Thermodynamics of Formation of Molecular Sieves

Thesis by
Patrick Manuel Piccione

In Partial Fulfillment of the
Requirements for the Degree of
Doctor of Philosophy

California Institute of Technology
Pasadena, California

2002
(Submitted 04 September 2001)

Past, Present and Future:

"I mean, after all; you have to consider we're only made out of dust. That's admittedly not much to go on and we shouldn't forget that. But even considering, I mean it's a sort of bad beginning, we're not doing too bad."

Philip K. Dick, *The Three Stigmata of Palmer Eldritch*, 1964.

"It's not what you look like, or what planet you were born on. It's how kind you are. The quality of kindness, to me, distinguishes us from rocks and sticks and metal, and will forever, whatever shape we take, wherever we go, whatever we become."

Philip K. Dick, afterword to "Human Is", 1976.

"[...] he was reaping the harvest of his years. He had done well with the thousands upon thousands of days behind him, with the result that age had brought a curious joy into his manner, as though each experience meant one more treat before the long bleak dark closed in."

Cordwainer Smith, *Norstrilia*, 1975.

Till Mamma

A Papá

Acknowledgments

I wish to thank my advisor Dr. Mark Davis for giving me the freedom to pursue the problems I was interested in, while giving me enough guidance to enable me to efficiently tackle them. By example, he has taught me how to systematically tackle a broad scientific problem and how to determine which questions it is important to answer. The experimental calorimetry work could never have been carried out without the assistance and interest of Dr. Alexandra Navrotsky of the University of California at Davis, who graciously gave me full access to the Thermochemistry Facility. I have also enjoyed the collaboration with Dr. Juliana Boerio-Goates and Dr. Brian Woodfield of Brigham Young University for the entropy measurements. Dr. Stacey Zones of Chevron took an interest in this project from the beginning, and I thank him for many fruitful discussions and zeolite samples. I am further indebted to Dr. Stephen Kinrade of Lakehead University for his suggestions on the ^{29}Si NMR experiments. Dr. Miguel Angel Camblor of Industrias Quimicas del Ebro kindly provided samples and also helped me surmount some of the hurdles when I first synthesized samples in fluoride media.

Dr. Sonjong Hwang has been an invaluable help for NMR-related issues and I thank him most gratefully. My second summer at Caltech was marked by having to get the AM300 NMR spectrometer working again; often alone in slightly

surreal surroundings (no windows, track lights and that hum!), I appreciated every time Tom Dunn came to the subbasement and helped me. I also wish to thank Mike Roy from the instrument shop and Rick Gerhart from the glassblowing shop for their help in making calorimeter cells, sample transfer cells and the occasional Rube Goldberg device. Further thanks are due to Joseph Abril and to George Wayrynen at UC-Davis for their assistance with mechanical matters. Martha Hepworth provided competent and friendly help with many administrative matters.

In the Mark Davis group, I particularly want to express my thanks to Dr. Hector Gonzalez for tirelessly discussing organic chemistry with me. Dr. Larry Beck first introduced me to experimental NMR and I appreciate his patience much more now that I have had to train people myself. Takahiko Takewaki always generously provided me with samples whenever he could. Later, I enjoyed working on the decomposing SDA project together with Dr. Brian Santora. At UC-Davis, Drs. Christel Laberty and Irina Molodetsky first taught me the essentials of experimental calorimetry, always gracefully and with a smile. Later, I collaborated with Dr. Sanyuan Yang and I thank him, too. I further wish to acknowledge Mike Gordon for countless conversations trying to "think outside the box," as well as for his great willingness to help me with design issues and to keep the mind alive.

My years here at Caltech have been made richer and more pleasant by the friends I made here and with whom I wish to keep in touch (so, please, write, call, come visit): Mike Gordon, Ramesh Srinivasan, Sonjong Hwang, Mohan Sankaran,

Marco Casari, Bruce Lambert, Ashish Bhardwaj, Don Kuklo, Ganesh Subramanian, Nathalie Bellocq, Victoria "Foxy Princess" Johnson, Martha Hepworth.

Mike "Chief" ("boss frog") Gordon, you are like a brother to me. We have gone on trips, seen things, talked nonsense and too much sense–with what relish! I think there is nothing we couldn't guess now. Leopard sharks, colorful nudibranchs, mutant crabs, and experimental SCUBA at Christmas Tree Cove. The (nuclear) Hale–Bopp mosqitoes, mineral origami and other great astronomical events. May the NexStar be your next finderscope! Remember that you will always underestimate the shower of Z particles if you fail to account for *dé Hyperion faktor*. Suitably bad movies beget good conversation if it is late enough. *Altered States* and isolation tanks. Ba-ba-ba-barjo and lovely Æon. Kris Kelvin and Hari. Lake Mono and its pH. "U-hu-hu" and the kitten which climbed the tree on the 110. The H_2SO_4/HF/urushiol-clad plants of the American West and "let's explore off the trail" with the reward of the *amaranth sentinels* (snow plants) and the risk of ticks (in the desert? helloooo, idiosyncratic tetracycline). Thank you for handing me a dull toothpick and telling me "*Do what you can*" while the coyotes threatened to eat me alive. Finally, this list would be incomplete without the old favorite: "*Be good, and be real; but don't be real good!*" We have grown together.

Ramesh has probably travelled a harder path here at Caltech than most. Of course, when one is fortified with much wisdom and philosophy, such a path is... who am I kidding? It's still hard! To see changes in personality induced by altering

quantum level populations, Mike, Mohan, and I were discussing the development of megatesla magnetic fields. We have Sonjong, King of the Sharpies, to thank for the alternative approach, much less invasive, of cooling people down to 4K. The TLAIPVMLSSNMRFAC (Three-Letter Acronym Infested Per Vacuumed Master Labelled Solid-State Nuclear Magnetic Resonance Facility At Caltech)-007 is in good hands. I greatly enjoyed my many conversations with Martha Hepworth, from literary science-fiction to its real-life alternatives in Tujunga Canyon.

I have also made good friends at UC-Davis. Jean Tangeman will always be welcome, as will Ulli Troitzsch, Kate Helean, Juro Majzlan, Mandar Ranade. Sergey "shutterbug" and Lena Ushakov kindly saved me from sleeping in the calorimetry suite. Irina Molodetsky, you did three Ph.Ds, but are r-e-a-l-l-y done now! (And yes, I will come visit–I will be living quite close to you.)

John McMaster listened in difficult times and shared much-needed and hard-acquired wisdom at all times. *May you never need it.* Further away from everyone else, Charles Duchenij has been most instrumental to my sanity. Que ton pays d'adoption t'apporte le bonheur esperé! My dear friends, I wish you all well. At different stages, Stephani and Nathalie provided emotional support and I wish them well, too. I also thank my uncle Alfredo for his continual encouragement.

I further wish to thank Dean Parandeh Kia of the International Student Office for all her help, as well as Dr. Sharyn Slavin Miller. Dr. Jo-Ann Ruffolo of the Caltech Career Centre helped me decide which immediate path to follow. Alice

Sogomanian and Divina Bautista have taken good care of me (and everyone else) over the last five years and I will miss them.

I am further grateful to the many sources of inspiration which I have drawn upon since I first came here: particularly, Cordwainer Smith ("The Lady who Sailed *The Soul*," "The Ballad of Lost C'Mell," *Norstrilia*, "A Planet Named Shayol," "Angerhelm"), Philip K. Dick (*The Three Stigmata of Palmer Eldritch, Ubik, The Transmigration of Timothy Archer, A Maze of Death*, "Human Is") and Tom Tykwer (*Run Lola Run*, that infused me with energy when it was much needed).

Finally, I wish to thank my Mom and Dad for their unwavering support and, more fundamentally, for their love. **I love you, too!** I could not have done it without you.

Abstract

Molecular sieves, porous, crystalline frameworks with pore sizes of molecular dimensions, are of great industrial importance as detergents, catalysts and absorbants. Despite their technological importance, the syntheses of these materials are still not well understood and typically rely on extensive series of trials to produce new framework structures.

Thermodynamic investigations are undertaken to better understand the energetic differences amongst molecular sieve frameworks and the mechanisms and interactions important in molecular sieve self-assembly. The enthalpies relative to quartz at 298.15 K are determined by high-temperature solution calorimetry for a collection of calcined pure-silica molecular sieves with diverse structural features. SiO_2 molecular sieves are shown to be only modestly (6.8-14.4 kJ/mol) metastable with respect to quartz. A strong linear correlation between enthalpy and molar volume is observed, implying that the overall packing quality determines the relative enthalpies of SiO_2 molecular sieves. Silanol (Si-O-H) defect sites lead to an additional destabilization of no more than 2.4 kJ/mol. The entropies of four pure-silica molecular sieves spanning the entire range of molar volumes available to SiO_2 frameworks are determined by the integration of heat capacity measurements from 5 to 400 K. The entropies of these structures are almost identical (3.2-4.2 $J \cdot K^{-1} \cdot mol^{-1}$ above quartz), hence the empty pore volume and cages do not

contribute appreciably to the vibrational density of states. The enthalpy and entropy data are combined to calculate the Gibbs free energies of transition from quartz to eight other silica polymorphs, including four molecular sieves as well as silica glass. At typical synthesis conditions, the available thermal energy is RT = 3.5 kJ/mol. The molecular sieve Gibbs free energies are only slightly larger than RT at 5.5-12.6 kJ/mol above quartz and lie in the same energetic region as the amorphous precursors used for molecular sieve preparation. There are therefore no significant thermodynamic barriers to transformations among silica polymorphs. Thus the role of SDA in molecular sieve syntheses is not the stabilization of *otherwise* very unstable phases.

Interaction enthalpies between inorganic frameworks and organic SDAs are measured by HF solution calorimetry for six molecular sieve/SDA pairs. The enthalpies are only moderately exothermic (-1.1 to -5.9 kJ/mol SiO_2), as expected if the predominant interactions are van der Waals contacts between the hydrophobic silica frameworks and the hydrocarbon portions of the SDAs. Interaction entropies can be estimated for three framework/SDA pairs, and, when used in combination with the interaction enthalpies, allow the calculation of the Gibbs free energies of interaction between these three inorganic/organic pairs. The latter values range from –2.0 to –5.4 kJ/mol SiO_2, smaller in magnitude than twice the available thermal energy at molecular sieve synthesis temperatures. This energy range is comparable to the range observed for the molecular sieve frameworks alone, showing that energetics of both the frameworks and of the molecular

sieve/SDA interactions must be considered in order to adequately describe molecular sieve synthesis. The energetics of the synthesis of molecular sieves (considering all components present in the synthesis mixture) are examined here and also reveal small differences between various molecular sieve/SDA combinations. The energetic contribution of the effective dilution experienced by the SDA upon occlusion is similar in magnitude to the other energetic effects. The strong selectivity of organic SDAs experimentally observed in the face of the comparatively small energetic differences suggests that kinetic factors dominate in molecular sieve preparation.

Table of Contents

CHAPTER ONE

INTRODUCTION 1

ZEOLITE SYNTHESIS **8**

HISTORICAL PERSPECTIVE 8

SUCCESSFUL ORGANIC STRUCTURE–DIRECTING AGENTS (SDAS) 9

A TYPICAL SYNTHESIS 9

ASSEMBLY MECHANISM 10

THERMODYNAMICS OF MOLECULAR SIEVE STRUCTURES **12**

GENERALITIES 12

PREVIOUS WORK 14

REFERENCES **20**

CHAPTER TWO

OBJECTIVES 23

REFERENCES **26**

CHAPTER THREE

THERMOCHEMISTRY OF PURE-SILICA ZEOLITES 27

ABSTRACT **28**

INTRODUCTION **29**

EXPERIMENTAL SECTION **32**

SAMPLES 32

CHARACTERIZATIONS 37

CALORIMETRY 39

RESULTS **40**
CHARACTERIZATION 40
ENTHALPIES OF TRANSITION (QUARTZ → MOLECULAR SIEVE), ΔH_{trans}^{298} 43

DISCUSSION **45**
ENTHALPIES OF TRANSITION, ΔH_{trans}^{298} 45
DEFECT ENERGETICS 48
IMPLICATIONS FOR ZEOLITE SYNTHESIS 49
RELATIONSHIP BETWEEN STRUCTURE AND ENERGETICS 52

CONCLUSIONS **62**

ACKNOWLEDGMENTS **63**

REFERENCES **75**

CHAPTER FOUR
ENTROPIES OF PURE-SILICA MOLECULAR SIEVES 78

ABSTRACT **79**

INTRODUCTION **80**

EXPERIMENTAL SECTION **83**
SAMPLE PREPARATION 83
CHARACTERIZATIONS 85
CALORIMETRY 88

RESULTS **89**

DISCUSSION **91**
STRUCTURE–ENTROPY RELATION FOR SILICA POLYMORPHS 91
GIBBS FREE ENERGY OF TRANSITION 93

CONCLUSIONS **95**

ACKNOWLEDGMENTS **96**

REFERENCES **102**

CHAPTER FIVE

SOLVENT CHOICE FOR AQUEOUS CALORIMETRY OF MS/SDA INTERACTIONS 105

INTRODUCTION 106

PREVIOUS WORK 107

SILICATES-PREVIOUS WORK 109

DISSOLUTION IN BASE 113

EXPERIMENTAL 113

RESULTS 115

HYDROFLUORIC ACID DISSOLUTION 119

EXPERIMENTAL 120

RESULTS 122

REFERENCES 138

CHAPTER SIX

ESTIMATED THERMODYNAMIC PROPERTIES OF SYMMETRIC TETRAALKYLAMMONIUM HALIDES AND HYDROXIDES 140

ABSTRACT 141

INTRODUCTION 143

ENTHALPIES OF FORMATION OF TETRAALKYLAMMONIUM HALIDES AND HYDROXIDES 144

GENERALITIES 144

ESTIMATION PROCEDURES 146

TETRAPROPYLAMMONIUM HEAVY HALIDE SALTS 146

FLUORIDES AND HYDROXIDES 148

ENTHALPY OF FORMATION OF TPA^+ 150

ENTROPIES OF TETRAALKYLAMMONIUM HALIDES AND HYDROXIDES 151

ENTROPIES OF TEACl, TEABr, TPACl AND TPABr 152

ENTROPIES OF FLUORIDE AND HYDROXIDE SALTS 153

RELATIONSHIP BETWEEN ΔH_F AND S° **155**

IMPLICATIONS FOR THE THERMODYNAMICS OF THE TPA-MFI INTERACTION **156**

SUMMARY **159**

REFERENCES **171**

CHAPTER SEVEN

THERMODYNAMICS OF PURE-SILICA MOLECULAR SIEVE SYNTHESIS 173

ABSTRACT **174**

INTRODUCTION **175**

EXPERIMENTAL SECTION **180**

MOLECULAR SIEVE SAMPLES 180

ORGANIC STRUCTURE-DIRECTING AGENTS 183

CHARACTERIZATIONS 185

CALORIMETRY 186

THERMODYNAMIC CYCLES 188

RESULTS **193**

MOLECULAR SIEVE CHARACTERIZATIONS **193**

CALORIMETRY **196**

ENTHALPIES OF SOLUTION IN AQUEOUS HF, ΔH_{soln}^{323} 196

DISCUSSION **200**

ENTHALPIES OF TRANSITION (QUARTZ → MOLECULAR SIEVE), ΔH_{trans}^{323} 200

ENTHALPIES OF INTERACTION, ΔH_{int}^{323} 201

GIBBS FREE ENERGIES OF MS/SDA INTERACTION 211

MOLECULAR SIEVE FORMATION FROM AMORPHOUS PRECURSORS 217

THERMODYNAMIC ANALYSIS OF THE FULL SYNTHESIS MIXTURES 219

IMPLICATIONS FOR MOLECULAR SIEVE SYNTHESIS 224

CONCLUSIONS.....226

ACKNOWLEDGMENTS.....229

REFERENCES.....250

CHAPTER EIGHT

CONCLUSIONS.....253

List of Tables

TABLE 1.1 PUBLISHED ENTHALPY AND ENTROPY VALUES FOR Si-MFI 18

TABLE 3.1 RESULTS FROM THERMOGRAVIMETRIC ANALYSIS OF SILICA MATERIALS 64
TABLE 3.2 MEASURED CALORIMETRIC DATA 64
TABLE 3.3 CALCULATED CALORIMETRIC DATA 65
TABLE 3.4 RELATIONSHIP BETWEEN STRUCTURE AND ENERGETICS 66
TABLE 3.5 MEASURED ENTHALPIES OF TRANSITION VS. PREDICTED VALUES BASED ON MOLAR VOLUME CORRELATION 67
TABLE 3.6 FRACTIONAL CONTRIBUTIONS OF LOOP CONFIGURATION TYPES TO SILICA STRUCTURES 68
TABLE 3.7 ENTHALPY CONTRIBUTIONS FOR LOOP TYPES 68
TABLE 3.8 MEASURED ENTHALPIES OF TRANSITION VS. PREDICTED VALUES BASED ON LOOP CONFIGURATION CORRELATION 69

TABLE 4.1 THERMOGRAVIMETRIC ANALYSES OF MOLECULAR SIEVE SAMPLES . 97
TABLE 4.2 THIRD-LAW ENTROPIES OF PURE-SILICA MOLECULAR SIEVES 98
TABLE 4.3 THIRD-LAW ENTROPIES AT 298.15 K, MOLAR VOLUMES AND FRAMEWORK DENSITIES FOR TETRACOORDINATED SILICA POLYMORPHS 99
TABLE 4.4 ENTROPY, ENTHALPY AND GIBBS FUNCTION OF TRANSITION (QUARTZ ↔ OTHER POLYMORPHS) FOR TETRACOORDINATED SILICA POLYMORPHS 99

TABLE 5.1 EFFECT OF VARYING METAL CATIONS AND MINERALIZING ANIONS OF DISSOLUTION IN BASIC SYSTEMS 128
TABLE 5.2 EFFECT OF TMA AND MEOH ON DISSOLUTION IN BASIC SYSTEMS . 129
TABLE 5.3 CHEMICAL SHIFTS OF FLUOROSILICATE SPECIES 130
TABLE 5.4 NMR EXPERIMENTS LIST: DSX-500 130
TABLE 5.5 INOVA 500 RESULTS: DISSOLUTION KINETICS 131
TABLE 5.6 INOVA 500: VT EXPERIMENT 131

TABLE 6.1 REPORTED ENTHALPIES OF SOLUTION FOR MONOVALENT HALIDES (KJ/MOL) 161

TABLE 6.2 REPORTED ENTHALPIES OF FORMATION FOR MONOVALENT HALIDES AND HYDROXIDES (KJ/MOL) 162
TABLE 6.3 ESTIMATION OF ENTHALPIES OF TPACl, TPABr, TPAI (KJ/MOL) 163
TABLE 6.4 DIFFERENCES BETWEEN HALIDE/HYDROXIDE PAIR ENTHALPIES BASED ON REPORTED VALUES (KJ/MOL) 164
TABLE 6.5 ESTIMATION OF TETRAALKYLAMMONIUM FLUORIDE AND HYDROXIDE ENTHALPIES (KJ/MOL) 165
TABLE 6.6 REPORTED ENTROPIES FOR MONOVALENT HALIDES AND HYDROXIDES (J/MOL·K) 166
TABLE 6.7 DIFFERENCES BETWEEN HALIDE/HYDROXIDE PAIR ENTROPIES (J/MOL·K) 166
TABLE 6.8 ESTIMATED TETRAALKYLAMMONIUM HALIDE AND HYDROXIDE ENTROPIES(J/MOL·K) 167

TABLE 7.1 UNIT CELL COMPOSITIONS 230
TABLE 7.2 MEASURED ENTHALPIES OF SOLUTION (MASS BASIS) 231
TABLE 7.3 MEASURED ENTHALPIES OF SOLUTION (MOL BASIS) 231
TABLE 7.4 COMPARISON OF SOLUTION ENTHALPIES TO LITERATURE VALUES ... 232
TABLE 7.5 ENTHALPIES OF TRANSITION FROM QUARTZ 233
TABLE 7.6 ENTHALPIES OF INTERACTION 234
TABLE 7.7 GIBBS FREE ENERGIES OF INTERACTION 235
TABLE 7.8 GIBBS FREE ENERGIES OF FORMATION FROM AMORPHOUS PRECURSORS AND SDAS 236
TABLE 7.9 SYNTHESIS MIXTURE COMPOSITIONS 237
TABLE 7.10 GIBBS FREE ENERGIES OF FORMATION AND EFFECTIVE DILUTION FOR COMPLETE SYNTHESIS MIXTURES 238

List of Figures

FIGURE 1.1 TYPES OF SHAPE SELECTIVITY 19

FIGURE 3.1 POSSIBILITIES FOR SILICATE SELF-ASSEMBLY IN HYDROTHERMAL SYNTHESES 70
FIGURE 3.2 ENTHALPY OF TRANSITION VS. FRAMEWORK DENSITY 71
FIGURE 3.3 ENTHALPY OF TRANSITION VS. MOLAR VOLUME 72
FIGURE 3.4 ENTHALPY OF TRANSITION VS. δ 73
FIGURE 3.5 CONFIGURATION LOOPS PRESENT IN ZEOLITES 74

FIGURE 4.1 THIRD-LAW ENTROPIES OF PURE-SILICA MOLECULAR SIEVES RELATIVE TO THAT OF QUARTZ VS. TEMPERATURE 100
FIGURE 4.2 THIRD-LAW ENTROPIES VS. MOLAR VOLUME FOR SILICA POLYMORPHS 101

FIGURE 5.1 ^{29}Si NMR SPECTRUM OF 1 MOL/L Na SILICATE 132
FIGURE 5.2 ^{29}Si NMR SPECTRUM OF 1 MOL/L TMA SILICATE 133
FIGURE 5.3 ^{29}Si NMR SPECTRUM OF 1 MOL/L TMA SILICATE IN 50% MeOH ... 134
FIGURE 5.4 ^{29}Si NMR SPECTRUM OF 1 MOL/L TMA SILICATE FROM CAB-O-SIL M5 AND AT CALORIMETRIC CONCENTRATION 135
FIGURE 5.5 TYPICAL ^{19}F SPECTRUM OF FLUOROSILICATE SOLUTIONS 136
FIGURE 5.6 DISSOLUTION KINETICS OF MFI:TPA: TIME EVOLUTION OF ^{19}F NMR SIGNALS 137

FIGURE 6.1 ENTHALPIES OF FORMATION OF TAA HALIDES VS. n 168
FIGURE 6.2 EMPIRICAL RELATION BETWEEN ΔH_F (TAAX) AND ΔH_F (NH_4X) 169
FIGURE 6.3 RELATIONSHIP BETWEEN ΔH_F AND S° FOR TAA HALIDES AND HYDROXIDES 170

FIGURE 7.1 SETARAM C-80 MICROCALORIMETER 239
FIGURE 7.2 HF RESISTANT CELLS 240
FIGURE 7.3 HF RESISTANT CELLS 241
FIGURE 7.4 ^{1}H SOLID-STATE NMR SPECTRA OF SDA-CONTAINING MOLECULAR SIEVES 242

FIGURE 7.5 ^{1}H SOLID-STATE NMR SPECTRA OF CALCINED MOLECULAR SIEVES 243
FIGURE 7.6 ^{29}Si SOLID-STATE NMR SPECTRA OF SDA-CONTAINING MOLECULAR SIEVES 244
FIGURE 7.7 ^{29}Si SOLID-STATE NMR SPECTRA OF CALCINED MOLECULAR SIEVES 245
FIGURE 7.8 ^{13}C SOLID-STATE NMR SPECTRA OF SDA-CONTAINING MOLECULAR SIEVES 246
FIGURE 7.9 REPRESENTATIVE HEAT FLOW CURVES 247
FIGURE 7.10 GENERAL TRENDS IN MS/SDA INTERACTIONS 248

Chapter One

Introduction

A catalyst is defined as a substance that modifies the rate at which a chemical reaction takes place without being consumed itself.[1] The first patent on catalysis was awarded in 1831 to Phillips on the oxidation of sulfur dioxide to sulfur trioxide over platinum.[2] Berzelius coined the word *catalysis* in 1835, unifying earlier reports where small amounts of a substance were found to greatly effect the rates of reactions.[3] The modern definition of catalysis was given by Oswald in 1894, and the early 1900s saw a flurry of Nobel prizes being awarded for studies related to catalysis:[2] Oswald (1909) for the study of rates over catalysts, Sabatier (1912) for the catalytic hydrogenation of organics, Haber (1919) for the synthesis of ammonia, Langmuir (1932) for studies of surface chemistry.

Today catalysts have an enormous economic impact; in fact, the exact composition of the catalysts is often the most secret and therefore highly guarded part of an industrial chemical process. The US sales of process catalysts alone had a value of over 1 billion dollars in 1990.[1] More impressively, perhaps, it has been estimated that about one-sixth of the material equivalent to the GNP of the US contains a catalytic process at some stage of its manufacture.[4]

Catalysts are traditionally classified as follows.[1] *Homogeneous* catalysts are typically fairly small molecules and are present in the same physical state as the main reagents. For instance, hydrofluoric and sulfuric acids are used in liquid-phase alkylation reactions, such as the production of isooctane from isobutane and

butene. *Heterogeneous* catalysts, by contrast, are present in a *different* physical phase from one or more of the reactants. The alumina-supported silver solid catalyst used for the gas-phase partial oxidation of ethylene to ethylene oxide is such a catalyst.[5] Finally, enzymatic catalysts are large, complex molecules of biological origin that often are present in the same phase as the main reagents. They are typically proteins, in other words polypeptides with multidimensional structures. They are considered separate from homogeneous catalysts because the mechanism whereby they act is often different in nature from those latter ones, to the point of being specific to a single molecule sometimes. The enzyme amylase, for instance, is found in saliva and enables the hydrolysis of starch.[1]

Two important concepts in the study of catalysis are *activity* and *selectivity*.[6] Activity refers to the rates of reaction. Selectivity, on the other hand, refers to the ratio of the amounts of the desired and undesired products. Obviously the highest possible values are desirable for each of these quantities. Practical considerations must also be kept in mind for industrial scale processes and a quick summary of the trade-offs follows.[2]

Homogeneous catalysts exhibit good *enantio* selectivity (ability to form only one of a pair of mirror image isomers, crucial for a compound such as naproxen where one enantiomer is beneficial but the other is a liver toxin[7]), *regio* selectivity (ability to react only at a specific site of the reagent molecule) and are quite tunable (the properties of an organometallic complex can easily be varied by

changing the ligands around the metal center). Heterogeneous catalysts, on the other hand, are more environmentally benign (compare a solid zeolite to liquid H_2SO_4 for alkylation!), more thermally stable and easier to separate since they are present in a different phase from the product. These latter advantages become more marked for processes carried out on very large scales. As a result, there is a tendency in modern chemical engineering practice to shift towards heterogeneous catalysts whenever possible for the production of bulk commodity chemicals, whereas the more selective homogeneous catalysts are preferentially used in the fine chemicals and pharmaceutical industries. This distinction is obviously not a sharp one, and each individual process uses the most appropriate catalyst.

A particular class of heterogeneous catalysts is composed of the porous materials called molecular sieves. The dimension of their pores is on the molecular level, i.e., in the 10^{-10} meter range. Only molecules smaller than the pores can diffuse in and out of them. This characteristic is the basis for *shape-selective catalysis* that uses size differences to discriminate among reagents and products.[8] The first application for these molecular sieves was in separations, and even molecules of fairly similar sizes such as *n*-butane and *i*-butane can be separated with a high degree of selectivity.

A particularly successful class of molecular sieves consists of the *zeolites*. These materials are crystalline aluminosilicates first discovered in 1756 by Swedish mineralogist A.F. Cronstedt.[9] They are composed of MO_4 tetrahedra (M=Al or Si)

where each apical oxygen is shared between adjacent tetrahedra.[10] Over 100 different structures exist, each designated by a three-letter code.[11] Their pores are uniformly sized, with pore diameters ranging from 4 to 13 Å. Both one- and multi-dimensional networks exist. Zeolites can discriminate between molecules whose dimensions differ by less than 1 Å; for instance, *i*-butane and *n*-butane, whose sizes differ by 0.3 Å, can be separated.[8] The high surface-to-volume ratio and thermal stability of zeolites are also desirable characteristics.[12] In addition to their use in the large-scale shape-selective separation of hydrocarbons, zeolites are used as solid acids for applications such as cracking (they can have acid site concentrations[2] equivalent to 4 M H_2SO_4), solid base catalysis[13] and even as catalysts for redox reactions: H_2O_2 over the zeolite TS-1 performs partial oxidations with selectivities and yields unattainable by other routes.[14] Furthermore, zeolites are extremely benign environmentally and easily regenerated by burning off any accumulated coke.[15] While zeolite research in the 1970s and 1980s concentrated on changing their transport properties (on a 10^{-2}-10^{-8} m length scale), current efforts focus on changing the structure around the active site.[16] In other words, the manipulations involved now take place on a molecular (10^{-10} m) length scale, and aim to improve the complementarity of the product, reactant and intermediates with the active site. For molecular sieves such as zeolites, the catalytic activity observed can be broadly classified into three patterns:[17] *reactant*, *product*, and *transition-state* shape selectivity, as depicted in Figure 1.1.[8]

Reactant shape selectivity is based on a difference in size between different reactant molecules in a mixture.[17] Only the molecules which are small enough to enter the pores of the zeolite can react at its active sites. Zeolite A contains acid sites that can dehydrogenate alcohols to water and the corresponding alkene. In the example shown (Figure 1.1), the zeolite is presented with a mixture of 1-butanol and 2-butanol. Only 1-butanol has a kinetic diameter small enough to enter the pores of the zeolite and therefore it is the only one of the two isomers to react. Product shape selectivity is based on the difference in sizes of a mixture of possible products at thermodynamic equilibrium. While all possible products are formed in the zeolite pore, only the product(s) small enough to escape the pores will actually be observed. The example (Figure 1.1) shows the synthesis of *p*-xylene from toluene over the zeolite ZSM-5. This zeolite, like many others, includes cavities within its pore structure. In the cavity, a mixture of the three xylenes is formed. However, *p*-xylene diffuses through the zeolite pores at a rate approximately 1000 times faster than the other isomers and can lead to the production of nearly pure *p*-xylene. Finally, transition-state shape selectivity occurs when the space in the pores does not allow all possible transition states for a set of reactions to form. In this case the reactants and products from the different pathways considered can diffuse from and to the pores, but the essential step for converting some reactants to some products simply cannot be taken. The example shows that the zeolite mordenite converts 1,5-pentadiene to cyclopentadiene. The zeolite ZSM-5, however, even though it has the requisite active sites, cannot effect

this transformation. Yet it is known that cyclopentadiene as well as 1,5-pentadiene can travel freely in the pores of ZSM-5. If no cyclopentadiene product is observed from a 1,5-pentadiene feed, it must therefore be the case that the requisite intermediate cannot form: in other words, there is evidence for transition-state shape selectivity. Although rare, transition-state shape selectivity is potentially the most useful type of shape selectivity. Consider first that for both reactant and product shape selectivity, activity and selectivity are inversely related. The reason for this is that selectivity gains can only be achieved by narrowing the pores, thus greatly reducing diffusion rates and, hence, activity. In the case of transition-state shape selectivity, it is not necessary to narrow the pores but only to get to the point where certain conformations within the pores are impossible.

In view of the remarkable catalytic activity of zeolites, and the benefits of transition-state shape selectivity, it is desirable to reach the stage where transition-state shape selectivity can be obtained in zeolites by *design* and not by chance for a given reaction. In order to reach this ambitious goal, we must better understand the assembly mechanism of zeolites. In fact, such an understanding will be helpful to achieve reactant and product shape selectivity by design as well. This project aims at increasing our understanding of zeolite syntheses by determining thermodynamic parameters for different SiO_2 structures, as well as organic-inorganic interactions. To set the stage for the rest of this work a brief discussion of zeolite syntheses follows.

Zeolite Synthesis

Historical Perspective

Several zeolites occur in nature;[18] therefore, the earliest attempts at zeolite synthesis mimicked geological conditions (pressure over 100 bar, temperature over 200 °C).[10] Indeed, the first zeolite without naturally occurring counterpart was synthesized by Barrer using this approach in 1948.[19] By the late 1940s, however, zeolite synthesis had already taken a turn toward lower temperature, hydrothermal conditions: temperatures around 100-150 °C and autogenous pressures were used for aluminosilicate gels, crystallizing high-Al zeolites such as LTA and FAU. The use of water-soluble organic molecules (Structure-Directing Agents, SDAs) to assist the synthesis burgeoned in the 1960s,[20] resulting in new structures and more siliceous systems.[10] Nowadays, over 100 zeolite structures are officially recognized.[11] In addition to the naturally occurring, aluminosilicate zeolites, crystalline porous oxide frameworks incorporating several other elements such as B, Ti, Zn, Ga, and Ge have been synthesized;[21-23] these are more generally referred to as *molecular sieves*. While the exact mechanism of zeolite self-assembly (and thus structure direction) is only imperfectly understood (see below), some general comments about the SDAs are in order.

Successful Organic Structure–Directing Agents (SDAs)

Most obviously, a molecule must be stable at the severe conditions (pH>10, $100 \leq T \leq 200$ °C, reaction times of up to several months) of hydrothermal syntheses to successfully serve as a zeolite SDA. Organic amines and especially quaternary ammonium ions constitute the most successful series of SDAs, but other compounds such as crown ether-metal complexes have also been used.[24] For alkylammonium ions, Zones determined that the optimal structural-directing activity was exhibited by cations with $11 \leq C/N^{+} \leq 15$.[25] A necessary balance between the hydrophobic and hydrophilic nature of the organic cations was invoked to explain this narrow range.

A Typical Synthesis

In a generic zeolite synthesis, an aqueous solution of the organic SDA (except for the very few frameworks that can be synthesized in the absence of any organic), a mineralizing agent (fluoride or hydroxide) and, if applicable, an aluminum source (sulfate, hydroxide) is first prepared.[26] A silica source (e.g., sodium silicate, colloidal silica, silicon alkoxides) is added, forming a gel or, less frequently, a clear solution. After a so-called "aging" period at room temperature,

the mixture is loaded into a Teflon liner and inserted into a metal "bomb" container; the reaction is then allowed to proceed in 100-250 °C ovens for several days, sometimes months. For reference, a typical pure–SiO_2 ZSM-5 synthesis follows.

To an aqueous solution of 2.94 g sodium hydroxide in 165.14 g water, 9.8 g tetrapropylammonium (TPA) bromide were added. 22.11 g Cab-O-Sil M-5 silica were blended in until an even paste resulted. After being allowed aging for an hour, the paste was transferred into a Teflon vessel and heated at 100 °C for ten days. The resulting suspension was filtered and dried, yielding Si-ZSM-5 identified by its X-Ray Diffraction (XRD) powder pattern.[27]

Assembly Mechanism

The assembly mechanism for zeolites is still poorly understood despite intensive current efforts.[28] The formation of the ordered silicate framework depends on the ability to reversibly form and break Si-O-Si bonds by condensation/decondensation steps.[29] These local-equilibrium conditions are most easily established in the presence of alkali metal cations (that increase the rates of polymerization/depolymerization up to 15 times)[30] and "mineralizing agents": the anions OH^- and F^- which solubilize SiO_2 and produce 5- and 6–coordinated intermediates in solution.[26] Several *modus operandi* for the SDA have been

proposed. Although the size and shape of the guest certainly match those of the framework pores, there typically is no templating in the biological "hand-in-glove" sense of the notion.[29] The interactions between SDA and zeolite framework are weak, van der Waals forces and in some cases the SDA has even been demonstrated to retain some rotational degrees of freedom.[31] In fact, there is seldom a one-to-one guest-host correspondence, as exemplified by 1,6-hexanediamine ($H_2N(CH_2)_6NH_2$) that forms MFI at 120 °C but ZSM-48 at 150 °C.[32] In addition, MFI can also be made using tens of other SDAs.

Because of the industrial importance of the MFI structure and because of the high specificity between tetrapropylammonium (TPA) ions and MFI, nucleation and growth studies have concentrated on the TPA-MFI system. TPA ions are thought to first arrange water molecules around them in a hydrophobic hydration sphere (HHS).[32] The ordered structure of the water induces an ordered structure in the soluble silicate species present in the solution. When two HHSs start to overlap, the water molecules are displaced (an entropically favorable process) and a composite species of TPA and silicate is left behind. This "primary unit" can be detected by Small-Angle X-Ray Scattering (SAXS) and its size is approximately 2.8 nm.[33] The presence of precursor species with significant organic-silica interactions has also been demonstrated by ^{1}H-^{13}C cross-polarization, magic-angle spinning nuclear magnetic resonance (CP-MAS NMR) experiments.[32]

Once formed, these composite species can follow several pathways. First, if an extended crystalline structure is already present, the composite species can diffuse to its surface to form a new layer of zeolite. Another possibility is the aggregation of several of the composite species to form structures on the 5-10 nm length scale that have also been detected by SAXS.[33-35] A non-crystalline aggregate is first formed that can either fall apart or rearrange to give the thermodynamically more stable crystalline unit. These crystalline 5-10 nm aggregates are the nucleation sites first detectable by XRD: once formed, they are too stable to be redissolved. They can either diffuse to an already-formed crystal or grow by aggregation to form larger structures. While these crystallization data explain the sequence of events in zeolite formation, they do not help understand why a *particular* framework topology is formed under given synthesis conditions.

Thermodynamics of Molecular Sieve Structures

Generalities

The reactions producing complex materials such as a pure molecular sieve phase often depend on a complicated combination of kinetic and thermodynamic factors. As discussed above, nucleation studies do not concern themselves with the

variety of frameworks that can be synthesized. By contrast, while thermodynamic data do not answer all the questions about these materials, they enable one to know what the relative energetics of different molecular sieves are and which transformations are at all possible.[36] They further provide magnitudes for the driving forces of the relevant processes, thereby helping understand which mechanisms are most important in the assembly of a given material.[37]

Thermodynamics predicts (see below) that α-quartz is the most stable phase of SiO_2.[26] In other words, all-silica molecular sieves are metastable polymorphs of silicon dioxide that would have no right to existence based on thermodynamic considerations alone. Due to the industrial importance of zeolites, an insight in the factors governing the relative stabilities of these materials (both variations with composition and with framework structure are of interest here) is obviously desirable.[38] Actual syntheses, however, do not produce pure inorganic frameworks but rather inorganic-organic composites (SDAs enclathrated within the molecular sieve). In addition to the relative framework stabilities, the interaction of the SDA with the zeolite must therefore be considered in order to give a full thermochemical description of zeolite syntheses.[26] Indeed, the hydrothermal crystallization reaction (shown here for the simplest case, that of a pure-silica molecular sieve) is not

$$\text{dissolved silicates} \rightarrow \text{MS but rather}$$

$$\text{water} + \text{dissolved silicates} + \text{SDA (solution)} \rightarrow \text{MS·SDA (s)} + \text{water}$$

where MS represents an empty molecular sieve framework, and MS·SDA represents the corresponding as-made molecular sieve with the SDA occluded inside.

A brief summary of the earlier experimental work on zeolite and molecular sieve thermochemistry follows.

Previous Work

A large body of data has been generated for natural zeolites by low-temperature, heat capacity calorimetry and solution calorimetry.[39-50] It is hard to evaluate the relative thermodynamics of different structures from an analysis of this work due to the changing compositions of natural materials. In addition to these studies, Johnson *et al.*[51] published a complete set of thermodynamic properties for pure–Si MFI (a synthetic material) determined from low-temperature heat-capacity, fluorine-combustion, high-temperature drop calorimetric and HF solution calorimetric measurements. At 298.15 K, these authors reported an enthalpy of formation of ΔH°_{f} = -905.20 ± 0.84 kJ/mol and a third-law entropy of S° = 46.29 ± 0.23 J/(mol·K) that are energetically rather close to the values for α-quartz (-910.70 ± 1.0 kJ/mol and 41.5 ± 0.1 J/(mol·K) respectively[50]).

Petrovic and co-workers[38] used combinations of drop solution (DS) and transposed temperature drop (TTD) calorimetry to obtain ΔH°_{f} values for a

collection of high-silica molecular sieves (MFI, MTW, FAU, EMT, MEL and AFI). These six structures span a narrow range of 7 kJ/mol and are only 7 kJ/mol less stable than α-quartz. This energy range overlaps with that of amorphous silicas and confirms that pure-silica molecular sieves are only modestly metastable with respect to quartz. The authors further concluded that the role of the SDA is not the stabilization of *otherwise* very unstable structures. When the enthalpies of formation were plotted against molecular sieve structural parameters, no correlation to either density or mean Si-O-Si angles was found. A slight correlation of the overall energy with the fraction of Si-O-Si angles below 140° was illustrated, in accord with some theoretical considerations.[52] At the time of this study, fewer molecular sieves were available as pure-SiO_2 polymorphs than today. Since the phases available tended to have rather similar structural features the conclusions of the Petrovic study are somewhat limited. Further studies by the same group found similar energetic trends for the $AlPO_4$ class of molecular sieves.[53-54] Finally, despite their much larger pore sizes, the mesoporous materials such as MCM-41 are only slightly less stable than the molecular sieves at about 15 kJ/mol above quartz.[55]

The publications described so far concerned themselves with calcined materials. Molecular sieve syntheses, however, typically produce inorganic frameworks with *occluded SDAs* within them so the enthalpy of the framework alone may not be the most synthetically relevant quantity. Patarin *et al.*[56-57] studied the interaction between three SDAs and pure–Si MFI by HF calorimetry and found

tetrapropylammonium cations (TPA^+) to stabilize MFI considerably more than either di- or tri-propylammonium cations. The enthalpy of stabilization for the reaction

$$MFI\ (96\ SiO_2) + 4\ TPA^+F^-\ (aq) \rightarrow MFI{\cdot}4\ TPAF\ (s)$$

is reported to be -6.2 ± 2.4 kJ/mol SiO_2 whereas it is positive for the other cations. The authors suggested that TPA may interact intimately with the MFI silicate framework whereas di- and tri-propylammonium cations only serve as pore-filling agents.

Table 1.1 summarizes the published data for pure-SiO_2 MFI, the only material for which several measurements are available. These data are not within experimental error of each other; this discrepancy may be due in part to differences in the synthetic procedures used. These discrepancies illustrate the necessity for obtaining data from a collection of isocompositional molecular sieves using a single thermochemical technique. To summarize, the energetic differences between empty molecular sieve frameworks appears to be small, of the order of the thermal energy. Such low barriers of transformation would explain the multitude of possible molecular sieve phases. To firmly establish this conclusion data were needed from a collection of molecular sieves that more comprehensively displayed most of the possible structural features of this set of polymorphs. Furthermore, only very scarce data are available on the organic-inorganic interaction. To better understand this interaction and the self-assembly process and also to provide

parameters for calculations, interaction enthalpy data for various MS-SDA pairs are needed.

Table 1.1. Published Enthalpy and Entropy Values for Si-MFI

Measurement Method	Reference	ΔH°_{f} (kJ/mol)	S° (J/(mol·K))
F_2 combustion, low-T Cp	51	-905.20 ± 0.84	46.29 ± 0.23
TTD/DS	38	-902.5 ± 1.3	N/A
HF solution	56	-908.51 ± 1.69	N/A

Figure 1.1. Types of Shape Selectivity[17]

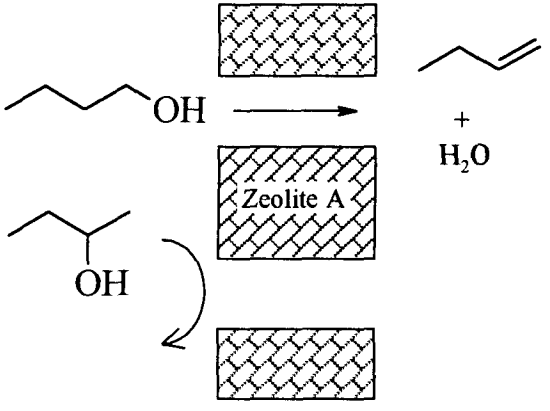

Reactant Shape Selectivity (based on differences in sizes of reactant molecules)

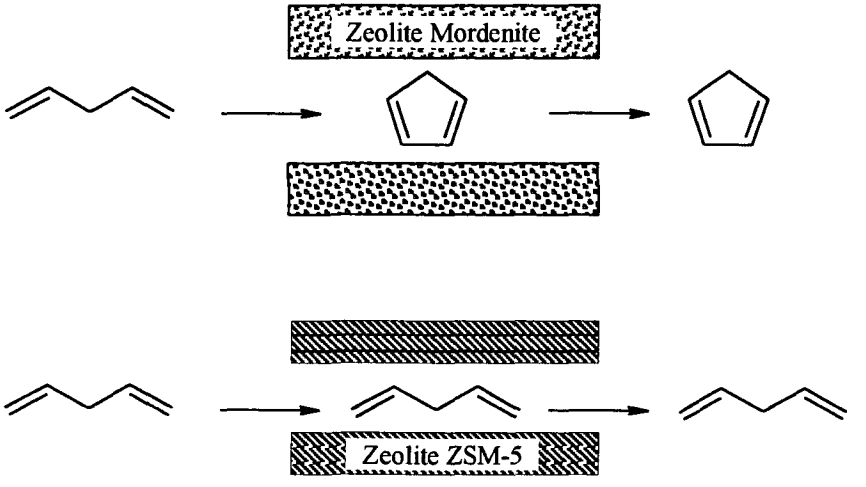

Transition-State Shape Selectivity (transition state is too large to form inside ZSM-5 channels)

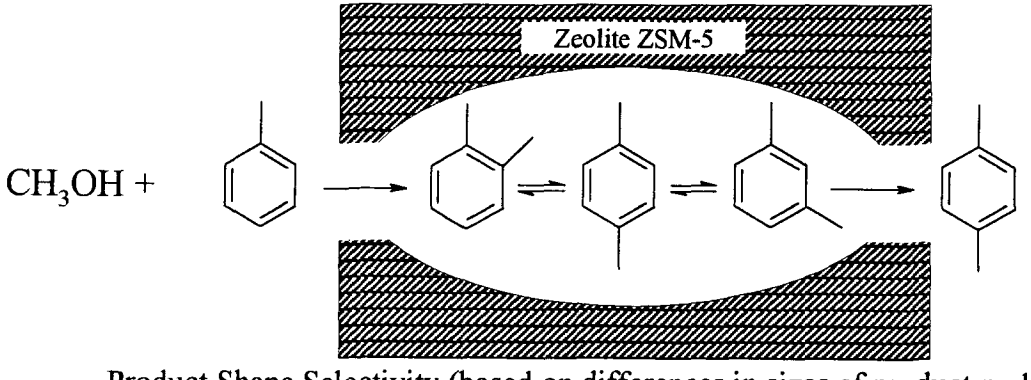

Product Shape Selectivity (based on differences in sizes of product molecules)

References

[1] Oyama, S.T.; Somorjai G.A. *J. Chem. Edu.* **1988**, *65*, 765.

[2] Davis, M.E. *Unpublished Notes* **1997**.

[3] Berzelius, J. J., *Årsberättelse om framstegen i fysik och kemi* **1835**, Stockholm.

[4] Haensel, V.; Burwell, R.L. *Sci. Am*, **Dec 1971**, *225*, 46.

[5] Gates, B.C., *Catalytic Chemistry* **1992**, Wiley, New York.

[6] Fogler, S.H., *Elements of Chemical Reaction Engineering* **1992**, Prentice Hall, Englewood Cliffs.

[7] Haupt, D.; Petterson, C.; Westerlund, D. *J. Biochem. and Biophys. Methods* **1992**, *25*, 273.

[8] Davis, M.E.; Katz, A.; Ahmad, W.R. *Chem. Mater.* **1996**, *8*, 1821.

[9] Cronstedt, A.F. *Svenska Vetenskaps Akademiens Handlingar*, **1756,** *17*, 120.

[10] Davis, M.E.; Lobo, R.F. *Chem. Mater.* **1992**, *4*, 756.

[11] See http://www.iza.sc.ethz.ch/IZA-SC/Atlas/AtlasHome.html.

[12] Davis, M.E. *ChemTech* **1994**, September, 22.

[13] Tanabe, K.; Misono, M.; Ono,Y.; Hattori, H. *New Solid Acids and Bases, Their Catalytic Properties*, **1989**, Elsevier, Amsterdam.

[14] Notari, B. in Grobet, P.J.; Mortier, W.J.; Vansant, E.F.; Schulz-Ekloff, G., Eds. *Innovation in Zeolite Materials Science*, **1988**, Elsevier, Amsterdam, cited by Dartt, C.B.; Khouw, C.B.; Li, H.-X.; Davis, M.E. *Microp. Mat.*, **1994**, *2*, 425.

[15] Satterfield, C.N. *Heterogeneous Catalysis in Industrial Practice*, **1991**, McGraw-Hill, New York.

[16] Davis, M.E. *Acc. Chem. Res.* **1993**, *26*, 111.

[17] Csicsery, S. M. *Zeolites* **1984**, *4*, 203.

[18] De Michele, V. *Atlante/Dizionario di Mineralogia* **1972**, Istituto Geografico De Agostini, Novara, Italy.

[19] Barrer, R.M. *J. Chem. Soc.* **1948**, 127.

[20] Barrer, R.M.; Denny, P.J. *J. Chem. Soc.* **1961**, 971.

[21] Toshikawa, M.; Zones, S.I.; Davis, M.E. *Microporous Mater.* **1997**, *11*, 137.

[22] Newsam, J.M.; Vaughan, D.E.W.; Strohmaier, K.G. *J. Phys. Chem.* **1995**, *99*, 9924.

[23] Tuilier M.H.; Lopez A.; Guth, J.L. *Zeolites* **1991**, *11*, 662.

[24] Delprato, F.; Delmotte, L.; Guth, J.L.; Huve, L. *Zeolites* **1990**, *10*, 546.

[25] Kubota, Y.; Helmkamp, M.M.; Zones, S.I.; Davis, M.E. *Microporous Materials* **1996**, *6*, 213.

[26] Helmkamp, M.M.; Davis, M.E. *Annu. Rev. Mater. Sci.* **1995**, *25*, 161.

[27] M. E. Davis group **1996**, *Synthesis Book*, Unpublished.

[28] Gies, H.; Marler, B. *Zeolites,* **1992**, *12*, 42.

[29] Burkett, S.L.; Davis, M.E. in *Comprehensive Supramolecular Chemistry*, Lehn, J.M., ed, **1994**, vol. *7* chapter 4.

[30] Brady, P.; Walther, J.V. *Chem. Geol.* **1990**, *82*, 253.

[31] Hong, S.B.; Cho, H.M.; Davis, M.E. *J. Phys. Chem.* **1993**, *97*, 1662.

[32] Burkett, S.L.; Davis, M.E. *Chem. Mater.* **1995**, *7*, 1453.

[33] de Moor, P.-P.E.A.; Beelen, T.P.M.; Komanschek, B.U.; Beck, L.W.; Wagner, P.; Davis, M.E.;van Santen, R.A. *Chem. Eur. J.* **1999**, *5*, 7.

[34] Dokter, W.H.; Van Garderen, H.F.; Beelen, T.P.M.; van Santen, R.A.; Bras, W. *Angew. Chem. Int. Ed. Engl.* **1995**, *34*, 73.

[35] de Moor, P.-P.E.A.; Beelen, T.P.M.; Komanschek, B.U.; Diat, O.; van Santen, R.A. *J. Phys. Chem. B* **1997**, *101*, 11077.

[36] Navrotsky, A.N. *Mat. Res. Soc. Symp. Proc.* **1997**, *432*, 3.

[37] Navrotsky, A.N. *MRS Bulletin* **1997**, May, 35.

[38] Petrovic, I.; Navrotsky, A.; Davis, M.E.; Zones S.I. *Chem. Mater.* **1993**, *5*, 1805.

[39] Belitskiy, I.A.; Gabunda, S.P.; Drebushchak, V.A.; Naumov, V.N.; Notgeva, V.V. *Geochemistry International* **1984**, *21*, 21.

[40] Paukov, I.E.; Belitskii, I.A.; Fursenko, B.A.; Kovalevskaya, Yu.A. *Geochemistry International* **1997**, *35*, 946.

[41] Paukov, I.E.; Belitskii, I.A.; Kovalevskaya, Yu.A. *Geochemistry International* **1998**, *36*, 663.

[42] Paukov, I.E.; Fursenko, B.A. *Geochemistry International* **1998**, *36*, 471.

[43] Paukov, I.E.; Belitskii, I.A.; Berezovskii, G.A. *Geochemistry International* **1998**, *36*, 565.

[44] Kiseleva, I.; Navrotsky, A.; Belitsky, I.A.; Fursenko, B.A. *Amer. Mineral.* **1996**, *81*, 658.

[45] Johnson, G.K.; Flotow, H.E.; O'Hare, P.A.G.; Wise, W.S *Amer. Mineral.* **1985**, *70*, 1065.

[46] Johnson, G.K.; Flotow, H.E.; O'Hare, P.A.G.; Wise, W.S. *Amer. Mineral.* **1983**, *68*, 1134.

[47] Johnson, G.K.; Flotow, H.E.; O'Hare, P.A.G.; Wise, W.S. *Amer. Mineral.* **1982**, *67*, 736.

[48] Johnson, G.K.; Tasker, I.R.; Flotow, H.E.; Wise, W.S. *Amer. Mineral.* **1992**, *77*, 85.

[49] Donahoe, R.J.; Hemingway, B.S.; Liou, J.G. *Amer. Mineral.* **1980**, *75*, 188.

[50] Robie, R.A.; Hemingway, B.S. *USGS Bulletin* **1995**, *2131*.

[51] Johnson, G.K.; Tasker I.R.; Howell, D.A.; Smith, J.V. *J. Chem. Thermodynamics* **1987**, *19*, 617.

[52] Newton, M.D.; Gibbs, G.V. *Phys. Chem. Miner.* **1980**, *6*, 221.

[53] Hu, Y.; Navrotsky, A.; Chen C.-Y.; Davis, M.E. *Chem. Mater.* **1995**.

[54] Yang, S.; Navrotsky, A. *Microporous Mesoporous Materials* **2000**, *37*, 175.

[55] Petrovic, I.; Navrotsky, A.; Chen, C.-Y.; Davis, M.E. *Stud. Surf. Sci. Catal.* **1994**, *84*, 677.

[56] Patarin, J.; Kessler, H.; Soulard, M.; Guth, J.L. **1989**, in *Zeolite Synthesis;* Occelli, M.L.; Robson, H.E. Eds.; *ACS Symposium Series 298*, American Chemical Society, Washington, DC, Ch. 16 .

[57] Patarin, J.; Soulard, M.; Kessler, H.; Guth, J.L.; Diot, M. *Thermochim. Acta* **1989**, *146*, 21.

Chapter Two

Objectives

The broad aim of this thesis is to determine thermodynamic quantities of interest to better understand the formation of molecular sieves, with particular emphasis on the factors that lead to the formation of different frameworks. Since the adsorption and catalytic properties depend critically on the framework structure (pore and cage sizes), this work has considerable practical relevance. Pure-SiO_2 molecular sieves were studied so as to: first, eliminate differences due to compositional variations; second, benefit from the use of hydrophobic samples (small water contents yield small corrections due to water vaporization, etc., in thermochemistry experiments).

The synthesis of zeolites can be investigated from several different perspectives since it involves both the formation of a large, ordered, crystalline network and the interaction of this network with organic species. The theoretical complexity of the systems studied and corresponding experimental difficulties were progressively increased as follows. First, a model for pure-SiO_2 lattice energetics had to be provided; to this end, thermodynamic data for different porous SiO_2 polymorphs frameworks were obtained and correlated with structural data. After the energetics of these polymorphs had been better characterized, the interaction between selected MS-SDA pairs was studied, with particular attention to SDA molecules capable of directing syntheses towards several different frameworks.

This thesis is organized as follows. In Chapter Three, pure-SiO_2 molecular sieve samples are investigated by high-temperature (974 K) drop solution

calorimetry in molten lead borate to obtain their relative enthalpies. These samples comprise a range of molecular sieve structural features significantly more varied than those available to previous investigators.[1] In particular, several low framework density materials were studied, along with an extra-large pore (14-membered rings) framework and the only all-silica zeolite containing 7- and 9-membered rings. Correlations between structural features and enthalpies were investigated as well. To complement the data presented in Chapter Three, a study of pure-SiO_2 molecular sieve entropies was undertaken employing low-temperature heat capacity calorimetry. The results are presented in Chapter Four. The entropy and enthalpy data, together, fully characterized the thermodynamics of porous SiO_2 polymorphs. NMR studies for near-room temperature calorimetry showed the solvent of choice for molecular sieve investigations to be aqueous HF and are documented in Chapter Five. Chapter Six presents estimation procedures for the enthalpies and entropies of halides and hydroxides of some symmetric tetraalkylammonium ions used in zeolite synthesis. Finally, thermodynamic cycles following the methodology of Patarin *et al.*[2] were constructed to obtain the enthalpies for the interaction MS + SDA (aq. HF) $\rightarrow$ MS·SDA from solution calorimetry studies performed on six MS-SDA pairs. These pairs were chosen to provide representative values for the enthalpy of interaction between various classes of SDAs and molecular sieves. The results along with their implications for zeolite synthesis are given in Chapter Seven. These data constitute a

thermodynamic characterization of *molecular sieves as they are actually synthesized,* i.e., of the organic–inorganic composite materials.

References

[1] Petrovic, I.; Navrotsky, A.; Davis, M.E.; Zones S.I. *Chem. Mater.* **1993**, *5*, 1805.

[2] Patarin, J.; Soulard, M.; Kessler, H.; Guth, J.L.; Diot, M. *Thermochim. Acta* **1989**, *146*, 21.

Chapter Three

Thermochemistry of Pure-Silica Zeolites

Abstract

A series of pure-silica molecular sieves (structural codes AST, BEA, CFI, CHA, IFR, ISV, ITE, MEL, MFI, MWW and STT) is investigated by high-temperature drop solution calorimetry using lead borate solvent at 974 K. The enthalpies of transition from quartz at 298 K are: AST: 10.9 ± 1.2 kJ/mol, BEA: 9.3 ± 0.8 kJ/mol, CFI: 8.8 ± 0.8 kJ/mol, CHA: 11.4 ± 1.5 kJ/mol, IFR: 10.0 ± 1.2 kJ/mol, ISV: 14.4 ± 1.1 kJ/mol, ITE: 10.1 ± 1.2 kJ/mol, MEL: 8.2 ± 1.3 kJ/mol, MFI: 6.8 ± 0.8 kJ/mol, MWW: 10.4 ± 1.5 kJ/mol and STT: 9.2 ± 1.2 kJ/mol. The range of energies observed is quite narrow at only 6.8-14.4 kJ/mol above quartz, and these data are consistent with and extend earlier findings of Petrovic *et al.*[1] The enthalpy variations are correlated with the following structural parameters: framework density, non-bonded distance between Si atoms and framework loop configurations. A strong linear correlation between enthalpy and framework density is observed, implying that it is the overall packing quality that determines the relative enthalpies of zeolite frameworks. The presence of internal silanol groups is shown to result in a slight (≤2.4 kJ/mol) destabilization of the calcined molecular sieves by comparing calorimetric data for MFI and BEA samples synthesized in hydroxide (containing internal silanol groups) and fluoride (low internal silanol group density) media.

Introduction

During the past decade, interest in new inorganic materials with complex structures and their assembly mechanisms has increased.[2] An industrially useful class of materials is the zeolites that are porous, crystalline aluminosilicates that can act as molecular sieves for shape-selective adsorption and heterogeneous catalysis. These materials can be endowed with strongly acidic or basic sites in the pores by suitable modifications. Pure-SiO_2 zeolites, more properly termed pure-silica molecular sieves, are particularly interesting for practical applications because of their high temperature persistence and hydrophobic nature[3]. Despite the industrial importance of zeolites, their syntheses are still not well understood and typically rely on extensive series of trials that use different organocations (structure-directing agents, SDAs) and conditions to produce new framework structures.[4-7]

While purely thermodynamic data cannot answer questions about the kinetics of zeolite syntheses, knowledge of the energetics of different structures provides a framework for rationalizing the driving forces for synthesis, the differences amongst various structures, and the mechanisms and interactions important in the assembly of these materials.

All silica molecular sieves are metastable with respect to α-quartz, the thermodynamically stable polymorph at ambient conditions. Petrovic *et al.*[1]

obtained calorimetric data for six high-silica molecular sieves (structural codes[8] FAU, EMT, AFI, MEL, MFI, and MTW; all pure-silica except EMT) and found them to be energetically higher than quartz by only 7-14 kJ/mol, and higher than SiO_2 glass by only 0-7 kJ/mol. They argued that this very modest metastability presented no great hindrance to molecular sieve formation, and that the role of the structure-directing agent in hydrothermal syntheses was thus kinetic in nature (selection amongst configurations that in the pure state would have very similar energetics). Petrovic *et al.*[1] found no strong correlation between enthalpy (relative to quartz) and structural parameters such as framework density (number of tetrahedral atoms per nm^3, FD). Henson *et al.*[9] calculated lattice energies relative to quartz for a collection of 26 structures over a wide range of FD values and found a strong correlation between enthalpy and framework density for their calculated values. They also found a linear correlation between Petrovic's measured values and their calculated ones by ignoring the EMT data point. The work of Petrovic *et al.*[1] was limited in the variety and quality of materials available a decade ago. Indeed, neither one of their two low-framework density samples (FAU and EMT) was prepared as a pure-SiO_2 material by direct synthesis and the enthalpy values for these samples cannot be regarded as accurate as those for the more dense materials (AFI, MEL, MFI and MTW). These latter materials, however, cover only a very small range (FD = 17.8-19.4 Si atoms/nm^3) of framework densities.

To reach more definitive conclusions on the effect of various structural parameters on molecular sieve energetics, experimental thermodynamic data were needed for pure-SiO_2 materials *made from direct syntheses* and with FD smaller than 17.8. Fortunately, in the past few years, the use of fluoride instead of hydroxide as the mineralizing agent in zeolite syntheses has enabled the synthesis of pure-SiO_2 materials with lower framework densities (FD = 15.4-17.3) than the materials available to Petrovic *et al.*[10]

The enthalpy for the transition from quartz to molecular sieve, ΔH_{trans}^{298}, for the following pure-SiO_2 molecular sieves: AST (all-silica $AlPO_4$-16), BEA, CHA, IFR (ITQ-4), ISV (ITQ-7), ITE (ITQ-3), MWW(ITQ-1), is determined here in order to obtain thermodynamic data for structures with low FD values. As discussed above, this region of framework density (FD smaller than 17.8) was hitherto unexplored. Also the enthalpy for CFI (CIT-5) was measured, to determine whether energetics for such a large pore structure follow the trends seen for samples with smaller pore sizes; it was long believed that extra-large pore materials were hard to synthesize due to thermodynamic instability. Enthalpies for MFI and BEA samples synthesized both in fluoride and hydroxide media were investigated as well. While the fluoride materials are essentially free of internal silanol defects, the hydroxide materials contain such defects and are more typical of those used for industrial applications. From these samples, an estimate of the defect energetics can be obtained.

High-temperature drop solution calorimetry using lead borate solvent at 974 K is employed here to measure enthalpies of transformation from quartz with a standard error of ±1 to ±2 kJ/mol. The results and their implications with regard to the stability of the different frameworks, the correlations with framework structural features and comparisons with previously reported trends are presented.

Experimental Section

Samples

Unless noted otherwise, the SiO_2 source for the synthesis of all molecular sieves was tetraethoxysilane (TEOS). For BEA:F and BEA:OH the complete reaction mixture was formulated to the compositions specified below and the TEOS completely hydrolyzed before heating the synthesis gel. The ethanol generated by hydrolysis was removed by evaporation at room temperature. For AST, CFI, CHA, IFR, ISV and STT the reaction mixture omitting HF was formulated to the compositions specified below and the TEOS completely hydrolyzed before heating the synthesis gel. The ethanol generated by hydrolysis was removed by evaporation at room temperature and the HF added to the correct composition.

AST. The *t*-butyltrimethylammonium (TBTMA) mediated synthesis of pure-SiO_2 AST used a gel composition of 1 SiO_2: 0.5 TBTMAF: 13 H_2O.[12] After reaction at 423 K and autogeneous pressure for 6 days in a Teflon-lined stainless steel reactor that was rotated at 60 rpm, the product was collected by cooling the mixture to room temperature, filtering and washing with water, then acetone. The sample was calcined four times in air at 1223 K for 3 hours to remove the occluded organics.

BEA:F. The TEAF-mediated synthesis of pure-SiO_2 zeolite beta employed a reaction composition of 1 SiO_2: 0.5 TEAF: 7.25 H_2O.[13] In this synthesis, two rotary evaporations were performed to remove the ethanol formed by hydrolysis. The synthesis was conducted at 413 K and autogeneous pressure for 14 days in a Teflon-lined stainless steel reactor and the products were collected by cooling the mixture to room temperature, filtering and washing with water, then acetone. The sample was calcined at 823 K in air for 6 hours to remove the occluded organics. This sample will be denoted here as BEA:F to distinguish it from the hydroxide mediated sample of zeolite beta.

BEA:OH. For the trimethylenebis(*N*-methyl,*N*-benzylpiperidinium) hydroxide mediated synthesis of pure-SiO_2 BEA (BEA:OH), the gel composition was 1 SiO_2: 0.10 $R(OH)_2$: 35 H_2O where R is trimethylenebis(*N*-methyl,*N*-benzyl,piperidinium), synthesized as described previously.[14] After reaction at 408 K and autogeneous pressure for 9 days in a Teflon-lined stainless steel reactor, the

products were collected by cooling the mixture to room temperature, filtering and washing with water, then acetone. The sample was calcined in air at 873 K for 8 hours to remove the occluded organics.

CFI. A sample of pure-SiO_2 CFI was prepared from a gel composition of 1 SiO_2 : 0.50 TOH: 0.50 HF: 15 H_2O where T is the *N*-methyl-(-)-sparteinium cation.[15] After reaction at 448 K and autogeneous pressure for 4 days in a Teflon-lined stainless steel reactor with rotation at 60 rpm, the product was collected by cooling the mixture to room temperature, filtering and washing with water, then acetone. The sample was calcined in air at 923 K for 3 hours to remove the occluded organics.

CHA. For the *N,N,N*-trimethyladamantammonium mediated synthesis of pure-SiO_2 CHA, the gel composition was 1 SiO_2: 0.5 TMAdaF: 3 H_2O where TMAda is *N,N,N*- trimethyladamantammonium.[16] After reaction at 423 K and autogeneous pressure for 40 hours in a Teflon-lined stainless steel reactor that was rotated at 60 rpm, the products were collected by cooling to room temperature, filtering and washing with water and then acetone. The sample was calcined at 853 K for 3 hours in air to remove the occluded organics.

IFR. The *N*-benzyl-1-azoniumbicyclo[2,2,2]-octane mediated synthesis of pure-SiO_2 IFR utilized the gel composition 1 SiO_2: 0.50 $C_{14}H_{20}N^+OH^-$: 0.50 HF: 15 H_2O where $C_{14}H_{20}N^+$ is *N*-benzyl-1-azoniumbicyclo[2,2,2]-octane.[17] After reaction at 423 K and autogeneous pressure for 12 days in a Teflon-lined stainless

steel reactor rotating at 60 rpm, the products were collected by cooling to room temperature, filtering and washing with water and then acetone. The sample was calcined at 923 K for 3 hours in air to remove the occluded organics.

ISV. A sample of pure-SiO_2 ISV was prepared from a gel composition of 1 SiO_2 : 3 $C_{14}H_{26}NOH$: 3 HF : 1 H_2O where $C_{14}H_{26}N^+$ is 1,3,3-trimethyl-6-azoniumtricyclo[3.2.1.$4^{6,6}$] dodecane.[18] After reaction at 423 K and autogeneous pressure for 15 days in a Teflon-lined stainless steel reactor rotating at 60 rpm, the products were collected by cooling to room temperature, filtering and washing with water and then acetone. The sample was calcined in air at 853 K to remove the occluded organics.

ITE. Pure-SiO_2 ITE was prepared from a gel composition of 1 SiO_2 : 0.5 $C_{12}H_{24}NOH$: 0.5 HF :7.7 H_2O where $C_{12}H_{24}N^+$ is 1,3,3,6,6-pentamethyl-6-azoniabicyclo[3.2.1]octane[19]. After reaction at 423 K and autogeneous pressure for 19 days in a Teflon-lined stainless steel reactor rotating at 60 rpm, the products were collected by cooling to room temperature, filtering and washing with water. The sample was calcined in air at 853 K to remove the occluded organics.

MEL. Pure-SiO_2 MEL was produced from a gel of composition 1 SiO_2: 0.25 ROH: 0.05 KOH: 18 H_2O where R is *N,N*-diethyl-3,5-dimethylpiperidinium.[11] The silica source for this synthesis was Cab-O-Sil M-5. After reaction at 443 K in a rotating Teflon-lined stainless steel reactor, the product was collected by cooling

the mixture to room temperature, filtering and washing with water, then acetone. The sample was calcined in air at 873 K to remove the occluded organics.

MFI:F. For the TPA-mediated synthesis of pure-SiO_2 MFI in fluoride media (denoted MFI:F), the gel composition was 1 SiO_2: 0.44 TPAOH: 0.5 HF: 50 H_2O. The silica source for this synthesis was Cab-O-Sil M-5. After reaction at 448 K and autogeneous pressure for 5 days in a Teflon-lined stainless steel reactor, the products were collected by cooling to room temperature, filtering and washing with water then acetone. The sample was calcined in air at 823 K for 6 hours to remove the occluded organics.

MFI:OH. A sample of pure-SiO_2 MFI made with hydroxide as the mineralizer (denoted MFI:OH) was prepared from a gel of composition 1 SiO_2: 0.1 TPABr: 0.5 $C_4H_{10}N_2$: 50 H_2O where $C_4H_{10}N_2$ is piperazine. The silica source for this synthesis was Cab-O-Sil M-5. The gel was seeded with 0.6% MFI which had been previously prepared with tetrapropylammonium (TPA) ions as the SDA. After reaction at 423 K and autogeneous pressure for 8 days in a Teflon-lined stainless steel reactor, the products were collected by cooling to room temperature, filtering and washing with water then acetone. The sample was calcined in air at 823 K for 7 hours to remove the occluded organics.

MWW. Pure-SiO_2 MWW was made from a gel of composition 1 SiO_2: 0.25 TMAdaOH: 0.40 HMI: 44 H_2O where TMAda is *N,N,N*-trimethyl-1-adamantammonium and HMI is hexamethyleneimine.[20] The silica source for this

synthesis was Aerosil 200. After reaction at 423 K and autogeneous pressure for 17 days in a Teflon-lined stainless steel reactor rotating at 60 rpm, the products were collected by cooling to room temperature, filtering and washing with water, then acetone. The as-made sample was calcined in air at 853 K to remove the occluded organics and to produce the fully-connected three-dimensional framework.[20]

STT. For the $TMAda^+$ mediated synthesis of pure-SiO_2 STT, the gel composition was $1SiO_2$: 0.50TMAdaOH: 0.50HF: $15H_2O$.[21] After reaction at 423 K and autogeneous pressure for 30 days in a Teflon-lined stainless steel reactor, the products were collected by cooling to room temperature, filtering and washing with water, then acetone. The sample was calcined in air at 853 K for three hours to remove the occluded organics.

Before calorimetry the samples were pressed into approximately 15 mg pellets and dried in air overnight at 473 or 573 K to remove most of the absorbed water. All sample pellets were stored in an Ar-filled glove box prior to calorimetry.

Characterizations

Room temperature, powder X-ray diffraction (XRD) patterns were collected on a Scintag XDS 2000 diffractometer (liquid nitrogen cooled Ge

detector, Cu Kα radiation, λ=1.54184 Å) operating in a Bragg-Bretano geometry. The data were obtained in a stepwise mode with 2θ ranging from 2 to 51° (step size=0.01°, count time=4s) in order to identify the crystalline phases present before and after drying. Thermogravimetric analyses (TGA) were performed on 35-50 mg sample using a Netzsch STA409 system to measure the mass fraction of water present in the samples introduced into the calorimeter. The heating rate was 10 K/min to 1473 K and dry Ar was used as the carrier gas to avoid sample rehydration. Buoyancy corrections were performed for all runs by allowing the sample to cool down to room temperature and heating it back to 1473 K. Alternatively, the measurement was performed on approximately 15 mg samples using a Dupont 2100 instrument. The heating rate was 10 K/min to 1173 K and the buoyancy correction was based on a run with 15 mg Pt.

Solid-state ^{29}Si NMR spectra for the BEA:OH and MFI:OH samples were collected on a Bruker AM300 spectrometer equipped with a Bruker cross-polarization, magic angle spinning (MAS) accessory. The samples were packed into 7mm ZrO_2 rotors and spun in air at 4 kHz . Proton-decoupled ^{29}Si NMR spectra (59.63 MHz) referenced to tetrakis(trimethylsilyl)silane (downfield peak at δ= -10.053 ppm) were collected using MAS. The results were analyzed with the Tecmag MacFID software; simulations using Gaussian lines were carried out to estimate the defect density (Q_3 /Q_4 ratio).

The adsorption capacity of the BEA:OH sample for cyclohexane was measured at room temperature using a McBain-Bakr balance. The C_6H_{12} vapor was delivered from the liquid phase. The microporous volume was determined at a relative vapor pressure P/P_0 of 0.33. Prior to the adsorption experiment, the sample was dehydrated at 473 K under a vacuum of 10^{-3} Torr for 2 hours. The adsorption capacity is reported in milliliters of liquid per gram of dry zeolite, assuming bulk liquid density for the adsorbate in the micropores.

Calorimetry

Drop solution calorimetry was employed to obtain the heats of solution of the molecular sieves. In each experiment, the sample pellet was dropped from room temperature into the molten $2PbO{\cdot}B_2O_3$ solvent in the calorimeter at 973 K. SiO_2 is well known to be soluble in lead borate, so the same final state is obtained for all molecular sieves upon dissolution.[1] A quartz sample (Fluka, 99.5%) was used in addition to the molecular sieves so that the enthalpy for the transition **quartz (298 K) → molecular sieve (298 K),** ΔH^{298}_{trans}, could be obtained by difference. All thermochemical measurements were performed using a Tian-Calvet twin microcalorimeter that has been described in detail elsewhere[22] and operating under flowing Ar to assist in the removal of any water vapor. The calibration

factor for the calorimeter (J/μV) was obtained by dropping ~15 mg pellets of alumina (Aldrich, 99.99%) stabilized in the corundum phase by heating overnight at 1773 K. The overall methodology is now standard and has been described previously.[1,23,24]

Results

Characterization

The X-ray powder diffraction (XRD) patterns indicated the presence of a single molecular sieve phase for each sample. All powder patterns except for BEA:OH displayed sharp peaks and were in excellent agreement with published data (AST,[12] BEA,[13] CFI,[25] CHA,[16] IFR,[17] ISV,[18] ITE,[19] MEL,[26] MFI,[27] MWW,[20] STT[28]). For the BEA:OH sample, repeated attempts to completely remove the large, bulky organic SDA without degrading the XRD pattern, e.g., calcinations at lower temperature, extractions, were unsuccessful. This is a common problem for pure-silica zeolite beta prepared in hydroxide media. To quantify the degree of structural damage, cyclohexane adsorption was performed on the BEA:OH sample calcined in air at 873 K. The adsorption capacity for cyclohexane with this material

was found to be 0.24 mL/g and compares favorably to literature data.[29] Thus, the structure is not significantly collapsed by the calcination procedure.

For all materials other than BEA:OH, the crystal sizes were larger than 1 μm. For particles larger than 1 μm, surface energy effects do not significantly affect the measured energetics[1]; hence, they were neglected in this work.

The TGA results are shown in Table 3.1, along with the calculated molar mass (per mol SiO_2) and water contents. The amount of water present in the dehydrated samples was calculated by taking the difference of the mass losses at 1373 or 1073 K and at the dehydration temperature of 473 or 573 K. The water contents are typically below 1% for all the materials synthesized in fluoride media, indicating successful dehydration. These water contents are non-zero, however, because only a partial dehydration is carried out by heating to 473-573 K; treatment at higher temperatures could have achieved complete dehydration, but with the possible risk of damaging the molecular sieve frameworks, at least for the hydroxide mediated samples. Two of the materials synthesized using hydroxide ions as the mineralizer (BEA:OH and MWW) contain slightly larger amounts of water (0.5-2.0%) as expected due to the hydrophilic nature of their defect sites (see below). The calorimetry experiments with MWW were performed on the air-exposed material since the mechanical properties of the pellets prepared from the oven-dried material were poor and the pellets could not be made to retain their

shape. This fact further explains the higher (1.8%) amount of water in this material.

The ^{29}Si solid-state NMR spectra of the MFI:OH and BEA:OH samples confirmed the presence of Q_3 (defect) Si sites in both samples (peak below –105 ppm). A quantitative deconvolution into Gaussian lineshapes carried out with the MacFID software gave Q_3/Q_4 ratios of 0.43 for BEA:OH and 0.041 for MFI:OH. The corresponding percentages of silicon present as Q_3, denoted here as Si_d, are Si_d = 29.9% (BEA:OH) and 4.0% (MFI:OH). The unusually low defect site density for the MFI:OH sample is undoubtedly due to the use of piperazine as the SDA. The mass losses corresponding to complete annealing of the defect sites calculated from these Si_d values are 0.37% and 0.02%, respectively. Since the TGA mass losses are comprised of both (possibly incomplete) annealing and the loss of water bound in molecular form, the TGA losses are expected to be higher than those calculated from the ^{29}Si NMR data. Indeed, the TGA mass losses for the BEA:OH and MFI:OH are 0.93% and 0.37% respectively, so the ^{29}Si NMR and TGA data are consistent.

Enthalpies of Transition (quartz → molecular sieve), ΔH_{trans}^{298}

The enthalpies of transition for the reaction **quartz → molecular sieve** at 298 K were calculated by taking the difference between the heats of drop solution for quartz and the molecular sieve. The following thermodynamic cycle was used to determine the energetics of the molecular sieve frameworks, where MS is a generic designation for any of the molecular sieve frameworks and h is the number of moles of water present per mole of SiO_2:

(1) SiO_2 (soln, 974) + hH_2O (g, 974) → MS·hH_2O (s, 298)

(2) H_2O (l, 298) → H_2O (g, 974)

(3) SiO_2 (α-quartz, 298) → SiO_2 (soln, 974)

Adding these equations yields ΔH_{trans}^{298} for the formation of MS from α-quartz:

(4) SiO_2 (α-quartz, 298) + hH_2O (l, 298) → MS·hH_2O (s, 298)

where $\Delta H_4 = \Delta H_1 + h\,\Delta H_2 + \Delta H_3 = \Delta H_{trans}^{298}$.

The enthalpies ΔH_1 and ΔH_3 are the experimentally measured heats of drop solution for the molecular sieves and quartz, respectively: ΔH_2 was obtained from a linear interpolation of the water enthalpies at 900 and 1000 K to 974 K (from ref. 30), giving 70.85 kJ/mol H_2O. The ΔH_2 contribution to the overall transition enthalpy represents the heat required to completely vaporize and heat the residual amount of water in the dehydrated molecular sieves from 298 K to the calorimeter

operating temperature of 974 K. This correction assumes that the residual H_2O present is energetically the same as liquid water; that is, any enthalpy of hydration of the framework is neglected. Hu *et al.*[31] measured enthalpies of hydration for microporous $AlPO_4$ materials and reported values of –12 kJ/mol relative to liquid water. The pure-SiO_2 molecular sieves are more hydrophobic than the aluminum phosphates. Therefore, it is likely that they interact less favorably with water leading to enthalpies of hydration less negative than –12 kJ/mol. Indeed, the enthalpy of hydration for pure-silica, defect-free zeolite BEA has been shown to be small compared to the heat of vaporization of water[32] and this is expected to be true for all defect-free, hydrophobic samples. To estimate the impact of nonzero hydration energetics on the ΔH_{trans}^{298}, enthalpy of transition values assuming both an enthalpy of hydration of -10 kJ/mol (slightly less exothermic than the value for the $AlPO_4$ materials) and an enthalpy of hydration of 10 kJ/mol (an endothermic, physically unreasonable overestimate) were calculated in addition to the ΔH_{trans}^{298} values derived from a zero enthalpy of hydration.

Measured calorimetric data and calculated enthalpies of transition are shown in Tables 3.2 and 3.3. Table 3.3 lists the transition enthalpy ΔH_{trans}^{298}, for each molecular sieve with the associated standard error that includes and neglects the ±10 kJ/mol hydration enthalpies as discussed above. The 95% confidence intervals were calculated as $\sigma_{95} = \frac{1.96}{N-1}\sqrt{\sigma_1^2 + \sigma_3^2 + (10h)^2 + 0.7^2}$ where σ_1 and σ_3 are the standard deviations for ΔH_1 and ΔH_3, respectively and the third and fourth

terms account for the uncertainty in the nonzero water interaction energy (± 10 kJ/mol) and TGA mass loss, respectively. An uncertainty of approximately 0.7 kJ/mol due to TGA errors was calculated by a propagation-of-errors approach assuming an estimated mass loss uncertainty of ± 0.3%. N is the number of drop solution measurements for each sample.

Discussion

Enthalpies of Transition, ΔH_{trans}^{298}

The measured drop solution enthalpies for quartz are within experimental error of the previous value[33] of 39.1 ± 0.3 kJ/mol. Furthermore, the measured value for MEL (8.2 ± 1.3) is in good agreement with the previously measured value of 8.2 ± 1.0 kJ/mol.[1] Since the measured ΔH_{trans}^{298} values of MEL and MFI:OH are essentially identical (8.2 and 8.0 kJ/mol), the presence[11] of MFI intergrowths in the previously synthesized MEL sample cannot have significantly affected the reported enthalpy.[1] The MFI:F value of 6.8 ± 0.8 kJ/mol is also close to the previously reported 8.2 ± 0.8 kJ/mol.[1] The range of ΔH_{trans}^{298} values for the molecular sieves studied here is 6.8–14.4 kJ/mol; in good accord with a similar

range (7-14 kJ/mol) reported by Petrovic *et al.*[1] The uncertainty in ΔH_{trans}^{298} is 1-1.5 kJ/mol, typical of this class of calorimetry experiments.[22]

The contribution of the water vaporization to the enthalpies ($h\Delta H_2$) is below 1.6 kJ/mol for all samples synthesized in fluoride media since they contain less than 0.6% water (see Table 3.3). For the fluoride samples, the water contribution amounts to no more than 20% of the total enthalpy measured. For the samples synthesized in hydroxide media, the water correction takes on generally higher values since the solids contain more water. For MEL and MFI:OH, this correction is only 0.87 kJ/mol, but with MWW and BEA:OH, the corrections are 4 kJ/mol. The enthalpies of these last two samples, therefore, are somewhat more uncertain than the other enthalpies reported here.

The ΔH_{trans}^{298} values calculated with ±10 kJ/mol hydration enthalpies do not differ significantly from the ΔH_{trans}^{298} values that ignore this contribution (see Table 3.3): the discrepancy is less than 0.2 kJ/mol for all fluoride-synthesized samples. For the hydroxide-synthesized samples, the discrepancy is larger (up to 0.5 kJ/mol for MWW), but still well within the reported uncertainties. The assumption that the water behaves as liquid water, therefore, does not significantly impact the final enthalpy values and trends. For the remainder of these discussions, the values calculated assuming that the physically adsorbed water behaves as bulk liquid water will be used. The data for BEA:F and MFI:F must be considered the most accurate determination of the BEA and MFI framework enthalpies since they

consist of a SiO_2 framework with very low silanol defect densities. For further discussion see the defect energetics section below. Before undertaking a closer study of the correlation between structure and energetics, some general remarks are in order.

This study focuses on determining ΔH_{trans}^{298} for a set of molecular sieves with significantly different frameworks (lower density for pure-SiO_2 materials, larger and different ring sizes) than those examined in earlier studies.[1] Notwithstanding this wider range of structural features, the enthalpies of the molecular sieves studied here still fall within the same narrow range of enthalpies of 6.8-14.4 kJ/mol less stable than quartz. Pure-silica molecular sieves are therefore energetically quite close to quartz. This is also true for CFI which, despite its pores of 14-membered rings, is only 8.8 kJ above quartz. The enthalpy for STT also falls in this range and shows that frameworks comprised of seven and nine membered rings (7 and 9 MR), extremely rare in zeolites and only found in STT amongst pure-silica materials, do not display unusual energetics. Thus, there appears to be nothing intrinsically unstable in frameworks containing 7 and 9 MR despite their scarcity among zeolites. The same conclusion has been reached from lattice energy minimizations of the STT structure using the program GULP,[34] although the calculated enthalpy of STT relative to quartz (13.85 kJ/mol) was larger than the experimental one.[28] The systematic tendency of the GULP calculations to overestimate pure-silica molecular sieve enthalpies was already

evident in the early work by Henson *et al.*[9] Most SiO_2 molecular sieves currently known have structural features (pore sizes and framework densities) that fall within the range of those molecular sieves for which the enthalpies have now been determined.[1,8] We conclude that ΔH_{trans}^{298} values for all SiO_2 molecular sieves presently known can be expected to lie within a narrow region at approximately 6.8–14.4 kJ/mol less stable than quartz.

Defect Energetics

A comparison of the ΔH_{trans}^{298} values for the samples of MFI and BEA synthesized in both hydroxide and fluoride media gives higher values for the hydroxide samples. Despite the limited number of data points available, the presence of silanol defects is shown to have a slight destabilizing effect (1.2 kJ/mol for MFI, 2.4 kJ/mol for BEA). Since zeolite BEA is well-known to have the largest number of defects of all pure-silica molecular sieves, these results place an upper bound of 2.4 kJ/mol on the energetic effect of the defects for any crystalline silica phase. This value is smaller than the observed total range of enthalpies for the silica molecular sieves, so for these materials the presence of defects does not significantly alter the relative energetics of the various frameworks.

Finally, note that among pure-SiO_2 molecular sieves prepared in hydroxide media, BEA is known to contain the largest numbers of defect sites so the MEL

and MWW ΔH_{trans}^{298} values are assumed to be good indications of the corresponding idealized framework enthalpies despite the fact that the samples were synthesized in the presence of OH- ions. MWW, in particular, is known to have a large concentration of defects in the as-made layered form, but the large majority of these anneal upon calcination to produce the 3-D framework.[20]

Implications for Zeolite Synthesis

The ΔH_{trans}^{298} values of pure-silica molecular sieves are shown here to be 6.8-14.4 kJ less stable than quartz. The enthalpies of amorphous silicas derived from gels lie in the same energetic region as the molecular sieve enthalpies (the former are 0-10 kJ/mol less stable[35,36] than silica glass which is itself 9.1 kJ/mol less stable than quartz[31]) so the formation of pure-SiO_2 molecular sieves from amorphous precursors is not appreciably hindered on enthalpy grounds. In fact, for the most stable molecular sieves ($\Delta H_{trans}^{298} \leq 9.1$ kJ/mol), the **amorphous** $\rightarrow$ **molecular sieve** transformation is even exothermic by at least 0-2.5 kJ/mol. The entropies of the amorphous species, however, are necessarily higher than those of the crystalline, *ordered* molecular sieves, so whether ΔG will favor the amorphous or crystalline phases is not certain. In any event, the magnitude of ΔG for the **amorphous** $\rightarrow$ **molecular sieve** transformation is clearly quite small. Since the available thermal energy at the typical synthesis temperature of 373 K is RT=3.1

kJ/mol all pure-SiO_2 molecular sieve frameworks are within twice the available thermal energy (2RT= 6.2 kJ/mol) of each other and are not significantly less stable than quartz. Further, even mesoporous silicas such as the MCM-41 materials have been shown to be no more than 14-15 kJ/mol less stable than quartz. Thus, they must be considered to lie in the same general enthalpy region even though their pore sizes and molar volumes are several times larger than even the most porous molecular sieve.[37] Therefore, there are no large thermodynamic barriers to the interconversions among the many polymorphs of SiO_2.

The narrowness of the enthalpy range covered by different frameworks undoubtedly explains the multiplicity (around 30) of known SiO_2 polymorphs.[8] Indeed, similar energetics are expected for other isocompositional classes of dehydrated microporous materials, e.g., the $AlPO_4$ materials.[31] The role of the structure-directing agent cannot then be to help stabilize otherwise very unstable structures, but rather to form organic-inorganic composites that select one set of structures over another. The presumably exothermic nature of the interaction to form such organic-inorganic composites can be invoked to explain the preferential formation of ordered porous frameworks over amorphous silicas in molecular sieve syntheses, even though the amorphous silicas would be expected to be favored on entropic grounds.

More instructively, perhaps, the self-assembly of the various silica polymorphs can be understood by considering the organic species present in the synthesis gel or solution. These organic species participate in three essentially

different types of interactions: organic-organic (O-O), organic-inorganic (O-I), and organic-water (O-W) interactions. The relative strengths of these three interactions presumably determine the kind of structure that the self-assembly process will yield. If sufficiently strong O-O attractive interactions are present, organized organic structures are formed. These structures, in turn, may be able to organize the water and silicate species around themselves, leading to structures with large pores due to the relatively large size of the O-O aggregates. A typical example is the synthesis of mesoporous materials using surfactants as the SDAs. If the O-I interactions predominate, precursors to molecular sieves with the organic and inorganic species in intimate contact can form. In this case, crystalline materials can result after self-assembly; because of the intimate O-I contact, they are typically porous, i.e., they are molecular sieves. If neither O-O nor O-I interactions are sufficiently strong to lead to ordered structures, there is no opportunity to form either micelles or precursors to molecular sieves. In such cases, either amorphous or dense materials are synthesized, probably depending in large part on the general conditions (pH, temperature, silica concentration and synthesis time). A schematic representation of these various processes is shown in Figure 3.1. While this mechanism does not explicitly include the energy contribution of removing water from the hydrophobic hydration sphere around the organic to replace it with silicate species, the relative magnitudes of the O-I and O-W interactions discussed above determine the energetics of the replacement process.

Relationship between Structure and Energetics

Previous studies reported no strong correlation between enthalpies and framework structure. Petrovic *et al.* attempted to correlate enthalpies of formation with both framework density and mean Si-O-Si angle without success.[1] *Ab initio* calculations[38] suggest that while large Si-O-Si angles (for reference, the angle is 143.6° for quartz, while it ranges from 132 to 179° for molecular sieves) do not appreciably destabilize these structures, angles below about 135° will do so. A weak correlation between the overall enthalpy and the fraction of Si-O-Si angles below 140° was indeed found by Petrovic *et al.*[1] by ignoring the data for the dense phases that did not fit within the trend. As discussed above, these findings suffered from the relative narrowness of the density range for which pure-silica molecular sieves could be prepared. The later work by Henson *et al.*[9] reanalyzed the experimental values of Petrovic *et al.*[1] and concluded that after ignoring the EMT data point, they showed a dependence of ΔH_{trans}^{298} on the framework density. Henson *et al.*[9] presented theoretical calculations for additional structures that confirmed this trend. Having more than doubled the number of molecular sieves for which experimental ΔH_{trans}^{298} values are available, we are now in a better position to determine how well the enthalpies and FD correlate. The FD values considered in this paper are those derived from the structural data available for the calcined silica materials. These values may differ significantly from the values

collected in ref. 8 (corresponding to the "Type Materials," which frequently are high alumina zeolites or aluminophosphates) or from the FD_{Si} values in ref. 8 (derived from the DLS minimized silica structure).

The structural and thermodynamic data for all tetrahedrally coordinated SiO_2 polymorphs for which ΔH_{trans}^{298} values have been experimentally determined are listed in Table 3.4 with the respective references. In addition to the molecular sieves, data for the dense phases cristobalite (cr), tridymite (tr), coesite (co) and moganite (mo) are included. Data for the dense phase stishovite is not included since its Si coordination is not tetrahedral, but rather octahedral. The EMT data measured by Petrovic *et al.*[1] have also been excluded due to the relatively high (Si/Al=14.5) Al content. Crystal structures derived from single-crystal studies are available for FER and quartz and must be considered more reliable than those for the other frameworks that were obtained by refinements of powder data (except for MFI: it was not powder but it was a "twin crystal" with one twin much smaller than the other, and the overlapping reflections from both twins were treated mathematically to derive the "true" intensities for the larger twin). This point is relatively unimportant for bulk parameters, such as the framework density and molar volume. The δ parameter discussed below, however, is much more sensitive to atomic configuration and its precision is affected by uncertainties in the crystal structure accordingly.

Framework Density and Molar Volume. Figures 3.2 and 3.3 show the relationship between the ΔH_{trans}^{298} values and the FD and molar volume, respectively. It is evident from the heat content data of Petrovic *et al.*[1] that the relative enthalpies of empty pure-silica molecular sieves are very insensitive to temperature. Trends observed for ΔH_{trans}^{298} values should be closely followed at other temperatures, such as the 373-473 K range of interest in zeolite synthesis. The data in Figure 3.2 clearly exhibit a roughly linear correlation between the ΔH_{trans}^{298} values and the framework density for FD ≤ 26.55 (quartz). Such a trend can be understood in terms of a "quality of packing" argument: in the molecular sieves, the creation of void volumes is only possible with an associated energetic cost corresponding to the inherent instability of the Si atoms that are prevented from collapsing into the void spaces. As the density increases (eliminating void volume) the silica polymorphs become progressively more stable until the most stable structure (quartz) is reached. Further increases in density lead to unfavorable compression, explaining the unstable nature of coesite. The only structure for which the enthalpy differs significantly from the trend above is mo: its relatively high ΔH_{trans}^{298} (3.4 kJ/mol) cannot be rationalized on the basis of FD since it has almost exactly the same density as quartz. The enthalpy of moganite was not obtained by a direct measurement, but rather by extrapolating measured enthalpies of mo-q intergrowths with varying mo contents to 100% mo.[50] Hence the reported ΔH_{trans}^{298} cannot be considered to be as reliable as those for the other silica

polymorphs. Furthermore, the Si-O-Si bonds in mo are more strained than in q; in particular, 4-membered Si rings are present in mo but not in quartz. Because of the tighter packing, dense silica phases generally have less room for the atoms to rearrange away from the optimal (quartz) configuration than with higher void volumes (molecular sieves). Hence the destabilizing effect of bonding distortions is expected to be the largest for the most dense phases. This observation most likely explains the higher than expected enthalpy of mo and the corresponding departure of the mo data point from the general trend.

The data in Figure 3.3 show the trends in the ΔH_{trans}^{298} versus the molar volume of the various silica phases. Since molar volume is inversely proportional to FD, a good correlation is observed between the enthalpies and molar volume. For predictive purposes, a linear regression of the ΔH_{trans}^{298} and molar volume data was performed for the phases less dense than quartz and the results give ΔH_{trans}^{298} =(-10.1 ± 1.9) + (0.55 ± 0.06)V_m where V_m is the molar volume in cm^3/mol. The molar volume was chosen for the regression rather than the framework density because it allows the regression results to be extended to structures without a regularly repeating framework. Quartz is thermodynamically required to represent a minimum in the enthalpy vs. molar volume curve. The coesite data was thus excluded from the correlation since co is a denser, yet less stable phase than quartz. Table 3.5 compares the predicted and experimentally measured ΔH_{trans}^{298} values. The calculated value is typically within less than 2 kJ/mol

of the experimentally measured ΔH_{trans}^{298}, i.e., the error in the predicted value is only slightly larger than the uncertainty in the measurement itself. Clearly, this empirical correlation is useful to interpolate the enthalpies of transition for other silica phases whose molar volumes are between those of q (22.71 cm^3/mol) and FAU (44.77 cm^3/mol).

For SiO_2 polymorphs less dense than FAU, the above correlation does not lead one to expect large framework instabilities. Recall that the MCM-41 mesoporous materials (admittedly not crystalline) are much less dense than even the most porous molecular sieve, yet have enthalpies of only 14-15 kJ/mol above quartz. This observation suggests that the linear molar volume-ΔH_{trans}^{298} trend may plateau at high molar volumes (low FD values) as has already been observed for the $AlPO_4$ materials.[31] Therefore, very porous materials cannot be sufficiently unstable for their syntheses to be ruled out based on framework thermodynamics. As pointed out by Davis,[53] a purely physical limitation in zeolite syntheses is that the crystal must not float in order for its growth to take place at an appreciable rate in an aqueous system. This restriction does not exclude the formation of frameworks considerably less porous than the ones currently known.[53] The difficulty in synthesizing silica polymorphs with FD $\leq$ FD (FAU), so far, defies explanation.

Above, the enthalpies have been shown to correlate well with the packing parameters FD and molar volume. These parameters are easy to obtain and are not

very sensitive to uncertainties in the crystallographic structure solution. They do not, however, provide significant insight into the nature of the interactions affecting porous silica energetics: in other words, what is the atomic/molecular origin of the destabilization relative to quartz of the silica molecular sieves? To address this issue, we attempted to explore whether other parameters that are based on crystal chemistry concepts would correlate well with the ΔH_{trans}^{298} values.

O'Keeffe noted that crystallographic evidence shows that for an element in a lattice such as Si in four-coordinated SiO_2, there is an optimal Si-Si distance below which electrostatic repulsion becomes excessive.[54] He therefore suggested correlating framework energetics with non-bonded distances, i.e., the distances between non-neighboring atoms. To examine the effect of such non-bonded distances on the framework energetics, we defined a parameter, δ, as the average absolute value of the deviation from the Si-Si distance in quartz (3.0568Å, calculated from the data in ref. 39 and taken as the optimum non-bonded distance for this class of materials):

$$\delta = \frac{\sum_{i=1}^{N}\sum_{j=1}^{4} | d(Si_i - Si_j) - 3.0586 |}{4N}$$

where $d(Si_i\text{-}Si_j)$ is the distance from Si atom *i* to each of its four neighbors *j* and N is the total number of Si atoms per unit cell. No δ value was calculated for the BEA since its structure is faulted and no single meaningful average non-bonded distance can be defined.

The δ parameter is a *local* measure of the atomic configuration in direct contrast to the *global* description afforded by the framework density FD. An even more local description is given by the loop configuration (defined in the *Zeolite Atlas*[8] as a collection of graphs showing how many 3- or 4- membered rings each type of T atom in a given framework is residing within). The determination here of thermodynamic data for a much more varied collection of silica polymorphs than previously available permitted a conclusive examination of the quality of the correlation between ΔH_{trans}^{298} and both of these structural parameters.

Non-Bonded Distances. The correlation between ΔH_{trans}^{298} and the δ parameter as illustrated by Figure 3.4 is much weaker than the correlation between ΔH_{trans}^{298} and the simple structural parameters FD and molar volume. While the dense phases that are relatively close in enthalpy to quartz all have low δ values, two of the most unstable silica phases, CHA and FAU, have δ values in the same range (0–0.04 nm). Conversely, the structures with the largest distortions (AST and especially STT) are not the most unstable polymorphs. The structures in the middle δ region ($0.04 \leq \delta \leq 0.08$) show no clear trend either. Rather, the enthalpies appear to plateau at slightly above 10 kJ/mol for high values of δ. This observation is at variance with the expected physical behavior: namely, the progressive destabilization with increasing δ until the frameworks become so strained that they cannot form under any condition. A comparison between Figures 3.3 and 3.4 conclusively shows that the ΔH_{trans}^{298} values correlate much better with

the molar volume than with δ. Local distortions of the framework, then, do not uniformly determine structural enthalpies; indeed, the large flexibility of T-O-T bonds is traditionally invoked to explain the large number of silica polymorphs that can be synthesized.

Loop Configuration. The loop configuration is a graph representing the number of 3- and 4- membered rings (3,4 MR) each type of T atom in a framework is residing within. Currently known zeolites and related materials exhibit 12 different types of loop configurations and they are shown in Figure 3.5. Calculations predict that 3,4 MR are less stable than six-membered rings (6MR) by approximately 2.8 (3MR) and 1.1 (4MR) kJ/mol.[55] Five-membered rings, by contrast, are only slightly (0.08 kJ/mol) destabilized relative to 6MR.[55] The frameworks whose T atoms are mostly bonded within multiple 3,4 MR, then, are expected to be less stable than structures devoid of them. Table 3.6 lists the fractions, f, of T atoms engaged in the various loop configuration types for each silica phase for which enthalpy data are available. Six of the twelve possible loops are represented, and the frameworks contain from 0% 3,4 MR (q, tr, cr, FER) up to 100% loops containing three 4MR (CHA, FAU). Unfortunately, no pure-SiO_2 material with 3MR has yet been prepared by direct synthesis so only the effect of 4MR will be examined here. The molecular sieves that consist mostly ($f_0 + f_1 \geq$ 75%) of zero or only one 4MR (AFI, MTW, MFI, MEL, FER and CFI) are the most stable frameworks: they all have $\Delta H_{trans}^{298} \leq 8.8$ kJ/mol. Conversely, the

structures that contain mainly ($f_{3A}+f_{3B} \geq 50\%$) triple 4 MR (CHA, ISV, FAU, AST) are the least stable frameworks, with $\Delta H_{trans}^{298} \geq 10.8$ kJ/mol. The presence of large fractions of multiple 4MR, then, seems to lead to a destabilization of the framework. When the dense phases are examined as well, however, the trend becomes less evident: q, tr and cr have the same loop configuration as FER, yet are up to 6.6 kJ/mol more stable. Further, coesite consists solely of loops containing two 4MR , yet it is only 2.9 kJ/mol less stable than quartz.

To evaluate these data more quantitatively, a linear regression was performed to fit the enthalpy data to the distribution of loop types, according to $\Delta H_j = e_0 + \sum_{i \neq 0} e_i f_{ij}$ where f_{ij} is the fraction of loop type i present in structure j and e_i is the energetic contribution of loop type i (to be determined). Since only 20 data points are available to determine 5 parameters, the results must be interpreted with caution; Table 3.7 lists the e_i coefficients with their associated standard errors while Table 3.8 compares the calculated enthalpy from this relation, ΔH_j, to the measured ΔH_{trans}^{298}. A comparison between the data in Tables 3.5 and 3.8 clearly shows that the correlation based on molar volume is much more accurate in its ΔH_{trans}^{298} predictions than the loop configuration correlation, despite the much larger number of independent variables in the latter. In particular, the loop configuration correlation severely overestimates the enthalpies of transition of the dense phases. This systematic error is due to the fact that the loop descriptions for the most stable molecular sieves and the dense phases q, tr and cr are quite similar (f_0 >

0.70), even though there are significant enthalpy differences between the two groups.

In summary, the data presented here for low-FD, directly synthesized, SiO_2 phases show that ΔH^{298}_{trans} correlates well with the molar volume (or, equivalently, the FD) of SiO_2 polymorphs. This correlation expresses the effect of the overall quality of packing on the framework enthalpies. The new data conclusively discredit any correlation between ΔH^{298}_{trans} and the non-bonded parameter δ. While large fractions of Si atoms involved in 4MR result in less stable structures, the quantitative correlation between ΔH^{298}_{trans} and loop configuration is not very good. This is especially true for the dense phases where the enthalpies of the 4MR-containing phases coe and mo are severely overestimated. Finally, the enthalpies for the large number of high quality SiO_2 polymorphs reported here conclusively show the class of crystalline SiO_2 materials lie within a narrow range and are not dramatically destabilized from quartz.

Conclusions

The enthalpies of transition for a series of pure-SiO_2 molecular sieves with varied structural features (low density, large rings) have been determined by drop solution calorimetry in lead borate at 974 K. All samples in this study have enthalpies in a narrow range 6.8-14.4 kJ/mol less stable than quartz and are in excellent agreement with previously reported values. This range (7.6 kJ/mol) is comparable to twice the available thermal energy (6.2 kJ/mol) at typical synthesis conditions. All known tetrahedrally coordinated SiO_2 polymorphs, then, are only slightly metastable with respect to quartz. This low barrier to transformation explains the large diversity (around 30 structures) of SiO_2 polymorphs. Furthermore the role of the organic structure-directing agents used in zeolite synthesis cannot be the stabilization of otherwise very unstable structures. They may, however, stabilize one structure at the expense of others by forming inorganic-organic composites.

The pure-SiO_2 molecular sieve enthalpies correlate well with molar volume and framework density but rather poorly with non-bonded Si-Si distances and loop configuration. The overall quality of packing of the SiO_4 tetrahedra is thus the most important parameter affecting the framework stability. Finally, the presence of silanol defect groups has been shown to slightly raise the enthalpies of transition relative to quartz when compared to the low-defect density frameworks.

Acknowledgments

Financial support for this work was provided by the Chevron Research and Technology Co. The calorimetric studies were supported by NSF grant DMR 97-31782. PMP thanks Katsuyuki Tsuji for providing one of the samples used in this study, and Michael Gordon (Caltech) for helping in the design of sample transfer vessels. Comments by Dr. Stacey I. Zones (Chevron) are appreciated.

Table 3.1. Results from Thermogravimetric Analysis of Silica Materials

Sample	%mass loss TGA (wt)	mol H_2O Per mole SiO_2	MW per mole SiO_2
Quartz	0.27	0.009	60.25
MEL	0.38	0.013	60.31
MWW	1.8	0.061	61.19
IFR	0.55	0.018	60.42
ITE	0.42	0.014	60.34
AST	0.39	0.013	60.32
STT	0.42	0.014	60.34
CHA	0.66	0.022	60.48
BEA:F	0.12	0.004	60.16
MFI:F	0.06	0.002	60.12
CFI	0.59	0.020	60.44
ISV	0.05	0.002	60.12
BEA:OH	0.93	0.031	60.65
MFI:OH	0.37	0.012	60.31

Table 3.2. Measured Calorimetric Data

Sample	$\Delta H_{dropsol}$ (J/mg)	Stdev (J/mg)	Number of data points	Error (95% c.i.) (J/mg)	$\Delta H_{dropsol}$ Uncorrected (kJ/mol SiO_2)	$\Delta H_{dropsol}$ 95%c.i. (kJ/mol SiO_2)
Quartz	0.6765	0.0199	9	0.0138	40.76	0.83
MEL	0.5442	0.0144	6	0.0126	32.82	0.76
MWW	0.5561	0.0104	4	0.0118	34.03	0.72
IFR	0.5194	0.0054	4	0.0061	31.38	0.37
ITE	0.5144	0.0092	6	0.0081	31.04	0.49
AST	0.5005	0.0078	6	0.0069	30.19	0.41
STT	0.5291	0.0098	6	0.0086	31.93	0.52
CHA	0.5003	0.0163	5	0.0159	30.26	0.96
BEA:F	0.4921	0.0056	7	0.0045	29.60	0.27
MFI:F	0.5317	0.0034	6	0.0030	31.96	0.18
CFI	0.5160	0.0031	7	0.0025	31.19	0.15
ISV	0.4170	0.0144	7	0.0116	25.07	0.69
BEA:OH	0.4808	0.0060	8	0.0044	29.16	0.27
MFI:OH	0.5219	0.0046	7	0.0037	31.48	0.22

Table 3.3. Calculated Calorimetric Data (all data in kJ/mol SiO_2)

Sample	Water correction	$\Delta H_{dropsol}$ corrected	ΔH^{298}_{trans}	ΔH^{298}_{trans}	$\Delta H_{dropsol}$ corrected	ΔH^{298}_{trans}	$\Delta H_{dropsol}$ corrected	ΔH^{298}_{trans}
				95% c.i.	With 10 kJ/mol hydration		With -10 kJ/mol hydration	
Quartz	0.64	40.12	0.00	N/A	40.21	0.00	40.03	0.00
MEL	0.90	31.92	8.19	1.34	32.05	8.16	31.80	8.23
MWW	4.33	29.70	10.42	1.45	30.31	9.90	29.08	10.94
IFR	1.31	30.08	10.04	1.17	30.26	9.95	29.89	10.14
ITE	1.00	30.04	10.08	1.21	30.18	10.03	29.90	10.13
AST	0.93	29.26	10.86	1.18	29.39	10.82	29.13	10.90
STT	1.00	30.93	9.19	1.22	31.07	9.14	30.79	9.24
CHA	1.57	28.69	11.43	1.47	28.91	11.30	28.47	11.56
BEA:F	0.28	29.32	9.29	0.82	29.36	9.25	29.28	9.33
MFI:F	0.14	31.82	6.78	0.80	31.84	6.76	31.80	6.80
CFI	1.40	29.79	8.82	0.81	29.98	8.62	29.59	9.02
ISV	0.13	24.94	14.37	1.07	24.96	14.36	24.92	14.39
BEA:OH	2.22	26.94	11.67	0.88	27.25	11.35	26.63	11.98
MFI:OH	0.88	30.60	8.01	0.82	30.72	7.88	30.48	8.13

Table 3.4. Relation Between Structure and Energetics

Sample	Framework Density (Si/nm^3)	Molar Volume (cm^3/mol)	δ (nm)	Structure Reference	ΔH_{trans}^{298} (kJ/mol SiO_2)	Enthalpy Reference
Quartz	26.52	22.71	0	39	0.0	---
MEL	17.80	33.83	0.0496	26	8.2	This work
MWW	16.51	36.47	0.0688	20	10.4	This work
IFR	17.03	35.36	0.0434	17	10.0	This work
ITE	16.26	37.04	0.0617	19	10.1	This work
AST	17.29	34.83	0.0867	12	10.9	This work
STT	16.83	35.78	0.0845	28	9.2	This work
CHA	15.40	39.10	0.0225	16	11.4	This work
BEA	15.60	38.60	N/A	13	9.3	This work
MFI	17.97	33.51	0.0516	27	6.8	This work
CFI	18.28	32.94	0.0376	25	8.8	This work
ISV	15.36	39.21	0.0593	18	14.4	This work
AFI	17.80	33.83	0.0543	40	7.2	8
MTW	19.39	31.06	0.0532	41	8.7	8
FAU	13.45	44.77	0.0242	42	13.6	8
FER	18.43	32.67	0.0494	43	6.6	48
cr	23.37	25.77	0.0127	44	2.84	49
mo	26.22	22.97	0.0379	45	3.4	50
co	29.26	20.58	0.0442	46	2.93	51
tr	22.61	26.63	0.0311	47	3.21	52

Table 3.5. Measured Enthalpies of Transition vs. Predicted Values based on MV correlation

Sample	ΔH_{trans}^{298} exptl (kJ/mol SiO_2)	ΔH_{trans}^{298} predicted (kJ/mol SiO_2)	Error (kJ/mol SiO_2)
Quartz	0	2.4	2.4
MEL	8.2	8.5	0.3
MWW	10.4	9.9	-0.5
IFR	10.0	9.3	-0.7
ITE	10.1	10.2	0.2
AST	10.9	9.0	-1.8
STT	9.2	9.6	0.4
CHA	11.4	11.4	0.0
BEA	9.3	11.1	1.8
MFI	6.8	8.3	1.5
CFI	8.8	8.0	-0.8
ISV	14.4	11.4	-2.9
AFI	7.2	8.5	1.3
MTW	8.7	7.0	-1.7
FAU	13.6	14.5	0.9
FER	6.6	7.8	1.2
cr	2.84	4.0	1.2
mo	3.4	2.5	-0.9
tr	3.21	4.5	1.3
co	2.93	1.2	-1.7

Table 3.6. Fractional Contributions of Loop Configuration Types to Silica Structures

Loop type	0	1	2A	2B	3A	3B
	0 ring	1 ring	2 rings	2 rings	3 rings	3 rings
Structure						
AFI	0.00	1.00	0.00	0.00	0.00	0.00
AST	0.20	0.00	0.00	0.00	0.00	0.80
BEA	0.25	0.25	0.50	0.00	0.00	0.00
CHA	0.00	0.00	0.00	0.00	1.00	0.00
MTW	0.71	0.29	0.00	0.00	0.00	0.00
MFI	0.83	0.17	0.00	0.00	0.00	0.00
MEL	0.58	0.42	0.00	0.00	0.00	0.00
FAU	0.00	0.00	0.00	0.00	1.00	0.00
MWW	0.22	0.50	0.17	0.00	0.00	0.11
FER	1.00	0.00	0.00	0.00	0.00	0.00
CFI	0.75	0.00	0.25	0.00	0.00	0.00
IFR	0.00	0.25	0.50	0.25	0.00	0.00
ITE	0.00	0.25	0.50	0.25	0.00	0.00
STT	0.13	0.31	0.38	0.13	0.06	0.00
ISV	0.25	0.25	0.00	0.00	0.00	0.50
Quartz	1.00	0.00	0.00	0.00	0.00	0.00
tr	1.00	0.00	0.00	0.00	0.00	0.00
cr	1.00	0.00	0.00	0.00	0.00	0.00
co	0.00	0.00	1.00	0.00	0.00	0.00
mo	0.00	0.67	0.00	0.33	0.00	0.00

Table 3.7. Enthalpy Contributions for Loop Types

Loop type	Enthalpy Contribution (kJ/mol)	Std error (kJ/mol)
0	4.9	1.3
1	4.5	3.1
2A	3.0	3.0
2B	-0.5	7.8
3A	7.6	2.6
3B	10.2	3.8

Table 3.8. Measured Enthalpies of Transition vs Predicted Values based on Loop Configuration Correlation

Structure	ΔH_{trans}^{298} exptl (kJ/mol SiO_2)	ΔH_j (fit) (kJ/mol SiO_2)	error (kJ/mol SiO_2)
AFI	7.2	9.5	2.3
AST	10.9	13.1	2.2
BEA	9.3	7.6	-1.7
CHA	11.4	12.5	1.1
MTW	8.7	6.2	-2.5
MFI	6.8	5.7	-1.1
MEL	8.2	6.8	-1.4
FAU	13.6	12.5	-1.1
MWW	10.4	8.8	-1.6
FER	6.6	4.9	-1.7
CFI	8.8	5.7	-3.1
IFR	10.0	7.5	-2.6
ITE	10.1	7.5	-2.6
STT	9.2	7.9	-1.3
ISV	14.4	11.2	-3.2
q	0	4.9	4.9
tr	3.2	4.9	1.7
cr	2.8	4.9	2.1
co	2.9	7.9	5.0
mo	3.4	7.8	4.4

Figure 3.1. Possibilities for Silicate Self-Assembly in Hydrothermal Syntheses

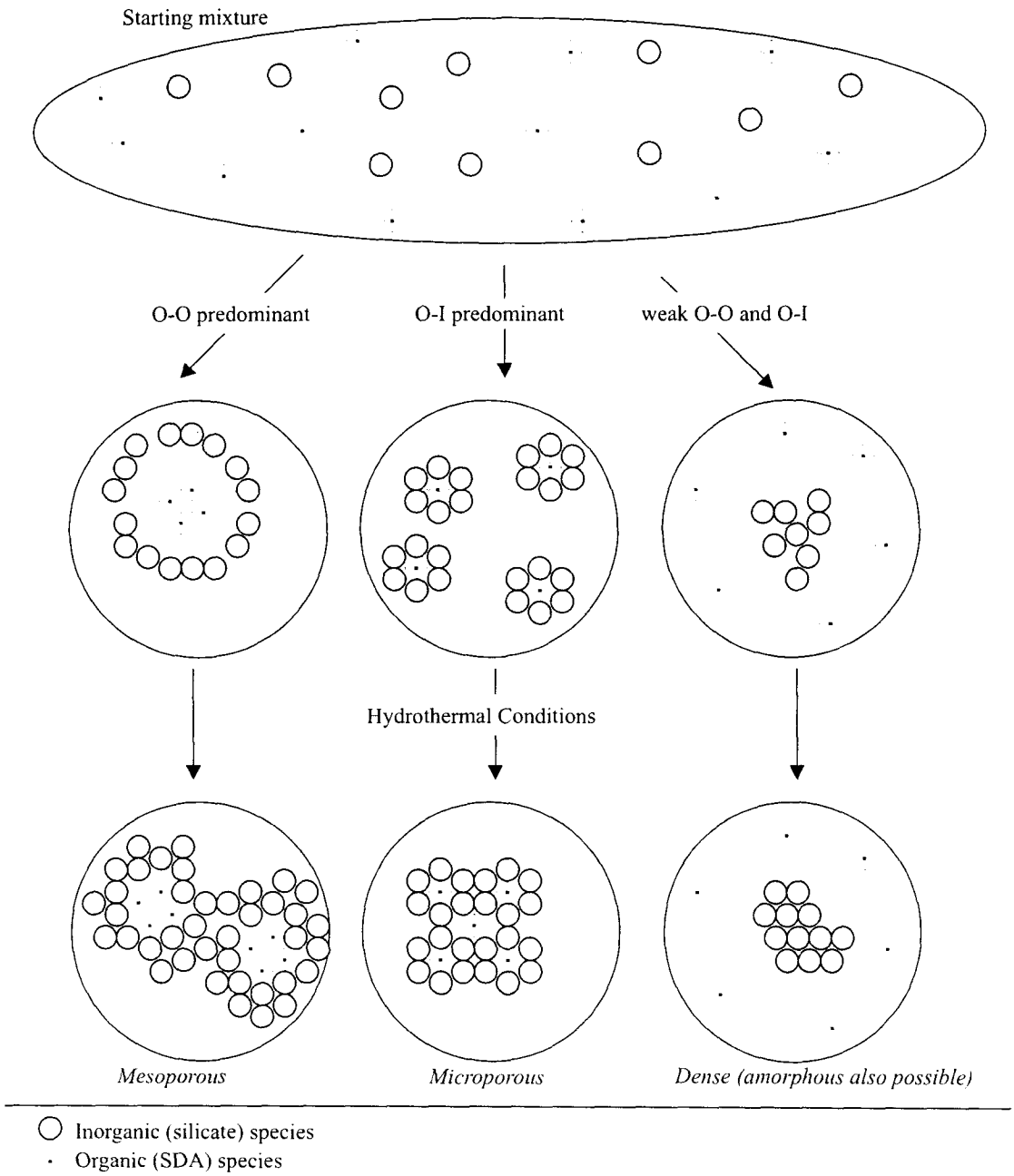

Figure 3.2. Enthalpy of Transition vs. Framework Density

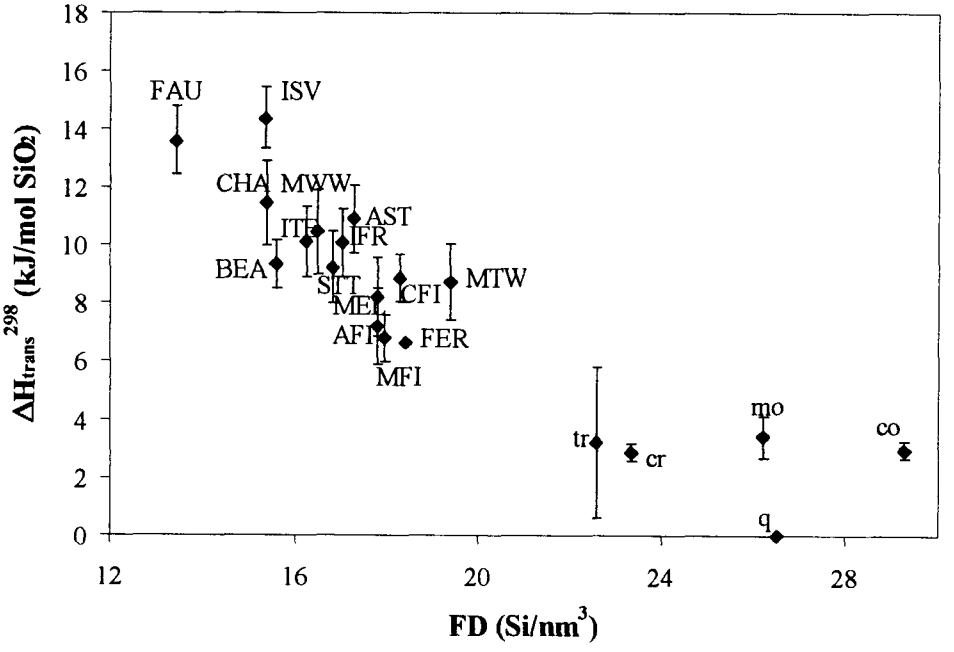

Figure 3.3. Enthalpy of Transition vs. Molar volume

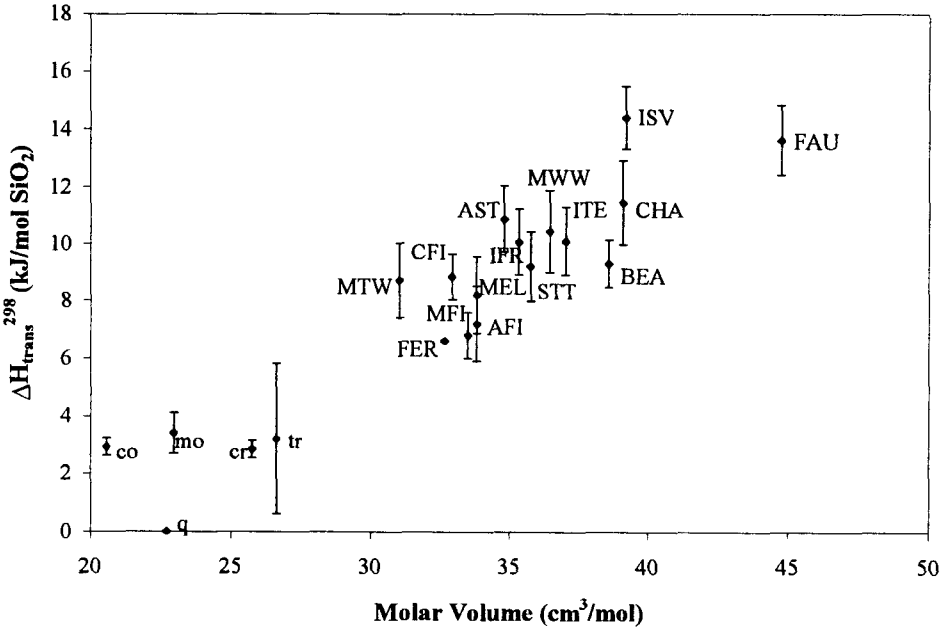

Figure 3.4. Enthalpy of Transition vs. δ

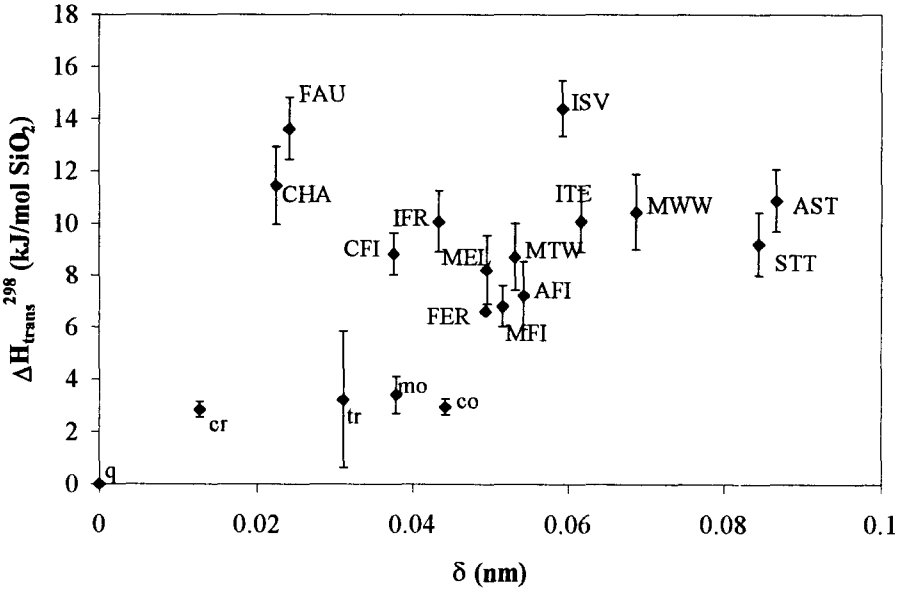

Figure 3.5. Configuration Loops Present in Zeolites

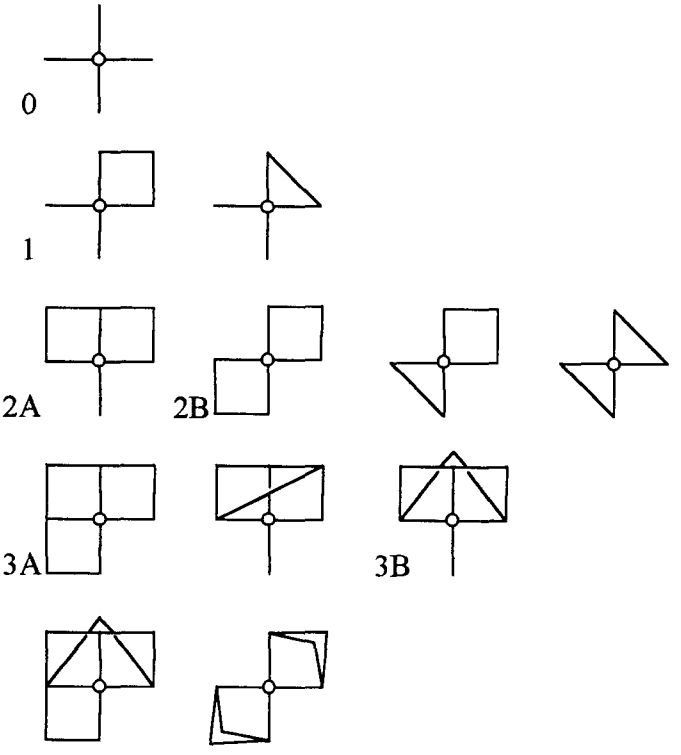

References

[1] Petrovic, I.; Navrotsky, A.; Davis, M. E.; Zones, S. I. *Chem. Mater.* **1993**, *5*, 1805.

[2] Navrotsky, A. *MRS Bull*, May **1995**, *35*.

[3] Breck, D. W. *Zeolite Molecular Sieves*, **1974**, Wiley: NY.

[4] Gies, H.; Marler, B. *Zeolites*, **1992**, *12*, 42.

[5] Lobo, R. F.; Zones, S. I.; Davis, M. E. *J. Incl. Phen. Mol. Recogn. Chem.* **1995**, *21*, 47.

[6] Davis, M. E.; Zones, S. I. in Occelli, M. L.; Kessler, H. *Synthesis of Porous Materials*, **1997**, Marcel Dekker: NY.

[7] Helmkamp, M. M.; Davis, M. E. *Annu. Rev. Mater. Sci.*, **1995**, *25*, 161.

[8] http://www.iza-sc.ethz.ch/IZA-SC/Atlas/AtlasHome.html.

[9] Henson, N. J.; Cheetham, A. K.; Gale, J. D. *Chem. Mater.* **1994**, *6*, 1647.

[10] Camblor, M. A.; Villaescusa, L. A.; Díaz-Cabañas, M.-J. *Top. Catal.* **1999**, *9*, 59.

[11] Ohsuna, T.; Terasaki, O.; Nakagawa, Y.; Zones, S.I.; Hiraga, K. *J. Phys. Chem. B.* **1997**, *101*, 9881.

[12] Villaescusa, L. A.; Barrett, P. A.; Camblor, M. A. *Chem. Mater.* **1998**, *10*, 3966.

[13] Camblor, M. A.; Corma, A.; Valencia, S. *Chem. Comm.* **1996**, 2365.

[14] Tsuji, K.; Beck, L. W.; Davis, M. E. *Micro. Meso. Mater.* **1999**, *28*, 519.

[15] Barrett, P. A.; Díaz-Cabañas, M.-J.; Camblor, M. A.; Jones, R. H. *J. Chem. Soc. Faraday Trans.* **1998**, *94, 2475.*

[16] Díaz-Cabañas, M.-J.; Barrett, P. A.; Camblor, M. A. *Chem. Comm.* **1998**, 1881.

[17] Barrett, P. A.; Camblor, M. A.; Corma, A.; Jones, R. H.; Villaescusa, L. A. *Chem. Mater.* **1997**, *9*, 1713.

[18] Villaescusa, L. A.; Barrett, P. A.; Camblor, M. A. *Angew. Chem. Int. Ed.* **1999**, *38*, 1997.

[19] Camblor, M. A.; Corma, A.; Lightfoot, P.; Villaescusa, L. A.; Wright, P. A. *Angew. Chem. Int. Ed.* **1997**, *36*, 2659.

[20] Camblor, M. A.; Corma, A.; Díaz-Cabañas, M.-J.; Baerlocher, Ch. *J. Phys. Chem. B* **1998**, *102*, 44.

[21] Camblor, M. A.; Díaz-Cabañas, M.-J.; Perez-Pariente, J.; Teat, S. J.; Clegg, W.; Shannon, I. J.; Lightfoot, P.; Wright, P. A.; Morris, R. E. *Angew. Chem. Int. Ed.* **1998**, *37*, 2122.

[22] Navrotsky, A. *Phys. Chem. Miner.* **1977**, *2*, 89.

[23] Navrotsky, A. *Phys. Chem. Miner.* **1997**, *24*, 3.

[24] Navrotsky, A.; Rapp, R.P.; Smelik, E.; Burnley, P.; Circone, S; Chai, L.; Bose, K. *Am. Mineral.* **1994**, *79*, 1099.

[25] Yoshikawa, M.; Wagner, P.; Lovallo, M.; Tsuji, K.; Takewaki, T.; Chen, C-Y.; Beck, L.W.; Jones, C.; Tsapatsis, M.; Zones, S. I.; Davis, M. E. *J. Phys. Chem. B.* **1998**, *102,* 7139.

[26] Terasaki, O.; Ohsuna, T.; Sakuma, H.; Watanabe, D.; Nakagawa, Y.; Medrud, R. C. *Chem. Mater.* **1996**, *8*, 463.

[27] van Koningsveld, H.; Jansen, J. C.; van Bekkum, H. *Zeolites* **1990**, *10*, 235.

[28] Camblor, M. A.; Díaz-Cabañas, M.-J.; Cox, P. A.; Shannon, I. J.; Wright, P. A.; Morris, R. E. *Chem. Mater.* **1999**, *11*, 2878.

[29] Nakagawa, Y.; Lee, G. S.; Harris, T. V.; Yuen, L. T.; Zones, S. I. *Micro Meso. Mater.* **1998**, *22*, 69.

[30] Robie, R. A.; Hemingway, B. S. *USGS Bulletin 2131,* **1995**.

[31] Hu, Y.; Navrotsky, A.; Chen, C.-Y.; Davis, M.E. *Chem. Mater.* **1995**, *7*:1816.

[32] Blasco, T.; Camblor, M. A.; Corma, A.; Esteve, P.; Guil, J. M.; Martínez, A.; Perdigón-Melón, J. A.; Valencia, S. *J. Phys. Chem. B.* **1998**, *102*, 75.

[33] Kiseleva, I.; Navrotsky, A.; Belitsky, I. A.; Fursenko, B. A. *Am. Mineral.* ***1996,*** *81*, 658.

[34] GULP (the General Utility Lattice Program) written and developed by J. D. Gale, Royal Institution/Imperial College: United Kingdom, 1992-1994.

[35] Maniar, P. D.; Navrotsky, A.; Rabinovich, E. M.; Ying, J. Y.; Benziger, J. B. *J. Non-Cryst. Solids* **1990**, *124*, 101.

[36] Ying, J. Y.; Benziger, J. B.; Navrotsky, A. *J. Am. Ceram. Soc.* **1993**, *76*, 257.

[37] Petrovic, I.; Navrotsky, A.; Chen, C.-Y.; Davis, M. E. *Stud. Surf. Sci. Catal.* **1994,** *84*, 677.

[38] Newton, M. D.; Gibbs, G. V. *Phys. Chem. Miner.* **1980**, *6*, 221.

[39] Levien, L.; Prewitt, C. T.; Weidner, D. J. *Amer. Mineral.* **1980**, *65*, 920.

[40] Bialek, R.; Meier, W. M.; Davis, M.; Annen, M. J. *Zeolites* **1991**, *11*, 438.

[41] Fyfe, C. A.; Gies, H.; Kokotailo, G. T.; Marler, B.; Cox, D. E. *J. Phys. Chem.* **1990**, *94*, 3718.

[42] Hriljac, J. A.; Eddy, M. M.; Cheetham, A. K.; Donohue, J. A.; Ray, G. J. *J. Solid State Chem.* **1993**, *106*, 66.

[43] Lewis Jr., J. E.; Freyhardt, C.C.; Davis, M. E. *J. Phys. Chem.* **1996**, *100*, 5039.

[44] Pluth, J. J.; Smith, J. V.; Faber Jr., J. *J. Appl. Phys.* **1985**, *57*, 1045.

[45] Miehe, G.; Graetsch, H. *Eur. J. Mineral.* **1992**, *4*, 693.

[46] Smyth, J. R.; Smith, J. V.; Artioli, G.; Kvick, A. *J. Phys. Chem.* **1987**, *91*, 988.

[47] Dollase, W. A.; Baur, W. H. *Amer. Mineral.* **1976**, *61*, 971.

[48] Petrovic, I.; Navrotsky, A., *Unpublished Results.*

[49] Richet, P.; Bottinga, Y.; Denielou, L.; Petitet, J. P.; Tequi, C. *Geochim. Cosmochim. Acta* **1982**, *46*, 2639.

[50] Petrovic, I.; Heaney, P. J.; Navrotsky, A. *Phys. Chem. Minerals* **1996**, *23*, 119.

[51] Akaogi, M.; Navrotsky, A. *Phys. Earth Planet. Inter.* **1984**, *36*, 124.

[52] Robie, R. A.; Hemingway, B. S.; Fisher, J. R. *USGS Bulletin 1452*, **1978**.

[53] Davis, M.E. *Chem. Eur.J.* **1997**, *3*, 1745.

[54] O'Keeffe, M.; Hyde, B. G. in O'Keeffe, M.; Navrotsky, A. *Structure and Bonding in Crystals*, **1981**, Academic Press: NY.

[55] Gibbs, G. V. *Personal Communication*, **1998**.

Chapter Four

Entropy of Pure-Silica Molecular Sieves

(reproduced with permission from Piccione, P. M; Woodfield, B.F.; Boerio-Goates, J.; Navrotsky, A.; Davis, M. E. *J. Phys. Chem. B* **2001,** *105,* 6025-6030.

Abstract

The entropies of a series of pure-silica molecular sieves (structural codes *BEA, FAU, MFI and MTT) are obtained by calorimetric measurements of low-temperature heat capacity. The third-law entropies at 298.15 K are (on the basis of one mole of SiO_2): *BEA: 44.91±0.11 $J \cdot K^{-1} \cdot mol^{-1}$, FAU: 44.73±0.11 $J \cdot K^{-1} \cdot mol^{-1}$, MFI: 45.05±0.11 $J \cdot K^{-1} \cdot mol^{-1}$, MTT: 45.69±0.11 $J \cdot K^{-1} \cdot mol^{-1}$, while the corresponding entropies of transition from quartz at 298.15 K are *BEA: 3.4 $J \cdot K^{-1} \cdot mol^{-1}$, FAU: 3.2 $J \cdot K^{-1} \cdot mol^{-1}$, MFI: 3.6 $J \cdot K^{-1} \cdot mol^{-1}$, MTT: 4.2 $J \cdot K^{-1} \cdot mol^{-1}$. The entropies span a very narrow range at 3.2-4.2 $J \cdot K^{-1} \cdot mol^{-1}$ above quartz, despite a factor of two difference in molar volume. This confirms that there are no significant entropy barriers to transformations between SiO_2 polymorphs. Finally, the Gibbs free energy of transformation with respect to quartz is calculated for eight SiO_2 phases and all are found to be within twice the available thermal energy of each other at 298.15 K.

Introduction

Aluminosilicates are of great technical commercial importance and are used in a variety of different applications. Over the last two decades, improved syntheses, processing and characterization techniques have revolutionized materials science by increasing the variety of available materials and enabling a better understanding of how they are made. Zeolites (porous, crystalline aluminosilicates) have been shown to be especially valuable by providing unique environments for chemical reactions to take place. These controlled environments have lead to many applications such as in shape-selective separations and heterogenous catalysis.[1] The sizes, shapes and dimensionality of the pore systems vary with the frameworks and determine which chemical species can diffuse into and out of the zeolite. Zeolites and their pure-silica analogues are synthesized at temperatures below 473 K in aqueous media.[1] To date, there is no consistent thermodynamic understanding of zeolite synthesis. In earlier work, some of us have explored the relationship between zeolite structure and enthalpy.[2,3] Here, we measure entropies in order to determine and interpret the Gibbs free energy of the different zeolite structure types.

The thermochemistry of zeolites has long been difficult to study since their syntheses usually proceed by a sequence of irreversible steps progressively leading to more stable structures.[4] Since no phase equilibria are established, the

determination of thermodynamic quantities must be made directly by calorimetry and such measurements are time-consuming and difficult. Considerable effort has resulted in the availability of enthalpy and entropy values for over 20 zeolites, mostly hydrated natural phases of geological interest.[2-19] Entropy values for several dense silica phases have been determined as well.[20-26] Comparisons between the energetics of different frameworks, however, have been complicated by the changing composition of the natural samples. Following the initial work of Petrovic *et al.*,[3] Piccione *et al.*[2] overcame this difficulty by focusing on a collection of synthetic, pure-silica molecular sieves with varied structural features and concluded that the enthalpies of porous silica polymorphs are only slightly (6.6-14.4 $kJ \cdot mol^{-1}$ SiO_2) destabilizing relative to quartz. In order to assess conclusively the degrees of instability of the various SiO_2 polymorphs, the entropies of those polymorphs must be measured as well.

Prior studies on the entropies of SiO_2 materials have mostly been performed on dense phases: values for quartz (q),[21,27] cristobalite (cr),[24,27] tridymite (tr),[24,26,27] coesite (co),[21,25] moganite (mo)[22] and stishovite (st)[21,25,27] have all been reported. The entropy of silica glass has been determined as well.[23] In contrast, only one microporous phase has been previously studied: namely, synthetic pure-SiO_2 ZSM-5 (MFI).[5] The recent increase in the number of synthetic pure-SiO_2 polymorphs available from structure-directed syntheses now allows for the measurement of the entropies of a series of SiO_2 molecular sieves.

There are a number of advantages associated with pure-SiO_2 molecular sieves that make them particularly attractive candidates for comparison of the energetics of different framework structures. They are iso-compositional and have a simple chemical makeup. Since there are no transition metals and only a single kind of tetrahedral atom, one can expect there to be no contributions to the third law entropy from configurational or magnetic disorder. Crystalline SiO_2 is hydrophobic, so there will be relatively little adsorbed water, thus minimizing complications associated with hydration.

Pure-silica analogues of *BEA (zeolite beta), MFI (ZSM-5) and MTT (ZSM-23) were all synthesized in the presence of fluoride ions as the mineralizing agent since F^- ions are known to produce samples essentially free of silanol (Si-O-H) defect groups.[28] Furthermore, such samples are considerably more hydrophobic than the zeolite materials synthesized in hydroxide media. A sample of commercial high-silica faujasite (FAU) was studied as well, since FAU is the most porous crystalline SiO_2 phase known to date, with a density about half that of quartz. The frameworks studied were chosen to possess as widely varying structural features as possible, from very porous (FAU and *BEA) to comparatively much denser (MTT).[29] The MFI measurement further enabled a comparison of the data obtained with that already published.[5]

The third-law entropies, S°(298.15 K)-S°(0 K) were determined for *BEA, FAU, MFI and MTT by low-temperature heat capacity measurements using the

following relationship: $S^{\circ}(298.15K) - S^{\circ}(0K) = \int_{0K}^{298.15K} \frac{C_p}{T} dT$. We assume that S°(0 K) = 0 and adopt the simpler notation S°(298.15 K) for the entropy at 298.15 K. Here, we report the entropy for a series of pure-silica molecular sieves and discuss the implications regarding the stability of SiO_2 polymorphs. In particular, the entropy measurements enable the calculation of the change in the Gibbs free energy on going from quartz to the molecular sieve phases when used in conjunction with previously measured enthalpies.[2,3]

Experimental Section

Sample Preparation

*BEA. Pure-SiO_2 *BEA was synthesized using a gel composition of 1 SiO_2: 0.5 TEAF: 7.25 H_2O where TEA is the tetraethylammonium cation.[30] The SiO_2 source for this synthesis was tetraethoxysilane (TEOS). The complete reaction mixture was formulated to the composition specified above and the TEOS hydrolyzed before heating the synthesis gel. Two rotary evaporations ensured the removal of all the EtOH formed by hydrolysis. After reaction at 413 K and autogeneous pressure for 14 days in a Teflon-lined stainless steel reactor, the product was collected by cooling the mixture to room temperature, filtering and

washing with water, then acetone. The sample was calcined in air at 823 K for 6 hrs to remove the occluded organics.

FAU. The high-silica faujasite, Tosoh 390 HUA, is a commercial material from the Tosoh Chemical Co., Japan, and was kindly provided by Dr. John Cook of Tosoh USA.

MFI. Pure-SiO_2 MFI was synthesized using a gel composition of 1 SiO_2: 0.44 TPAOH: 0.5 HF: 50 H_2O where TPA is the tetrapropylammonium cation. The silica source was Cab-O-Sil M-5. The synthesis was conducted at 448 K and autogeneous pressure for 5 days in a Teflon-lined stainless steel reactor and the product was collected by cooling the mixture to room temperature, filtering and washing with water then acetone. The sample was calcined in air at 823 K for 6 hrs to remove the occluded organics.

MTT. Pure-SiO_2 MTT was prepared from a gel composition of $1SiO_2$: 0.2 ImOH: 0.087 NaOH: 0.016 NaF : 24.0 H_2O where Im is *N,N*-diisopropylimidazolium. The silica source was Cab-O-Sil M-5 and 0.3% previously synthesized boron-MTT were added as seed. After reaction at 423 K and autogeneous pressure for 5 days in a Teflon-lined stainless steel reactor, the product was collected by cooling the mixture to room temperature, filtering and washing with water, then acetone. The sample was calcined at 921 K in air to remove the occluded Im. After calcination, the sample appeared brown-and-black, indicating incomplete removal of the organic material. Increasing the temperature further did not successfully remove the colored impurities.

Characterizations

Room temperature, powder X-ray diffraction (XRD) patterns were collected on a Scintag XDS 2000 diffractometer (liquid nitrogen cooled Ge detector, Cu Kα radiation, λ=1.54184 Å) operating in a Bragg-Bretano geometry. The data were obtained in a stepwise mode with 2θ ranging from 2 to 51° (step size = 0.01°, count time = 4s) in order to identify the crystalline phases present before and after drying. The X-ray powder diffraction patterns indicated the presence of a single molecular sieve phase for each sample. The dehydration treatment effected no significant degradation of the crystalline structures.

Previously published structural data[31] for MTT were calculated from a sample treated with NH_4F that the sample studied here does not contain. To obtain a more accurate molar volume determination, the 22 most intense XRD reflections were used to index the pattern (M_{20}=22, F_{20}=38) with the TREOR90 software package,[32] yielding a primitive orthorhombic unit cell with a=21.582(7), b=11.173(3) and c=5.046(1) Å. These unit cell parameters yield a unit cell volume of V = 1216.8 ± 1.0 Å^3 compared to the previously reported[31] value of 1203.4 ± 0.4 Å^3. While synchrotron diffraction data are necessary to distinguish between the monoclinic and orthorhombic symmetry in MTT,[31] they are not required to determine the unit cell volume (and, hence, the molar volume) of MTT.

With 24 Si atoms per unit cell, a molar volume of 30.53 ± 0.03 $cm^3 \cdot mol^{-1}$ is obtained.

Since it remained off-white after every calcination attempt, the MTT specimen was also analyzed by Galbraith Laboratories, Inc., Knoxville, TN, for the following elements: F, C, N, H. Chemical analysis of the MTT sample gave 34 ppm F, 0.32% C, 0.26% N, < 0.5% H. The nonzero C content is consistent with a slightly incomplete calcination. In the analysis of the entropy, a heat capacity contribution equal to the equivalent amount of solid graphite was used to correct for the carbon impurity.[33] The N content is surprisingly high. Although no Si_3N_4 was visible in the powder X-ray pattern of the MTT sample, the entropy contribution[34] due to an equivalent amount of Si_3N_4 was used to correct for the nitrogen impurity. Previously reported[3] chemical analysis of the FAU sample, in terms of weight percent, gave 95.73% SiO_2, 0.119% Al, 0.005% Ca, 0.001% Mg and 0.013% Na. The calculated correction to the heat capacity due to such a low Al content is sufficiently small to be neglected.

Thermogravimetric analyses (TGA) were performed on approximately 15 mg samples using a TA Instruments 951 Analyzer to measure the mass fraction of water present for the materials used in the calorimetric experiments. The heating rate was 10 K/min to 1073 K and a buoyancy correction based on a run with 15 mg Pt was applied. The TGA results are shown in Table 4.1, along with the calculated molar mass (per mol SiO_2) and compositions. The amount of water present in the dehydrated samples was calculated by taking the difference of the

mass losses at 1073 K and the dehydration temperature of 493 K. For MTT the water content was calculated by taking the difference between the TGA weight loss and the amount of C and Si_3N_4 determined by elemental analysis. For BEA and MFI, the water contents are below 1% as expected for materials synthesized in fluoride media. These water contents are non-zero, however, because only a partial dehydration is carried out by heating to 493 K; treatment at higher temperatures could have achieved complete dehydration but with the possible risk of damaging the molecular sieve frameworks. For MTT, the mass loss on TGA may partially be due to decomposing organic residues even though the sample still appears colored after TGA.

For FAU the water content is slightly higher at 0.77% since this material is made by dealumination of an aluminosilicate faujasite. It is also known to contain silanol defect (SiOH) groups. A solid-state ^{29}Si NMR spectrum for the FAU sample was collected on a Bruker Avance 200 spectrometer equipped with a Bruker cross-polarization, magic angle spinning (MAS) accessory to quantify the amount of silanol groups present. The sample was packed into a 7mm ZrO_2 rotor and spun in air at 4 kHz. A proton-decoupled ^{29}Si NMR spectrum (operating frequency 39.760 MHz, $\pi/2$ = 4μs, 90° pulse angle, recycle delay = 60 s, 2000 transients) referenced to tetrakis(trimethylsilyl)silane (downfield peak at δ =-10.053) was collected using MAS. This spectrum showed a single sharp peak at -107.8 ppm, as expected since FAU only has one kind of crystallographic Si position.[29] A small peak at −101.0 ppm was present below the sharp peak and is

typical of Q_3 (defect) sites; a broader feature is present below the two FAU peaks and may be due to small amounts of amorphous material. The sum of the intensities of the latter two features was estimated at <7.6% of the total amount of Si present. No method to estimate the entropy contribution due to the defects is presently available.

Calorimetry

Heat capacity measurements on the molecular sieves were obtained over the temperature interval from 12 K to 400 K using an intermittent heating technique in an adiabatic calorimeter. The details of the calorimetric apparatus and experimental procedure have been reported elsewhere.[35] Sample masses ranged from 3.1 g (FAU) to 5.0 g (MFI). The molecular sieve heat capacities were typically 15-30 percent of the measured heat capacity. The largest contribution to the total measured heat capacity is that of the empty calorimeter. Corrections have been made for the differences in the masses of helium exchange gas, gold gaskets, and Apiezon-T grease used in the molecular sieve experiments relative to those used in the heat capacity measurements on the empty calorimeter.

Hemingway and Robie[15] have shown that the heat capacity of zeolitic water changes with increasing water content. Also, values for the contribution of water to the entropy of natural zeolites have been shown to range from 32 to 57 $J \cdot K^{-1} \cdot (\text{mol water})^{-1}$.[17] The water content in our samples, however, is

significantly below those reported in these two studies. Thus, there is no definitive heat capacity curve for the small amount of water present in the pure-silica molecular sieves upon which we have made our heat capacity measurements and so, we have made no corrections for water. We estimate, based on the results in reference 17, that the neglect of water corrections should affect the entropies at 298.15 K by no more than 0.1 $J \cdot K^{-1} \cdot mol^{-1}$.

Results

The detailed results of the thermodynamic measurements on these four molecular sieves will be reported elsewhere.[36] The focus here is on the entropies and their contributions to the thermodynamic stabilities of the zeolites. Table 4.2 presents the entropies calculated from the integration of the heat capacity curves as a function of temperature. The entropies of the four samples are very close to one another over the entire temperature region; at 298.15 K, they differ by less than 1 $J \cdot K^{-1} \cdot mol^{-1}$. Since the FAU entropy is very similar to the values for the other frameworks, the presence of defects appears not to influence the entropy significantly. The entropies begin to diverge more significantly above 300 K but still differ only by 1.5 $J \cdot K^{-1} \cdot mol^{-1}$ at 400 K.

The entropies for MFI reported in Table 4.2 for temperatures above 250 K include a contribution due to the monoclinic to orthorhombic phase transition, observed as a small anomaly in the heat capacity from 250 to 375 K. This transition, first reported by by Hay *et al.*,[37] is associated with a deformation of the zeolite framework[38] due to a shift of neighboring (010) pentasil layers along **c**. The total contribution from this transition is only 0.39 $J \cdot K^{-1} \cdot mol^{-1}$. This small entropy effect is consistent with the displacive mechanism proposed by van Koningsveld *et al.*[38] for the transition.

Because of the similarities in the molecular sieve entropies, it is easier to see the differences by considering the entropy relative to that of quartz, S°(molecular sieve) – S°(quartz). This entropy difference vs. temperature for the four molecular sieves is shown in Figure 4.1. The entropies for quartz reported by Gurvich and Khlyustov,[39] augmented by the value at 400 K reported by Richet *et al.*,[23] have been used to generate this figure. The shape of the ΔS vs. temperature curve for *BEA is different from those for the other three molecular sieves in that it shows a maximum near 230 K. We currently have no explanation for this behavior.

Discussion

Structure–Entropy Relation for Silica Polymorphs

The enthalpies of formation of pure SiO_2 crystalline polymorphs have been shown to correlate with their molar volume. It is of interest to consider whether the molar entropies show a similar correlation. Table 4.3 lists the third-law entropies at 298.15 K and molar volumes of various phases of tetracoordinated SiO_2 including the molecular sieves studied in this work. (Stishovite, which has six-coordinated silicon, is not included in this list, because an increase in coordination numbers is known to change the entropy in a complex fashion.[45]) The q, co, tr and cr values have been determined by several investigators with good agreement.

The entropies at 298.15 K from Table 4.3 are plotted versus molar volume in Figure 4.2. An approximately linear correlation is found between the two variables for the dense silica phases (quartz, coesite, trydimite and cristobalite), but the molecular sieves do not follow this trend. Despite having relatively large variations in molar volume, the molecular sieves exhibit nearly identical entropies. Thus, it appears that the entropies of pure-silica phases with molar volumes larger than 27-30 $cm^3 \cdot mol^{-1}$ reach a constant entropy of 45.1 ± 0.7 $J \cdot K^{-1} \cdot mol^{-1}$.

Framework structures based upon SiO_4 tetrahedra have remarkable constancy in the length of the SiO-bond.[46] Changes in volume are associated with

changes in the Si-O-Si bond angle and/or the framework topology. Thus, the vibrational density of states associated with Si-O bond stretching is expected to be relatively constant from polymorph to polymorph. Changes will be expected in the lower frequency regions associated with bending of the Si-O-Si angles and the very low frequency region associated with the long-wavelength motions of the unit cell. These motions contribute to the heat capacity at very low temperatures. The differences among the various molecular sieve topologies are reflected in the complex behavior of the molecular sieve entropies relative to one another below 50 K and the effect of topological differences on the total entropy at room temperature is not significant.

The S°(298.15) values for *all crystalline* SiO_2 phases only span 7.2 $J \cdot K^{-1} \cdot mol^{-1}$. The available thermal energy at 423.15 K, a common synthesis temperature, is RT = 3.5 $kJ \cdot mol^{-1}$. At that same temperature T[S°(molecular sieve) – S°(quartz)] is 1.7 $kJ \cdot mol^{-1}$ for the molecular sieve with the highest entropy (MTT) whereas T[S°(coe) – S°(quartz)] is –1.1 $kJ \cdot mol^{-1}$ for coesite, the lowest entropy silica polymorph. Comparing those values with the available thermal energy, it is evident that there is no significant entropic barrier to transformations between crystalline SiO_2 phases.

Gibbs Free Energy of Transition

In combination with the previously reported[2,3] enthalpies of transition from quartz to other SiO_2 phases, ΔH_{trans}^{298}, the entropies of transition from quartz at 298.15 K, ΔS_{trans}^{298}, determined in this work enable the calculation of the changes in the Gibbs free energy among the different SiO_2 polymorphs:

$$\Delta G_{trans}^{298} = \Delta H_{trans}^{298} - (298.15)\Delta S_{trans}^{298}$$

Table 4.4 lists the ΔG_{trans}^{298} values relative to quartz, i.e., for the reaction **quartz → crystalline SiO_2**, for all SiO_2 polymorphs where experimental data are available for both ΔH_{trans}^{298} and ΔS_{trans}^{298}. Since a measured value for MTT has not been reported, the expected value for MTT based on a linear interpolation of ΔH_{trans}^{298} values at the appropriate molar volume is used here (MV = 30.53 $cm^3 \cdot mol^{-1}$ for MTT,[29] giving ΔH_{trans}^{298} = 6.7 $kJ \cdot mol^{-1}$). Clearly, all phases have nearly the same ΔG_{trans}^{298} as the values range from 0 to 12.6 $kJ \cdot mol^{-1}$. Thus, there are no large thermodynamic barriers to interconversions between SiO_2 polymorphs. It is important to point out that pure-SiO_2 molecular sieves cannot be synthesized directly as empty frameworks. Rather, inorganic-organic composites are synthesized and the organic material is removed by calcination. Therefore, the relatively frequent occurrence of all-SiO_2 molecular sieves as pure-phase materials must be due either to very slow transformation kinetics, or to significant

interactions between the organic guest and inorganic host. While guest-host interactions do not serve to stabilize highly unstable silica polymorphs, the presence of the organic SDAs may favor one set of organic-inorganic precursors over another. Upon self-assembly, even a modest initial preferential stabilization can thus lead to phases each consisting of a single framework topology. These findings are consistent with the scheme of silica self-assembly presented by Piccione *et al.*[2]

The relative contributions of enthalpy and entropy to the Gibbs free energy are shown here for eight SiO_2 polymorphs. For molecular sieves at 298.15 K, the enthalpy term ranges from 6.6-14.4 $kJ \cdot mol^{-1}$ while the $T\Delta S$ entropy term spans the region of 1.0 to 1.2 $kJ \cdot mol^{-1}$. The far larger contribution to Gibbs free energy differences among pure-silica molecular sieves is thus due to variations in the enthalpy for different frameworks, while the entropies contribute little to these differences. An examination of the temperature behavior of the zeolite entropies in Figure 4.1 shows that this conclusion remains true at typical zeolite synthesis temperatures (e.g., 350-450 K).

Conclusions

The third-law entropies for a series of pure-SiO_2 molecular sieves with varied structural features have been determined by low-temperature heat capacity measurements from 5 to 400 K. The four samples used in this study have entropies that lie in a narrow range of 3.2-4.2 $J \cdot K^{-1} \cdot mol^{-1}$ higher than quartz. The entropy at 298.15 K reported here for MFI is in excellent agreement with the previously reported value.[5] This range of $T\Delta S$ is smaller than the available thermal energy at typical synthesis conditions. The entropy contribution to the overall thermodynamics of SiO_2 phase transformations is much smaller than the enthalpy contribution. Since all SiO_2 phases are energetically in close proximity, the role of the organic structure-directing agents used in molecular sieve synthesis cannot be the stabilization of *otherwise* very unstable structures. Rather, the formation of inorganic-organic composites must play a crucial role in the early stages of these syntheses in order to explain why crystallographically single-phase products are so often formed. Finally, the entropies of crystalline silica polymorphs only vary linearly with molar volume for the dense phases, whereas for the molecular sieves they reach an approximately constant value of 45.1 ± 0.7 $J \cdot K^{-1} \cdot mol^{-1}$.

Acknowledgments

Financial support for this work was provided by the Chevron Research and Technology Co. PMP thanks Dr. Stacey Zones (Chevron) for providing the ZSM-23 (MTT) sample. JBG and BFW thank Rebecca Stevens and B. Hom for assistance with the heat capacity measurements and B. Lang for calculations. AN thanks the National Science Foundation (Grant DMR/97-31782) for support.

Table 4.1. Thermogravimetric Analyses of Molecular Sieve Samples

Sample	water loss, 493-1073 K (%)	Composition	Molar mass ($g \cdot mol^{-1}$)
*BEA	0.16	SiO_2/ 0.005 H_2O	60.18
FAU	0.77	SiO_2/ 0.026 H_2O	60.55
MTT	0.21	SiO_2/0.007 H_2O/ 0.027C/ $4.6 \cdot 10^{-3}$ Si_3N_4	60.58
MFI	0.17	SiO_2/0.006 H_2O	60.19

Table 4.2. Third-Law Entropies of Pure-Silica Molecular Sieves ($J \cdot K^{-1} \cdot mol^{-1}$). The Relative Errors are ±0.25% (Based on the Measured Heat Capacities for NIST Synthetic Sapphire NIST-SRM 270)[35]

T/K	S(*BEA)	S(FAU)	S(MFI)	S(MTT)
5	0.002	0.003	0.002	0.002
10	0.029	0.029	0.017	0.023
15	0.180	0.167	0.118	0.155
20	0.530	0.475	0.399	0.479
25	1.036	0.920	0.853	0.963
30	1.635	1.456	1.420	1.541
35	2.290	2.052	2.051	2.170
40	2.984	2.695	2.719	2.834
45	3.709	3.376	3.410	3.524
50	4.461	4.087	4.122	4.240
60	6.027	5.579	5.601	5.739
70	7.648	7.138	7.147	7.314
80	9.299	8.744	8.747	8.945
90	10.97	10.39	10.39	10.62
100	12.65	12.06	12.06	12.32
110	14.34	13.75	13.75	14.05
120	16.04	15.47	15.46	15.79
130	17.74	17.18	17.19	17.55
140	19.45	18.90	18.92	19.31
150	21.16	20.62	20.66	21.07
160	22.86	22.33	22.39	22.83
170	24.56	24.04	24.12	24.58
180	26.24	25.73	25.83	26.32
190	27.91	27.42	27.54	28.05
200	29.56	29.09	29.23	29.76
210	31.20	30.74	30.91	31.46
220	32.82	32.39	32.58	33.14
230	34.42	34.02	34.24	34.80
240	36.01	35.63	35.88	36.44
250	37.58	37.23	37.50	38.07
260	39.14	38.82	39.10	39.69
270	40.68	40.39	40.69	41.28
273.15	41.16	40.88	41.19	41.78
280	42.20	41.95	42.26	42.86
290	43.70	43.49	43.81	44.42
298.15	44.91	44.73	45.07	45.69
300	45.19	45.02	45.35	45.97
320	48.12	48.02	48.38	49.02
340	50.97	50.96	51.36	52.00
360	53.77	53.83	54.32	54.91
380	56.50	56.64	57.16	57.76
400	59.16	59.38	59.81	60.54

Table 4.3. Third-Law Entropies at 298.15 K, Molar Volumes and Framework Densities for Tetracoordinated Silica Polymorphs

Name	Code	Entropy	Error	Reference	Molar Volume	Framework Density	Reference
		($J \cdot K^{-1} \cdot mol^{-1}$)	($J \cdot K^{-1} \cdot mol^{-1}$)	(Entropy)	($cm^3 \cdot mol^{-1}$)	($Si \cdot nm^{-3}$)	(Structure)
Quartz	q	41.5	0.1	27	22.69	26.54	40
Cristobalite	cr	43.4	0.1	27	25.77	23.37	41
Tridymite	tr	43.9	0.4	27	26.63	22.61	42
Coesite	coe	38.5	0.3	21	20.58	29.26	43
MFI	MFI/OH	46.3	0.2	5	33.52	17.97	38
Silica glass	g	48.5	1.0	23	27.27	22.08	20
ZSM-5	MFI/F	45.1	0.1	This work	33.52	17.97	38
ZSM-23	MTT	45.7	0.1	This work	30.53	19.94	This work
Faujasite	FAU	44.7	0.1	This work	44.29	13.60	44
Zeolite beta	*BEA	44.9	0.1	This work	38.56	15.62	30

Table 4.4. Entropy, Enthalpy and Gibbs Free Energy of Transition (Quartz ↔ Other Polymorphs) for Tetracoordinated Silica Polymorphs

Name	Code	ΔS^{298}_{trans}	Error	ΔH^{298}_{trans}	Error	Reference	ΔG^{298}_{trans}	Error
		($J \cdot K^{-1} \cdot mol^{-1}$)	($J \cdot K^{-1} \cdot mol^{-1}$)	($kJ \cdot mol^{-1}$)	($kJ \cdot mol^{-1}$)	ΔH^{298}_{trans}	($kJ \cdot mol^{-1}$)	($kJ \cdot mol^{-1}$)
Quartz	q	0	0	0	0	0	0	0.0
Cristobalite	cr	1.9	0.1	2.8	0.3	23	2.3	0.3
Tridymite	tr	2.4	0.4	3.2	2.6	47	2.5	2.6
Coesite	coe	-3.0	0.3	2.9	0.3	21	3.8	0.3
MFI	MFI/OH	4.8	0.3	6.8	0.8	2	5.4	0.8
Silica glass	g	7.0	1.0	9.1	2.3	27	7.0	2.3
ZSM-5	MFI/F	3.6	0.1	6.8	0.8	2	5.7	0.8
ZSM-23	MTT	4.2	0.1	6.7	2.6	2	5.4	2.6
Faujasite	FAU	3.2	0.1	13.6	0.7	3	12.6	0.7
Zeolite beta	*BEA	3.4	0.1	9.3	0.8	2	8.3	0.8

Figure 4.1. Third-Law Entropies of the Pure-Silica Molecular Sieves Relative to that of Quartz vs. Temperature (the Error Bars Associated with the Results are Smaller than the Symbols Used)

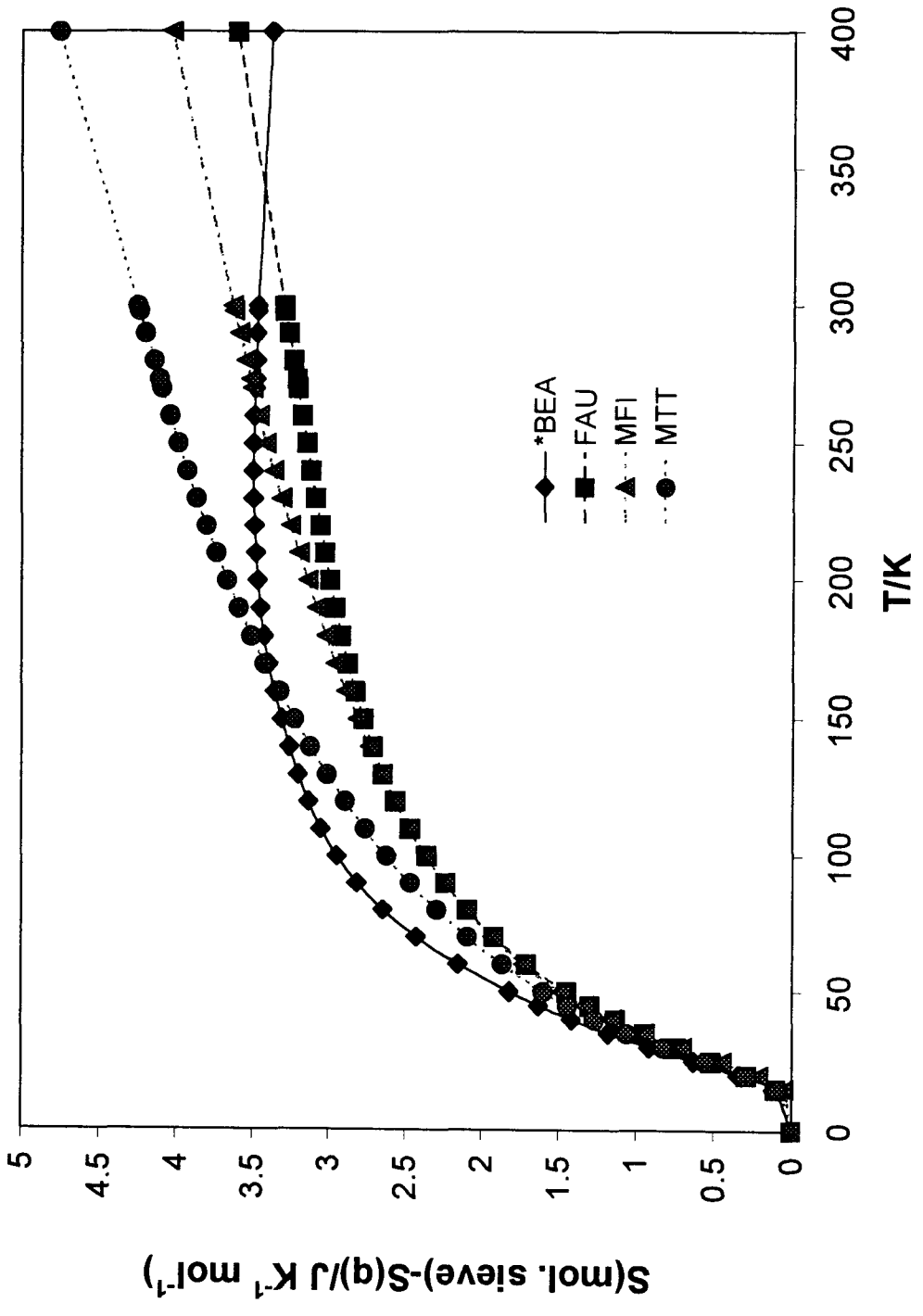

Figure 4.2. Third-Law Entropies vs. Molar Volume for Silica Polymorphs

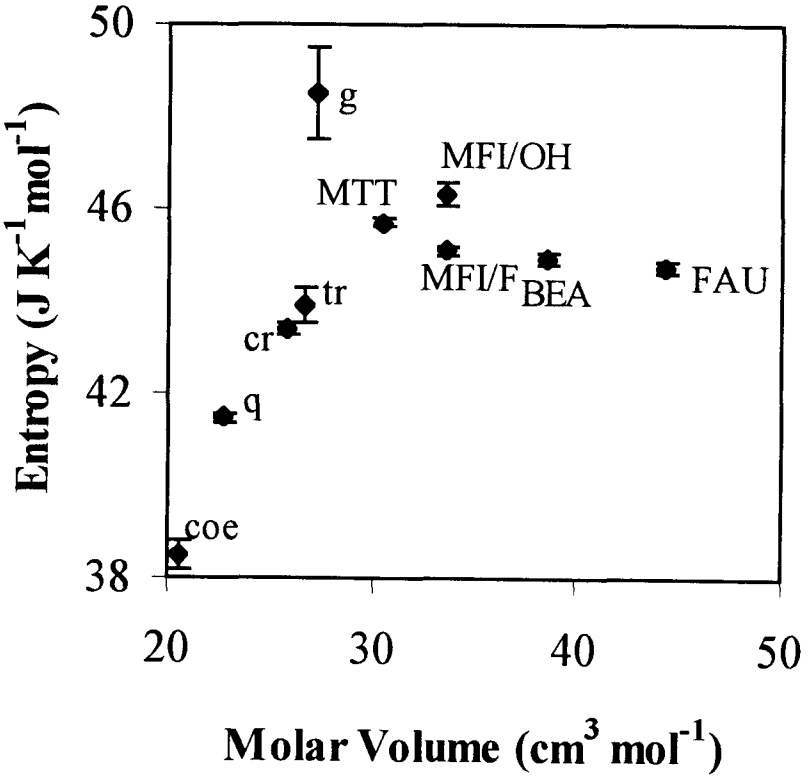

References

[1] Breck, D. W. *Zeolite Molecular Sieves,* **1974**, Wiley: NY.

[2] Piccione, P. M.; Laberty, C.; Yang, S.; Camblor, M. A.; Navrotsky, A.; Davis, M. E. *J. Phys. Chem. B* **2000,** *104,* 10001.

[3] Petrovic, I.; Navrotsky, A.; Davis, M. E.; Zones, S. I. *Chem. Mater.* **1993**, *5*, 1805.

[4] Howell, D. A.; Johnson, G. K.; Tasker, I. R.; O'Hare, P. A. G.; Wise, W. S. *Zeolites* **1990**, *10*, 525.

[5] Johnson, G..K.; Tasker, I. R.; Howell, D. A.; Smith, J. V. *J. Chem. Thermodynamics* **1987**, *19*, 617.

[6] Belitskiy, I. A.; Gabunda, S. P.; Drebushchak, V. A.; Naumov, V. N.; Notgeva, V.V. *Geochemistry International* **1984**, *21*, 21.

[7] Paukov, I. E.; Belitskii, I. A.; Fursenko, B. A.; Kovalevskaya, Yu. A. *Geochemistry International* **1997**, *35*, 946.

[8] Paukov, I. E.; Belitskii, I. A.; Kovalevskaya, Yu. A. *Geochemistry International* **1998,** *36*, 663.

[9] Paukov, I. E.; Fursenko, B. A. *Geochemistry International* **1998,** *36*, 471.

[10] Paukov, I. E.; Belitskii, I. A.; Berezovskii, G. A. *Geochemistry International* **1998,** *36*, 565.

[11] Kiseleva, I.; Navrotsky, A.; Belitsky, I. A.; Fursenko, B. A. *Amer. Mineral.* **1996**, *81*, 658.

[12] Johnson, G. K.; Flotow, H. E.; O'Hare, P. A. G.; Wise, W. S *Amer. Mineral.* **1985**, *70*, 1065.

[13] Johnson, G. K.; Flotow, H. E.; O'Hare, P. A. G.; Wise, W. S. *Amer. Mineral.* **1983**, *68*, 1134.

[14] Petrovic, I.; Navrotsky, A. *Microporous Materials* **1997**, *9*, 1.

[15] Hemingway B. S.; Robie, R. A. *Amer. Mineral.* **1984**, *69*, 692.

[16] Johnson, G. K.; Flotow, H. E.; O'Hare, P. A. G.; Wise, W. S. *Amer. Mineral.* **1982**, *67*, 736.

[17] Johnson, G. K.; Tasker, I. R.; Flotow, H. E.; Wise, W. S. *Amer. Mineral.* **1992**, *77*, 85.

[18] Donahoe, R. J.; Hemingway S. B.; Liou, J. G. *Amer. Mineral.* **1980**, *75*, 188.

[19] Yang, S.; Navrotsky, A. *Microporous Mesoporous Materials* **2000,** *37*, 175.

[20] Melchakova, L. V.; Ogorodova, L. P.; Kiseleva, I. A.; Belitskii, I. A.; Fursenko, B. A. *Geokhimiya* **1999**, *12*, 1357

[21] Akaogi, M.; Navrotsky, A. *Phys. Earth Planet. Inter.* **1984**, *36*, 124.

[22] Gislason, S. R.; Heaney, P. J.; Oelkers, E. H.; Schott, J. *Geochim. et Cosmochim. Acta* **1997**, *61*, 1193.

[23] Richet, P.; Bottinga, Y.; Denielou, L.; Petitet, J. P.; Tequi, C. *Geochim. et Cosmochim. Acta* **1982**, *46*, 2639.

[24] Thompson, A. B.; Wennemer, M. *Amer. Mineral.* **1979**, *64*, 1018.

[25] Holm, J. L.; Kleppa, O. J.; Westrum, E. F. *Geochim. et Cosmochim. Acta* **1967**, *31*, 2289.

[26] Anderson, C. T. *JACS* **1936**, *58*, 568.

[27] Robie, R. A.; Hemingway, B. S. *US Geological Survey Bulletin* 2131, **1995.**

[28] Camblor, M. A.; Villaescusa, L. A.; Díaz-Cabañas, M.-J. *Top. Catal.* **1999**, 9, 59.

[29] http://www.iza-sc.ethz.ch/IZA-SC/Atlas/AtlasHome.html.

[30] Camblor, M. A.; Corma, A.; Valencia, S. *Chem. Comm.* **1996**, 2365.

[31] Marler, B.; Deroche, C.; Gies, H.: Fyfe, C. A.; Grondey, H.; Kotokailo, G. T.; Feng, Y.; Ernst, S.; Weitkamp, J.; Cox, D.E. *J. Appl. Crystall.* **1993**, *26*, 636.

[32] Werner, P. E.; Eriksson, L.; Westdahl, M. *J. Appl. Crystall.* **1985**, *18*, 367.

[33] Desorbo, W.; Taylor, W.W. *J. Chem. Phys.*, **1953**, *21*, 1660.

[34] Beard, M. C. "Heat capacity of α- and β- Silicon Nitride, D-ribose and modifications to low-temperature cryostat," Brigham Young University, Provo, UT, M.S. Thesis **1997**.

[35] Shapiro, J. L.; Woodfield, B. F.; Stevens, R.; Boerio-Goates, J.; Wilson, M. L. *J. Chem. Thermodyn.* **1999,** *31,* 725 and references cited therein.

[36] Boerio-Goates, J.; Stevens, R.; Hom, B.; Woodfield, B. F.; Piccione, P. M.; Davis, M. E.; Navrotsky, A. *J. Chem. Thermodyn., submitted.*

[37] Hay, D. G.; Jaeger, H.; West, G. W. *J. Phys. Chem.* **1985**, *89*, 1070.

[38] van Koningsveld, H.; Jansen, J. C.; van Bekkum H. *Zeolites* **1990**, 10, 235.

[39] Gurvich, V. M.; Khlyustov, V. G. *Geokhimya* **1979,** *6*, 829.

[40] Levien, L.; Prewitt, C. T.; Weidner, D. J. *Amer. Mineral* **1980**, *65*, 920.

[41] Pluth, J. J.; Smith, J. V.; Faber Jr., J. *J. Appl. Phys.* **1985**, *57*, 1045.

[42] Dollase, W. A.; Baur, W. H. *Amer. Mineral.* **1976**, *61*, 971.

[43] Smyth, J. R.; Smith, J. V.; Artioli, G.; Kvick, A. *J. Phys. Chem.* **1987**, *91*, 988.

[44] Hriljac, J. A.; Eddy, M. M.; Cheetham, A. K.; Donohue, J. A.; Ray, G. J. *J. Solid State Chem.* **1993**, *106*, 66.

[45] Richet, P.; Robie, R. A.; Hemingway, B. S. *Geochim. et Cosmochim. Acta* **1993**, *57*, 2751.

[46] Flanigen, E. M.; Khatami, H.; Szymanski, H. A. *Adv. Chem. Ser.* **1971**, *101*, 201.

[47] Robie, R. A.; Hemingway, B. S.; Fisher, J. R. *US Geological Survey Bulletin 1452*, **1978**.

Chapter Five

Solvent Choice for Aqueous Calorimetry of MS/SDA Interactions

Introduction

As was shown in Chapters Three and Four, the enthalpies and entropies of crystalline silica polymorphs differ by only small amounts. It must be stressed again, however, that typical hydrothermal syntheses do not yield pure SiO_2, but rather composite materials: inorganic frameworks with enclathrated organic molecules. In fact, the great majority of aluminosilicate frameworks *cannot* be synthesized in the absence of organic structure-directing agents. This simple observation proves the existence of a synthetically significant organic-inorganic interaction.

To quantify the organic–inorganic interaction in thermodynamic terms (as opposed to studying the relative stabilities of calcined materials) it is necessary to determine the enthalpy of interaction, ΔH_i, for the reaction

$$MS(s) + SDA(ref) \rightarrow MS{\cdot}SDA(s) \qquad (1)$$

where MS is an empty (i.e., calcined) molecular sieve, SDA is a structure-directing agent, MS·SDA is the corresponding as-made molecular sieve and ref designates an appropriate reference state for the SDA. The quantity ΔH_i is expected to play a crucial role in actual syntheses since the enthalpy of transformation between different SiO_2 polymorphs is small. In an attempt to measure the enthalpy of interaction, high-temperature (974 K) calorimetry experiments have been conducted on both calcined and as-made molecular sieves.[1] The SDA was assumed

to burn completely, yielding N_2, H_2O and CO_2 as the combustion products. The strongly exothermic heat effects measured, however, yielded errors too large to produce interpretable results. The best approach, then, consists in effecting dissolutions near room temperature in aqueous systems that leave the SDA intact according to the following conceptual cycle:

$$MS(s) \rightarrow SiO_2 * \qquad (2a)$$

$$SDA(ref) \rightarrow SDA* \qquad (2b)$$

$$SiO_2* + SDA* \rightarrow MS{\cdot}SDA(s) \qquad (2c)$$

$$\overline{MS(s) + SDA(ref) \rightarrow MS{\cdot}SDA(s) \quad (1)}$$

In this cycle the asterisk * indicates the dissolved species. To perform such a study, an appropriate solvent must be found and this chapter is concerned with this search.

Previous Work

Only one study of interaction enthalpies was available prior to this work: Patarin *et al.* used 25% hydrogen fluoride (HF) in water as a solvent to study the dissolution enthalpies of MFI with a series of different enclathrated alkylammonium ions: tetrapropylammonium (TPA), tripropylammonium (TRIPA) and dipropylammonium (DIPA).[2] The calorimetry experiment was conducted near

room temperature (T = 298.15 K) with the sample lying as a powder in a capsule floating on top of a thin oil layer over the HF; tumbling of the calorimeter achieved contact of the solid and liquid. This procedure yielded ΔH_i values of -6.2 ± 2.4, 4.5 ± 2.4 and 5.3 ± 2.2 kJ/mol SiO_2 respectively for TPA, TRIPA and DIPA. Note that the errors are rather large and the absolute values are perhaps surprisingly small. In fact, with such values of the same order as the enthalpy differences between empty SiO_2 frameworks (6.6-14.4 kJ/mol, see Chapter Three), there are no strong thermodynamic grounds to explain molecular sieve single phase selectivity. A factor which was not studied by Patarin *et al.* was the variation in ΔH_i observed for interactions of the same organic with different frameworks: such a set of values is clearly of interest to determine whether it can be said that a given organic *preferentially* favors the formation of a specific structure. It should also be pointed out at this point that the dissolution of molecular sieve samples in HF was found to be strongly exothermic (~ -2500 J/g), clearly a desirable property since it means small sample masses can yield strong signals.

Johnson *et al.* also used HF (24.4%) to study the dissolution of calcined MFI[3] and found that the concentration of SiO_2 had quite a small effect on the enthalpies measured: when the SiO_2 concentration was varied from 0.5 to 4 g/dm,[3] the difference in measured enthalpy of dissolution was less than 0.2%. The enthalpy of dissolution, however, was quite sensitive to the concentration of HF, suggesting that if repeated sample dissolutions are to be carried out, they should all

be performed using a large batch of HF of precisely known concentration and that attention must be paid not to introduce significant additional amounts of water into the system (e.g., upon studying SDA dilution).

Silicates-Previous work

Whereas HF is the most well-known and effective solvent for silica species, it is an extremely hazardous substance: reactive and volatile, HF is particularly corrosive to most equipment as well as to living tissues and HF vapors attack the lungs. Several alternatives to HF have been reported in the literature within the context of various etching and dissolution studies of silicates. Most commonly, inorganic bases such as the alkali metal hydroxides were used,[4-6] but since the dissolution depends on the pH of the solution, strong organic bases such as the tetraalkylammonium hydroxides are capable of dissolving SiO_2 as well.[7] Iler[8] reported that a catechol (0.2 catechol/ 0.4 NH_4OH/ 0.4 H_2O) and a quinoline (0.2 quinoline/ 0.4 KOH/ 0.4 H_2O) based systems also dissolve silica, possibly via the chelation of silicate species in solution by the aromatic derivatives.

The requirements on the solvent system for calorimetry are as follows: first, the dissolution must be fast, so that integrated baseline drift does not compete with the dissolution signal itself. Second, the final state of the silicon species must be a

single, well-defined state so that all thermodynamic cycles close properly. For the first of these points, a dissolution that was complete within 2, preferably 1, hour both for the molecular sieve as a pellet and as a powder was deemed sufficiently fast (at this stage the exact means of contacting the molecular sieve and solvent were not known since they would be partially determined by the solvent system itself). For the second point, >95% of the silicon present as a single species was the target.

The corrosive action of the strongest inorganic bases, the alkali-metal hydroxides, on silicates forms the basis for the often used "base baths" to clean laboratory glassware. A few layers of glass are etched away at a time. The rates of glass dissolution increase quickly for pH values between 10 and 12, the approximate range of pK_A values of silicic acids.[9] A comparative study[4] of the etching of quartz in different alkali-metal hydroxides found that the dissolution was faster in NaOH than in KOH; the difference was attributed to the higher polarizability of Na^+. A study of quartz etching in neutral media found that among the alkali and alkali-earth cations, Ba^{2+} promoted the fastest etching rates.[10]

Most literature studies, however, did not aim to dissolve silica polymorphs completely, but rather to etch them. One dissolution study showed MFI to remain undissolved after 400 minutes[5] in 5 M NaOH at 60 °C; admittedly, the concentration of 25 g MFI/L solvent is 6-7 times higher than the probable concentration range used for calorimetry (compare Patarin[2] at 3.7 g/l). To completely dissolve possibly micron-sized molecular sieve crystals, then, it was

suspected that aqueous solutions of inorganic bases might not effect sufficiently fast dissolution. Furthermore, ^{29}Si NMR studies of sodium and potassium silicates have shown the resulting aqueous solutions to consist of a mixture of a large number of silicon containing species.[7,11] Alkali-metal hydroxides by themselves, then, would most likely not be adequate solvents for calorimetry purposes. They might, however, still be useful as *additives* to increase the pH and to catalyze depolymerization of the molecular sieve crystals. Indeed, many molecular sieve syntheses starting from polymeric species such as silicic acid or fumed silica must contain trace amounts of Na^+ to proceed at a reasonable rate.[12]

The importance of generating solutions with well-defined final states suggested the use of tetramethylammonium (TMA) derivatives since TMA^+ ions have been shown to preferentially order silicon species in basic solutions to cubic octamers[11,13-18] ("Q_8 species"). TMAOH itself is a very strong base (comparable to the alkali-metal hydroxides) and is commercially available as the solid pentahydrate from Aldrich. The cubic octamers are readily identified in ^{29}Si NMR spectra as a single intense peak -99 ppm from TMS.[11] To form the Q_8 species, fairly high silica concentrations are needed as expected from the law of mass action; at room temperature, silica concentrations of 0.02 mol/l or lower show no Q_8 peak.[14] Higher temperatures, especially higher than 50 °C, also favor dissociation of the Q_8 species to simpler oligomers.[17] Large concentrations of Na^+ and K^+ also favor dissociation of the cubic species,[18] which is unfortunate in view of the possible use of NaOH and KOH as additives to the system. Most importantly for calorimetry

purposes, the addition of methanol or other organic co-solvents has been shown by several workers to disproportionately shift the equilibrium of all the silicate species in aqueous solutions containing TMA ions to the cubic octamer.[14-15] A 1 mol % SiO_2 solution with SiO_2/TMAOH=2 contains about 10% of its silica as the Q_8 species.[15] If the solvent is 25% methanol, the silicon in solution is virtually 100% Q_8.

In summary, hydroxide-based systems are much less hazardous than HF. The use of TMAOH as a base, especially in the presence of an organic co-solvent, was expected to promote preferential organization of any silicate species to Q_8 species. Alkali or alkaline-earth cations as Na^+ or Ba^{2+} may play a catalytic role to ensure fast dissolution. Experimental studies focusing on the dissolution of different silica species in solvents containing these components were undertaken to examine their kinetics and completeness. HF remained the alternative option in case the dissolution behavior of the basic systems was inadequate.

Dissolution in Base

Experimental

Five series of experiments were carried out to identify an alkaline system to dissolve molecular sieves. In the first series, several SiO_2 materials (Cab-O-Sil M5 amorphous silica, MFI/TPA, MFI/ calc, and quartz) were introduced as powders (~10mg) into approximately 5 ml solvent at 65 °C. This yields a silicon concentration of 0.033 mol/l (2g/l) that is in the middle range of the concentration range studied by Johnson[3] (0.5-4 g/l). Aqueous 1 mol/l NaOH, 1 mol/l NaF and saturated (0.14 mol/l) $Ba(OH)_2$ were the solvents tested in order to examine the effect of Ba^{2+} versus Na^+ as a catalyst for silica depolymerization and also to observe the relative rates of dissolution in the presence of the only two anions (OH^- and F^-) known to mineralize silica. The solution was visually inspected at regular time intervals to see if all the cloudiness caused by the powder redispersion had disappeared, a prerequisite (but not proof) for complete dissolution.

In the second set of experiments, the effect of the addition of TMA ions and of methanol was examined to establish whether a quantitative yield of octamers could be obtained. Cab-O-Sil M5 was chosen as one of the two silica source for this study since it had been the easiest SiO_2 polymorph to dissolve in the study above, and so its dissolution was taken as a "minimal prerequisite." Pure-silica zeolite beta with *N*-methyl,*N*-benzyl,trimethylenebispiperidinium enclathrated

(BEA/bispip/OH) was chosen as a good indicator of the behavior of the molecular sieves that would be used in the actual experiments. In each case, the total hydroxide concentration was 1 mol/l and the hydroxide source was either NaOH or an equimolar mixture of Na and TMA hydroxides; the solvent was either water or 40% methanol (by mass) in water. As in the previous series, dissolutions at 65 °C were carried out and the cloudiness of the resulting solutions examined at regular intervals. 8 mg pellets were dispensed in 4 ml solvent, yielding the same concentration as in the previous series.

In the third series, the effect of the organic additives suggested by Iler[8] was investigated. A solution of 40%KOH/ 20%quinoline/ 40%H_2O and a solution of 20%catechol/ 40% NH_4OH/ 40%H_2O (both by mass) were prepared and Cab-O-Sil M5 pellets were pressed to perform dissolution tests.

In the fourth series, the best solvent identified from the previous experiments, 0.5 mol/l TMAOH: 0.5 mol/L NaOH in 40% methanol-water, was tested to see if it would dissolve pellets of both Cab-O-Sil M5 and the as-made BEA/bispip/OH sample described above. 7 mg sample pellets were introduced in 3.5 ml solvent at 65, 50 and 40 °C. Once again, the observed solutions were checked periodically to estimate their cloudiness. Since 65 °C is the boiling point of methanol, significant evaporation/recondensation processes start to happen at this temperature; the formation of droplets and their eventual return into the main body of the solution is a discontinuous process that could negatively impact the

stability of the calorimeter baseline. At lower temperatures, these processes do not happen, which is why dissolutions were also performed at 40 and 50 °C and in the same manner.

Finally, ^{29}Si NMR spectra were obtained on a Bruker AM500 instrument operating at 99.363 MHz ($\pi/2$ pulse = 16.7μs, recycle delay = 60s, 600 transients), externally referenced to hexamethyldisiloxane (δ = 7 ppm wrt TMS, measured). 1 mol/l aqueous solutions of Na silicate and of TMA silicate, and TMA silicate in 50% methanol were prepared to compare the data to published spectra. Pellets pressed from 8 mg Cab-O-Sil M5 amorphous silica and pure-silica ZSM-12 (with *N*-methyl,*N*-benzyl,trimethylenebispiperidinium ion enclathrated) were dissolved in 4 ml of a 0.5 mol/L TMAOH: 0.5 mol/L NaOH solution in 50% methanol/H_2O. These ^{29}Si NMR spectra were examined to see if the cubic octamers coveted did indeed form; the solutions were also visually examined for sample dissolution.

Results

The results of the first series of experiments are shown in Table 5.1. NaOH dissolves the silica samples much more completely than either NaF or $Ba(OH)_2$. The use of hydroxide as the mineralizing anion and Na^+ as the metal cation is recommended from these data. Quartz and the as-made molecular sieve are the least quickly dissolved silica phases; this observation confirms that the kinetics of

silica dissolution are strongly dependent on the internal surface accessible to the depolymerizing species. The results of the second series of experiments are presented in Table 5.2. Of the solutions considered, only the mixed Na^+ and TMA^+ hydroxides with methanol added achieved complete dissolution in less than 70 min for all cases. Presumably, the Na^+ cations increased the kinetics of depolymerization as has been already reported in the context of the molecular sieve syntheses,[12] whereas the TMA^+ cations and methanol helped stabilize the silicon species in solution.

In the third series of experiments, the effects of aromatic derivatives were studied with the hope of finding a system where the possible chelation of Si in solution would result in quantitative conversion of all the Si into a single species. The quinoline system, however, did not yield a single phase but an emulsion; such a system is clearly inappropriate for dissolution studies. While the catechol system yielded a single phase, its oxidation in air was readily detected by the progressive change in the color of the solution (from almost colorless to green to brown within minutes). This oxidation is a well-known characteristic of catechol and is doubtlessly accompanied by a corresponding exothermic heat effect. Since the extent of reaction within the calorimeter cannot be monitored in time, the corresponding heat of oxidation cannot be accounted for. The catechol system, then, is not going to be useful for calorimetry.

The fourth series of experiments, owing to the failure of the aromatic systems, returned to the $TMAOH/NaOH/H_2O$/methanol system to examine it in

more detail. At 65 °C, both Cab-O-Sil M5 and BEA *mostly* dissolved within 75 minutes, but a small amount of suspended powder was still visible in the solution. The masses involved were too small to try to quantify the amount of undissolved SiO_2. Sixteen hours later, this powder was still visible; its amount was very small, yet essentially 100% dissolution is crucial for the thermodynamic cycles to close properly. At 50 °C, Cab-O-Sil M5 dissolved in approximately 3 hours: at 40 °C, this process took between 3 and 19 hours. In each case, a small amount of solid remained; dissolution of the BEA pellets was significantly incomplete both at 50 and at 40 °C after 3 hours. Regular weighing of the solutions indicated that at 65 °C and in a sample vessel comparable to the standard calorimetry cell (a shortened NMR tube) a mass loss with significant heat effects compared to the expected heat of dissolution of the molecular sieve was present. A tight seal on top of the calorimeter would be necessary to prevent this evaporation. The presence of small amounts of undissolved solids was very problematic; the first possible explanation was the presence of an impurity but the inability of the solvent to dissolve this solid, even given an extra day at 65 °C, suggested that this solvent system may not be adequate for all samples and conditions. This conclusion was further strengthened by the NMR results shown below.

Figures 5.1, 5.2 and 5.3 show the ^{29}Si NMR spectra, respectively, of Na silicate, TMA silicate and TMA silicate in 50% methanol. These spectra are in excellent agreement with the literature (Figures 2 of ref. 15 and 2A and D of ref. 7,

respectively). The relatively good signal-to-noise ratio of these spectra is due to the fact that they were obtained from long runs (10 hours each) of quite concentrated (1 mol/l Si in each case) solutions. Figure 5.4 shows the ^{29}Si spectrum for the actual silicon concentration intended in the calorimeter experiments (from Cab-O-Sil M5). While only a single peak was observed, corresponding to the monomeric silicate (δ = -71 ppm), the poor signal-to-noise ratio hardly allows the identification of species present in smaller amounts. Hexamethyldisiloxane, while a useful chemical shift reference, cannot adequately be used as a concentration standard for such spectra. Furthermore, even after 10 hours, in the case of MTW the solution was still cloudy at the end of the experiment. No variable temperature experiment was attempted, since the signal-to-noise ratio degrades even further upon elevation of the temperature.

In summary, the dissolution of sample pellets in the only basic system yielding fast powder dissolution (TMAOH/NaOH/H_2O/methanol) was problematic at best, tending to leave a small residue of unidentified solid. At the concentrations used, the silicon species did not aggregate to the cubic octamer but seemed to form mostly monomer. Other Si species may be present but not detected by NMR (all raw spectra have a large amorphous hump due to the silicon in the glass NMR tube and in the probe, seen in the upfield third of Figure 5.4; at the concentrations of interest this hump would obscure any small, possibly broadened peaks in the same chemical shift range). Not only is the final state not the desired one, but

furthermore the poor NMR characteristics of ^{29}Si make these solutions very difficult to characterize.

Based on these results, hydroxide-based systems were deemed unsatisfactory for accurate calorimetry studies. As anticipated earlier, hydrofluoric acid must therefore be used.

Hydrofluoric Acid Dissolution

HF is well-known to dissolve silicates even at room temperature, so no preliminary tests with powders were carried out. Instead, experiments were performed to ensure that *pellets* would dissolve quickly and to verify that a single Si species is produced by dissolution. A major advantage of the HF system over the basic systems studied above is the high receptivity of ^{19}F for NMR (83.4% of proton receptivity with fast relaxation times). The equation usually invoked to represent the dissolution of SiO_2 in HF is[19]:

$$SiO_2 + 6HF \rightarrow H_2SiF_6 + 2H_2O.$$

Hexafluorosilicic acid, however, is a very strong acid (its extent of ionization is comparable to that of sulfuric acid) and so H_2SiF_6 is expected to be completely dissociated in aqueous solution to yield SiF_6^{2-} ions. The only other fluorosilicate species reported are SiF_4 (a colorless gas[19]) and the SiF_5^- anion

(prepared at low temperatures by the interaction of SiF_4 and tetraalkylammonium fluorides).[20] Table 5.3 lists the ^{19}F and ^{29}Si NMR chemical shifts of each of these species. While the ^{29}Si chemical shifts are more widely separated, the ^{19}F signals seemed sufficiently far apart to allow determination of which $[SiF_x]^{(x-4)-}$ species are present unless the ^{19}F signals suffered from extreme line broadening.

As expected, the most fluorinated species have the least negative (least shielded) δ_F values: each additional F atom can capture less of the Si electron cloud. Note that the HF chemical shift has been shown to vary with the solution conditions, doubtlessly due to changes in the $HF \leftrightarrow F^- \leftrightarrow HF_2^-$ equilibrium.[26] The approach used was to monitor the dissolution of various molecular sieves by obtaining ^{19}F NMR spectra and to obtain the more time-consuming ^{29}Si spectra later only if necessary.

Experimental

The ^{19}F NMR spectra were obtained both on a Bruker DSX-500 instrument operating at 470.598 MHz ($\pi/2$ pulse = 10μs, recycle delay = 1 s, 256 transients) and on a 500 MHz Inova instrument operating at 470.627 MHz ($\pi/2$ pulse = 11.4μs, recycle delay = 0 s, 32 transients). Teflon-FEP liners within 5mm Pyrex tubes were used in each case to contain the hydrofluoric acid. For the Avance 500 experiments, the annular region was filled with an external reference:

$F_2ClCCCl_3$ in hexadecane (δ = -65 ppm)[25] for ^{19}F NMR, hexamethyldisiloxane (δ = 6.6 ppm, measured) for the ^{29}Si experiments. For the Inova experiments, trifluoroacetic acid was used as an internal reference (δ = -78.5 ppm).[25]

Partially deuterated 24% hydrofluoric acid was prepared by mixing equal masses of HF (48%, Mallinckrodt) and D_2O (Cambridge Isotope Laboratories). Samples of the pure-SiO_2 molecular sieves MFI, BEA and MTW prepared in fluoride media according to procedures detailed elsewhere in this thesis (see Chapter Six) were pressed into pellets. Approximately 12.5 mg pellets or pellet shards were dropped into approximately 3.5 g HF/D_2O solution. Note that the dissolution of as-made samples was expected to be slower than for calcined materials since the blocked pores allow far less internal diffusion of the HF; this behaviour had been already observed for the basic systems. The initial set of NMR spectra was obtained on the DSX-500 spectometer to ensure that the same species were formed both in the absence and presence of the various tetraalkylammonium ions of interest. Table 5.4 summarizes the DSX-500 experiments. ^{19}F NMR spectra were recorded at varying times in each case, and the samples were periodically inspected to see if they were visually clear.

The difficulty in obtaining reliable integration values from the DSX-500 data (vide infra) led to following the dissolution in time on the Inova 500 (a liquid-state instrument with much narrower linewidths). MFI with occluded TPA was chosen as the molecular sieve sample to study in time: due to the tight fit of the organic guest, its dissolution had been earlier seen to be among the slowest, so it

was expected to give reliable "slowest case" values for the dissolution kinetics. The composition of the HF solution was as follows: 4.643 g D_2O : 5.063 g 48% HF : 0.14 g trifluoroacetic acid (internal reference). 0.7031g of this solution were added to 4.3 mg pure-silica MFI/TPA (prepared in fluoride media).

While the initial series of experiments were carried out at room temperature, a series of variable-temperature (VT) experiments were also performed for MFI/TPA on the Inova 500. The use of HF meant probable use of Teflon components to build the calorimeter cells; since Teflon undergoes a reversible phase transition[26] at 27 °C any calorimetry experiments must be carried out at a temperature sufficiently above 27 °C that the enthalpy of the phase transition be unobservable. Of course, the rate of dissolution will be higher at the higher temperature as well.

In addition to the spectra taken at different times, which were all obtained at 25 °C, spectra were also recorded at 5, 45 and 65 °C, in each case after a 30 min temperature equilibration period and after the 25 °C relative spectral intensities had ceased to vary significantly.

Results

In all the experiments on the DSX-500 instrument, only two peaks were identified in the ^{19}F NMR spectrum: a very strong peak attributed to HF species (HF, F^-, HF_2^-) at δ = -166.4 ppm and a smaller peak which must be the

fluorosilicate species (δ = -130.3 ppm). The linewidths (Full Width at Half Maximum, FWHM) for these signals are very broad at >1000 Hz, suggesting that exchange processes may be taking place; as a comparison, the FWHM for the external reference ($F_2ClCCCl_3$) is 220 Hz.

The exchange process is best characterized using the data obtained on the narrower-line Inova 500 instrument (see below). The fact that the same two peaks are observed for all samples proves that the presence of tetraalkylammonium ions does not affect the equilibrium of fluorosilicate solutions. A typical spectrum is shown in Figure 5.5 for the dissolution of MFI/TPA and shows the external reference along with the fluorosilicate and hydrofluoric acid peaks.

Integrations were made difficult by the presence of rolling baselines of fairly large amplitude. It is this difficulty, in fact, that motivated the re-examination of MFI/TPA on the Inova 500 described below. The time taken to obtain a visually clear solution for each sample is shown in Table 5.4. The calcined BEA sample clearly dissolves in less than 1 hour even at room temperature. The as-made materials, however, do not all dissolve in less than 2 hours at room temperature. Unfortunately, the calorimeter can be stirred or tumbled no more than the NMR tubes (that are actually spinning at 20Hz). The kinetics in the NMR experiments should therefore correspond well to the actual kinetics in the calorimeter. At 50 °C the dissolution of MFI/TPA (the slowest case) was complete in less than 2 hours.

Tables 5.5 and 5.6 show the dissolution kinetics results from the Inova 500 instrument and the variable temperature results, respectively. In accordance with

the DSX-500 data, only two peaks were identified in the ^{19}F NMR spectrum. They again correspond to the HF and fluorosilicate species. For the Inova spectrum, the FWHM for the internal reference is 3Hz, while the HF and the fluorosilicate peaks are much broader. The integrals of the fluorosilicate and HF species relative to the peak of the internal reference are shown in Figure 5.6. Clearly, there is no further reaction after 40 min. At that time, the solution was inspected and found to look visually clear. The composition of the solution leads to expected relative intensities of 3.2 (reference): 4.4 (fluorosilicate): 95.3 (free F) that are relatively close to the observed values. The small discrepancy is probably due to the uncertainty in measuring the very small silica mass introduced into the Teflon-FEP liners. Since the reaction kinetics for the sample expected to be hardest to dissolve are sufficiently fast for powders at 25 °C, they certainly will be so at 50 °C as well. At the time when the Inova experiment was performed, design of the calorimetry cells had already progressed to the point where it was known that the molecular sieve samples would be present as powders, not pellets.

The chemical shift observed for the fluorosilicate peak (-132 ppm) is close but not quite equal to the reported value of −128 ppm. This fluorosilicate line is broad and the FWHM increases dramatically upon heating to 45 °C. A possible reason for this discrepancy is the solvent dependence of the chemical shift of the SiF_6^{2-} species that has already been documented.[25] The FWHM of the HF line increases as well, albeit less dramatically so. Upon heating, the fluorosilicate peak shifts to the right, i.e., towards the HF peak. Such a move indicates that chemical

exchange on the NMR time scale is taking place. The HF peak, however, shifts towards the right, away from the fluorosilicate signal. While puzzling at first, this behavior can be easily understood in terms of a shift in the {HF, F^-, HF_2^- } equilibrium. Since the "free" fluoride species are present in an approximately 20-fold excess, the chemical exchange is expected to affect the HF peak much less than the fluorosilicate peak. Even a weak change in the {HF, F^-, HF_2^-} equilibrium with temperature, then, would suffice to mask any shift due to chemical exchange. In this context, it is surprising that the "total" free fluoride + fluorosilicate integral value with respect to the trifluoroacetic acid internal reference seems to diminish upon heating.

This effect may, however, be an artifact of data processing: large phasing and baseline corrections were necessary in all cases. The reference peak, unaffected by chemical exchange, did not broaden and hence its ^{19}F population was correctly described by the corresponding integral. For the strongly broadened HF and fluorosilicate peaks above room temperature, however, the baseline correction may well have subtracted out part of the real intensity along the wide "tails" of the peaks and hence the calculated integrals are underestimates of the real populations of these species present. Another possibility is the decomposition of hexafluorosilicate to form some free SiF_4 gas that would be unobservable; this decomposition has been described in the literature for very strong H_2SiF_6 solutions, but is not expected to take place at the range of concentration and temperatures of interest here.[26] In order to investigate this possibility more fully,

some thermochemistry calculations were undertaken to estimate the likelyhood of SiF_4 formation.

The system formed upon addition of SiO_2 to a 25% HF solution in H_2O at the concentration of the TPA/MFI experiment above (total HF concentration C_{HF} = 12.5 mol/l, $[H_2O]$ = 38.5 mol/l, total silicon concentration $[Si]_T$ = 0.09 mol/l) was assumed to consist only of the following species: SiF_6^{2-}, SiF_4, HF, F^-, H_2O, H^+. The five equations needed to determine the concentrations other than $[H_2O]$ are as follows:

- F conservation: $6\,[SiF_6^{2-}] + 4\,[SiF_4] + [HF] + [F^-] = C_{HF}$
- Si conservation: $[SiF_6^{2-}] + [SiF_4] = [Si]_T$
- charge conservation: $[H^+] = [F^-] + 2\,[SiF_6^{2-}]$
- dissociation constant for HF: $K_A = [H^+]\,[F^-] / [HF] = 10^{-3.45}$
- equilibrium constant of $[SiF_6^{2-}]$ formation: $K = [SiF_6^{2-}] / [SiF_4]\,[F^-]^2$

From the thermodynamic data in the *CRC Handbook of Chemistry and Physics*[27], K can be estimated to be 1.2×10^5 (this is a lower estimate; other reported values range up to 10^6) at 298 K. Note that while the simple aqueous K_A value cannot be expected to correctly describe the dissociation of a solution as concentrated as 25% in HF, it gives a simple estimate for this process. These equations lead to $[SiF_6^{2-}]/[SiF_4]$ = 55. In other words, no more than 1.8% of hexafluorosilicate species are expected to dissociate. This is a very small relative amount of dissociation, so significant SiF_4 formation is not the cause of apparent

signal loss at higher temperatures. Presumably, excessive line broadening must be blamed instead.

In summary, the ^{19}F NMR data show that only SiF_6^{2-} species are present upon the dissolution of silica species in HF, even in the presence of tetraalkylammonium cations. While the dissolution kinetics are slightly too slow for pellets at room temperature, powders at 50 °C dissolve readily. Therefore, 25% aqueous HF at 50 °C is a good solvent for pure-silica molecular sieves and thus adequate for the solution calorimetry experiments. Operation above 27 °C has the additional benefit of avoiding the Teflon phase transition region.

Table 5.1. Effect of Varying Metal Cations and Mineralizing Anions on Silica Dissolution in Basic Systems at 65 °C

Silica Sample	Solvent	Dissolution Time (min)
Cab-O-Sil M5	1 M NaOH	20
MFI as made	1 M NaOH	Incomplete (80min)
MFI calcined	1 M NaOH	20
quartz	1 M NaOH	Incomplete (80min)
Cab-O-Sil M5	0.14 M $Ba(OH)_2$	Incomplete (80min)
MFI	0.14 M $Ba(OH)_2$	Incomplete (80min)
Cab-O-Sil M5	1 M NaF	Incomplete (80min)
MFI	1 M NaF	Incomplete (80min)

Table 5.2. Effect of TMA and MeOH on Dissolution in Basic Systems at 65 °C

Silicate	Solvent[#]	Observations
Cab-O-Sil M5	TMA	dissolution incomplete (70min)
Cab-O-Sil M5	TMA/Na	dissolution incomplete (22min)
Cab-O-Sil M5	TMA/Me	dissolution incomplete (70min)
Cab-O-Sil M5	TMA/Me/Na	dissolution complete (22min)
BEA/bispip	TMA	dissolution incomplete (70min)
BEA/bispip	TMA/Na	dissolution complete (70min)
BEA/bispip	TMA/Me	dissolution incomplete (70min)
BEA/bispip	TMA/Me/Na	dissolution complete (22min)
BEA/bispip	0.02M TMAOH in H_2O	dissolution incomplete (70min)

[#] The solvent contains 1 M hydroxide. When the solvent label includes "Na," 0.5 M Na^+ is present; all other hydroxide ions are balanced by TMA^+. The solvent is water or, if the indication "Me" is given, 35% MeOH/ 65% water.

Table 5.3. Chemical Shifts of Fluorosilicate Species

Species	δ, ^{19}F, ppm from $CFCl_3$	Ref.	δ, ^{29}Si, ppm from TMS	Ref.
SiF_4	-163	21	-114	21
SiF_5^-	-136	20	Expect ~ -163	22
SiF_6^{2-}	-128	23	-185	24
HF	-165	25	---	

Table 5.4. NMR Experiments List: DSX-500

Experiment	Temperature (°C)	Nucleus	Times after drop (min)	Sample Nature	Dissolution Time (visual)(min)
PPN140	RT[#]	^{19}F	8.5, 15.5, 31.5, 37.5, 45.5, 90.5, 134.5, 270	BEA/calc	< 60
PPN142	RT	^{19}F	9, 18, 25, 37, 156, 508	MFI/TPA	52-156
PPN143	RT	^{19}F	9, 14, 40, 106, 118, 176, 641	MTW/bispip	90-118
PPN147	50 °C	^{19}F	9, 50,86, 157, 317, 747	MFI/TPA	<120
PPN130 (Inova) 3 mg/ 0.62220 DF	RT	^{19}F	30, 60, 80, 150	BEA/TEA	N/A

[#] Room Temperature

Table 5.5. Inova 500 Results: Dissolution Kinetics

Time (min)	Reference Integral	SiFx Integral	Fluoride Integral	Relative SiFx Integral	Relative Fluoride Integral
41	348	411	9241	1.18	26.55
82	346	416	9238	1.20	26.70
107	362	399	9239	1.10	25.52
146	353	410	9237	1.16	26.17
246	365	404	9232	1.11	25.29
369	364	332	9305	0.91	25.56
460	367	368	9266	1.00	25.25

Table 5.6. Inova 500: VT Experiment

Temperature (°C)	SiFx Integral	Fluoride Integral	δ(SiFx) (ppm)	δ(HF) (ppm)	FWHM (SiFx) (Hz)	FWHM (HF) (Hz)
5	1.04	25.34	-131.9	-167	60	61
25	1.11	25.29	-132	-168.5	450	126
45	0.45	23.67	-132.78	-170	2500	360
65	--	21.22	--	-171.3	--	990

Figure 5.1. ^{29}Si NMR Spectrum of 1 mol/l Na Silicate

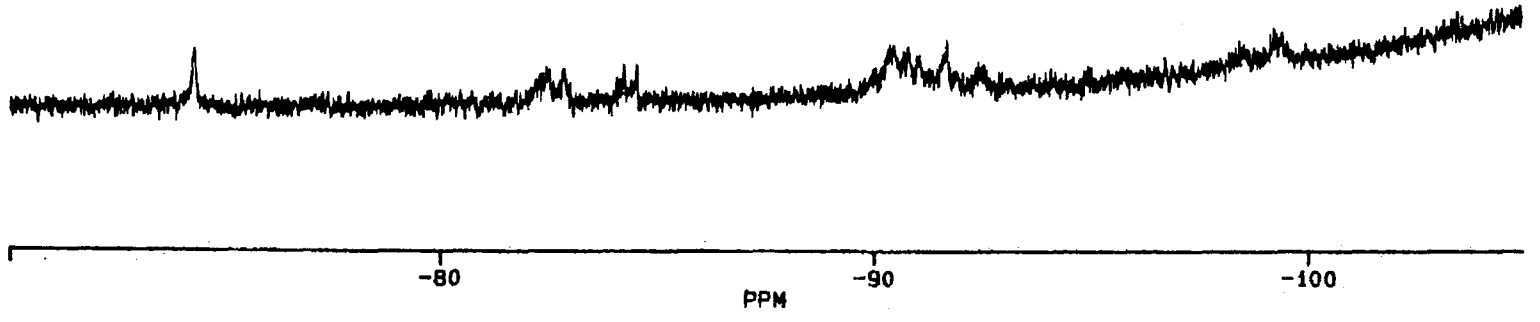

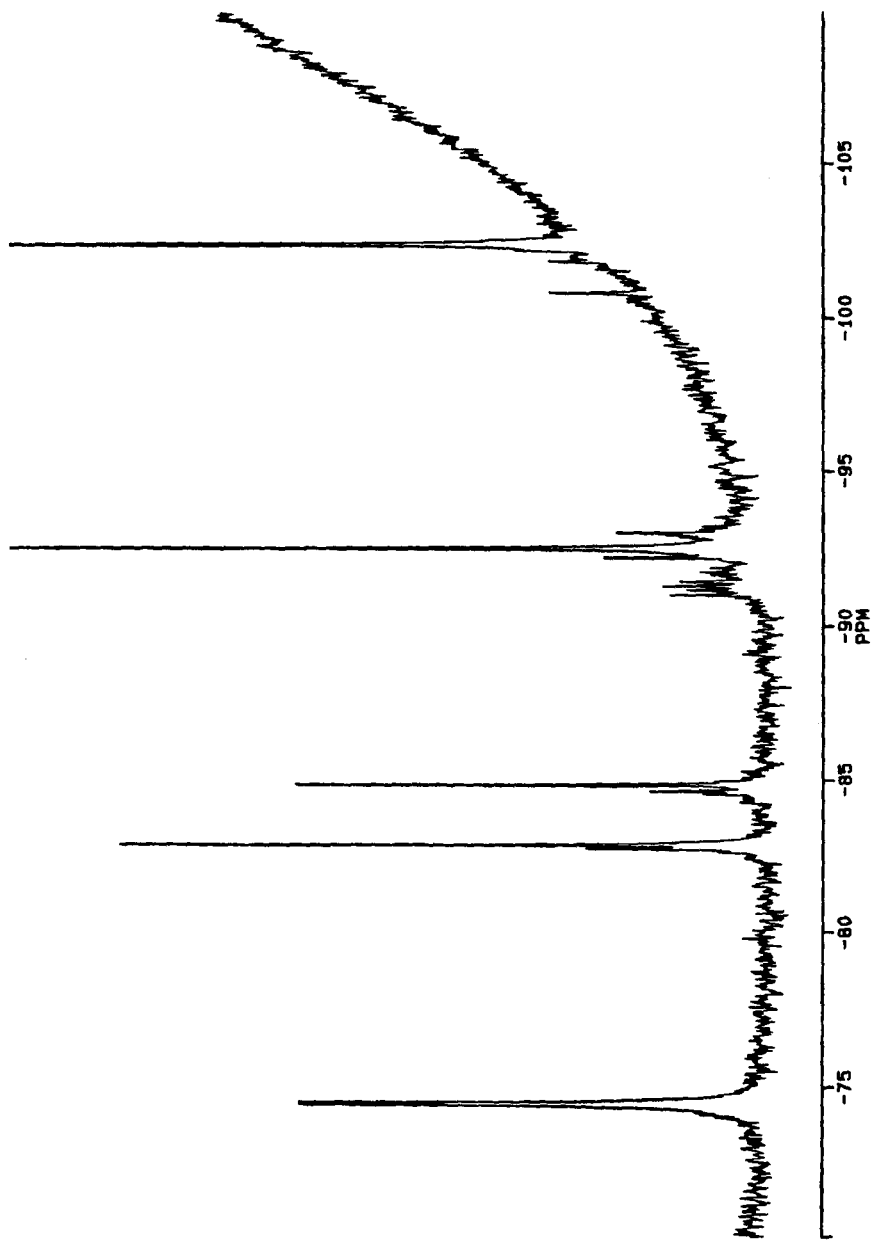

Figure 5.2. ^{29}Si NMR Spectrum of 1 mol/l TMA Silicate

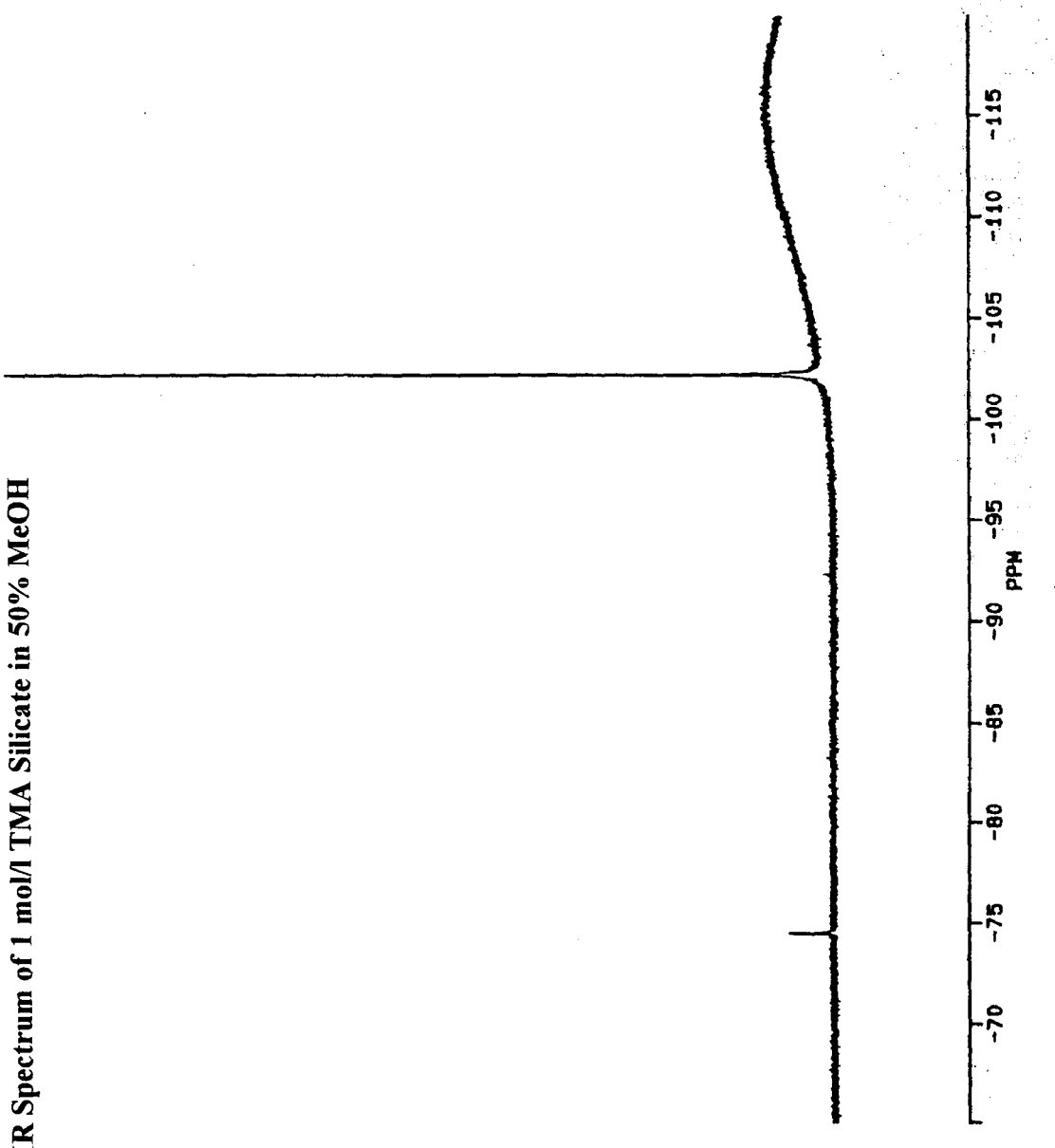

Figure 5.3. ^{29}Si NMR Spectrum of 1 mol/l TMA Silicate in 50% MeOH

Figure 5.4. ^{29}Si NMR Spectrum for TMA Silicate from Cab-O-Sil M5 and at the Calorimetric Concentration

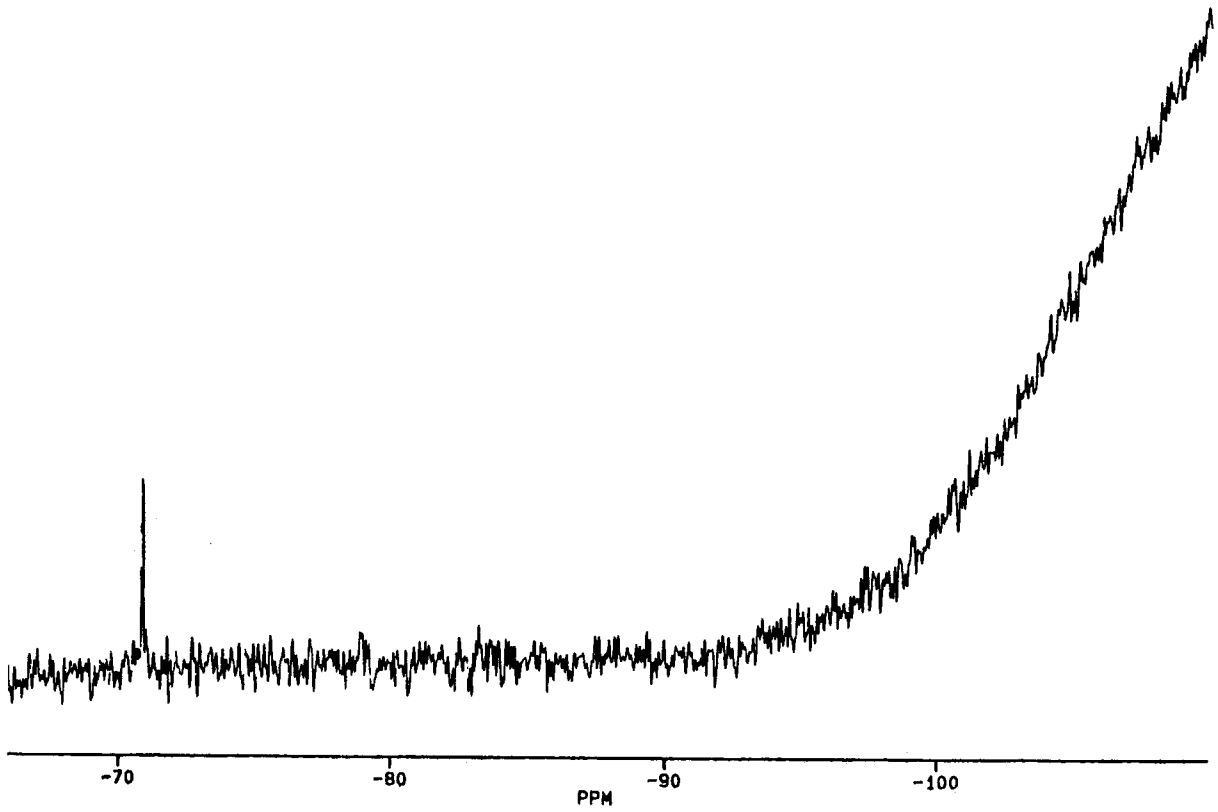

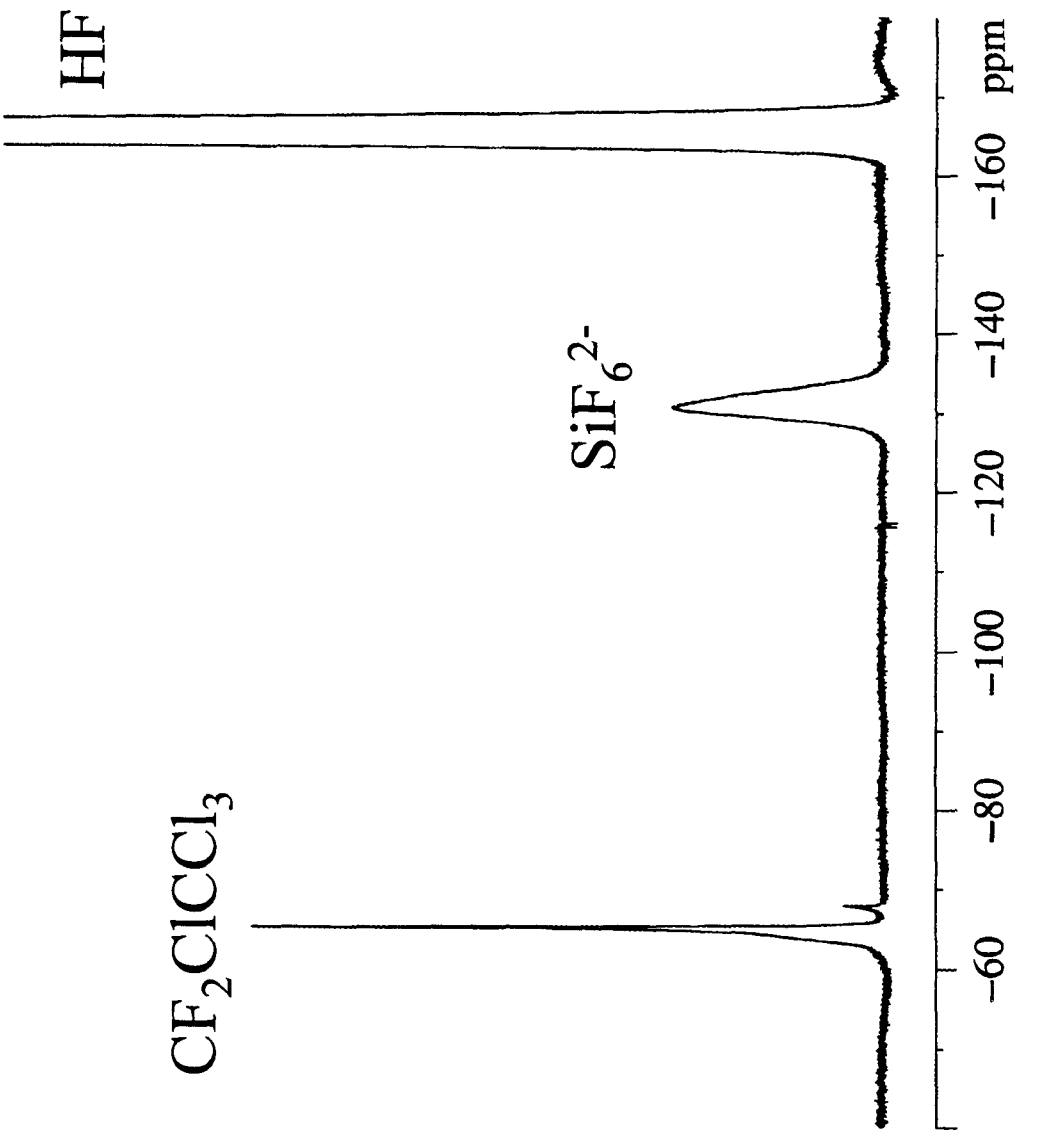

Figure 5.5 Typical ^{19}F Spectrum of Fluorosilicate Solutions

Figure 5.6. Dissolution Kinetics of MFI:TPA: Time Evolution of ^{19}F NMR Signals

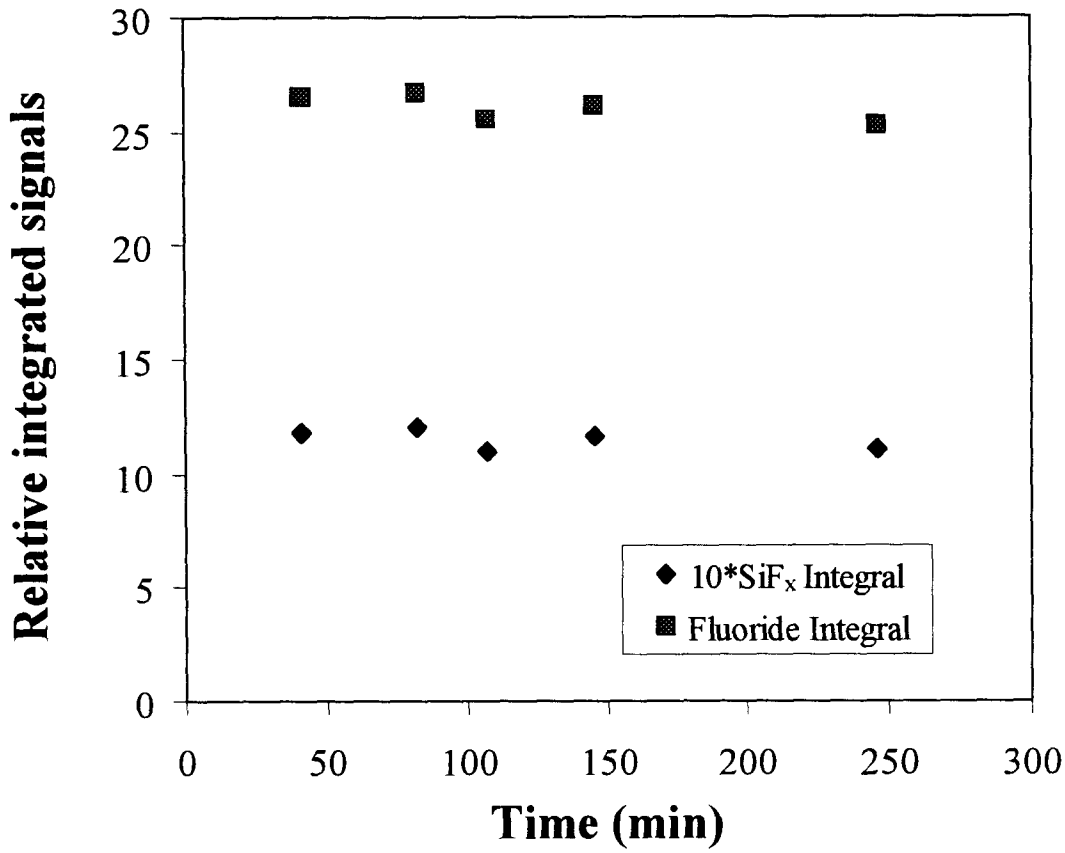

References

[1] Geilfuss, J. S.; Kniaz, K.; Navrotsky, A. N.; Davis, M. E. *Unpublished manuscript* **1997**.

[2] Patarin, J.; Kessler, H.; Soulard, M.; Guth, J. L. in *Zeolite Synthesis* **1989**; Occelli, M. L.; Robson, H. E.; Eds.ACS Symposium Series American Chemical Society, Washington, DC, **298**, Ch.16.

[3] Johnson, G. K.; Tasker, I. R.; Howell, D. A.; Smith, J. V. *J. Chem. Thermodynamics* **1987**, *19*, 617.

[4] Deleuze, M.; Goiffon, A.; Ibanez, A.; Philippot, E. *Journal of Solid State Chemistry* **1995**, *118*, 254.

[5] Cizmek, A.; Komunjer, L.; Subotic, B.; Aiello, R.; Crea, F.; Nastro, A. *Zeolites* **1994** *14*, 182.

[6] Iwasaki, A.; Sano, T. *Zeolites* **1997,** *19*, 41.

[7] Thouvenot, R.; Hervé, G.; Guth, J.- L.; Wey, R. *Nouveau Journal de Chimie/New Journal of Chemistry* **1986**, *10*, 479.

[8] Iler, R. K. *The Chemistry of Silica* **1979**, Wiley: NY.

[9] Dean, J. A. *Lange's Handbook of Chemistry* **1985**, McGraw-Hill:NY.

[10] Dove, P.M.; Nix, C. J. *Geochimica et Cosmoschimica Acta* **1997**, *61*, 3329.

[11] Harris, R. K.; Knight, C. T. G. *Journal of Molecular Structure* **1982**, *78*, 273.

[12] Goepper, M.; Li, H.-X.; Davis, M. E. *J. Chemical Soc. Chem. Comm.* **1992**, 1665.

[13] Knight, C. T. G.; Kirkpatrick, R. J.; Oldfield, E. *J. Chem. Soc. Chem. Commun.* **1986**, 66.

[14] Knight, C. T. G. *Zeolites* **1989,** *9*, 448.

[15] Hendricks, W. M.; Bell, A. T.; Radke, C. J., *J. Phys. Chem.* **1991,** *95*, 9519.

[16] Groenen, E. J. J.; Kortbeek, A. G. T. G.; Mackay, M.; Sudweijer, O. *Zeolites* **1986**, *6*, 403.

[17] Kinrade, S. D.; Knight, C. T. G.; Pole, D. L.; Syvitski, R. T. *Inorg. Chem.* **1998**, *37*, 4272.

[18] Kinrade, S. D.; Knight, C. T. G.; Pole, D. L.; Syvitski, R. T. *Inorg. Chem.* **1998**, *37*, 4278.

[19] Bailar, J. C.; Emeléus, H. D.; Nyholm, R.; Trotman-Dickenson, A. F. *Comprehensive Inorganic Chemistry* **1973**, Pergamon Press: Oxford.

[20] Klanberg, F.; Muetterties, E. L. *Inorg. Chem.* **1968**, *7*, 155.

[21] Suresh, B. S.; Thompson J. C. *JCS Dalton* **1987**, 1123.

[22] Johnson, S. E.; Day, R. O.; Holmes R. R. *Inorg. Chem.* **1989**, *28*, 3182.

[23] Dean, P. A. W.; Evans, D. F. *J. Chem. Soc. (A)* **1967**, 698.

[24] Harris, R. K. in Harris, R. K.; Mann, B. E., eds. *NMR and the Periodic Table* **1978**, Academic Press: London.

[25] Berger, S.; Braun, S.; Kalinowski, H.-O. *NMR Spectroscopy of the Non-Metallic Elements,* **1997**, Wiley: Chichester.

[26] *Gmelins Handbuch der Anorganischen Chemie, Silicium* Teil B, **1959**, Verlag Chemie: Weinheim.

[27] Lide, D. R., ed. *CRC Handbook of Chemistry and Physics* **1991-1992**, CRC Press: Boca Raton.

Chapter Six

Estimated Thermodynamic Properties of Symmetric Tetraalkylammonium Halides and Hydroxides

Abstract

The enthalpies of formation of tetraalkylammonium halides and hydroxides, $N[(CH_2)_nH]_4X$, (n = 1-4, X=F, Cl, Br or I and also X=OH) for which measurements have not been reported are estimated by group additivity methods or by linear regression yielding values of the following:

$$\Delta H_f \text{ (TPACl)} = -467.8 \pm 7.4 \text{ kJ/mol}$$

$$\Delta H_f \text{ (TPABr)} = -442.5 \pm 10.7 \text{ kJ/mol}$$

$$\Delta H_f \text{ (TPAI)} = -399.8 \pm 5.2 \text{ kJ/mol}$$

$$\Delta H_f \text{ (TMAF)} = -374.0 \pm 15.1 \text{ kJ/mol}$$

$$\Delta H_f \text{ (TEAF)} = -461.0 \pm 3.4 \text{ kJ/mol}$$

$$\Delta H_f \text{ (TPAF)} = -558.3 \pm 11.5 \text{ kJ/mol}$$

$$\Delta H_f \text{ (TBAF)} = -653.0 \pm 6.4 \text{ kJ/mol.}$$

$$\Delta H_f \text{ (TMAOH, } \infty H_2O) = -308.5 \pm 12.8 \text{ kJ/mol}$$

$$\Delta H_f \text{ (TEAOH, } \infty H_2O) = -398.8 \pm 3.4 \text{ kJ/mol}$$

$$\Delta H_f \text{ (TPAOH, } \infty H_2O) = -497.1 \pm 11.1 \text{ kJ/mol}$$

$$\Delta H_f \text{ (TBAOH, } \infty H_2O) = -593.4 \pm 5.7 \text{ kJ/mol}$$

where TMA, TEA, TPA and TBA denote, respectively, the tetramethylammonium, tetraethylammonium, tetrapropylammonium and tetrabutylammonium cations.

Previously unreported entropies are estimated for these compounds by group additivity methods to give the following results:

$$S^\circ (TEACl) = 293.8 \pm 5.2 \text{ J/(mol·K)}$$

$$S^\circ (TEABr) = 303.9 \pm 4.1 \text{ J/(mol·K)}$$

$$S^\circ (TPACl) = 414.8 \pm 5.2 \text{ J/(mol·K)}$$

$$S^\circ (TPABr) = 424.9 \pm 4.1 \text{ J/(mol·K)}$$

$$S^\circ (TMAF) = 177.8 \pm 10.5 \text{ J/(mol·K)}$$

$$S^\circ (TEAF) = 280.9 \pm 10.5 \text{ J/(mol·K)}$$

$$S^\circ (TPAF) = 401.9 \pm 10.5 \text{ J/(mol·K)}$$

$$S^\circ (TMAOH) = 183.7 \pm 10.0 \text{ J/(mol·K)}$$

$$S^\circ (TEAOH) = 286.8 \pm 10.0 \text{ J/(mol·K)}$$

$$S^\circ (TPAOH) = 407.8 \pm 10.0 \text{ J/(mol·K)}$$

Suggestions for steps that should be employed in the thermodynamic cycle for zeolite formation are provided.

Introduction

Alkylammonium halides, $NR_nH_{4-n}X$, where R designates an alkyl group and X can be F, Cl, Br or I, are important compounds for preparative chemistry both as large cations to stabilize otherwise unstable complex anions and as ion-pair reagents.[1] Quaternary alkylammonium ions, in particular, have by far been the most successful class of structure-directing agents (SDAs) for zeolite syntheses.[2] Within our ongoing studies of the thermodynamics of zeolite formation,[3] both a need and a desire for the quantitative thermodynamic properties (enthalpy of formation and entropy) of tetraalkylammonium halides (TAAX) has developed. In the context of zeolite synthesis, tetrapropylammonium (TPA) fluoride is of particular interest. Since this organic species directs one of the most robust zeolite syntheses, namely the formation of MFI in fluoride media, the MFI-TPA interaction is an important case for which to obtain thermodynamic parameters. Surprisingly, the TPA halides have been the least studied among the symmetric tetraalkylammonium halides, NR_4X, where R = H, Me, Et, *n*-Pr, *n*-Bu and X = F, Cl, Br, I. Homologues with heavier alkyl chains are not of interest here since, being too hydrophobic, they only direct zeolite syntheses with difficulty or not at all.

Herein, the previously reported thermodynamic data on NR_4X salts are presented. For the species for which such quantities are not available, new estimates based on *the most recent measured data* are calculated.

Enthalpies of Formation of Tetraalkylammonium Halides and Hydroxides

Generalities

Experimental values for the heats of solution in water at room temperature, ΔH_{soln}, of several TAA chlorides, bromides and iodides are available and representative data are shown in Table 6.1.[4-11] The heat of solution values and the enthalpies of formation, ΔH_f, for the mono-, di- and tri-alkylammonium heavy halides can be calculated from the corresponding data of amines and hydrogen halides.[12] For quaternary species no such simple thermodynamic cycle is available and early work in this field estimated the formation enthalpies of the tetraalkylammonium halides by extrapolating the ΔH_f values for mono-, di- and tri-substituted ammonium species to the completely substituted quaternary salts.[13,14] More recently, Nagano and co-workers measured the enthalpies of formation for tetramethylammonium (TMA), tetraethylammonium (TEA) and tetrabutylammonium (TBA) iodides by oxygen bomb calorimetry.[15,16] They further used their iodide measurements to calculate the ΔH_f values for TMA, TEA and TBA chlorides by combining the ΔH_f (TAAI) values with the heats of solution of the corresponding chlorides and iodides. Since the objective in the work of Nagano et al. was to provide a thermodynamic description for the changes in the enthalpies

of solution upon the transition from hydrophilic to hydrophobic organic cations, they avoided the intermediate cation TPA that is neither strongly hydrophilic or strongly hydrophobic. This intermediate character is, of course, one of the factors that makes TPA so useful in zeolite synthesis. Here, the measurements of Nagano et al. are used to perform interpolations to estimate the enthalpies of formation of TPACl, TPABr and TPAI.

In sharp contrast to their higher halide homologues, tetraalkylammonium fluorides are extremely hygroscopic[17] and the anhydrous fluorides are kinetically very unstable. In particular, an E_2 elimination of trialkylamine from one of the neighbouring C atoms can take place to form an alkylammonium bifluoride, a trialkylamine and an olefin:[18]

$$2\ (n\text{-}C_4H_9)_4N^+F^- \rightarrow (n\text{-}C_4H_9)_4N^+HF_2^- + (n\text{-}C_4H_9)_3N + CH_3CH_2CH{=}CH_2.$$

Neither a heat of solution or a heat of formation has been reported for *any* simple tetraalkylammonium fluoride due to their strong hygroscopic nature and inherent instability, and the same is true for the hydroxides. The most closely related species for which enthalpy data are available are the alkali-metal cation and ammonium fluorides and hydroxides which, by contrast, can be prepared anhydrous (except NH_4OH). A linear regression procedure to estimate the enthalpies of formation of the TAA (TMA, TEA, TPA and TBA) fluorides and hydroxides, based on ΔH_f (NH_4F) and ΔH_f (NH_4OH), is described below.

Estimation Procedures

Table 6.2 presents the reported enthalpies of formation for Li, Na, K, Rb, Cs, NH_4, TMA, TEA, and TBA halides. For the alkali-metal cation and ammonium salts, the values were obtained from *The NBS Tables of Chemical Thermodynamic Properties* and are accurate to better than 0.8 kJ/mol.[19] The uncertainties in the values for TMA, TEA and TBA halides are all approximately 3.0 kJ/mol (TMAI: 2.7, TMABr: 2.8, TMACl: 2.8, TEAI: 3.2, TEABr: 3.3, TEACl: 3.4, TBAI: 2.7, TBABr: 3.2 and TBACl: 3.1 kJ/mol).[15,16]

All the corresponding values, as discussed above, were measured or calculated by oxygen bomb calorimetry. The main contributor to the reported uncertainties is the enthalpy of combustion of the organic species.

Tetrapropylammonium Heavy Halide Salts

The enthalpies of formation of TPACl, TPABr and TPAI were estimated using group additivity techniques. Specifically, the progressive addition of methylene units to the hydrocarbon branches of the TAA cations was assumed to consistently decrease the enthalpy of formation of $N[(CH_2)_nH]_4^+X^-$ salts by the same amount. This additional enthalpy is the enthalpy of formation of four new C-C and eight new C-H bonds for each unity increase of n. This procedure was

chosen, rather than a calculation from first principles, so as to use the available measured data. The NH_4 halides were excluded from this procedure, since they contain N-H bonds instead of the N-C bonds and cannot truly be considered "n = 0" lower homologues.

Figure 6.1 shows the enthalpies of formation, ΔH_f, for the TMA, TEA and TBA chlorides, bromides and iodides vs. the number of methylene units n. The remarkably linear relationships displayed by the heavy halides have already been noted.[16] This observation lends very strong confidence to an interpolation methodology to estimate ΔH_f (TPAX). A linear regression of ΔH_f (TAAX) to n was performed for n = 1, 2 and 4 for each halide X. Applying the resulting correlation to n = 3 (the TPA halides) yielded the estimated ΔH_f (TPAX) values listed in Table 6.3.

Since the standard errors of regression range from 4.0 to 10.2 kJ/mol (as compared to ~3.0 kJ/mol errors in the original data), the major contribution to the reported uncertainties of 5.2-10.7 kJ/mol is due to the interpolation procedure itself. While they are larger than the uncertainties in the measured data, the uncertainties in calculated TPAX enthalpies represent no more than 2.5% of the ΔH_f values.

The group additivity idea can be further justified by another observation. The difference in the enthalpy values for selected pairs of anions (e.g., ΔH_f (MI) - ΔH_f (MCl)) is given in Table 6.4 for each cation. The difference

between the ΔH_f values of bromides, chlorides and iodides of the same cation remains fairly constant (within 5.7 kJ/mol) among the TAA species when the chains progressively lengthen from TMA to TEA to TBA; this is the expected behavior when group additivity accurately describes the thermodynamics of such a set of compounds. By contrast, the corresponding values for the NH_4 halide pairs are noticeably different (16.9 - 46.8 kJ/mol higher), confirming that the qualitative bonding differences between NH_4 and NMe_4 justify the exclusion of the NH_4X enthalpies from the above correlation.

Fluorides and Hydroxides

Since the enthalpy differences between the NH_4 halides have been shown to take on considerably higher values than the differences between the TAA halides, a simple group additivity approach based on ΔH_f (NH_4F) or ΔH_f (NH_4OH) cannot be used to estimate the enthalpies of formation of the TAA fluorides. Empirically, however, a very nearly linear relation between the ΔH_f values of NH_4 and TAA halides was noticed, as shown in Figure 6.2. In the absence of more rigorous ways to perform the calculations, a linear regression based on the three heavy halides was performed for *each* TAA cation according to ΔH_f (TAAX) = $c_1 + c_2$ ΔH_f (NH_4X) where X is Cl, Br or I.

The resulting linear relationship was then extrapolated to ΔH_f ($NH_4F(s)$) and ΔH_f (NH_4OH, ∞H_2O), i.e.,

$\Delta H_f (TAAF) = c_1 + c_2 \Delta H_f (NH_4F)$.

$\Delta H_f (TAAOH) = c_1 + c_2 \Delta H_f (NH_4OH)$

No enthalpy value for $NH_4OH(s)$ is available, so the enthalpy at infinite dilution was used for the hydroxide correlation: ΔH_f (NH_4OH, ∞H_2O) = - 362.50 kJ/mol.[19] Correspondingly, the calculated enthalpies for the TAAOH species are at infinite dilution as well. The regression results are shown in Table 6.5 along with the corresponding uncertainties calculated by propagation of errors.

The formation of all TAAF species is strongly exothermic, as expected, and the TAA fluorides are in fact 90-100 kJ/mol more stable than their chloride homologues. The uncertainties vary from 3.4 (TEAF) to 15.1 (TMAF) kJ/mol. As expected, the major contributor is the standard error of regression for TBAF and TMAF. For TEAF the linear regression, fortituitously, gives an almost exact fit of the experimental data so the error in the original data dominates the uncertainty. Finally, for the case of TPA where *predicted* ΔH_f values must be used for the chloride, bromide and iodide salts, the much larger error in the data that the regression is based upon dominates the reported uncertainty. The uncertainty propagation for the hydroxides is similar to that for the fluorides and all enthalpies of formation are strongly negative, as expected. The accuracy of the ΔH_f (TAAOH) values, however, may be lower since no data are available to evaluate

how legitimate the extrapolation of the ΔH ($NH_4X(s)$) trend to aqueous NH_4OH really is.

Enthalpy of Formation of TPA^+

The enthalpy of formation of aqueous TPA^+ can be calculated from the heats of solution and formation of TPABr and TPAI according to:

$$\Delta H_f(TPA^+, aq) = \Delta H_f(TPAX) + \Delta H_{soln}(TPAX) - \Delta H_f(X^-, aq)$$

where X stands for Br or I.

The ΔH_{soln} values were obtained from Table 6.1. ΔH_f (Br^-, aq) and ΔH_f (I^-, aq) were taken from reference 19 and are -121.55 ± 0.8 and -55.19 ± 0.8 kJ/mol, respectively. The TPABr thermodynamic cycle leads to $\Delta H_f(TPA^+)$ = -325 ± 10.7 kJ/mol, whereas the TPAI cycle leads to $\Delta H_f(TPA^+)$ = -333 ± 5.3 kJ/mol. The largest contributor to the uncertainty is due to the ΔH_f (TPAX) estimates so the average ΔH_f (TPA^+) will be used and is -329 ± 12.5 kJ/mol. This value was used to calculate the enthalpy of solution of TPAF according to:

$$\Delta H_{soln}(TPAF) = \Delta H_f(TPA^+) + \Delta H_f(F^-, aq) - \Delta H_f(TPAF).$$

With ΔH_f (F^-, aq) = 332.63 ± 0.8 kJ/mol,[19] this expression leads to ΔH_{soln} (TPAF) = -103 ± 16.5 kJ/mol. Such a large negative enthalpy of hydration explains the strongly hygroscopic nature of TPAF. It should be emphasized that this value is

considerably more negative than the heats of solution of the heavier halides TPABr and TPAI (-4.3 and 11.6 kJ/mol, respectively), proving that the interaction between water and TAA halides depends significantly upon the nature of the halide anion.

Entropies of Tetraalkylammonium Halides and Hydroxides

Third-law entropies have been previously reported for TMA,[20] TEA[21] and TPA[21] iodides, as well as for TMACl[22] and TMABr.[22] All values were derived from low-temperature heat capacity measurements. Table 6.6 presents the available data along with the alkali-metal halide entropies. The associated uncertainties for the TAA halide entropies are all significantly lower than 1%: ± 1 J/(mol·K) for TEAI and TPAI, ± 0.2 J/(mol·K) for TMACl and TMABr, and 0.8 J/mol·K for TMAI. The standard entropies of Li, Na, K, Rb, Cs and NH_4 halides were obtained from *The NBS Tables of Chemical Thermodynamic Properties*[19] and are accurate to better than 0.8 J/(mol·K). The standard entropies of LiOH, NaOH and KOH were also from reference 19 and have the same associated uncertainty. The entropies of RbOH and CsOH were obtained from reference 23 and the associated uncertainties are not known.

Entropies of TEACl, TEABr, TPACl and TPABr

The entropies of these four salts, like the enthalpies of formation discussed above, were analyzed with group additivity concepts using the measured iodide entropies as starting points for the calculations. For the various TAA halides, replacing one halogen by another is expected to lead to similar changes in entropy. In other words, the entropy difference S°(MX)-S°(MY) should remain approximately constant for various monovalent cations M for any given halide pair (X, Y) and Table 6.7 shows the differences in entropy for such salt pairs. The differences between chloride and iodide salts, S°(MI)-S°(MCl), range from 17.3-27.5 J/(mol·K), while for bromide-iodide pairs the differences span 4-12 J/(mol·K). Since the spread for the chloride-iodide differences is 10.2 J/(mol·K), entropies of TAA chlorides calculated from those of TAA iodides are expected to have uncertainties of 5.1 J/(mol·K) due to the estimation procedure itself. For the TAA bromides, the corresponding contribution is 4 J/(mol·K). Because of the high accuracy of the data noted above, the numerical uncertainties in calculated entropies are due mostly to the estimation procedure itself.

Note that the entropy differences among the ammonium halides are quite different from those of the TMA salts for which data are available. The reason for this is most likely the significant qualitative change in bonding between NH_4 and

TMA as discussed for the enthalpies. The most appropriate group contribution corrections when comparing TAA chloride and bromide salts to the iodides, then, were chosen to be the entropy differences among TMA halides, since the trends in the entropies of the TEA and TPA salts are expected to be most similar to those of the TMAX entropies.

The entropies of TEA and TPA chlorides and bromides were thus estimated by:

$$S°(TAAX) = S°(TMAX) - S°(TMAI) + S°(TAAI).$$

This procedure yields S°(TEACl) = 293.8, S°(TEABr) = 303.9, S°(TPACl) = 414.81 and S°(TPABr) = 424.9 J/(mol·K). Since the uncertainty in the originally measured quantities was less than 1 J/(mol·K) and the inherent uncertainty in the estimation procedure were 5.1 J/(mol·K) (chlorides) and 4 J/(mol·K) (bromides), by propagation of errors the overall uncertainty in the TEA and TPA bromide and chloride entropies is estimated to be 5.1 (chlorides) and 4.1 (bromides) J/(mol·K) or less than 2 % of the entropy values themselves.

Entropies of Fluoride and Hydroxide Salts

When considering the fluoride salts, larger discrepancies are observed in the S°(MX) - S°(MF) values. For Cl-F pairs the entropy differences range from 8.2-23.6 J/(mol·K) and for I-F pairs the spread is even wider at 30-51 J/(mol·K). The calculated entropies for the fluoride salts, by contrast to those for the

chlorides and bromides discussed above, have a larger uncertainty of up to 10.5 J/(mol·K) introduced from the estimation procedure.

Since the changes in the entropies of the ammonium salts with varying halide ions are quantitatively quite different from that of TMA (see Table 6.7), the entropies of the heavier tetraalkylammonium fluorides cannot be estimated from that of NH_4F. With the monovalent cations, CsBr, CsCl and CsI show entropy differences among salt pairs numerically most similar to those of the TMA salts. Hence, the TAAF entropies were estimated by:

$$S°(TAAF) = S°(TAAI) - S°(CsI) + S°(CsF).$$

Note that since Cs is the largest alkali metal cation for which thermodynamic data are available, it is not unexpected that the TAAF entropies are best approximated using CsF as a starting point. The calculated entropies for TMAF, TEAF and TPAF are 177.8, 280.9 and 401.9 J/(mol·K), respectively. Similar calculations using the chloride and bromide salts (not shown) instead of the iodides are in reasonably good agreement (2.5-4.5 J/(mol·K) higher) with these values. Since the entropies of the iodides were the only measured values (except for TMA), the S°(TAAF) values derived from S°(TAAI) are reported here with the most confidence. As was the case for the heavier halides described above, the uncertainty is dominated by the uncertainty in the estimation procedure and is 10.5 J/(mol·K). This value represents 5.8% of the entropy of TMAF but only 2.6% of the entropy of TPAF. Similar calculations were performed to estimate the entropies of the TAAOH species by:

$$S^\circ (TAAOH) = S^\circ (TAAI) - S^\circ (CsI) + S^\circ (CsOH)$$

and yielded S° (TMAOH) = 183.7 ± 10.0 J/(mol·K), S° (TEAOH) = 286.8 ± 10.0 J/(mol·K) and S° (TPAOH) = 407.8 ± 10.0 J/(mol·K). The entropies of corresponding TAA fluorides and hydroxides are very similar, as expected, due to the closeness in size and bonding patterns between OH^- and F^-. Table 6.8 summarizes all previously unmeasured entropies which were calculated in this study.

Relationship between ΔH_f and S°

Figure 6.3 plots the entropies and enthalpies of the TAA halides and hydroxides against one another. Clearly, no single correlation can describe *all* species plotted on the graph; approximately linear relationships, however, are observed when only the cation or only the anion is varied. Such a result is expected since group additivity methods (which are intrinsically linear) were used for all estimations. The predictive power of Figure 6.3, however, is limited since neither ΔH_f or S° are available for many of the salts of interest for zeolite synthesis.

Implications for the Thermodynamics of the TPA-MFI Interaction

Since anhydrous TAA fluorides cannot be prepared, the original impetus for this work was to evaluate an alternative thermodynamic cycle for obtaining the heat of solution of any TAAF (s) salt; the heats of dissolution of TAABr, MBr and MF, where M is an alkali metal, are combined as follows:

$$MF(s) \rightarrow M^{+}(aq\ HF) + F^{-}(aq\ HF) \quad (1)$$

$$TAABr(s) \rightarrow TAA^{+}(aq\ HF) + Br^{-}(aq\ HF) \quad (2)$$

$$M^{+}(aq\ HF) + Br^{-}(aq\ HF) \rightarrow MBr(s) \quad (3)$$

$$TAAF(s) + MBr(s) \rightarrow MF(s) + TAABr(s) \quad (4)$$

$$TAAF(s) \rightarrow TAA^{+}(aq\ HF) + F^{-}(aq\ HF) \quad (5).$$

Note that the zeolite solution calorimetry experiments take place in HF (see next Chapter). Therefore, the dissolution of the TAAF salts must be conducted in HF and at the same concentration. The enthalpy of solution of the first three steps can easily be measured since all the relevant salts can be prepared anhydrous. To close the cycle and calculate the enthalpy of solution of solid TAAF (ΔH_5), the enthalpy of step (4) was first assumed to be 0 since it is a metathesis reaction. With the estimated TAAF and TAABr enthalpies presented in this note, ΔH_4 can also be evaluated by:

$$\Delta H_4 = \Delta H_f(TAABr) + \Delta H_f(MF) - \Delta H_f(TAAF) - \Delta H_f(MBr)$$

$$= [\Delta H_f(TAABr) - \Delta H_f(TAAF)] - [\Delta H_f(MBr) - \Delta H_f(MF)]$$

The two parts of this expression are the differences between (Br, F) halide pair enthalpies shown in Table 6.3 for the metal M and for the TAA cation. From a cursory examination of the data in Table 6.3, it is apparent that the metal cation for which halide pair enthalpy differences are closest to those for the TAA salts is cesium. This similarity is probably due to the large size of the Cs^+ cations, as noted above for the estimation of the TAAF entropies. In other words, ΔH_4 is expected to be closest to zero when CsBr and CsF are used for steps (1) and (3) above. To provide a numerical estimate of the consequences of the $\Delta H_4 = 0$ assumption, the special case of M = Cs and TAA = TPA was briefly examined. For the purposes of this calculation, the difference between the enthalpies of solution in water (from Table 6.1) and the enthalpies of solution in 25% HF (ΔH_1, ΔH_2, ΔH_3) was ignored. The following measured values are then used to calculate ΔH_4:

* $\Delta H_1 = -37.6$ kJ/mol, $\Delta H_2 = -4.3$ kJ/mol, $\Delta H_3 = -26.3$ kJ/mol,

and

* $\Delta H_4 = -31.9 \pm 16.5$ kJ/mol (estimated from the data in Tables 6.3, 6.4 and 6.5). Assuming $\Delta H_4 = 0$, then, leads to $\Delta H_5 = -68.2$ kJ/mol, compared to the more accurate value of -100.1 ± 16.5 kJ/mol based on the estimated TPA halide enthalpies. The difference between these two values is 30% and could possibly lead to quite large errors in the interaction enthalpies of the zeolite and TAAF salt.

The extent to which this 30% discrepancy affects the calculated interaction enthalpies was evaluated next.

The enthalpy of interaction between TPAF and pure-silica MFI was determined by Patarin and co-workers by HF calorimetry[23] and their heats of solution were used here to calculate ΔH_i with both ΔH_4 values. The relevant thermodynamic cycle can be denoted by

$$[(SiO_2)_{96}\ (MFI)] \rightarrow 96Si^* \qquad (6)$$

$$[(SiO_2)_{96} - 4TPAF] \rightarrow 4TPA^+(aq\ HF) + 4F^-\ (aq\ HF) + 96Si^* \qquad (7)$$

$$TPAF(s) \rightarrow TPA^+(aq\ HF) + F^-\ (aq\ HF) \qquad (5)$$

where Si* represents the silicate species in HF solution. The interaction enthalpy was calculated as $\Delta H_i = \Delta H_6 - \Delta H_7 + 4\ \Delta H_5$, and described by the reaction

$$(SiO_2)_{96}(MFI) + 4\ TPAF(s) \rightarrow [(SiO_2)_{96} - 4\ TPAF] \qquad (8).$$

The reported enthalpies of solution of MFI in 25% HF were $\Delta H_6 = -13250.8 \pm 86.5$ kJ/mol (calcined) and $\Delta H_7 = -12653 \pm 89$ kJ/mol (as-made).[23] When the enthalpy of the metathesis reaction was neglected and $\Delta H_5 = -68.2$ kJ/mol was utilized, an interaction enthalpy of -871 ± 124 kJ/ 96 mol SiO_2 was obtained. With $\Delta H_5 = -100.1$, by contrast, $\Delta H_i = -998.2 \pm 128$ kJ/ 96 mol SiO_2 was calculated. The difference between the two quantities is 13% and is at the extreme limit of the reported uncertainties. Note that the uncertainty introduced by the nonzero ΔH_4 does not lead to significantly higher uncertainties in the calculated ΔH_i. Patarin et al. reported $\Delta H_i = -596.8 \pm 230.3$ kJ/mol[23] when taking $\{TPA^+(aq)$

+ F^- (aq)} as the initial state of TPAF. When the initial state is chosen to be TPAF(s), correcting their value for the hydration of the salt lead to ΔH_i = -1008.8 ± 230 kJ/96 mol SiO_2. This value is in very close agreement with the -998.2 ± 128 kJ/96 mol SiO_2 value calculated with a nonzero ΔH_4, confirming the need to estimate the thermodynamics of the metathesis step if the cycle (1)-(4) is to be used to calculate the enthalpy of hydration of TAA fluorides.

For TEA and TPA, ΔH_4 can be estimated using the calculations above. Alternatively, if larger alkylammonium salts form less hygroscopic fluorides, the enthalpy of solution for both the bromide and fluoride of such a cation could be used in steps (1) and (3) above. Another possible choice, of course, was to take *aqueous* TAA^+ and F^- as the initial state of the SDA for the thermodynamic cycle of the interaction enthalpy since solutions of the TAAF species can easily be prepared. As is discussed in the next Chapter, the dilute TAA^+ and F^- ions in 25% HF provided a convenient reference state.

Summary

Enthalpies of formation for TPACl, TPABr and TPAI and entropy values for TEACl, TEABr, TPACl and TPABr are presented with high confidence (±2.5% or better uncertainty). Estimated values for the enthalpies and entropies of

TMAF, TEAF and TPAF and the corresponding hydroxides are necessarily more uncertain due to the lack of data for *any* TAA fluorides, but the uncertainty is no more than 5.5% (entropies) and 4.3% (enthalpies). Since the fluoride salt thermodynamics *cannot be determined* due to the difficulties in synthesizing anhydrous TAAF salts, these estimations will prove to be useful.

Table 6.1. Reported Enthalpies of Solution for Monovalent Halides (kJ/mol)

Cation	F	Cl	Br	I
Li	N/A	-37.2 [4]	-48.8 [5]	-63.2 [4]
Na	0.8 [4]	3.8 [6]	-0.6 [5]	-7.6 [6]
K	-17.6 [4]	17.2 [4]	19.9 [5]	20.4 [6]
Rb	-25.9 [4]	17.2 [4]	21.9 [5]	25.1 [5]
Cs	-37.7 [4]	18.0 [4]	26.3 [5]	31.2 [7]
NH4	N/A	15.0 [8]	17.3 [5]	N/A
TMA	N/A	4.1 [9]	24.5 [5]	41.8 [10]
TEA	N/A	-12.1 [11]	6.0 [5]	28.2 [10]
TPA	N/A	N/A	-4.3 [5]	11.6 [10]
TBA	N/A	-28.9 [11]	-8.2 [5]	15.0 [11]

Table 6.2. Reported Enthalpies of Formation for Monovalent Halides and Hydroxides (kJ/mol)

Cation	F	Cl	Br	I	Naked aq	Hydroxides
Li	-615.97	-408.61	-351.213	-270.41	-278.49	-479.139
Na	-573.647	-411.153	-361.062	-287.78	-240.12	-425.609
K	-567.27	-436.747	-393.798	-327.9	-252.38	-424.764
Rb	-557.7	-435.35	-394.59	-333.8	-251.17	-418.19
Cs	-553.5	-443.04	-405.81	-346.6	-258.28	-417.23
NH4	-463.96	-314.43	-270.83	-201.42	-132.51	-362.5
TMA	N/A	-276.4	-251.2	-203.9	-105.2	N/A
TEA	N/A	-369.4	-342.7	-300.2	-215.1	N/A
TPA	N/A	N/A	N/A	N/A	N/A	N/A
TBA	N/A	-564.8	-540.3	-498.6	-426.7	N/A
none	-332.63	-167.159	-121.55	-55.19	N/A	-229.994

Table 6.3. Estimation of Enthalpies of TPACl, TPABr, TPAI (kJ/mol)

Chlorides

n in $N[(CH2)_nH]^+$	ΔH_f exptl	ΔH_f predicted	Uncert.		Coefficients	Std. Error
1	-276.4	-275.1		Intercept	-178.7	3.1
2	-369.4	-371.4		Slope	-96.4	1.2
4	-564.8	-564.1			reg. error	6.6
3	N/A	-467.8	7.4			

Bromides

n in $N[(CH2)_nH]^+$	ΔH_f exptl	ΔH_f predicted	Uncert.		Coefficients	Std. Error
1	-251.2	-249.1		Intercept	-152.4	4.8
2	-342.7	-345.8		Slope	-96.7	1.8
4	-540.3	-539.2			reg.error	10.2
3	N/A	-442.5	10.7			

Iodides

n in $N[(CH2)_nH]^+$	ΔH_f exptl	ΔH_f predicted	Uncert.		Coefficients	Std. Error
1	-203.9	-203.1		Intercept	-104.7	1.9
2	-300.2	-301.4		Slope	-98.4	0.7
4	-498.6	-498.2			reg.error	4.1
3	N/A	-399.8	5.2			

Table 6.4. Differences between Halide Pair Enthalpies based on Reported Values (kJ/mol)

Cation	Cl-F	Br-F	I-F	Br-Cl	I-Cl	I-Br	OH-I
Li	207.4	264.8	345.6	57.4	138.2	80.8	-208.7
Na	162.5	212.6	285.9	50.1	123.4	73.3	-137.8
K	130.5	173.5	239.4	42.9	108.8	65.9	-96.9
Rb	122.4	163.1	223.9	40.8	101.6	60.8	-84.4
Cs	110.5	147.7	206.9	37.2	96.4	59.2	-70.6
NH4	149.5	193.1	262.5	43.6	113.0	69.4	-161.1
TMA	N/A	N/A	N/A	25.2	72.5	47.3	N/A
TEA	N/A	N/A	N/A	26.7	69.2	42.5	N/A
TPA	N/A	N/A	N/A	N/A	N/A	N/A	N/A
TBA	N/A	N/A	N/A	24.5	66.2	41.7	N/A
none	165.5	211.1	277.4	45.6	112.0	66.4	-174.8

Table 6.5. Estimation of Tetraalkylammonium Fluoride and Hydroxide Enthalpies (kJ/mol)

TMA			correlated			
Anion, X	$\Delta H_f(NH_4X)$	$\Delta H_f(TMAX)$	$\Delta H_f(TMAX)$		Coefficients	Std error
				Intercept	-74.6	7.4
Cl	-314.43	-276.4	-277.5	Slope	0.65	0.03
Br	-270.83	-251.2	-249.4			
I	-201.42	-203.9	-204.6			
F	-463.96	N/A	-374.0		reg error	14.9
OH	-362.5	N/A	-308.5		reg error	12.5

TEA			correlated			
Anion, X	$\Delta H_f(NH_4X)$	$\Delta H_f(TEAX)$	$\Delta H_f(TEAX)$		Coefficients	Std error
				Intercept	-176.9	5.9E-03
Cl	-314.43	-369.4	-369.4	Slope	0.61	2.2E-05
Br	-270.83	-342.7	-342.7			
I	-201.42	-300.2	-300.2			
F	-463.96	N/A	-461.0		reg error	0.01
OH	-362.5	N/A	-398.8		reg error	0.01

TPA			correlated			
Anion, X	$\Delta H_f(NH_4X)$	$\Delta H_f(TPAX)$	$\Delta H_f(TPAX)$		Coefficients	Std error
				Intercept	-278.7	2.7
Cl	-314.43	-467.8	-468.2	Slope	0.6	0.01
Br	-270.83	-442.5	-441.9			
I	-201.42	-399.8	-400.1			
F	-463.96	N/A	-558.3		reg error	5.3
OH	-362.5	N/A	-497.1		reg error	4.5

TBA			correlated			
Anion, X	$\Delta H_f(NH_4X)$	$\Delta H_f(TBAX)$	$\Delta H_f(TBAX)$		Coefficients	Std error
				Intercept	-380.6	2.8
Cl	-314.43	-564.8	-565.2	Slope	0.59	0.01
Br	-270.83	-540.3	-539.6			
I	-201.42	-498.6	-498.9			
F	-463.96	N/A	-653.0		reg error	5.6
OH	-362.5	N/A	-593.4		reg error	4.7

Summary Enthalpies		unc.(kJ/mol)
TMAF	-374.0	15.1
TEAF	-461.0	3.4
TPAF	-558.3	11.5
TBAF	-653.0	6.4
TMAOH	-308.5	12.8
TEAOH	-398.8	3.4
TPAOH	-497.1	11.1
TBAOH	-593.4	5.7

Table 6.6. Reported Entropies of Monovalent Halides and Hydroxides (J/(mol·K))

Cation	F	Cl	Br	I	Naked aq	OH
Li	35.65	59.33	74.27	86.78	13.4	42.8
Na	51.46	72.13	86.82	98.53	59	64.455
K	66.57	82.59	95.9	106.32	102.5	78.9
Rb	N/A	95.9	109.96	118.41	121.5	92
Cs	92.8	101.17	113.05	123.05	133	98.7
NH4	71.96	94.6	113	117	N/A	N/A
TMA	N/A	190.71	200.8	208	210	N/A
TEA	N/A	N/A	N/A	311.1	283	N/A
TPA	N/A	N/A	N/A	432.1	336	N/A
none	-13.8	56.5	82.4	111.3	N/A	10.75

Table 6.7. Differences between Halide and Hydroxide Pair Entropies (J/(mol·K))

Cation	S(MCl) -S(MF)	S(MBr) -S(MF)	S(MI) -S(MF)	S(MBr) -S(MCl)	S(MI) -S(MCl)	S(MI) -S(MBr)	S(M+,aq) -S(MI)	S(MOH) -S(MI)
Li	23.7	38.6	51.1	14.9	27.5	12.5	-73.4	-44.0
Na	20.7	35.4	47.1	14.7	26.4	11.7	-39.5	-34.1
K	16.0	29.3	39.8	13.3	23.7	10.4	-3.8	-27.4
Rb	N/A	N/A	N/A	14.1	22.5	8.5	3.1	-26.4
Cs	8.4	20.3	30.3	11.9	21.9	10.0	10.0	-24.4
NH_4	22.6	41.0	45.0	18.4	22.4	4.0	N/A	N/A
TMA	N/A	N/A	N/A	10.1	17.3	7.2	2.0	N/A
TEA	N/A	N/A	N/A	N/A	N/A	N/A	-28.1	N/A
TPA	N/A	N/A	N/A	N/A	N/A	N/A	-96.1	N/A
none	70.3	96.2	125.1	25.9	54.8	28.9	N/A	-100.6

Table 6.8. Estimated Tetraalkylammonium Halide and Hydroxide Entropies (J/(mol·K))

salt	S (J/mol·K)	Uncert. (J/mol·K)
TEACl	293.8	5.2
TEABr	303.9	4.1
TPACl	414.8	5.2
TPABr	424.9	4.1
TMAF	177.8	10.5
TEAF	280.9	10.5
TPAF	401.9	10.5
TMAOH	183.7	10
TEAOH	286.8	10
TPAOH	407.8	10

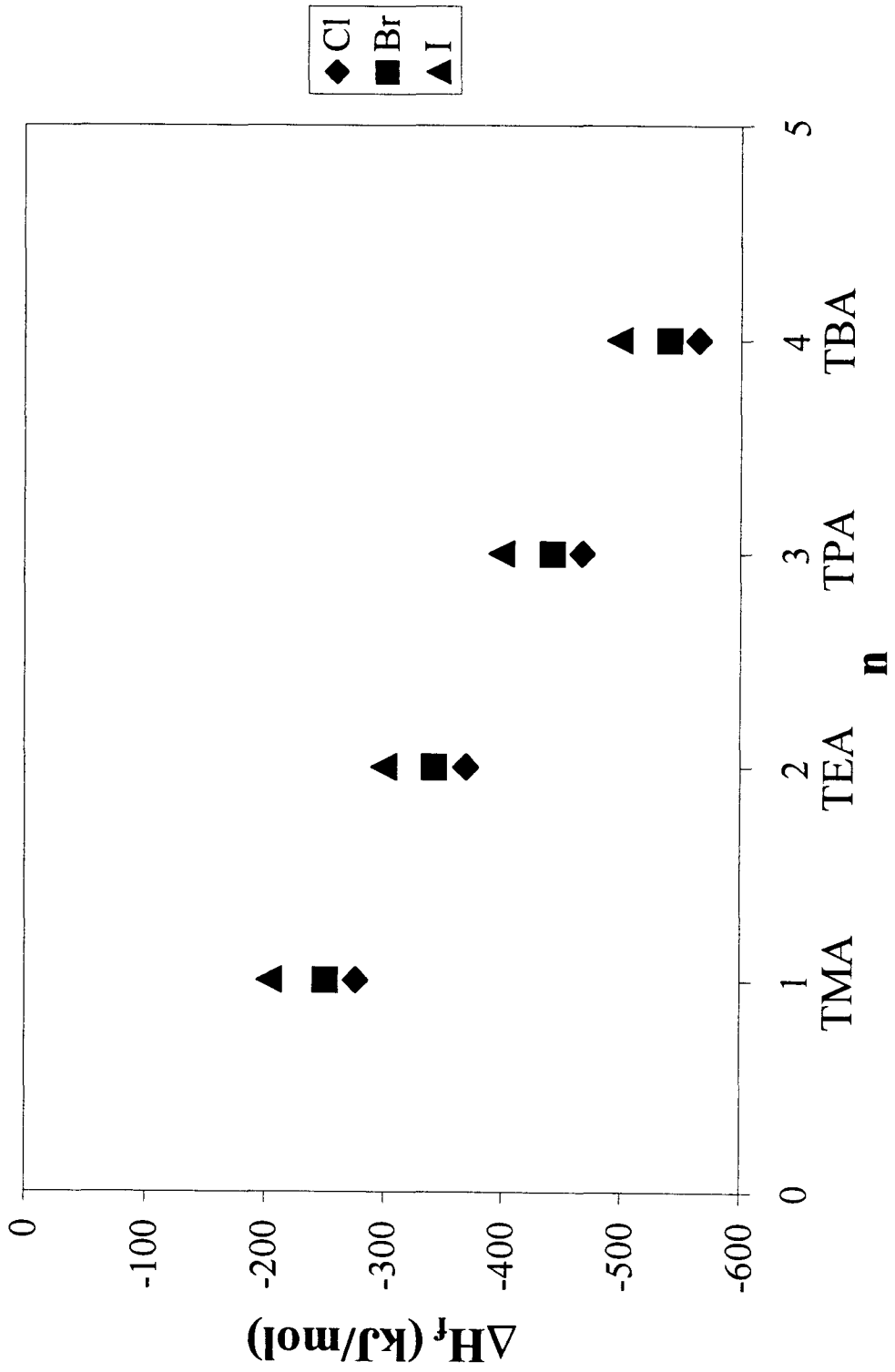

Figure 6.1. Enthalpy of Formation of TAA Halides vs. n

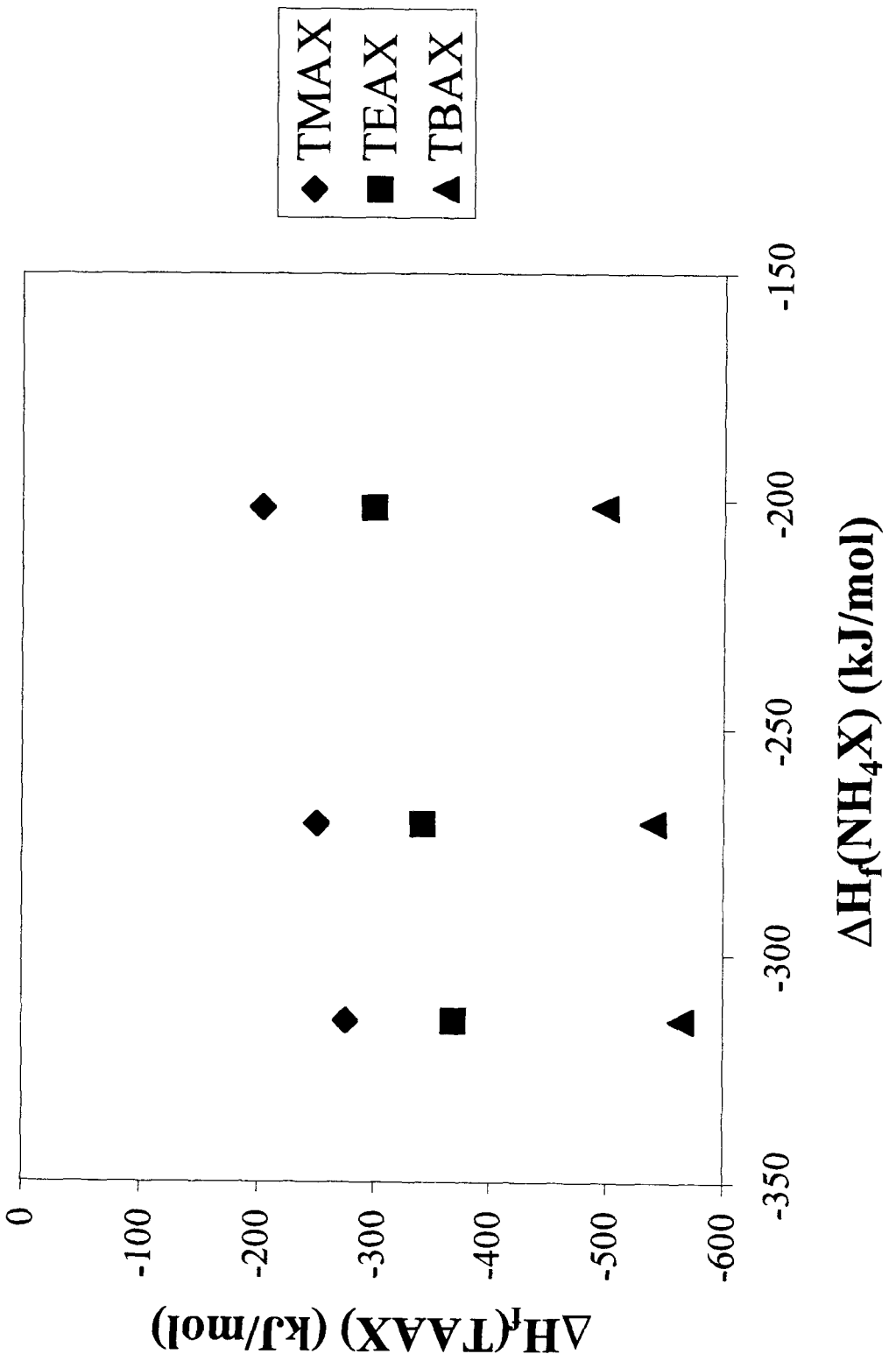

Figure 6.2. Empirical Relation between $\Delta H_f(TAAX)$ and $\Delta H_f(NH_4X)$

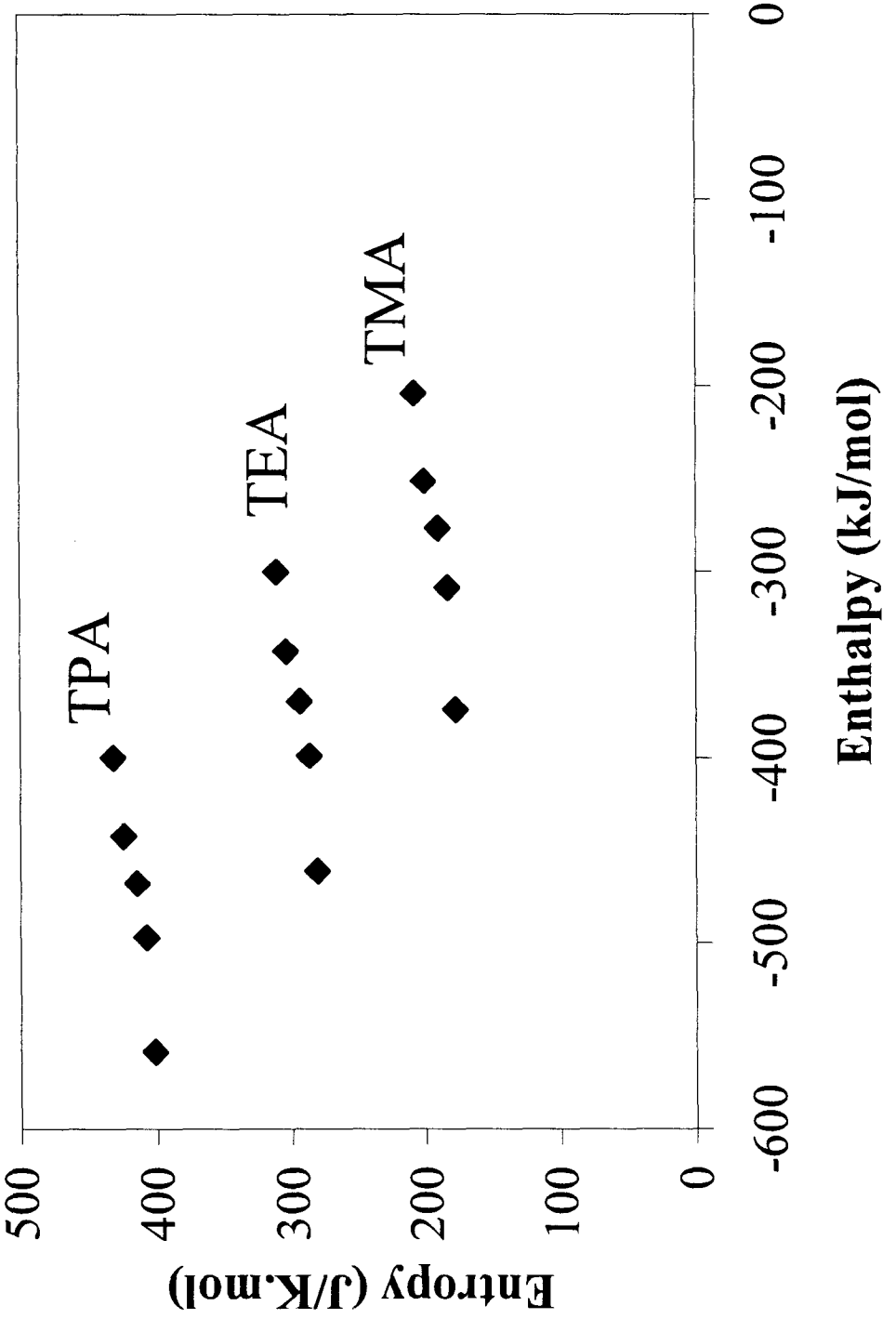

Figure 6.3. Relationship between ΔH_f and S° for TAA Halides and Hydroxides

References

[1] Kameyama, A.; Kiyota, M.; Nishikubo, T. *Tetrahedron Lett.* **1994**, *35*, 4571.

[2] Gies, H.; Marler, B. *Zeolites* **1992**, *12*, 42.

[3] Piccione, P. M.; Laberty, C.; Yang, S.; Camblor, M. A.; Navrotsky, A.; Davis, M. E. *J. Phys. Chem. B* **2000**, *104*, 10001.

[4] Cox, B. G.; Hedwig, G. R.; Parker, A. J.; Watts, D. W. *Aust. J. Chem.* **1974**, *27*, 477.

[5] Somsen, G. *Pure Appl. Chem.* **1993**, *65*, 983.

[6] Johnsson, M; Persson, I. *Inorg. Chim. Acta* **1987**, *127*, 25.

[7] Arnett, E. M. *J. Am. Chem. Soc.* **1966**, *88*, 2598.

[8] Juillard, J. *J. Chem. Soc. Faraday Trans. I* **1982**, *78*, 37.

[9] Parker, V.B. *Thermal Properties of Aqueous Uni-univalent Electrolytes* **1965**, NBS:Washington, DC.

[10] Bhatnagar, O. N.; Criss, C. M. *J. Phys. Chem.* **1969**, *73*, 174.

[11] Ahland, S.; Ishigmo, S.; Portanova, R. *Aust. J. Chem.* **1983**, *36*, 1805.

[12] Finch, A.; Hall, F. M. *J. Chem. Soc. Dalton Trans.* **1982**, 915.

[13] Wilson, J. W. *J.C.S. Dalton* **1975**, 890.

[14] Derakhsan, B. M.; Finch, A.; Gates, P. N.; Stephens, M. *J. Chem. Soc. Dalton Trans*, **1984**, 601.

[15] Nagano, Y.; Sakiyama, M.; Fujiwara, T.; Kondo, Y. *J. Phys. Chem.* **1988**, *92*, 5823.

[16] Nagano, Y.; Mizuno, H.; Sakiyama, M.; Fujiwara, T.; Kondo, Y. *J. Phys. Chem.* **1991**, *95*, 2356.

[17] Derweik, S.; Sasson, Y. *J. Org. Chem.* **1989**, *54*, 4827.

[18] Christe, K. O.; Wilson, W. W.; Wilson, R. D.; Bau, R.; Feng, J. *J. Am. Chem. Soc.* **1990**, *112*, 7619.

[19] Wagman, D.D.; Evans, W. H.; Parker, V. B.; Schumm, R. H.; Halow, I.; Bailey, S. M.; Churney, K. L.; Nuttall, R. L. *J. Phys. Chem. Ref. Data* **1982**, *11 suppl. 2*.

[20] Coulter, L. V; Pitzer, K. S.; Latimer, W. *J. Am. Chem.Soc.* **1940**, *62*, 2845.

[21] Johnson, D. A.; Martin, J. F. *J. Chem. Soc. Dalton Trans.* **1973**, 1585.

[22] Chang S.-S.; Westrum Jr., E. F. *J. Chem. Phy.* **1962**, *36*, 2420.

[23] Binnewies, M.; Milke, E. *Thermochemical Data of Elements and Compounds*, **1999**, Wiley-VCH: Weinheim.

[24] Patarin, J.; Soulard, M.; Kessler, H.; Guth, J.L.; Diot, M. *Thermochim. Acta* **1989**, *146*, 21.

Chapter Seven

Thermodynamics of Pure-Silica Molecular Sieve Synthesis

Abstract

The thermodynamics of pure-silica molecular sieves (structural codes *BEA, MFI, MTW, and STF) are investigated by solution calorimetry at 323.15 K using 25% aqueous HF as solvent. The enthalpies of solution are determined for both calcined (silica frameworks) and organic structure-directing agent occluded samples (SDAs: tetraethylammonium (TEA), tetrapropylammonium (TPA), trimethylenebis(*N*-methyl,*N*-benzylpiperidinium) (BISPIP) and 2,6-dimethyl-1-aza-spiro[5.4]decane (SPIRO)). These measurements provide data sufficient to calculate interaction enthalpies between the molecular sieve frameworks and SDAs at 323.15 K and they are as follows: *BEA/TEA: -3.1±1.4 kJ/mol SiO_2 (-32±15 kJ/mol SDA), *BEA/BISPIP: -5.9±0.7 kJ/mol SiO_2 (-181±21 kJ/mol SDA), MFI/TEA: -1.1±1.4 kJ/mol SiO_2 (-27±33 kJ/mol SDA), MFI/TPA: -3.2±1.4 kJ/mol SiO_2 (-81±34 kJ/mol SDA), MTW/BISPIP: -1.6±1.3 kJ/mol SiO_2 (-124±97 kJ/mol SDA), STF/SPIRO: -4.9±0.9 kJ/mol SiO_2 (-83±16 kJ/mol SDA). The magnitudes of the interaction energies between the pure-silica molecular sieves and their organic SDAs is consistent with that expected if the predominant interactions are van der Waals contacts between the hydrophobic silica frameworks and the hydrocarbon portions of the SDAs.

Interaction entropies can be estimated, and when used in combination with interaction enthalpies allow the calculation of the Gibbs free energies of

interaction: *BEA/TEA: -5.4±1.5 kJ/mol SiO_2; MFI/TEA: -2.0±1.4 kJ/mol SiO_2; and MFI/TPA: -4.9±1.4 kJ/mol SiO_2. These values are smaller than twice the available thermal energy at molecular sieve synthesis temperatures. This energy range is comparable to the range observed for the molecular sieve frameworks alone, showing that energetics of both the frameworks and of the molecular sieve/SDA interactions must be considered in order to adequately describe molecular sieve synthesis. The energetics of the synthesis of molecular sieves (considering all components present in the synthesis mixture) are examined here and reveal small differences between various molecular sieve/SDA combinations. Assuming complete transformation of the silica, the Gibbs free energy changes during molecular sieve crystallization are as follows: *BEA/TEA: -8.5±2.9 kJ/mol SiO_2; MFI/TEA: -4.9±2.8 kJ/mol SiO_2; and MFI/TPA: -8.1±2.8 kJ/mol SiO_2. The strong selectivity of organic SDAs experimentally observed in the face of the comparatively small energetic differences suggests that kinetic factors are of major importance in molecular sieve preparation.

Introduction

Zeolites and related materials are industrially very useful materials. These porous, crystalline aluminosilicates can act as heterogeneous catalysts, ion-

exchange materials, and absorbants.[1] Strongly acidic or basic sites, as well as catalytically active metal ions, can further be incorporated into these materials by suitable chemical modifications.[2] Other heteroatoms (B^{+3}, Ti^{+4}) than the naturally occuring Al^{+3} have also been incorporated into the framework of synthetic zeolite-like structures and the broad class of these materials is termed *molecular sieves*.[3] In sharp contrast to the amount of practical information available on various applications of molecular sieves, their syntheses are still not well understood at the fundamental level. Extensive screening of different organocations (structure-directing agents, SDAs) and conditions are the only currently available method for producing new framework structures.[4-6]

While purely thermodynamic data are not relevant to the kinetics of molecular sieve syntheses, knowledge of the energetics of different structures provides necessary data to rationalize the mechanisms and interactions important in molecular sieve self-assembly. The thermodynamically stable polymorph of silica at ambient conditions is the naturally occurring mineral, α-quartz. Pure-silica molecular sieves are therefore *metastable* polymorphs of SiO_2, with no thermodynamic stability field, at least not without considering the interactions between the silica and the other components (water, SDA).[7] A quantitative assessment of the energetics of the molecular sieve-SDA interaction, then, is clearly necessary and relevant to molecular sieve science in its effort to produce new materials with given desirable features (e.g., larger pores) by design.

Prior studies on molecular sieve thermodynamics have typically focused on obtaining the thermodynamic parameters for empty frameworks and very few studies determining interaction enthalpies are available. Petrovic and co-workers[8] and Piccione et al.[7] determined the enthalpy for the transition from quartz to molecular sieve, ΔH_{trans}^{298}, for 14 pure-SiO_2 molecular sieves covering a wide range of structural features:[9] FAU, AFI, MEL, MFI, MTW[8] and AST, *BEA, CHA, CFI, IFR, ISV, ITE, MEL, MFI, MWW, STT.[7] Both studies found that the range of enthalpies spanned by pure-silica molecular sieves is very narrow (6.6-14.4 kJ/mol less stable than quartz[7]) and showed that molecular sieve transformations are not appreciably hindered on the basis of enthalpy. They further argued that the role of the SDA in molecular sieve syntheses is in the formation of organic-inorganic composites that select one set of structures over another in early stages of the self-assembly process. Piccione et al.[7] further showed that the presence of silanol defect groups in calcined molecular sieves results in only very small destabilizing effects ($\leq$ 2.4 kJ/mol). Boerio-Goates et al.[10] and Piccione et al.[11] determined the heat capacities and entropies of four pure-silica molecular sieves by low-temperature adiabatic calorimetry. The molecular sieve entropies reported by these authors range from 3.2-4.2 J/(mol·K) above quartz, and the entropy differences between SiO_2 polymorphs affect the relative Gibbs free energies less than the enthalpy differences.[11] There are therefore no strong thermodynamic barriers to transformations between SiO_2 polymorphs. Extensive tabulations of

thermodynamic data for natural zeolites are also available,[12] but their interpretation is complicated by the changing composition of the natural minerals.

Patarin et al.[13-14] studied the effect of different SDAs on pure-Si MFI by HF calorimetry and found tetrapropylammonium ions (TPA^+) to stabilize MFI considerably more than either di- or tri-propylammonium cations. The enthalpy of stabilization from molecular sieve and aqueous TPA^+F^- was reported to be -6.2±2.4 kJ/mol SiO_2 whereas it is positive for the other cations. The authors attributed this difference to the high specificity of the TPA^+ cation toward the formation of MFI.[14] Helmkamp and Davis combined previous investigators' enthalpy data and estimated the entropy of interaction between MFI and TPA^+ by assuming that the state of the cation in the MFI cages is identical to that of TPA^+ in solid TPAF.[15] Their procedure yielded a Gibbs free energy of interaction between MFI and TPA, ΔG_{int}^{298} (MFI/TPA), of –7.9 kJ/mol SiO_2. They further calculated the Gibbs free energy of formation of MFI/TPA from aqueous TPA^+F^- and silica glass, a SiO_2 polymorph that should be representative of the actual amorphous silicas often used in molecular sieve synthesis. Their ΔG_{rxn}^{298} value is -10.9 kJ/mol SiO_2 and these workers concluded that there is a moderate thermodynamic driving force for the formation of MFI/TPA from amorphous silica precursors and aqueous TPA^+.[15]

Solution calorimetry near room-temperature using 25% aqueous HF solvent at 323.15 K is employed here to measure the enthalpies of interaction

between six pure-SiO_2 molecular sieve/organic SDA pairs with standard errors of ± 0.7 to ± 1.4 kJ/mol SiO_2. First, the interaction enthalpies of the commonly synthesized molecular sieve ZSM-5 (MFI) with the two symmetric SDAs tetraethylammonium (TEA^+) and TPA^+ were compared to examine the effect of changing cation sizes. The MFI/TPA^+ interaction enthalpy was also used to compare with the previously reported data.[13-14] To further investigate the dependence of the interaction enthalpy on cation size, the interaction between zeolite beta (*BEA) and the two organics TEA and trimethylenebis(*N*-methyl,*N*-benzyl,piperidinium) (BISPIP) was studied. The interaction enthalpy between the ZSM-12 (MTW) framework and the BISPIP SDA was determined to examine how the dimensionality of the inorganic framework affects the MS/SDA energetics: MTW is a one-dimensional (1-D) framework whereas *BEA is three-dimensional (3-D), yet both structures can be made from the BISPIP SDA. Finally, the interaction between the SSZ-35 (STF) framework and the 2,6-dimethyl-1-aza-spiro[5.4]decane (SPIRO) cation was investigated as a model for the case of a rigid, bicyclic SDA. All molecular sieves studied in this work were prepared using fluoride as the mineralizing agent;[16] this anion is well-known to minimize the formation of silanol (Si-O-H) defect groups.[17-18] The Gibbs free energies of interaction are calculated for the *BEA/TEA, MFI/TEA, and MFI/TPA pairs for which there are sufficient literature data to estimate the entropy of interaction. For these three pairs, estimates of the Gibbs free energy changes in the synthesis mixture during molecular sieve crystallization are also calculated. The

results and their implications with regard to which interactions are most important for the self-assembly of molecular sieves are presented.

Experimental Section

Molecular Sieve Samples

Each molecular sieve sample will be denoted here by MS/SDA where MS is the structural code of the framework and SDA is the occluded structure-directing agent (or calc for calcined materials).

*BEA/TEA. The TEAF-mediated synthesis of pure-SiO_2 *BEA employed a reaction composition of 1 SiO_2: 0.5 TEAF: 7.25 H_2O.[19] The SiO_2 source was tetraethoxysilane (TEOS) and the reaction mixture was hydrolyzed before starting the synthesis proper; two rotary evaporations ensured the removal of all the EtOH formed by hydrolysis. After reaction at 413 K and autogeneous pressure for 14 days in a Teflon-lined stainless steel reactor, the product was collected by cooling the mixture to room temperature, filtering and washing with water, then acetone.

*BEA/calc. The *BEA/TEA sample synthesized by the procedure listed above was calcined in air at 823 K for 6 hours to remove the occluded organic.

*BEA/BISPIP. The trimethylenebis(*N*-methyl,*N*-benzyl,piperidinium) fluoride mediated synthesis of pure-SiO_2 *BEA used a gel composition of 1 SiO_2:

0.27 BISPIP$(OH)_2$: 0.54 HF: 7 H_2O where BISPIP is trimethylenebis(*N*-methyl,*N*-benzyl,piperidinium), synthesized as described below.[20] The SiO_2 source was tetraethoxysilane (TEOS) and the reaction mixture was hydrolyzed before starting the synthesis proper; two rotary evaporations ensured the removal of all the EtOH formed by hydrolysis. 0.2% *BEA/BISPIP crystals prepared in a similiar manner were added as seeds. After reaction at 423 K and autogeneous pressure for 14 days in a Teflon-lined stainless steel reactor, the product was collected by cooling the mixture to room temperature, filtering and washing with water, then acetone.

MFI/TEA. The TEAF-mediated synthesis of pure-SiO_2 MFI employed a reaction composition of 1 SiO_2: 0.5 TEAF: 15 H_2O. The silica source for this synthesis was Cab-O-Sil M-5 and the gel was seeded with 5% calcined MFI. After reaction at 448 K and autogeneous pressure for 55 days in a Teflon-lined stainless steel reactor, the products were collected by cooling the mixture to room temperature, filtering and washing with water then acetone.

MFI/TPA. Pure-SiO_2 MFI was prepared from a gel composition of 1 SiO_2: 0.11 TPABr: 0.56 NH_4F: 21 H_2O where TPA is tetrapropylammonium.[21] The silica source for this synthesis was Cab-O-Sil M-5. After reaction at 469 K and autogeneous pressure for 5 days in a Teflon-lined stainless steel reactor, the product was collected by cooling the mixture to room temperature, filtering and washing with water then acetone. Syntheses performed in the presence of NH_4F were found to result in smaller amounts of silanol defects than syntheses performed in the absence of it.

MFI/calc. Pure-SiO_2 MFI was prepared from a gel composition of 1 SiO_2: 0.44 TPAOH: 0.5 HF: 8 H_2O where TPA is tetrapropylammonium. The silica source for this synthesis was Cab-O-Sil M-5. After reaction at 448 K and autogeneous pressure for 6 days in a Teflon-lined stainless steel reactor, the product was collected by cooling the mixture to room temperature, filtering and washing with water then acetone. This MFI/TPA sample was calcined in air at 823 K for 6 hours to remove the occluded organics.

MTW/BISPIP. The trimethylenebis(*N*-methyl,*N*-benzyl,piperidinium) fluoride mediated synthesis of pure-SiO_2 MTW used a gel composition of 1 SiO_2: 0.27 BISPIP$(OH)_2$: 0.54 HF: 40 H_2O where BISPIP is trimethylenebis(*N*-methyl,*N*-benzyl,piperidinium), synthesized as described below. The SiO_2 source was tetraethoxysilane (TEOS) and the reaction mixture was hydrolyzed before starting the synthesis proper; two rotary evaporations ensured the removal of all the EtOH formed by hydrolysis. After reaction at 448 K and autogeneous pressure for 23 days in a Teflon-lined stainless steel reactor, the products were collected by cooling the mixture to room temperature, filtering and washing with water, then acetone.

MTW/calc. The MTW sample above was calcined in air at 1173 K for 3 hours to remove the occluded organics. Calcinations at lower temperatures were not successful in completely removing the occluded cations (such samples were perceptibly colored).

STF/SPIRO. Pure-SiO_2 STF was prepared from a gel composition of 1 SiO_2: 0.5 SPIRO(OH): 0.5 HF: 15 H_2O where SPIRO is 2,6-dimethyl-1-aza-spiro[5.4]decane synthesized as described below. The SiO_2 source was tetraethoxysilane (TEOS) and the reaction mixture was hydrolyzed before starting the synthesis proper; the synthesis mixture was allowed to evaporate at room temperature for three days to remove the EtOH formed by hydrolysis. After reaction at 423 K and autogeneous pressure for 22 days in a Teflon-lined stainless steel reactor tumbling at 43 rpm, the products were collected by cooling the mixture to room temperature, filtering and washing with water, then acetone.[22]

STF/calc. The STF/SPIRO sample synthesized above was calcined in air at 1073 K for 3 hours to remove the occluded organics.

Organic Structure-Directing Agents

A solution of tetrapropylammonium fluoride was prepared by reacting stoechiometric amounts of TPAOH (40%, Alfa) and HF (48%, Mallinckrodt). A solution of tetraethylammonium fluoride was prepared by reacting stoechiometric amounts of TEAOH (40%, Alfa) and HF (48%, Mallinckrodt). The exact concentrations of the tetraalkylammonium hydroxide and HF solutions were determined by standard titration techniques.

Trimethylenebis(*N*-methyl,*N*-benzyl,piperidinium) **(I)** dibromide was prepared by the reaction of 9.580 g trimethylenebis(*N*-methylpiperidine) (40 mmol)

with 17.26 g (101 mmol) benzyl bromide in 240 ml ethyl acetate.[20] After reaction at room temperature for 19 hours, a white precipitate had separated that was recovered by suction filtration and washing with excess ethyl acetate. The diquaternary salt was recrystallized from a mixture of ethyl acetate and ethanol (overall yield: 79%). 5.81 g of BISPIP dibromide were dissolved in 50 ml water to yield a solution of approximately 0.2 mol/l. This solution was ion exchanged twice over BioRad Ag1-X8 hydroxide ion exchange resin. The fluoride salt was prepared by reacting the hydroxide solution with the stoechiometric amount of aqueous HF.

The SDA, 2,6-dimethyl-1-aza-spiro[5.4]decane **(II)** appears as entry 21 in Table 3 of reference 22. The SDA was made in its iodide form by a 1-step reaction between 2,6-dimethylpiperidine and 1,4-diiodobutane using methanol as the solvent and one equivalent of $KHCO_3$ as the base acceptor for the HI generated as a side product. SPIRO hydroxide was prepared by ion exchange of an aqueous solution of SPIRO iodide over BioRad Ag1-X8 hydroxide ion exchange resin. The fluoride salt was prepared by reacting this hydroxide solution with the stoechiometric amount of aqueous HF.

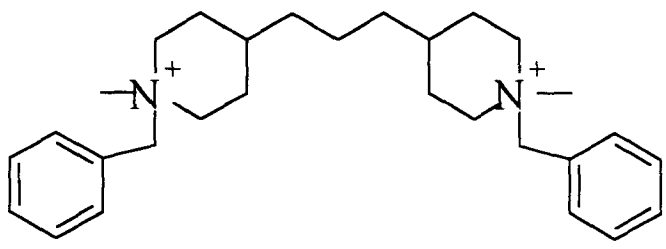

(I)

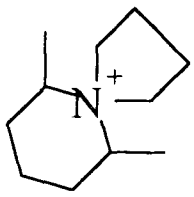

(II)

Characterizations

Room temperature, powder X-ray diffraction (XRD) patterns of the molecular sieves were collected on a Scintag XDS 2000 diffractometer operating in a Bragg-Bretano geometry (liquid nitrogen cooled Ge detector, Cu Kα radiation, λ=1.54184 Å). The patterns were collected in a stepwise mode with 2θ ranging from 2 to 51° (step size=0.01°, count time=4s) in order to identify the crystalline phases synthesized.

Thermogravimetric analyses (TGA) were performed on approximately 15 mg sample using a TA Instruments 2100 Analyzer to measure the mass fraction of water and organics present in the samples introduced into the calorimeter. The heating rate was 10 K/min to 1173 K, and buoyancy corrections were performed for all runs. Alternatively, the measurement was performed on approximately 10 mg sample using a Netzsch STA449C system. The heating rate for those cases was 10 K/min to 1573 K.

The molecular sieve specimens were also analyzed by Galbraith Laboratories, Inc., Knoxville, TN, for their carbon contents in order to confirm the organic SDA contents determined by TGA. Fluorine contents were also determined to confirm that no F species remained after calcination.

Solid-state ^{29}Si NMR spectra for all molecular sieve samples were collected on a Bruker DSX-200 spectrometer equipped with a Bruker cross-polarization (CP), magic angle spinning (MAS) accessory. The samples were packed into a

7mm ZrO_2 rotor and spun in air at 4 kHz. Proton-decoupled ^{29}Si NMR spectra (operating frequency 39.761 MHz, pulse angle 90°, pulse width 4μs) referenced to tetrakis(trimethylsilylsilane) (downfield peak at δ = -10.053 ppm) were collected using MAS.

Solid-state ^{13}C NMR spectra for the as-made molecular sieve samples were collected on a Bruker DSX-200 spectrometer. The samples were packed into a 7mm ZrO_2 rotor and spun in air at 4 kHz. ^{13}C NMR spectra (operating frequency 50.328 MHz, pulse angle 90°, pulse width 4μs) referenced to TMS (using adamantane as a secondary reference, upfield peak at δ = 38.47 ppm) were obtained by using CP MAS with ^1H decoupling.

Solid-state ^1H NMR spectra for all molecular sieve samples were collected on a Bruker DSX-500 spectrometer equipped with a Bruker cross-polarization, magic angle spinning (MAS) accessory. The samples were packed into 4mm ZrO_2 rotors and spun in air at 10-14 kHz. ^1H NMR spectra (operating frequency 500.248 MHz, pulse angle 90°, pulse width 4μs) were collected using MAS and referenced to tetrakis(trimethylsilylsilane) (upfield peak at δ = 0.247 ppm).

Calorimetry

Solution calorimetry was employed to obtain the heats of solution of the molecular sieves. The thermochemical measurements were performed using a

Setaram C-80 twin microcalorimeter equipped with HF-resistant cells developed jointly at our laboratories at the California Institute of Technology and at the Thermochemistry Facility at the University of California at Davis. A photograph of the calorimeter is shown in Figure 7.1. The enthalpy of solution of a commercial quartz sample (Fluka, purum, ≤0.3% loss on ignition, ≥230 mesh) was determined in addition to those of the molecular sieves in order to calculate the enthalpies of transition from quartz to the other silica polymorphs. These values allowed for comparison to the *quartz → molecular sieve* enthalpies of transition calculated from high-temperature calorimetry data.[7-8]

The solvent was 25 wt% aqueous HF at 323.15 K for both quartz and molecular sieve solution experiments. An amount of substance corresponding to approximately 0.18 mmol SiO_2 molecular sieves (10.8-13.7 mg) was contacted with 5.4 g HF solvent by the downward push of a retractable rod, as shown in Figures 7.2 and 7.3. This rod dropped a small plug into the HF solution, exposing the molecular sieve or quartz crystals to the solvent. All solid pieces in direct contact with the HF solution were made out of polytetrafluoroethylene (PTFE) or polychlorotrifluoroethylene (PCTFE); Viton o-rings were also used. While it was not possible to stir the reaction mixture, the completion of the dissolution reaction was easily identified by the return of the calorimeter heat rate signal to a stable constant value. The dissolution times ranged from two (*BEA, MTW, STF) to three hours (MFI) for the molecular sieves; four hours were necessary for the complete dissolution of quartz. Blank runs were also performed to determine the

heat effect of pushing the rod. Three to four measurements were performed on each molecular sieve sample in order to obtain acceptable uncertainty statistics. The calorimeter was calibrated by determining the enthalpy of solution of KCl in water at 300.15 K.[23]

Alkylammonium fluoride solutions in 25% aqueous HF were added to the HF solvent for the dissolution of the calcined materials. Where appropriate, minute amounts of water (less than 0.15 μL) were added as well. These additions were necessary for the thermodynamic cycles to close properly (see below).

Thermodynamic Cycles

The interaction enthalpy refers here to the enthalpy of the following reaction:

$$MS + nz\ F^-\ (ref) + n\ SDA^{z+}\ (ref) \rightarrow MS\cdot(SDAF_z)_n \qquad (1)$$

where MS is a generic designation for one mole of SiO_2 of any of the molecular sieve frameworks; n is the number of organic groups present per mole SiO_2; z is the charge on the organic SDA, and ref is an appropriate reference state for the fluoride and SDA ions. The conceptually simplest reference state is the solid organic fluoride, denoted here by RF_z (s). The salt is enclathrated in the inorganic host as $MS\cdot(R^{z+}(F^-)_z)$ and upon dissolution in HF, the salt dissociates into the ions without further reaction:

$$RF_z\ (s) \rightarrow R^{z+}(aq\ HF) + z\ F^-\ (aq\ HF). \qquad (2)$$

Tetraalkylammonium fluorides are extremely hygroscopic. Furthermore, the more water-rich systems present progressively lower melting points, so these fluorides are deliquescent and their hydration level cannot easily be controlled.[24-25] The uncertain water level in such samples would affect the enthalpy of solution of the solid salts to an unknown extent due to the salts' strong hydration enthalpies. To avoid the experimental difficulties associated with the solid fluorides, the dilute ions in 25% HF were therefore chosen as the reference states for the SDA fluorides. The highest SDA fluoride molality after the solution calorimetry experiments in this study was m = 0.003 mol/kg TEAF (for the case of *BEA/TEA). At such low molalities, the concentration dependence of the energetics of the SDA^{z+} and F^- ions can be neglected[26] and the SDA fluoride reference state is well-defined.

The idealized enthalpy of interaction at 323.15 K, ΔH_{int}^{323}, between the inorganic framework, MS, and its SDA, present in the dilute ion reference state, can be described by the following reaction:

$$MS + nz\ F^-\ (aq\ HF) + n\ SDA^{z+}\ (aq\ HF) \rightarrow MS{\cdot}(SDAF_z)_n \qquad (3)$$

The calcined and as-made forms of the molecular sieves contain different amounts of water (see Table 7.1 below): the MFI, MTW, and STF samples contained more water in their calcined forms, whereas the *BEA samples have more water in the as-made form. For the MFI, MTW, and STF specimens, the idealized enthalpy (reaction (3)) was approximated by that calculated from the reaction:

$$MS\cdot(H_2O)_c + n\ SDA^{z+}(aq\ HF) + nz\ F^-\ (aq\ HF) \rightarrow (c\text{-}w)\ H_2O\ (l) +$$
$$MS\cdot(SDAF_z)_n\cdot(H_2O)_w \qquad (4)$$

where c and w are the number of moles of water per mole SiO_2 occluded in the calcined and as-made forms of the molecular sieves, respectively.

The enthalpy for reaction (4) can be obtained by adding the enthalpies from reactions (5)-(7):

$$MS\cdot(H_2O)_c\ (s) + nz\ F^-\ (aq\ HF) + n\ SDA^{z+}\ (aq\ HF) + aq\ HF \rightarrow$$
$$c\ H_2O\ (aq\ HF) + SiF_6^{2-}\ (aq\ HF) + nz\ F^-\ (aq\ HF) +$$
$$n\ SDA^{z+}\ (aq\ HF) + aq\ HF \qquad (5)$$

$$H_2O\ (aq\ HF) \rightarrow H_2O\ (l) \qquad (6)$$

$$SiF_6^{2-}\ (aq\ HF) + n\ SDA^{z+}\ (aq\ HF) + nz\ F^-\ (aq\ HF) + c\ H_2O\ (aq\ HF) +$$
$$aq\ HF \rightarrow MS\cdot(SDAF_z)_n\cdot(H_2O)_w\ (s) + (c\text{-}w)\ H_2O\ (aq\ HF) +$$
$$aq\ HF \qquad (7)$$

according to $\Delta H_4 = \Delta H_5 + (c\text{-}w)\Delta H_6 + \Delta H_7$. The enthalpies ΔH_5 and ΔH_7 are the experimentally measured heats of solution for the calcined and as-made molecular sieves, respectively. The $(c\text{-}w)\Delta H_6$ contribution to the overall interaction enthalpy represents the difference between the heat evolved due to the dilution of the 25%

HF with an additional w moles of water (as-made molecular sieve) and the heat evolved due to the dilution of the 25% HF with an additional c moles of water (calcined material).

For this thermodynamic cycle to be exact, the final state after dissolution of the molecular sieves into the HF solutions must be the same for the as-made and calcined materials. This is the reason for the addition of n moles $SDAF_z$ to the HF solution into which the calcined material is dissolved and (c-w) moles water to the HF solution into which the as-made material is dissolved.

In the cases of *BEA/TEA and *BEA/BISPIP, the as-made materials contain more water than the calcined specimens, and the corresponding thermodynamic cycle is as follows:

$$MS\cdot(H_2O)_c\ (s) + (w\text{-}c)\ H_2O\ (aq\ HF) + nz\ F^-\ (aq\ HF) + n\ SDA^{z+}\ (aq\ HF) + aq\ HF \rightarrow SiF_6^{2-}\ (aq\ HF) + w\ H_2O\ (aq\ HF) + nz\ F^-\ (aq\ HF) + n\ SDA^{z+}\ (aq\ HF) + aq\ HF \quad (5')$$

$$H_2O\ (l) \rightarrow H_2O\ (aq\ HF) \quad (6')$$

$$SiF_6^{2-}\ (aq\ HF) + n\ SDA^{z+}\ (aq\ HF) + nz\ F^-\ (aq\ HF) + w\ H_2O\ (aq\ HF) + aq\ HF \rightarrow MS\cdot(SDAF_z)_n\cdot(H_2O)_w\ (s) + aq\ HF \quad (7')$$

$$MS\cdot(H_2O)_c\ (s) + n\ SDA^{z+}\ (aq\ HF) + nz\ F^-\ (aq\ HF) + (w\text{-}c)\ H_2O\ (l) \rightarrow MS\cdot(SDAF_z)_n\cdot(H_2O)_w\ (s) \quad (4')$$

Here, $\Delta H_4' = \Delta H_5' + (w\text{-}c)\Delta H_6' + \Delta H_7'$ is the experimentally determinable value closest to the enthalpy of interaction ΔH_{int}^{323}. For the *BEA specimens, n mol $SDAF_z$ and (w-c) water are added to the HF solution into which the *BEA/calc samples are dissolved (equation (5')).

By taking ΔH_4 (or $\Delta H_4'$) as the interaction enthalpy from empty pure-silica materials (equation (3)) the enthalpy of hydration of the molecular sieve is effectively neglected since only the heat of dilution is included in the "water correction" term $(c\text{-}w)\Delta H_6$. Piccione et al.[7] showed that the enthalpy of hydration of pure-SiO_2 molecular sieves prepared in fluoride media can be neglected since it leads to effects ≤ 0.2 kJ/mol SiO_2. This value is smaller than the uncertainty in the enthalpy of solution measurements (see *Results* below) and the idealized enthalpy of interaction $\Delta H_{\text{int}}^{323}$ is therefore taken here to be equal to the experimentally determined quantity, ΔH_4 (or $\Delta H_4'$). For clarity, ΔH_{int}^{323} is used in the remainder of this Chapter to designate ΔH_4 for the MFI, MTW, and STF samples and $\Delta H_4'$ for the *BEA samples. Similarly, ΔH_{soln}^{323}(MS/calc) and ΔH_{soln}^{323}(MS/SDA) are used to designate ΔH_5 or $\Delta H_5'$, and ΔH_7 or $\Delta H_7'$, respectively.

$\Delta H_6 = -\Delta H_6'$ can be shown to be equal to the opposite of the relative partial molal enthalpy of water in 25% aqueous HF at 323.15 K. The magnitude of $(c\text{-}w)\Delta H_6$ was expected to be much smaller than that of the enthalpies of solution since (c-w) is smaller than 0.046 for all MS/SDA pairs considered in this work. The temperature dependence of ΔH_6 was therefore neglected. Parker provided

extensive data on the thermal properties of aqueous uni-univalent electrolytes at 298.15 K.[27] From her tabulations of the relative apparent molal enthalpy of aqueous HF solutions, Φ_L, ΔH_6 was calculated as

$$\frac{Mm^{\frac{3}{2}}}{2000}\left(\frac{\partial\Phi_L}{\partial m^{\frac{1}{2}}}\right)$$

where M is the molecular weight of water in g/mol and m is the HF molality.[27] A linear interpolation of Φ_L versus $\sqrt{m}$ between m = 15.86 and m = 17.08 mol/kg using the data in reference 27 afforded the ΔH_6 value of 0.56 kJ/mol water for a 25 wt% HF solution (m = 16.67 mol/kg).

Results

Molecular Sieve Characterizations

The X-ray powder diffraction patterns indicate the presence of a single molecular sieve phase for each sample, and the crystal sizes were larger than 1μm (from microscopy). For particles larger than 1 μm, surface energy effects can be neglected in the measurement of energetics via calorimetry.[8] The X-ray powder diffraction patterns after the calcination treatment show that there is no degradation of the structures.

Table 7.1 shows the TGA data collected from the molecular sieve and quartz specimens, along with the calculated unit cell compositions. For the as-made materials, TGA mass losses below 423 K were attributed to water, while the remainder of the mass losses was assigned to enclathrated organic SDA fluoride. The low water contents (< 1.5% for all samples) are consistent with the hydrophobic nature of pure-silica molecular sieves prepared in fluoride media. For the samples where the SDA/uc amounts have been previously reported in the literature (MFI/TPA,[21,28] *BEA/TEA[29]), there is good agreement with those values. Since MFI has four channel intersections per unit cell,[9] the SDA/uc value near 4 for MFI/TEA is within experimental error of the expected value. The carbon contents determined by elemental analysis (also shown in Table 7.1) for the as-made materials are consistent with the SDA/uc ratios calculated from the TGA data. Furthermore, the carbon contents of the calcined materials confirm that complete removal of the organic SDA is achieved upon calcination. The fluorine contents determined by elemental analysis prove that essentially all F species are also removed by calcination.

All molecular sieve materials were prepared in fluoride-containing media so the Q_3 concentrations will be lower than those achieved in the presence of hydroxide.[17,21] The ^1H and ^{29}Si solid-state NMR spectra of all samples (shown in Figures 7.4 to 7.7) quantitatively confirmed the absence of significant concentrations of Q_3 (defect) Si sites (^1H NMR chemical shift at 10 ppm, ^{29}Si NMR chemical shift below –105 ppm) for all the calcined materials, as well as for

the MFI/TEA and MTW/BISPIP specimens. For the other samples, some Q_3 sites are observed. For MFI/TPA, the use of NH_4F in the syntheses mixture results in a lower density of defect sites than MFI/TPA prepared in the absence of this additive. Elemental analyses on MFI/TPA materials made in the presence and absence of NH_4F showed identical C/N ratios, proving that no NH_4^+ is incorporated in TPA/MFI when synthesized in the presence of NH_4F. The *BEA samples contain somewhat higher defect concentrations. No thermodynamic data are available for defects in as-made molecular sieves, and since significant amounts of Q_3 sites are absent for all the specimens studied here, no attempt was made to separate the effects of the defect energetics in the thermodynamic cycles for the interaction enthalpies. These effects, that are expected to be small (probably less than 1-2 kJ/mol SiO_2), are thus included implicitly in the interaction enthalpies.

The ^{13}C solid-state NMR spectra for the as-made materials, shown in Figure 7.8, were compared to liquid-state ^{13}C NMR spectra for the corresponding SDAs and in each case it was confirmed that the organic molecules had been occluded intact.

Calorimetry

Enthalpies of Solution in Aqueous HF, ΔH_{soln}^{323}

The typical heat effects for the HF solution experiments ranged from -25 to -27 J. The magnitude of the heat effect due to pushing the rod was approximately -0.06 J, i.e., less than 0.3% of the total heat of solution. Representative heat flow curves for the solution of MTW/calc, *BEA/TEA, and quartz in HF, as well as for the blank experiment are shown in Figure 7.9. The enthalpy of solution at 27 °C for KCl in water to a final concentration of 0.111 mol/kg is 0.2317 J/mg.[23] The experimentally determined enthalpies of solution are 0.230±0.001 and 0.233±0.001 J/mg, respectively, from measurements performed with the reference and sample cells. The corresponding calibration factors (relative to an electric calibration) of 1.008 (reference) and 0.994 (sample) are very close to unity, as expected for this class of calorimeter when operating near room temperature.

The measured enthalpies of solution of the molecular sieves and of quartz on a mass and mole basis are shown in Tables 7.2 and 7.3, respectively. The uncertainties (2 standard deviations from the mean) in ΔH_{soln}^{323} are 0.2-1.3 kJ/mol SiO_2, and never exceed 0.9% of the enthalpy of solution. Such errors compare favorably to the study of Patarin et al.[13-14]

Quartz. The enthalpy of solution of quartz in HF solutions at various HF concentrations and temperatures has been studied by several groups.[13-14,30-34]

While the values reported for solution in 25% HF between 348-353 K are all in good agreement with each other, larger discrepancies are observed at lower temperatures (possible causes for these differences are discussed in references 30 and 31). Kilday and Prosen performed a systematic study of the changes in ΔH^{T}_{soln}(quartz) with concentration (18-30 wt% HF) and temperature (298-358 K).[31] They presented correlations enabling the ΔH^{T}_{soln}(quartz) values of other investigators to be compared on the same basis by using these correlations for correcting for the concentration and temperature variations. The ΔH^{323}_{soln} values from the most recent studies corrected to 25% HF and 323.15 K using Kilday and Prosen's regressions are shown in Table 7.4. The ΔH^{323}_{soln} values range from -137.1±0.2[30] to -142.3±0.4[32] kJ/mol SiO_2. The value determined here of -140.2±1.1 kJ/mol SiO_2 falls well within the range of data determined by previous workers and confirms that the calorimeter used here had been well-calibrated.

MFI. The measured solution enthalpy for MFI is in very good agreement with the datum of Johnson et al.[34] but not with that of Patarin et al. (4.8% discrepancy, see Table 7.4).[13-14] The average ΔH^{323}_{soln}(MFI/calc) value from solution of the MFI/calc sample into HF containing traces of either TEAF or TPAF was used for the purposes of this comparison (see *MFI and *BEA Consistency* section below). Johnson et al.[34] documented the effect of the HF concentration on the enthalpy of dissolution of calcined MFI and found a difference in HF concentrations of 4.4% to lead to a discrepancy in the heat of

solution of 0.95 kJ/mol, i.e., 0.22 kJ/mol SiO_2/(%HF conc change). For the 0.6% HF concentration change between 24.4 and 25 this would yield a contribution of -0.13 kJ/mol, much smaller than the difference between the two reported values. The literature data[13-14,34] are therefore irreconcilable within experimental error. Since the experimental conditions used here (sample synthesized in fluoride media, calorimeter scale of ~5.4 g HF solution) are more similar to those used by Patarin than to those used by Johnson, it is unclear why our value is closer to that of Johnson.

Based upon additional data reported by Johnson and co-workers,[34] it can be shown that the 6.8 kJ/mol discrepancy between the ΔH_{soln}^{323}(MFI/calc) value reported here and in references 13-14 is also not attributable to differences in silica concentration. Unlike Patarin et al., Johnson and co-workers were able to continuously stir their reaction mixture. Since the value reported here is in good agreement with that of Johnson et al., and more exothermic than that of Patarin et al., it is plausible that molecular sieve dissolution may have been incomplete in the latter work. The value reported here and in reference 34 is believed to be a more accurate measure of the true ΔH_{soln}^{323}(MFI/calc). The ΔH_{soln}^{323}(MFI/TPA) value reported by Patarin et al. is also less exothermic (by 11.5 kJ/mol) than the value reported here. As-made molecular sieves dissolve slower than their calcined counterparts since their pores are filled with organics at the beginning of the calorimetry experiment. The larger discrepancy for the MFI/TPA data than for the

MFI/calc data are therefore consistent with incomplete dissolution in the previous work.[13-14]

*Enthalpy of Solution of Calcined MFI and *BEA.* The enthalpies of solution of MFI/calc and *BEA/calc were each determined in HF containing traces of two different organic cations. As noted above, the organic species in these solutions are always present at molalities less than 0.003 m. The final hexafluorosilicate molality after dissolution of the molecular sieves is 0.033 m. At such low concentrations, the SDA^{z+} and SiF_6^{2-} species are unlikely to interact with each other (for comparison the solvent molality is approximately 54.2 mol/kg). The ΔH_{soln}^{323}(MFI/calc) and ΔH_{soln}^{323}(*BEA/calc) values per mol SiO_2 are therefore expected to be independent of the presence and identity of the SDA species. Examination of the data in Table 7.3 shows the pairs of values for each structure to indeed be within experimental error of each other. The average ΔH_{soln}^{323} values for MFI/calc and *BEA/calc are -147.2±0.6 and −148.4±0.6 kJ/mol SiO_2, respectively.

Discussion

Enthalpies of Transition (quartz → molecular sieve), ΔH_{trans}^{323}

The enthalpy of transition from quartz to other silica polymorphs at 323.15 K, ΔH_{trans}^{323}, can be determined by the subtraction of the enthalpy of solution of the calcined molecular sieve from that of quartz:

$$\Delta H_{trans}^{323}(\text{quartz}\rightarrow\text{MS}) = \Delta H_{soln}^{323}(\text{quartz}) - \Delta H_{soln}^{323}(\text{MS/calc}) \qquad (8)$$

For the purposes of this discussion, the average ΔH_{soln}^{323}(MFI/calc) and ΔH_{soln}^{323}(*BEA/calc) values calculated above (–147.2±0.6 and -148.4±0.6 kJ/mol SiO_2, respectively) were used. Table 7.5 compares the ΔH_{trans}^{323} values calculated from the aqueous HF calorimetry in this work to the ΔH_{trans}^{298} values determined by Piccione et al.[7] and Petrovic et al.[8] using high-temperature drop solution calorimetry in lead borate near 974 K. Based on the heat capacity data of Boerio-Goates et al.,[11] the enthalpies of transition at 323.15 K differ from those at 298.15 K by no more than 0.5 kJ/mol SiO_2. Within their experimental errors,[7-8] ΔH_{trans}^{298} and ΔH_{trans}^{323} should therefore be equal. Since ΔH_{trans}^{298}(STF) has not been determined experimentally, the value in Table 7.5 was obtained by applying the molar volume-ΔH_{trans}^{298} correlation given in reference 7 to the STF framework, that has a molar volume of 34.86 cm^3/mol.[35] The enthalpies of transition from quartz determined by the two methods are within experimental error of each other for all

frameworks except MTW. The high-temperature calorimetry datum reported by Petrovic et al. is based on a sample that was made in fluoride media, but at basic pH.[8] As discussed by Barrett et al., molecular sieve materials made using fluoride as the mineralizing agent are only truly defect-free if the pH is sufficiently low.[18] The MTW sample used by Petrovic et al. may therefore have contained some silanol defect groups. Therefore the enthalpy of the defect-free MTW framework may have been overestimated in reference 8 by up to 2.4 kJ/mol.[7] Correcting for the energetic destabilization due to an unknown density of defect sites would lead to a smaller disparity between the MTW data determined by HF and lead borate calorimetry. The presence of destabilizing silanol groups in the previously studied MTW sample is also suggested by the relatively large discrepancy between the experimental ΔH_{trans}^{298}(MTW) value and that predicted from the molar volume-ΔH_{trans}^{298} correlation of reference 7. This correlation predicts a ΔH_{trans}^{298}(MTW) value of 7.0 kJ/mol, significantly closer to the value calculated from the HF solution enthalpy in this work. In conclusion, the sets of ΔH_{trans}^{T} data calculated from the two methods are in good agreement.

Enthalpies of Interaction, $\Delta H_{\text{int}}^{323}$

Experimental Values. The interaction enthalpy ΔH_{int}^{323} between each molecular sieve and its associated SDA are shown per mol SiO_2 and per mol

SDA in Table 7.6. The standard errors were calculated according to $\sigma = \sqrt{\sigma_5^2 + \sigma_7^2}$ where σ_5 and σ_7 are the standard deviations for ΔH_{soln}^{323}(MS/calc) and ΔH_{soln}^{323}(MS/SDA), respectively.

The contribution of the differential heat of dilution between the calcined and as-made molecular sieve samples, (c-w)ΔH_6, shown in the last column of Table 7.6, is less than 2.5% of the uncertainty in ΔH_{int}^{323}. The simplifying approximation that the relative apparent molal enthalpy of HF solutions is independent of temperature in the 298.15-323.15 K range, therefore, cannot have significantly altered the calculated ΔH_{int}^{323} values. Although the errors in ΔH_{int}^{323} may appear large in relative terms, ranging from 12% to 125%, the absolute uncertainties are quite narrow ($\leq$ 1.4 kJ/mol SiO_2) and are significantly smaller than those of Patarin et al.[13-14]

Interpretation. When viewed per mol SiO_2, ΔH_{int}^{323} characterizes the stabilization gained by silicate frameworks interacting with organic SDAs. Such a viewpoint expresses the inorganic/organic interaction in terms relevant to the polymerizing species–the silica tetrahedra. The ΔH_{int}^{323} values were also compared per mol SDA as a measure of the quality of the fit of the SDA molecules within each pore system.

The ΔH_{int}^{323} values in Table 7.6 range from -1.1 kJ/mol SiO_2 for the MFI/TEA interaction to -5.9 kJ/mol SiO_2 for the *BEA/BISPIP interaction. All

ΔH_{int}^{323} values are negative, implying that the MS/SDA interaction is exothermic, and thus favorable, for all inorganic/organic pairs studied here. At a typical synthesis temperature of 423.15 K, the available thermal energy per total number of moles in the system is RT = 3.5 kJ/mol. Since there are many Si atoms per SDA in the as-synthesized molecular sieves, the most appropriate quantity to compare to RT is ΔH_{int}^{323} per mol SiO_2. On such a basis, the interaction between the varied range of pure-silica molecular sieve frameworks and their SDAs studied here is seen to be in no case more exothermic than twice the thermal energy at synthesis conditions. Such a narrow ΔH_{int}^{323} range may explain why certain SDAs (e.g., TEA and BISPIP) can direct synthesis toward several frameworks depending on the reaction conditions. The relatively small magnitude of ΔH_{int}^{323} is consistent with the interpretation of the MS/SDA interaction as consisting predominantly of weak, van der Waals forces between the hydrophobic silica species and hydrocarbon moieties of the SDA.[36-37] Before performing a more rigorous description of molecular sieve synthesis that focuses on the Gibbs free energy of formation, the relationships between ΔH_{int}^{323} values and MS and SDA structures are examined. In this context, it was found particularly instructive to compare the ΔH_{int}^{323} values for MS/SDA pairs with the same MS or the same SDA.

TEA, TPA. The stabilizing effect of TEA towards the MFI framework is 2.1 kJ/mol SiO_2 less exothermic than that of TPA. This result is consistent with the observation that MFI is the sole product from TPA-directed

syntheses whereas TEA frequently yields other phases. On a silica basis ΔH_{int}^{323}(*BEA/TEA) is comparable to ΔH_{int}^{323}(MFI/TPA), roughly 2 kJ/mol SiO_2 more exothermic than ΔH_{int}^{323}(MFI/TEA). The stronger overall interaction between the *BEA framework and TEA, however, is not due to a stronger stabilization of TEA in the *BEA void spaces: ΔH_{int}^{323}(*BEA/TEA) per mol SDA is identical to ΔH_{int}^{323}(MFI/TEA) within experimental error. The more exothermic occlusion of TEA within *BEA, rather, is simply related to the larger *number* of interactions engaged in by the greater number of guest molecules in the larger *BEA cages. Note that the occlusion of fluoride ions within molecular sieves has been shown by ^{19}F-^{29}Si CP MAS NMR to result in the formation of five-coordinate Si units, $SiO_{4/2}F^-$.[38] Since all the materials studied in this work were prepared in fluoride media, it is not possible to separate the energetic effects of the interaction of the silica frameworks with the SDA cations and the F^- anions. If the penta-coordinate Si units preferentially stabilize certain kinds of Si structures (e.g., fused four-membered rings, such as those of *BEA), one can speculate that the use of fluoride as a mineralizing agent in molecular sieve syntheses might produce different crystalline phases than the use of hydroxide. In this context, the formation of metal-substituted molecular sieves in F^- media may also be affected by the relative stabilities of various frameworks. These stabilities, in turn, may differ from those of the pure-silica polymorphs depending on whether or not the changes in preferred bond angles upon substitution favor five-coordinate species.

BISPIP. The much larger organic, BISPIP, gives the highest enthalpy of interaction in this study when occluded inside *BEA. One might expect the large negative ΔH_{int}^{323} (*BEA/BISPIP) to be related to the greater number of interactions the organic molecule can participate in when compared to TEA. Based on the unit cell compositions, however, there are 50 C atoms/uc in *BEA/TEA and 60 C atoms/uc in *BEA/BISPIP. This difference is too small for it alone to account for the factor of two difference in ΔH_{int}^{323} (*BEA/SDA) per mol SiO_2. Instead, one could argue that it is the quality of the spatial fit of the organic guest inside the inorganic host that is important. Since the *BEA structure is three-dimensional, the large BISPIP molecule is expected to have significant freedom to orient itself into a minimum energy configuration. Once such a conformation is found, the BISPIP cations are not expected to reorient themselves significantly away from it since such motion would require the simultaneous motion of a large number of atoms. By contrast, the TEA molecules inside the *BEA cages have been shown by ^{13}C solid-state NMR to behave similarly to TEA cations in the liquid state.[6] Such fast rotating species would, on average, sample a larger number of less energetically favorable conformations, thus helping explain the less exothermic ΔH_{int}^{323} value for *BEA/TEA among the two *BEA/SDA materials. Note that such a preferential stabilization for *BEA/BISPIP is a purely enthalpic effect – entropy contributions to the overall energetics are expected to

favor the more mobile species, which in this case are the TEA cations (see also *Gibbs Free Energies of MS/SDA Interaction* below).

The BISPIP SDA was also occluded inside MTW, a one-dimensional structure with a distorted, unusually narrow 12-membered pore. Table 7.6 shows the interaction between BISPIP and MTW to be considerably less exothermic than the *BEA/BISPIP interaction. ΔH_{int}^{323} (*BEA/BISPIP) and ΔH_{int}^{323} (MTW/BISPIP) are significantly different on a per mol SDA basis, so the difference is not solely due to a greater packing of SDA molecules in the *BEA framework. Linear hydrocarbon chains can easily expand into one-dimensional pore systems, but bulkier groups (e.g., the *N*-benzyl substituted piperidinium groups of BISPIP) are less easily accommodated; such groups are expected to be more stable when residing within the intersections of multi-dimensional pore systems, or inside cage frameworks. Even though the SDAs can undergo conformational changes (e.g., the ring-flipping mechanism proposed by Tsuji and Davis for BISPIP inside MTW[39]) before incorporation into a 1-D framework that is more constrained, some parts of large, bulky SDAs may not be able to reside at the optimal distance to interact most favorably with the inorganic framework. Note further that MTW differs from the other three molecular sieves in this study in that 1/7 of its T atoms are not easily accessible for interactions with the SDA from the pore channels.[9] This inability would in turn lead to fewer MS/SDA interactions. To summarize, the significant difference between the ΔH_{int}^{323} (*BEA/BISPIP) and

ΔH_{int}^{323}(MTW/BISPIP) values may be due to the three-dimensional *BEA framework's greater ability in accommodating the SDA.

Synthetic data confirm the interpretation above: Tsuji and Davis[39] systematically studied the structure-directing effect of a collection of trimethylenebis(*N*-alkyl,*N*-methylpiperidinium) ions, **(III)**. They found such diquarternary SDAs to direct syntheses towards 1-D MTW for small linear chains (R = propyl, butyl), but towards larger 3-D *BEA for bulkier substituents (R = benzyl, cyclomethylhexyl). Camblor et al. reviewed molecular sieve syntheses in fluoride media and reported similar trends for several classes of diquarternary SDAs. For instance, among the three isomers of xylylenediquinuclidinium **(IV)**, only the most elongated para isomer can be used to prepare both MTW and *BEA; the ortho and meta isomers, whose quinuclidinium moieties are locked into bulkier arrangements, only allow the synthesis of *BEA.[17]

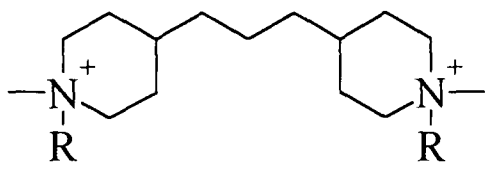

(III)

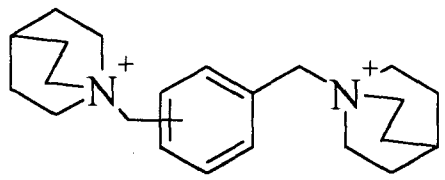

(IV)

As synthesis temperatures increase, molecular motions allow SDA cations to sample a larger set of conformations. One could speculate that eventually such motions occur to such a degree that SDAs enclathrated inside molecular sieves

begin to sample conformations farther away from those yielding the minimum energy. Such changes would adversely affect the MS/SDA pairs with more exothermic ΔH_{int}^{323} values to a greater extent, resulting in a net gain in apparent relative stability for frameworks such as MTW that, at least in the BISPIP case, do not interact as intimately with the SDAs.

SPIRO. The bicyclic derivative used to make STF is representative of a class of relatively small, globular, yet rather rigid, SDAs used by researchers at Chevron to make novel molecular sieve materials with notable success.[22] Such molecules do not lead to the crystallization of as varied a set of frameworks as more flexible molecules, and it has been suggested that the high specificity of the more rigid SDAs may be due to their role in preventing polymorphs of lower activation energy from crystallizing.[40] The best-known example of the rigid class of SDAs may be the propellane molecule **(V)** used for the synthesis of SSZ-26.[41]

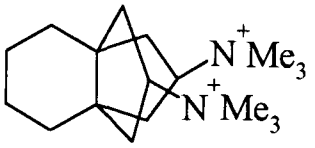

(V)

The comparatively strong exothermic ΔH_{int}^{323}(STF/SPIRO) value (the second highest per mol SiO_2 in this work) is consistent with the view that highly rigid SDAs such as SPIRO can only be occluded inside molecular sieves with which they have significant favorable interactions. Such organics are simply not flexible

enough to be easily accommodated into other frameworks. For SPIRO this lack of flexibility translates into the formation of STF that is best described as stacked cages connected by 10-ring portals.[35] These cages presumably provide necessary space for the rigid spiro moiety.

In summary, the interaction enthalpies between pure-silica molecular sieve frameworks and their organic SDAs depend to some extent on the quality of the fit between inorganic host and organic guest. Small and flexible molecules can produce three-dimensional or one-dimensional pore systems without strong energetic differences per mol SDA. In such cases, the greater overall number of interactions for more porous structures lead to somewhat more exothermic interaction enthalpies. More rigid and/or bulkier SDAs have more stringent spatial requirements, leading to the formation of three-dimensional structures or large one-dimensional structures, possibly containing unusually large rings such as STF. The more intimate contact between such SDAs and the inorganic framework is confirmed by the observation that more selective SDAs are often found to occupy a large fraction of the void space of the molecular sieves whose syntheses they facilitate.[22] Figure 7.10 summarizes the energetic trends observed in this work and extends the experimental findings to the expected behavior for some pure-SiO_2 cases not studied here. While such broad generalizations must be viewed with care, they are believed to adequately represent the typical regimes of molecular sieve synthesis. This figure is in good accordance with the large body of synthetic data available on molecular sieve syntheses.[5,17,39]

A cautionary note must be inserted here to mention that for substituted lattices such as aluminosilicates, bearing a charge, the energetic trends above will likely be affected by the extent of electrostatic lattice/SDA interactions. This may also be the case for pure-silica materials with very high defect concentrations, such as *BEA prepared from hydroxide-containing media.

Comparison to Calculated Values. Lewis et al. used energy minimization techniques to calculate nonbonded energies of interaction between the symmetric tetramethylammonium (TMA), TEA, TPA, and tetrabutylammonium (TBA) cations and the pure-silica MFI, *BEA, and ZSM-11 (MEL) frameworks.[42] They reported interaction energies for MFI/TEA, MFI/TPA, and *BEA/TEA of –92.1, -133.9, and –104.7 kJ/mol SDA, respectively. These values are several times more exothermic than the corresponding ΔH_{int}^{323} values of –27, -81, and –32 kJ/mol SDA. Nevertheless, the calculated values follow the correct energetic trends, suggesting that the stabilization of charged organic SDA cations within molecular sieves, at least in their pure-silica form, can be viewed as consisting primarily of nonbonded interactions as was assumed by Lewis et al.[42]

Endothermic MS/SDA Values. Strongly unfavorable MS/SDA interactions are only expected for SDA cations inside molecular sieve frameworks that they cannot produce. Of course, such specimens cannot be prepared by hydrothermal means, since an organocation under such conditions would facilitate the synthesis of other, more favorable frameworks instead. Small

endothermic enthalpies of interaction are possible, however, if other contributions to the energetic changes during synthesis are sufficiently exergonic for the overall ΔG to become negative. Patarin et al.[13-14] reported modestly endothermic enthalpies of interaction for MFI with tripropylammonium (TRIPA) and dipropylammonium (DIPA) cations (4.5±2.4 and 5.3±2.2 kJ/mol SiO_2, respectively). To synthesize MFI/TRIPA and MFI/DIPA specimens, they found it necessary to seed their gels with 4-5% as-made MFI crystals.[13] They reported the synthesis of pure-phase MFI/DIPA to be particularly difficult (MTT readily crystallizes under the same conditions). Two of the materials studied here (*BEA/BISPIP and MFI/TEA) were produced from seeded gels. Both materials, however, readily crystallize from the compositions used here even in the absence of seed crystals. Neither the *BEA/BISPIP nor the MFI/TEA MS/SDA pairs studied here therefore adequately represents systems that *require* seeding.

Gibbs Free Energies of MS/SDA Interaction

The Gibbs free energies of interaction between organic SDAs and calcined molecular sieve, ΔG_{int}(MS/SDA), are related to the interaction enthalpies determined in this work by

$$\Delta G_{int}(\text{MS/SDA}) = \Delta H_{int}(\text{MS/SDA}) - T\Delta S_{int}(\text{MS/SDA}),$$

where ΔS_{int}(MS/SDA) represents the entropy of interaction between framework

MS and its SDA. Unfortunately, no entropy data are available at this time for any organic-containing molecular sieve at any temperature so ΔS_{int}(MS/SDA) must necessarily be approximated. Note that the entropies for most tetraalkylammonium salts are only available at 298.15 K whereas the ΔH_{int}^{323} values determined above refer to interactions at 323.15 K. In the interest of simplicity, we assumed that the interaction enthalpies at 298.15 K are not significantly different from those at 323.15 K, i.e., $\Delta H_{int}^{298} = \Delta H_{int}^{323}$. Such an assumption is reasonable since the major contributor to the heat capacity on each side of reaction (1) is that of the solid molecular sieve, and this quantity is expected to be relatively unaffected by the presence or absence of organic guest molecules inside the pores. Following the same procedure as Helmkamp and Davis,[15] the entropies of interaction between organic SDA fluoride in the solution state and empty molecular sieve were estimated by the negative of the entropy of hydration of the solid SDA fluoride, i.e., per mol SDA $\Delta S_{int}^{298}(MS/SDAF_z) = -\Delta S_{soln}^{298}(SDAF_z)$. Tetraalkylammonium ions in aqueous solutions are well-known to order water around their alkyl chains.[15,43-44] The above approximation takes into account the gain in entropy of the water liberated by desolvation of the SDA cations as well as the change in environment experienced by the SDA cations upon enclathration in the molecular sieve framework.[15] It explicitly assumes that the entropy of the SDA fluoride occluded inside the molecular sieve framework is the same as that for the solid salt. Implicitly, it is assumed that the entropy of the inorganic framework is not

significantly affected by the presence of the occluded ions.[15] Using these approximations with a generic fluoride $SDAF_z$, one can write

$$\Delta S^{298}_{soln}(SDAF_z) = \Delta S^{298}_{soln}(SDAI_z) + z\{S[F^-(aq)] - S[I^-(aq)]\} + S^{298}(SDAF_z) - S^{298}(SDAI_z)$$

where $SDAI_z$ is the corresponding iodide. Johnson and Martin measured S(TEAI) = 311.1±1 J/(mol·K) and S(TPAI) = 432.1±1 J/(mol·K) by low-temperature heat capacity calorimetry.[45] They also calculated the entropies of solution for the two salts: $\Delta S^{298}_{soln}(TEAI)$ = 78.7±1.5 J/(mol·K) and $\Delta S^{298}_{soln}(TPAI)$ = 11±3 J/(mol·K). ΔS^{298}_{int} can thus be estimated for the MFI/TPA, MFI/TEA and *BEA/TEA molecular sieve/SDA pairs. The absolute entropies of aqueous F^- and I^- were taken from *The NBS Tables of Chemical Thermodynamic Properties*; their values are –13.8 and 111.3 J/(mol·K), respectively.[46] The entropies of the solid fluorides were unavailable, doubtlessly due to the difficulties in preparing these salts in the anhydrous state. I used group additivity methods to calculate the enthalpies and entropies of a collection of symmetric tetraalkylammonium salts (see previous Chapter) and estimated S(TEAF) = 280.9±10.5 J/(mol·K) and S(TPAF) = 401.9±10.5 J/(mol·K).

Table 7.7 lists the Gibbs free energies for the MS/SDA interactions, ΔG^{298}_{int}, as well as the entropy and TΔS (at 298.15 K) contributions to the MS/SDA interactions. The entropy of interaction for the MS/SDA interaction is positive in all cases; as noted by Helmkamp and Davis, this must be due to the

release of ordered water upon SDA enclathration.[15] The MS/SDA interaction is thus simultaneously favored by both its enthalpy (exothermic van der Waals contacts between hydrophobic silica species and hydrocarbon chains) and entropy (disordering of water around the SDA). $T\Delta S_{int}^{298}$ ranges from 0.9 to 2.2 kJ/mol SiO_2 (54-92% of ΔH_{int}^{298}) so the enthalpy and entropy of interaction are of the same order of magnitude. *Thus, the entropy contribution cannot be neglected when quantitatively describing the thermodynamics of formation of molecular sieves.*

The entropy of interaction per mol SDA is greater for TPAF (144±11 J/(mol·K)) than for TEAF (77±11 J/(mol·K)). The more positive ΔS_{int}^{298} per mol TPA is consistent with the expectation that larger, more hydrophobic cations would release a greater number of water molecules upon enclathration.[15] The magnitude of the entropy contribution to molecular sieve stabilization, however, is higher for the *BEA/TEA interaction (2.2 kJ/mol SiO_2 at 298.15 K) than for MFI/TPA. The reason for this apparent discrepancy is the greater organic content of the *BEA sample. Within the approximations of this work, the entropy of interaction per mol SDA depends neither on the framework into which that SDA is occluded nor on the amount of SDA occluded. ΔS_{int}^{298} therefore scales linearly with the SDA/Si ratio (n) when expressed per mol SiO_2. Effectively, the entropy contribution thus preferentially stabilizes higher organic contents, i.e., more porous frameworks. Note further that the approximations employed here do

not take into account differences in the tightness with which organic species are bound in different frameworks. A given organic SDA is intuitively expected to have a larger number of degrees of freedom, and thus entropy, when inside more porous structures. There thus exists an additional stabilizing factor for frameworks with higher void volumes. For the case of TEA, the entropy of the very mobile cations inside *BEA is expected to be higher than for TEA ions inside MFI that has smaller pores (5.6 Å vs. 7.6 Å for *BEA along the largest axis[9]). In fact, TEA inside *BEA represents the extreme case of a rather small SDA occluded inside a large-pore molecular sieve. ΔS_{int}^{298} (*BEA/TEA) may therefore be higher than estimated above, although it is doubtful that its true value is more than twice of that in Table 7.7. Note also that since the ordering of water is most pronounced for larger molecules,[15] the contribution of $T\Delta S_{int}^{298}$ per mol SDA may be expected to increase with the size of SDA cations. Extremely large molecules, however, are anticipated to be quite rigid upon enclathration, leading to reduced $T\Delta S_{int}^{298}$ values.

For comparison purposes, the last column of Table 7.7 shows ΔG_{int}^{423} extrapolated from the data at 298.15 K to the more typical synthesis temperature of 423.15 K assuming that both the enthalpy and entropy of interaction are independent of temperature. While this assumption is admittedly open to criticism, sufficient data are not available to adequately correct ΔH_{int}^{323} and ΔS_{int}^{298} to synthesis conditions. No uncertainty for ΔG_{int}^{423} is given since the assumption above is likely to lead to larger errors than the uncertainties in the original data.

Qualitatively, ΔG_{int}^{423} follows the same trend as ΔG_{int}^{298} with the values for MFI/TPA and *BEA/TEA approximately more stable than MFI/TEA by RT. Within this approximation higher temperatures only lead to slightly more favorable interactions ($\leq$0.9 kJ/mol SiO_2). Unless the enthalpy and entropy of interaction themselves change significantly with temperature closer to synthesis conditions, the relative importance of these two terms is only slightly altered. Furthermore, neither ΔG_{int}^{423} nor ΔG_{int}^{298} shows an interaction more exergonic than –2RT; the implication of such relatively small magnitudes are discussed below.

The fact that $T\Delta S_{int}^{298}$ is proportional to both temperature and organic content leads to the expectation that more porous phases be preferentially stabilized at higher temperatures. At variance with this prediction, typical F^--mediated syntheses more readily yield *less* porous phases upon heating to higher temperatures,[17] although some of the hydroxide mixtures studied by Gies and Marler[4] produced more porous clathrasils when heated to higher temperatures. Note also that more porous phases frequently are transformed to less porous phases with longer crystallization times. For instance, SSZ-25 is transformed to FER, then quartz in systems containing *N,N,N*-trimethyl-2-adamantammonium and piperidine as the SDAs.[47] When viewing molecular sieve crystallization as an example of Ostwald ripening, both longer synthesis times and higher temperatures should promote transformations to progressively more stable phases. The synthetic data therefore suggest that less porous phases may preferentially be stabilized with

increasing synthesis temperatures. The extent to which water is ordered around tetraalkylammonium ions presumably decreases with increases in temperature. If the magnitude of ΔS_{int}^{T} starts to decrease faster than 1/T above a certain temperature, the overall entropy contribution to the Gibbs free energy of interaction will decrease with temperature as well. Under such conditions, less porous structures would appear less destabilized due to their lower organic contents.

Molecular Sieve Formation from Amorphous Precursors

More representative of an actual synthesis than ΔG_{int}^{298} (MS/SDA) above is the Gibbs free energy of reaction between silica glass and an organic SDA leading to the formation of an as-made molecular sieve:

$$SiO_2\,(glass) + nz\ F^-\ (aq\ HF) + n\ SDA^{z+}\ (aq\ HF) \rightarrow MS{\cdot}(SDAF_z)_n \qquad (9)$$

The Gibbs free energy for this reaction, $\Delta G_9 = \Delta G_{rxn}^{298}$ (glass→MS/SDA), can be obtained by noticing that it is the sum of the two reactions:

$$MS\,(s) + nz\ F^-\ (aq\ HF) + n\ SDA^{z+}\ (aq\ HF) \rightarrow MS{\cdot}(SDAF_z)_n \qquad (1)$$

and

$$SiO_2\ (glass) \rightarrow MS \qquad (10)$$

The enthalpy and entropy of transition from quartz to silica glass are 9.1±2.3 kJ/mol SiO_2 and 7.0±1.0 J/(mol·K), respectively,[12] and at 298.15 K the Gibbs free

energy for reaction (10) is ΔG_{trans}^{298}(glass→MS) = ΔG_{trans}^{298}(quartz→MS) - ΔG_{trans}^{298}(quartz→glass). Therefore, the Gibbs free energy of formation of an organic-containing molecular sieve from amorphous precursors is ΔG_{rxn}^{298}(glass→MS/SDA) = ΔG_{int}^{298}(MS/SDA) + ΔG_{trans}^{298}(quartz→MS) - ΔG_{trans}^{298}(quartz→glass). Table 7.8 shows the various contributions to ΔG_{rxn}^{298}(glass→MS/SDA) for MFI/TPA, MFI/TEA, and *BEA/TEA. The large uncertainties in Table 7.8 are due to uncertainties in the literature values for the enthalpy and entropy of silica glass.[12] Since the energetic data for silica glass were obtained by high-temperature calorimetry, the ΔH_{trans}^{298}(quartz→MS) values measured by high-temperature calorimetry[7,8] were used to calculate ΔG_{rxn}^{298}(glass→MS/SDA) for the sake of consistency. Note that since the entropies of pure-silica molecular sieves are nearly identical,[11] the stabilities of calcined frameworks differ mostly because of enthalpy differences.

The Gibbs free energies of formation of MS/SDA from silica glass are not significantly more exothermic than the Gibbs free energies of interaction; they do not lead to stabilization energies greater than 2RT. When ΔG_{rxn}^{298}(glass→MS/SDA) is examined, the most favorable self-assembly among the materials in Table 7.8 is that for MFI/TPA, even if ΔG_{int}^{298}(MS/SDA) is higher for *BEA/TEA. This result is in accordance with the fact that TPA has a higher specificity than TEA (with which both MFI and *BEA can be crystallized). The difference in the stabilities of

the empty MFI and *BEA frameworks thus alters the relative energetics of the organic-inorganic composite materials. The interaction between *BEA and TEA is sufficiently exergonic for the formation of *BEA/TEA from amorphous precursors to occur spontaneously even though calcined *BEA is less thermodynamically stable than glass. Under hydrothermal synthesis conditions, calcined *BEA has been observed to redissolve,[48] showing that the framework is only metastable when not interacting with the SDA. When extrapolated to 423.15 K, a more typical synthesis temperature, the energetic trends for self-assembly from amorphous precursors are not strongly altered, so conclusions based on ΔG_{int}^{298} are expected to correlate well with behavior at synthesis temperatures.

Thermodynamic Analysis of the Full Synthesis Mixtures

The ΔG_{rxn}^{298} (MS/SDA) values discussed above represent only part of the actual synthesis reaction. To perform a more complete analysis, the energetic effects of the changes in state of the other components (water, free SDA^{z+} and F^- ions in the gel) must be considered as well. The crystallization of a pure-silica molecular sieve from a fluoride containing gel can be symbolized per mol silica as:

$$SiO_2\ (glass) + a\ SDA^{z+}\ (aq, molality\ m_i) + az\ F^-\ (aq, zm_i) + h\ H_2O \rightarrow$$
$$MS{\cdot}(SDAF_z)_n + (a-n)\ SDA^{z+}\ (aq, m_f) + (az-nz)\ F^-\ (aq, zm_f) +$$
$$h\ H_2O \qquad (11)$$

where the hydration of the molecular sieve is again neglected. Here m_i and m_f symbolize the initial and final molalities of the SDA fluoride in the synthesis gel. h and a are the initial amounts of substance of $SDAF_z$ and water, respectively. m_{cal} is the molality of the SDA fluoride in the calorimeter at the end of the solution experiments. Table 7.9 shows the initial and final concentrations of the three synthesis mixtures considered. A simpler synthesis composition than the actual mixture (without extra HF or NH_4F) was employed for MFI/TPA; this gel is known to also yield MFI/TPA. It is assumed that all the silica in each system is present as silica glass at the beginning and as MS/SDA at the end of the crystallization. This assumption is reasonable since the synthesis yield (on a silica basis) was greater than 85% for all three systems considered. Equation (11) is the sum of the following simpler steps:

$$SiO_2\ (\text{glass}) + n\ SDA^{z+}\ (\text{aq HF}, m_{cal}) + nz\ F^-\ (\text{aq HF}, zm_{cal}) \rightarrow MS{\cdot}(SDAF_z)_n \qquad (9)$$

$$n\ SDA^{z+}\ (\text{aq}, m_{cal}) + nz\ F^-\ (\text{aq}, zm_{cal}) \rightarrow n\ SDA^{z+}\ (\text{aq HF}, m_{cal}) + nz\ F^-\ (\text{aq HF}, zm_{cal}) \qquad (12)$$

$$\{n\ SDA^{z+}\ (aq, m_i) + nz\ F^-\ (aq, zm_i) + h\ H_2O\} \rightarrow$$

$$\{n\ SDA^{z+}\ (aq, m_{cal}) + nz\ F^-\ (aq, zm_{cal})\} +$$

$$\{(a\text{-}n)\ SDA^{z+}\ (aq, m_i) + (az\text{-}nz)\ F^-\ (aq, zm_i) + h\ H_2O\} \qquad (13)$$

Equation (9) is the idealized self-assembly of MS/SDA from silica glass and the $SDAF_z$ in its reference state in 25% aqueous HF solution. The energetics for this step were discussed in the previous section. Equation (12) represents the transfer of SDA and fluoride ions from 25% aqueous HF to water at the concentration present in the solution calorimetry experiments. Equation (13) is the fictitious dilution of n moles SDA and fluoride ions (in h mol water) from the initial concentration in the hydrothermal synthesis mixture to the concentration present in the solution experiments, and simultaneously of (a-n) moles SDA and fluoride ions (in h mol water) at the initial concentration of the hydrothermal synthesis mixture to (a-n) moles SDA and fluoride ions (in h mol water) at the final concentration of the hydrothermal synthesis mixture.

No data are available to estimate the energetics of SDAF transfer from water to 25% aqueous HF. The most similar compound to the SDA fluorides for which data are available is TEAI whose Gibbs free energy of transfer from water to methanol is 7.5 kJ/mol SDA at 298.15 K.[49] For the MS/SDA pair with the highest organic content (*BEA/TEA) such a value would lead to ΔG_{12} = 0.7 kJ/mol SiO_2. 25% aqueous HF is considerably more polar than methanol, and furthermore 77% of the solvent molecules are water. The magnitude of ΔG_{12} is

thus expected to be significantly smaller than the value calculated from the transfer to methanol of TEAI. ΔG_{12} was therefore neglected in the calculation of the energetic changes of the complete synthesis mixture due to the lack of data and to its small size. The Gibbs free energy of equation (13) is equal to:

$$\Delta G_{13} = \Delta G_{mix}(m_f) + n\mu(m_{cal}) - \Delta G_{mix}(m_i)$$

$$= \Delta G^{id}_{mix}(m_f) - \Delta G^{id}_{mix}(m_i) + \Delta G^{EX}(m_f) - \Delta G^{EX}(m_i) + 2RTn\ln(m_{cal}\gamma_{cal})$$

In this equation, the Gibbs free energies of mixing are calculated based on a synthesis mixture containing one mole of SiO_2. The standard state of the organic fluoride salts is the hypothetical ideal one molal solution. The excess Gibbs free energies of mixing were calculated from Pitzer's correlations for TEAF and TPAF.[50] The activity coefficients at the calorimetric concentration were obtained from the same source. The ideal Gibbs free energies of mixing for uni-univalent electrolytes at molality m are given by 2RTn(ln m –1).

Table 7.10 shows the Gibbs free energy of self-assembly from the actual synthesis mixture, $\Delta G_{11} = \Delta G^{298}_{SYN}$ (MS/SDA), as well as the contribution from the effective dilution of the SDA and fluoride ions, ΔG_{13}. Dilution (13) is exergonic for all cases, with ΔG_{13} ranging from -1.6 to –4.4 kJ/mol SiO_2, a range comparable to that of ΔG^{298}_{rxn} (glass→MS/SDA). Each of the three energetic contributions considered in this work (empty frameworks, MS/SDA interaction, and dilution of SDA fluorides in the synthesis mixture) contributes to the overall energetics to a similar extent. They must all be included in thermodynamic descriptions of

molecular sieve syntheses. Note also that at the high molalities present in these synthesis mixtures, the activity coefficients of the SDAF species in aqueous solution are among the highest reported for uni-univalent electrolytes.[51] The magnitudes of ΔG_{13} are therefore more negative than the corresponding dilutions for ideal solutions.

The Gibbs free energy changes during molecular sieve synthesis range from -4.9 to -8.5 kJ/mol SiO_2. While more exergonic than ΔG_{rxn}^{298} (glass→MS/SDA), these values still imply only slight thermodynamic differences between various phases. The ΔG_{SYN}^{298} (MS/SDA) values are comparable for MFI/TPA and *BEA/TEA, the more readily synthesized materials. Although the interaction between TPA and glass to produce MFI/TPA is more favorable (as befits the more selective SDA), the changes experienced by the water and SDAF unincorporated in the framework (ΔG_{13}) are more exergonic for the *BEA/TEA pair.

The last two columns of Table 7.10 present ΔG_{13} per mol SDA present in the initial synthesis mixture and per mol SDA incorporated in the molecular sieve, respectively. The ΔG_{13} values per mol SDA initially present differ by more than a factor of two between the two TEA systems. Table 7.10 also shows the calculated ΔG_{SYN}^{298} (*BEA/TEA) and ΔG_{13} values for the hypothetical synthesis of *BEA/TEA from the composition 1 SiO_2/ 0.5 TEAF/ 15 H_2O that in reality produces MFI/TEA. The ΔG_{13} value for this system is only slightly less exergonic than for the actual *BEA synthesis with H_2O/SiO_2 = 7.25, hence the propensity of

water-poor synthesis mixtures to crystallize more porous phases is not due to the higher activity of SDAF species in more concentrated mixtures. The preferential stabilization of *BEA/TEA over MFI/TEA seen in ΔG_{13} can be mostly related to the occlusion of a larger amount of substance of SDAF species into the more porous *BEA framework. The hypothetical ΔG_{SYN}^{298} (*BEA/TEA) is more negative than ΔG_{SYN}^{298} (MFI/TEA) by 2.6 kJ/mol SiO_2. While these values were calculated at 298.15 K and should be evaluated with caution, they suggest that the end products of molecular sieve crystallizations are not always the thermodynamically most stable phase.

Implications for Molecular Sieve Synthesis

Piccione et al. have shown that all crystalline silica polymorphs have Gibbs free energies within 2RT of each other.[11] The Gibbs free energies of interaction between inorganic host and organic guest calculated here are of comparable magnitude. The MS/SDA interaction thus significantly alters the free energy landscape during molecular sieve self-assembly. In some cases, the relative stability of silicate frameworks is modified to such an extent that structures less stable than silica glass become energetically favorable when their self-assembly takes place simultaneously with the interaction of the assembling framework with charged SDA species. While this interaction is favorable, it is not sufficiently exergonic to

explain the strong selectivity of many organic cations towards a relatively small subset of porous silica frameworks.

The role of organic SDAs in zeolite synthesis, then, cannot be to provide preferential stabilization for one structure with respect to others: the ΔH and ΔG differences seen here are too small in magnitude to explain the frequent formation of pure molecular sieve phases. By contrast, the moderate magnitude of the Gibbs free energy changes during crystallization readily explains the ability of most organocations to direct syntheses towards more than one molecular sieve framework. The relative magnitudes of the enthalpy and entropy contributions to the Gibbs free energy of self-assembly are similar, so the crystallization thermodynamics depend on the delicate interplay between a large number of interactions. The energetics of the empty molecular sieves, those of the organic/inorganic interaction, and the additional stabilizing factor contributed by the effective dilution of high-activity SDAF species upon enclathration must all be considered to fully describe molecular sieve syntheses. No single factor dominates ΔG_{SYN}^{298} (glass→MS/SDA). Although more porous molecular sieve frameworks are among the less stable silica polymorphs, several factors contribute to their stabilization in the as-made state. First, exothermic interactions with large, bulky SDAs can favor more porous phases due to the steric requirements for occlusion. A greater number of interactions with smaller, less specific SDAs can also lead to an enthalpy-based preference for more porous phases. In addition, the larger

amount of organic incorporated into more porous phases leads such systems to have greater entropies of interaction, and more exergonic Gibbs free energies for the effective dilution of SDA fluorides upon occlusion.

Since thermodynamic effects are relatively modest, kinetic factors must be at play to explain the crucial role of organic SDAs in molecular sieve synthesis. This conclusion is consistent with the observation that organic SDAs can be diverted away from those frameworks that they usually form by seeding with other molecular sieve phases.[13,40] This fact has been explained in terms of the nucleation step of molecular sieve synthesis having a higher energy of activation than the growth step.[40] It is plausible that activation energies be related to the interaction energetics, since conclusive evidence exists that precursors with intimate inorganic/organic contacts form in molecular sieve synthesis before long-range order is detectable by techniques such as X-ray diffraction.[52]

Conclusions

Enthalpies of solution in 25% HF at 323.15 K for a series of pure-silica molecular sieves in their as-made and calcined forms have been determined by solution calorimetry. The relative enthalpies of the calcined frameworks confirm previous findings[7,8] that crystalline silica polymorphs are within twice the available

thermal energy (RT) of each other. Such a low barrier to transformation explains the large diversity (over 20 structures) of silica polymorphs.

Enthalpies of interaction between organic guests and inorganic hosts were obtained by taking the difference between the enthalpies of solution of the as-made and calcined materials. The enthalpies of interaction determined in this work span the narrow exothermic range of –1.1 to –5.9 kJ/mol SiO_2. None of these values is more negative than -2RT, and such modest magnitudes explain why many SDAs can direct molecular sieve syntheses toward several different frameworks. The thermodynamic data, combined with published synthetic findings, suggest that small molecules engage in relatively non-specific interactions with pure-silica molecular sieves. Larger, bulkier, and/or more rigid SDAs are more selective in the frameworks that they interact favorably with, leading to stronger enthalpies of interaction, and in general, to more porous structures. It is suggested that the greater specificity of such SDAs is due to the more stringent steric requirements they place on the inorganic frameworks.

Entropies of interaction were estimated and Gibbs free energies of interaction calculated for the *BEA/TEA, MFI/TEA and MFI/TPA inorganic/organic materials. The entropy of interaction is found to be positive, thus favorable, in all cases. Within the approximations of this work, the entropy of interaction varies linearly with the organic content, thus preferentially stabilizing more porous structures. The magnitudes of the enthalpy and entropy contributions to the Gibbs free energy of interaction are comparable, proving that both must be

included in thermodynamic descriptions of MS/SDA interactions. The Gibbs free energy of transformation from amorphous precursors is also in no case more exergonic than 2RT, yet the organic/inorganic interactions can provide a thermodynamic stability field for some SiO_2 polymorphs less stable than glass (e.g., *BEA) relative to amorphous precursors. When all the components present in the synthesis mixture are considered, additional stabilizing contributions (-1.6 to -4.4 kJ/mol SiO_2) due to the effective dilution of the SDA and fluoride ions are recognized. Such contributions also favor more porous frameworks. The Gibbs free energy changes during molecular sieve syntheses starting with amorphous precursors are in no case more exergonic than 3RT. There is therefore no strong thermodynamic control in molecular sieve synthesis. Organic SDAs do not select one structure over others by strongly stabilizing a particular framework as the final product. Rather, a kinetic role for the SDA is argued for, where the activation energies for molecular sieve formation may be related to the energetics of the MS/SDA interaction.

Acknowledgments

Financial support for this work was provided by the Chevron Research and Technology Co. The calorimetric studies were supported by NSF grant DMR 98 XXX. PMP thanks Dr. Stacey Zones (Chevron) for providing the STF and 2,6-dimethyl-1-aza-spiro[5.4]decane samples used in this study, and Michael Gordon and Michael Roy (Caltech) for helping in the calorimeter cell design. Comments by Dr. Stacey Zones (Chevron) are appreciated.

Table 7.1. Unit Cell Compositions

Sample	% water loss*	% organic loss*	Si/uc[9]	SDA/uc*	H_2O/uc*	SDA/SiO_2*	H_2O/SiO_2*	MW (g/mol SiO_2)*	%C†	%F†	SDA/uc†
MFI/calc	1.32	–	96	–	4.29	–	0.045	60.89	0.25	0.0408	–
MFI/TEA	0.08	9.24	96	3.94	0.29	0.041	0.003	66.26	5.58	1.67	3.77
MFI/TPA	0.00	11.85	96	3.78	0.00	0.039	0.000	68.64	8.31	1.13	3.91
*BEA/calc	1.32	–	64	–	2.85	–	0.044	60.89	0.37	0.0192	–
*BEA/TEA	1.31	19.30	64	6.26	3.51	0.098	0.055	75.68	11.99	1.15	6.11
*BEA/BISPIP	1.45	19.56	64	2.08	3.92	0.032	0.061	76.06	15.17	1.18	2.14
MTW/calc	1.20	–	56	–	2.27	–	0.041	60.89	0.17	< 0.01	–
MTW/BISPIP	0.27	9.06	56	0.73	0.56	0.013	0.010	66.27	6.29	0.73	0.70
STF/calc	1.35	–	16	–	0.73	–	0.046	60.89	< 0.5	0.013	–
STF/SPIRO	0.07	15.58	16	0.95	0.04	0.059	0.003	71.23	10.93	1.03	0.96
Quartz	0.00	–	3	–	0.00	–	0.000	60.08	–	–	–

* By TGA. These compositions were used in the thermodynamic cycles.

† By elemental analysis.

Table 7.2. Measured Enthalpies of Solution (mass basis)

Framework	Organic SDA	ΔH_{soln}^{323} (MS/calc) (kJ/g)	Uncertainty (kJ/g)	ΔH_{soln}^{323} (MS/SDA) (kJ/g)	Uncertainty (kJ/g)
MFI	TPA	-2.407	0.012	-2.103	0.017
MFI	TEA	-2.428	0.021	-2.214	0.006
*BEA	TEA	-2.438	0.016	-1.920	0.014
*BEA	BISPIP	-2.437	0.011	-1.874	0.003
MTW	BISPIP	-2.391	0.020	-2.170	0.005
STF	SPIRO	-2.426	0.015	-2.005	0.003
Quartz	–	-2.334	0.018	–	–

Table 7.3. Measured Enthalpies of Solution (mol basis)

Framework	Organic SDA	ΔH_{soln}^{323} (MS/calc) (kJ/mol SiO_2)	Uncertainty (kJ/mol SiO_2)	ΔH_{soln}^{323} (MS/SDA) (kJ/mol SiO_2)	Uncertainty (kJ/mol SiO_2)
MFI	TPA	-146.56	0.70	-143.35	1.16
MFI	TEA	-147.84	1.30	-146.73	0.39
*BEA	TEA	-148.43	0.98	-145.30	1.07
*BEA	BISPIP	-148.41	0.64	-142.55	0.20
MTW	BISPIP	-145.44	1.23	-143.80	0.32
STF	SPIRO	-147.74	0.89	-142.80	0.23
Quartz	–	-140.23	1.09	–	–

Table 7.4. Comparison of Solution Enthalpies to Literature Values

Reference	ΔH^{T}_{soln} (kJ/mol SiO_2)	T*	HF%*	Correction† (kJ/mol SiO_2)	ΔH^{323}_{soln} (kJ/mol SiO_2)
Quartz					
This work	-140.2±1.1	323.15	25	–	-140.2±1.1
Johnson[34]	-138.2±1.4‡	298.15	24.4	-2.4	-140.7±1.4
Patarin[13]	-138.0±1.0	298.15	25	-2.4	-140.4±1.0
Hemingway[30]	-137.7±0.2	333.15	20.1	0.6	-137.1±0.2
Kilday[31]	-139.1±0.1	323.15	24.4	0.1	-139.1±0.1
Liou[32]	-142.3±0.1	322.62	24.4	0.1	-142.4±0.1
MFI/calc					
This work	-147.2±0.6	323.15	25	–	-147.2±0.6
Johnson[34]	-145.1±0.1	298.15	24.4	-2.5	-147.6±0.1
Patarin[13]	-138.0±1.8	298.15	25	-2.4	-140.4±1.8
MFI/TPA					
This work	-143.3±1.2	323.15	25	–	-143.3±1.2
Patarin[13]	-131.8±1.9	298.15	25	-2.4	-134.2±1.9

* Experimental conditions of the reported solution experiments closest to 25% HF and 323.15 K.

† Correction to 25% HF and 323.15 K. Temperature corrections for the MFI enthalpies of solution used the same correlations as for quartz.[31]

‡ Combination of HF solution and F_2 combustion measurements.

Table 7.5. Enthalpies of Transition from Quartz to other SiO_2 Polymorphs

Framework	ΔH_{trans}^{323} (This work) kJ/mol SiO_2	ΔH_{trans}^{298} (High-T calorimetry) kJ/mol SiO_2
*BEA	8.2±1.1	9.3±0.8[7]
MFI	7.0±1.1	6.8±0.8[8]
MTW	5.2±1.3	8.7±1.3[7], 7.0±2.7[8,*]
STF	7.5±1.2	9.1±2.8[8,*]

* Estimated.

Table 7.6. Enthalpies of Interaction

Framework	Organic SDA	ΔH_{int}^{323} (kJ/mol SiO_2)	Uncertainty (kJ/mol SiO_2)	ΔH_{int}^{323} (kJ/mol SDA)	Uncertainty (kJ/mol SDA)	(c-w)ΔH_6 (kJ/mol SiO_2)
MFI	TPA	-3.2	1.4	-81	34	0.03
MFI	TEA	-1.1	1.4	-27	33	0.02
*BEA	TEA	-3.1	1.4	-32	15	-0.01
*BEA	BISPIP	-5.9	0.7	-181	21	-0.01
MTW	BISPIP	-1.6	1.3	-124	97	0.02
STF	SPIRO	-4.9	0.9	-83	16	0.02

Table 7.7. Gibbs Free Energies of Interaction

Framework	Organic SDA	ΔS_{int}^{298} (J/(mol SDA·K))	$T\Delta S_{int}^{298}$ at 298.15 K (kJ/mol SiO_2)	ΔG_{int}^{298} (kJ/mol SiO_2)	ΔG_{int}^{423} * (kJ/mol SiO_2)
MFI	TPA	144±11	1.7±0.1	-4.9±1.4	-5.6
MFI	TEA	77±11	0.9±0.1	-2.0±1.4	-2.4
*BEA	TEA	77±11	2.2±0.3	-5.4±1.5	-6.3

* Extrapolated assuming no temperature dependence of ΔS_{int}^{T} or ΔH_{int}^{T}.

Table 7.8. Gibbs Free Energies of Formation from Amorphous Precursors and SDAs

Framework	ΔH_{trans}^{298} (glass→MS) (kJ/mol SiO_2)	$T\Delta S_{trans}^{298}$ (glass→MS) (kJ/mol SiO_2)	ΔG_{trans}^{298} (glass→MS) (kJ/mol SiO_2)
MFI	-2.3±2.4	-1.0±0.3	-1.3±2.5
*BEA	0.2±2.4	-1.1±0.3	1.3±2.5

Framework	Organic SDA	ΔH_{rxn}^{298} (glass→MS/SDA) (kJ/mol SiO_2)	$T\Delta S_{rxn}^{298}$ (glass→MS/SDA) (kJ/mol SiO_2)	ΔG_{rxn}^{298} (glass→MS/SDA) (kJ/mol SiO_2)	ΔG_{rxn}^{423}* (glass→MS/SDA) (kJ/mol SiO_2)
MFI	TPA	-5.5±2.8	0.7±0.1	-6.2±2.8	-6.4
MFI	TEA	-3.4±2.8	-0.1±0.1	-3.3±2.8	-3.3
*BEA	TEA	-2.9±2.8	1.2±0.2	-4.1±2.9	-4.6

* Extrapolated assuming no temperature dependence of ΔS_{rxn}^{T} or ΔH_{rxn}^{T}.

Table 7.9. Synthesis Mixture Compositions

Framework	Organic SDA	Initial Composition	Final Composition
MFI	TPA	1 SiO_2/ 0.44 TPAF/ 8.44 H_2O	1 MFI·$(TPAF)_{0.039}$/ 0.401 TPAF/8.44 H_2O
MFI	TEA	1 SiO_2/ 0.5 TEAF/ 15 H_2O	1 MFI·$(TEAF)_{0.041}$/ 0.459 TEAF/15 H_2O
*BEA	TEA	1 SiO_2/ 0.5 TEAF/ 7.25 H_2O	1 *BEA·$(TEAF)_{0.098}$/ 0.402 TEAF/7.25 H_2O

Table 7.10. Gibbs Free Energies of Formation and Effective Dilution for Complete Synthesis Mixtures

Framework	Organic SDA	ΔG_{SYN}^{298} (MS/SDA) (kJ/mol SiO_2)	ΔG_{13} (effective dilution) (kJ/mol SiO_2)	ΔG_{13} (kJ/mol SDA incorporated)	ΔG_{13} (kJ/mol SDA in synthesis mixture)
MFI	TPA	-8.1±2.8*	-2.0	-50	-4.4
MFI	TEA	-4.9±2.8	-1.6	-39	-3.2
*BEA	TEA	-8.5±2.9	-4.4	-45	-8.9
*BEA†	TEA†	-7.5±2.9†	-3.4†	-35†	-6.8†

* The largest error is assumed to be contributed by ΔG_{rxn}^{298} (glass→MS/SDA).

† For a hypothetical synthesis mixture 1 SiO_2/0.5 TEAF/ 15 H_2O.

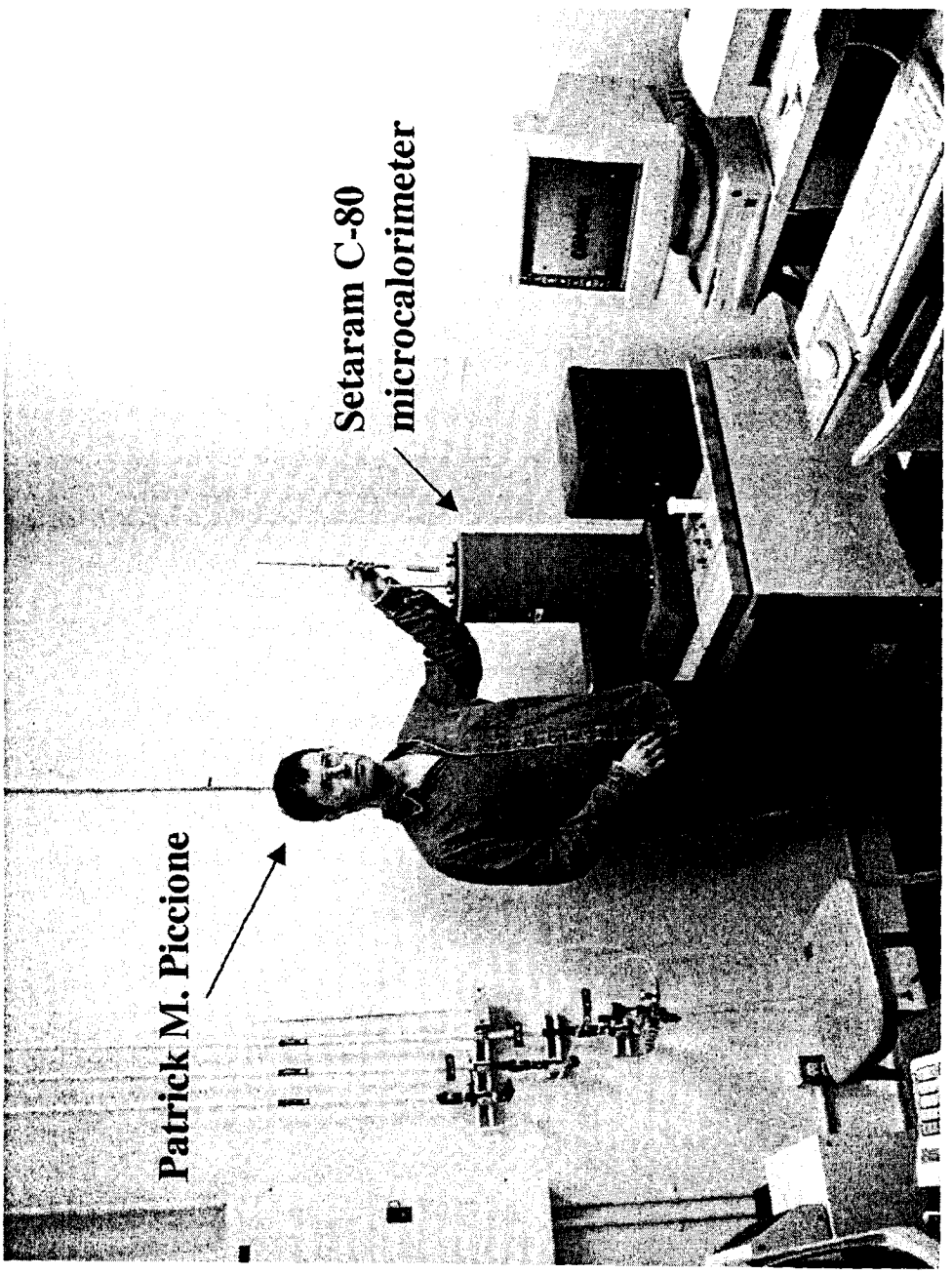

Figure 7.1. Setaram C-80 Microcalorimeter

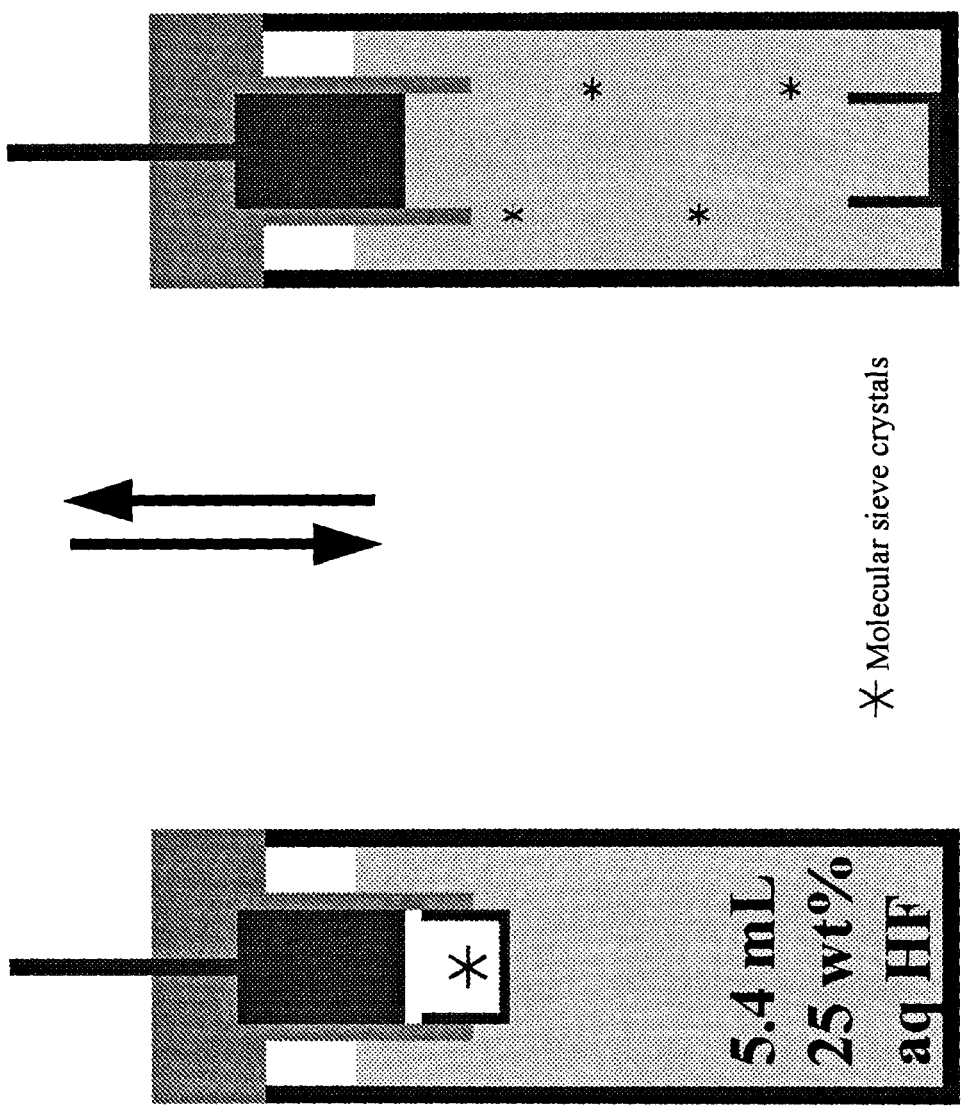

Figure 7.2. HF Resistant Cells

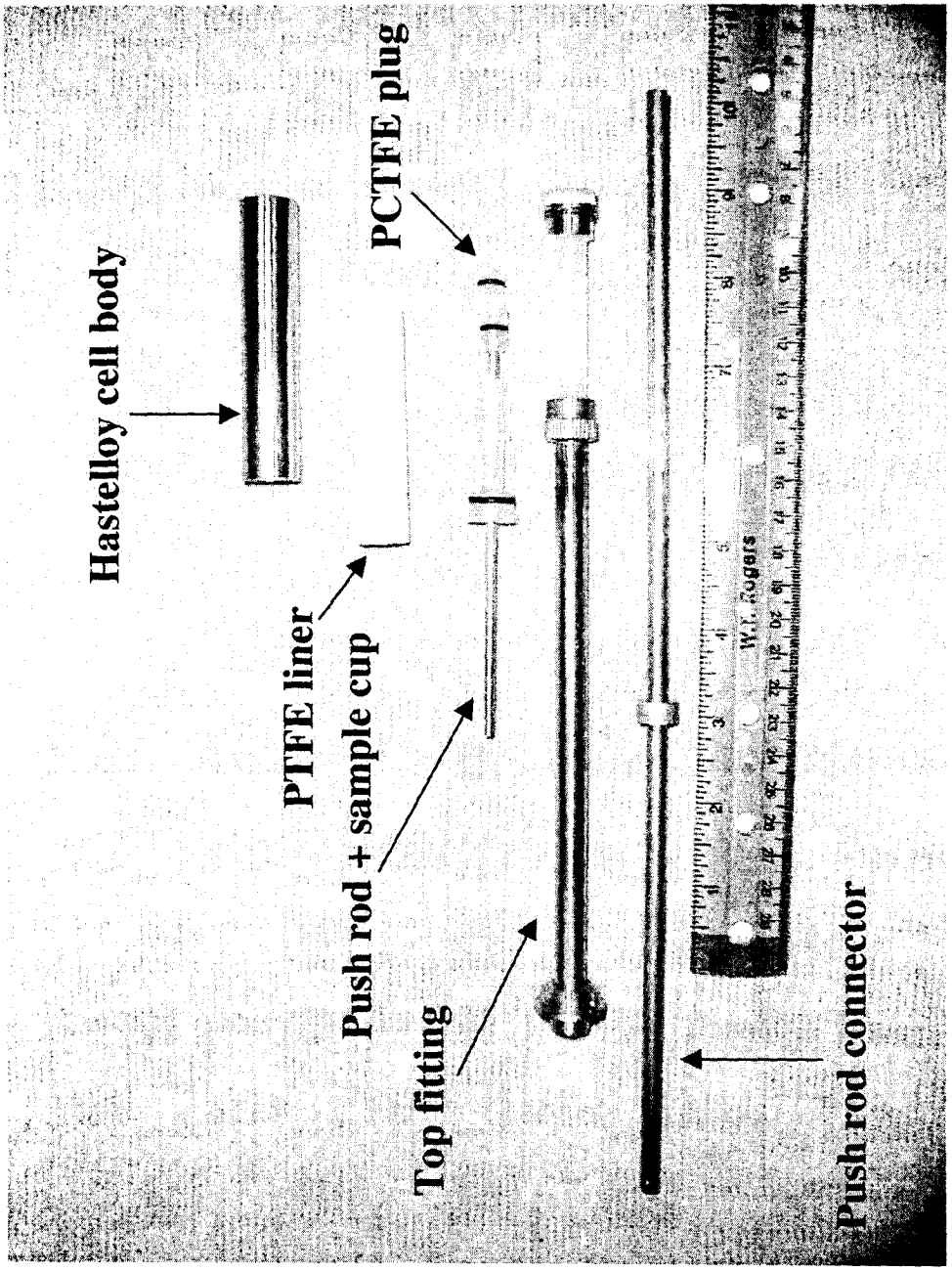

Figure 7.3. HF Resistant Cells

Figure 7.4. ^{1}H Solid-State NMR Spectra of SDA-Containing Molecular Sieves

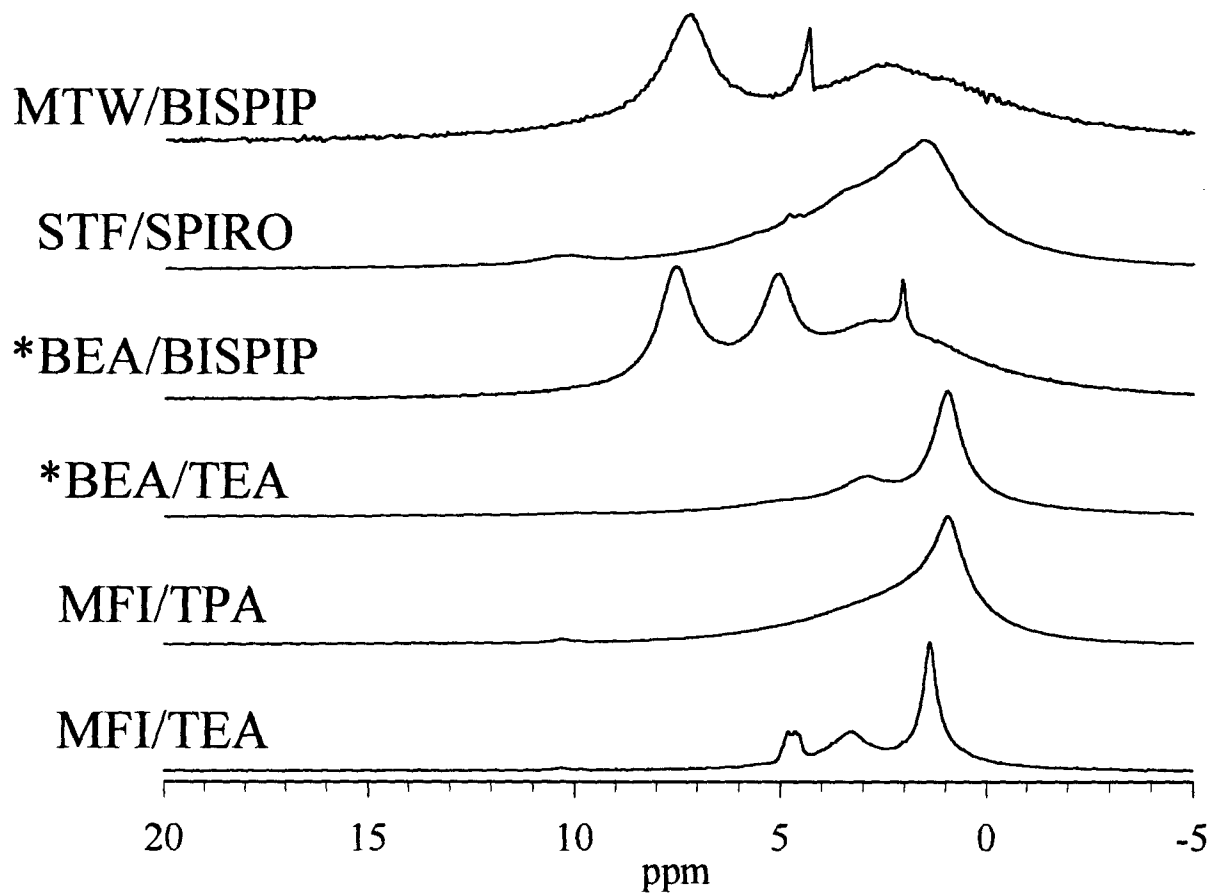

Figure 7.5. ^{1}H Solid-State NMR Spectra of Calcined Molecular Sieves

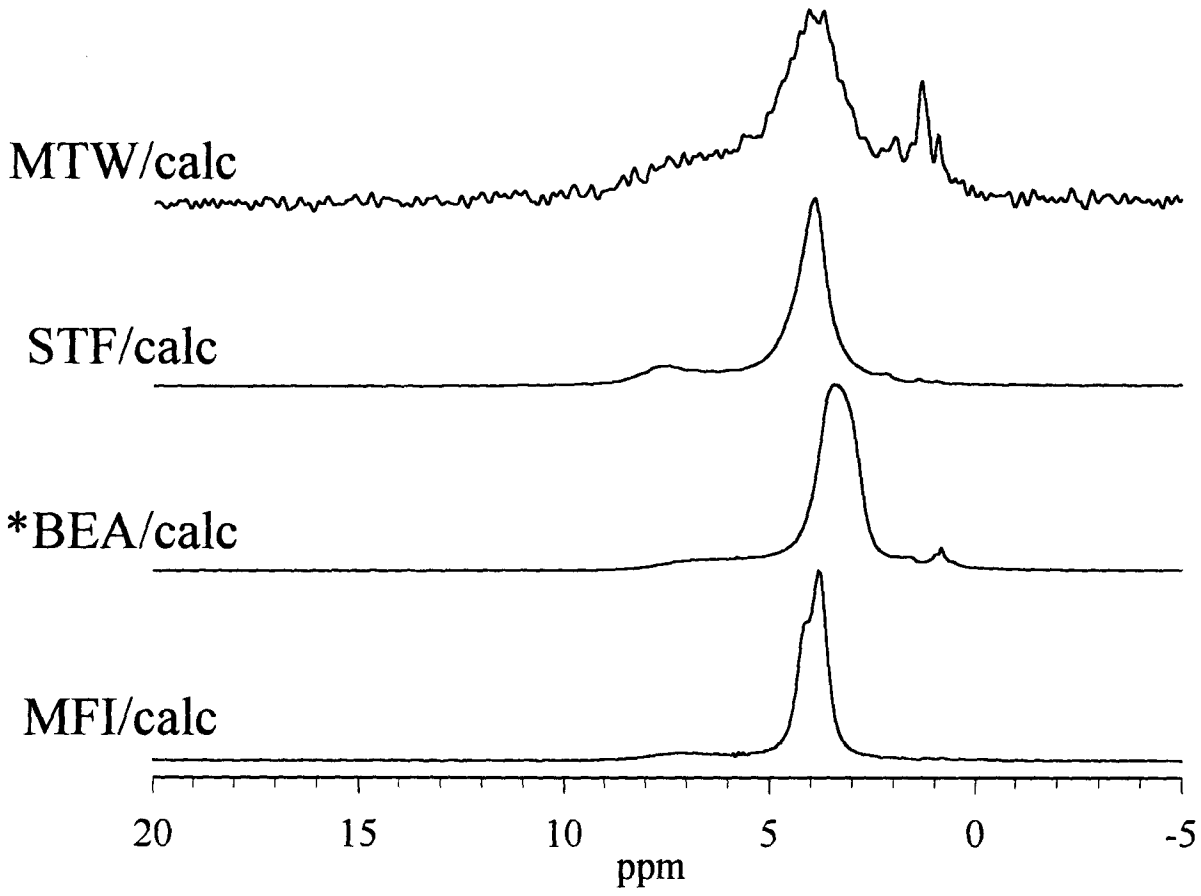

Figure 7.6. ^{29}Si Solid-State NMR Spectra of SDA-Containing Molecular Sieves

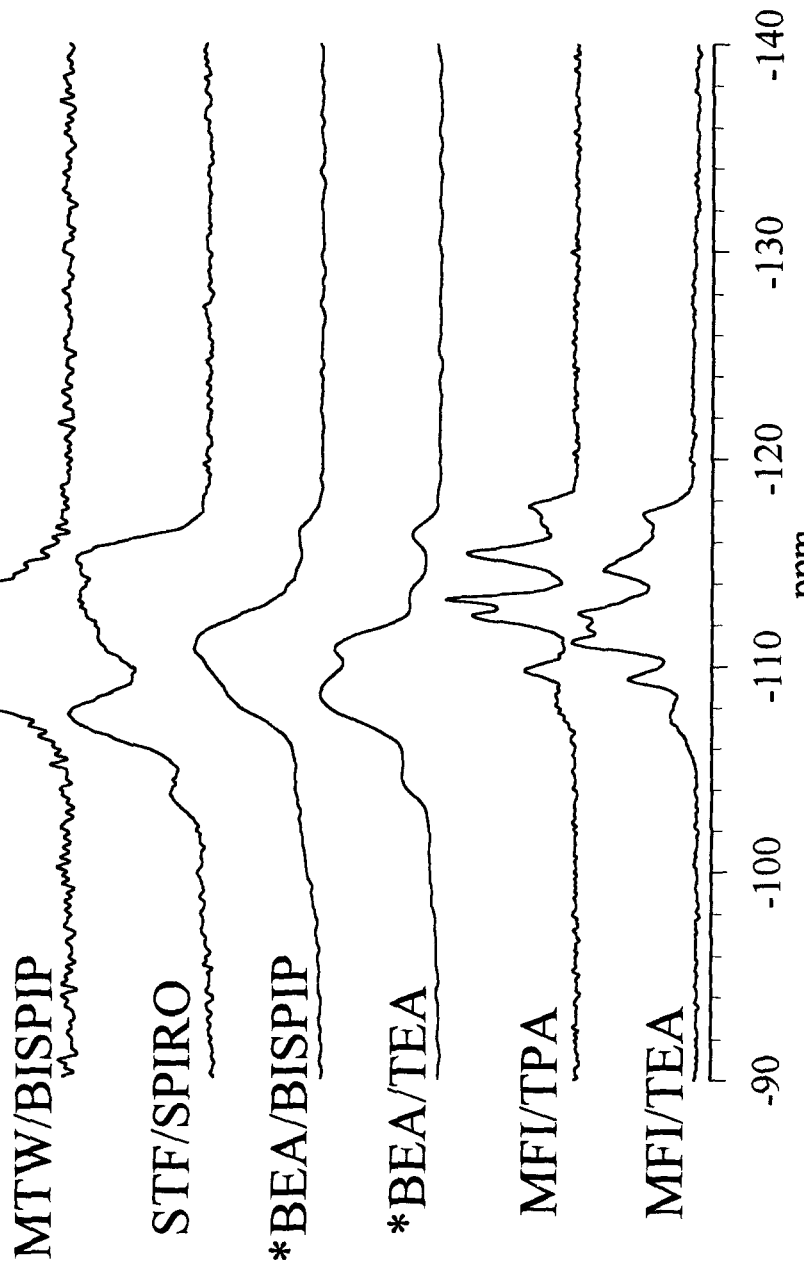

Figure 7.7. ^{29}Si Solid-State NMR Spectra of Calcined Molecular Sieves

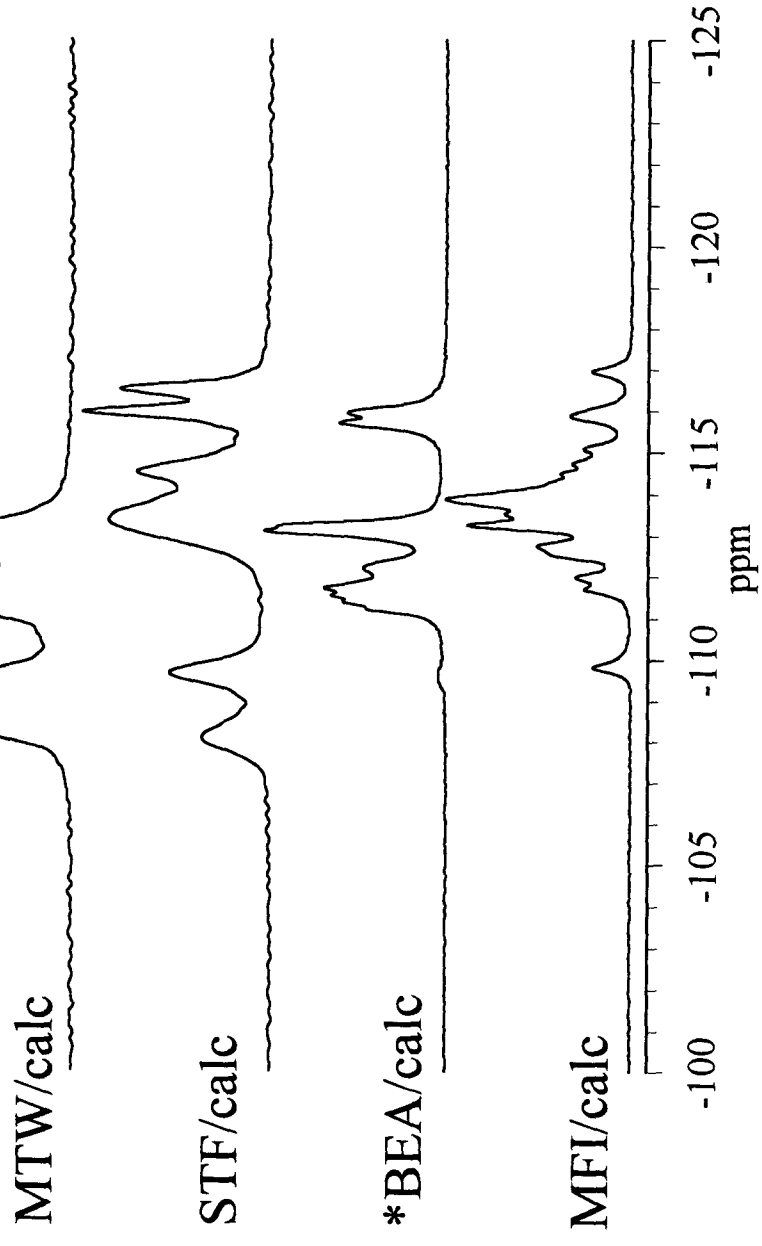

Figure 7.8. ^{13}C Solid-State NMR Spectra of SDA-Containing Molecular Sieves

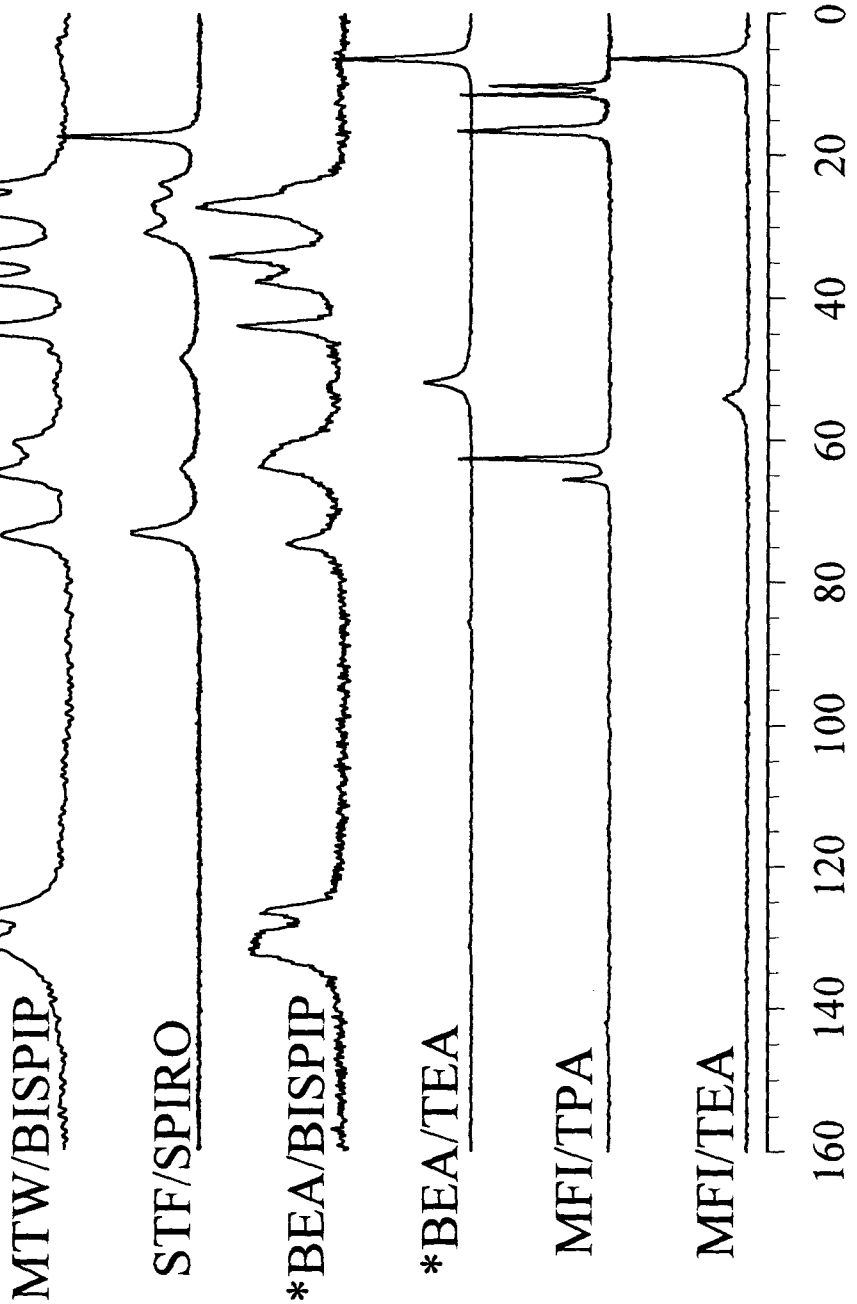

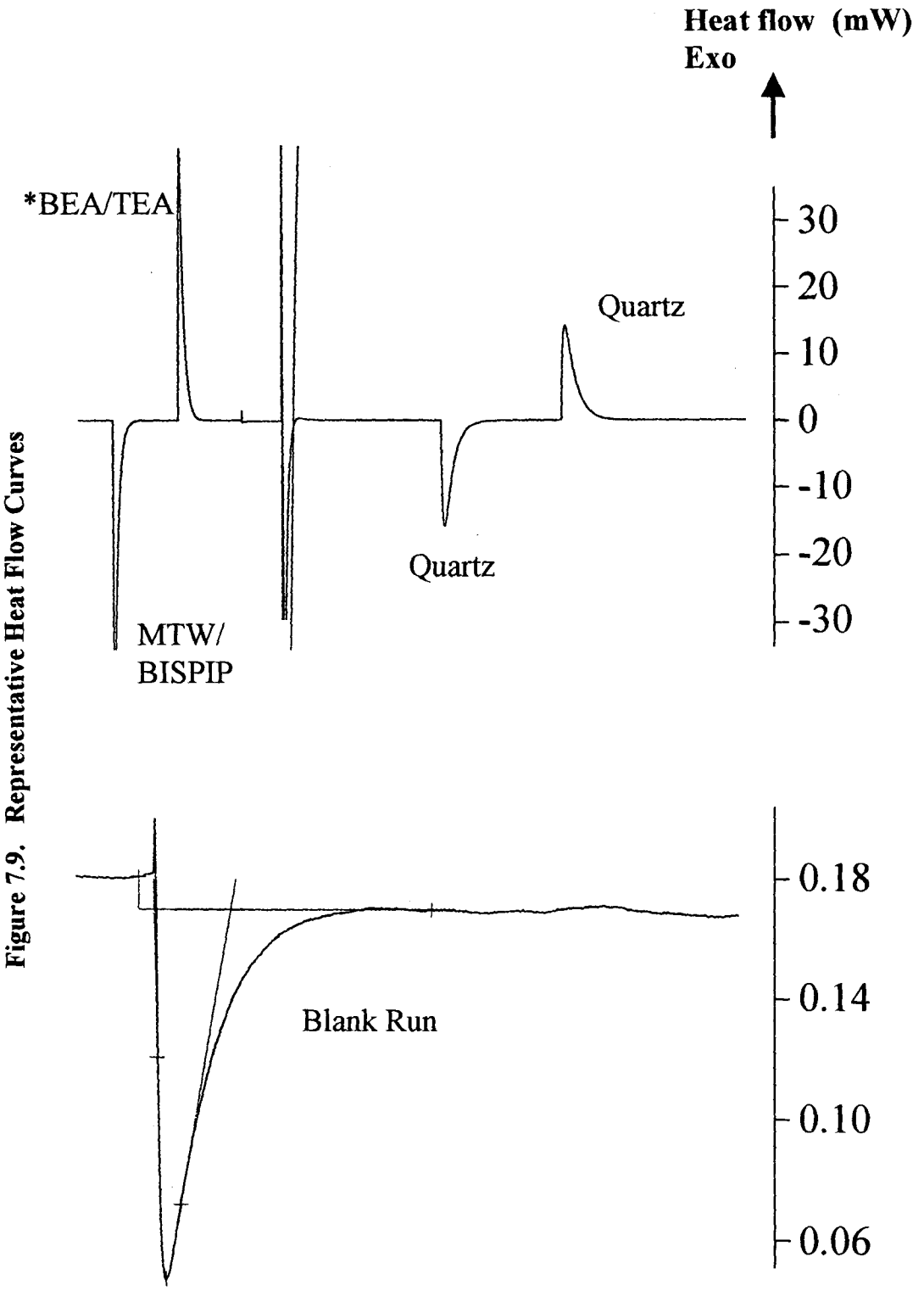

Figure 7.9. Representative Heat Flow Curves

Figure 7.10. General Trends in MS/SDA Interactions

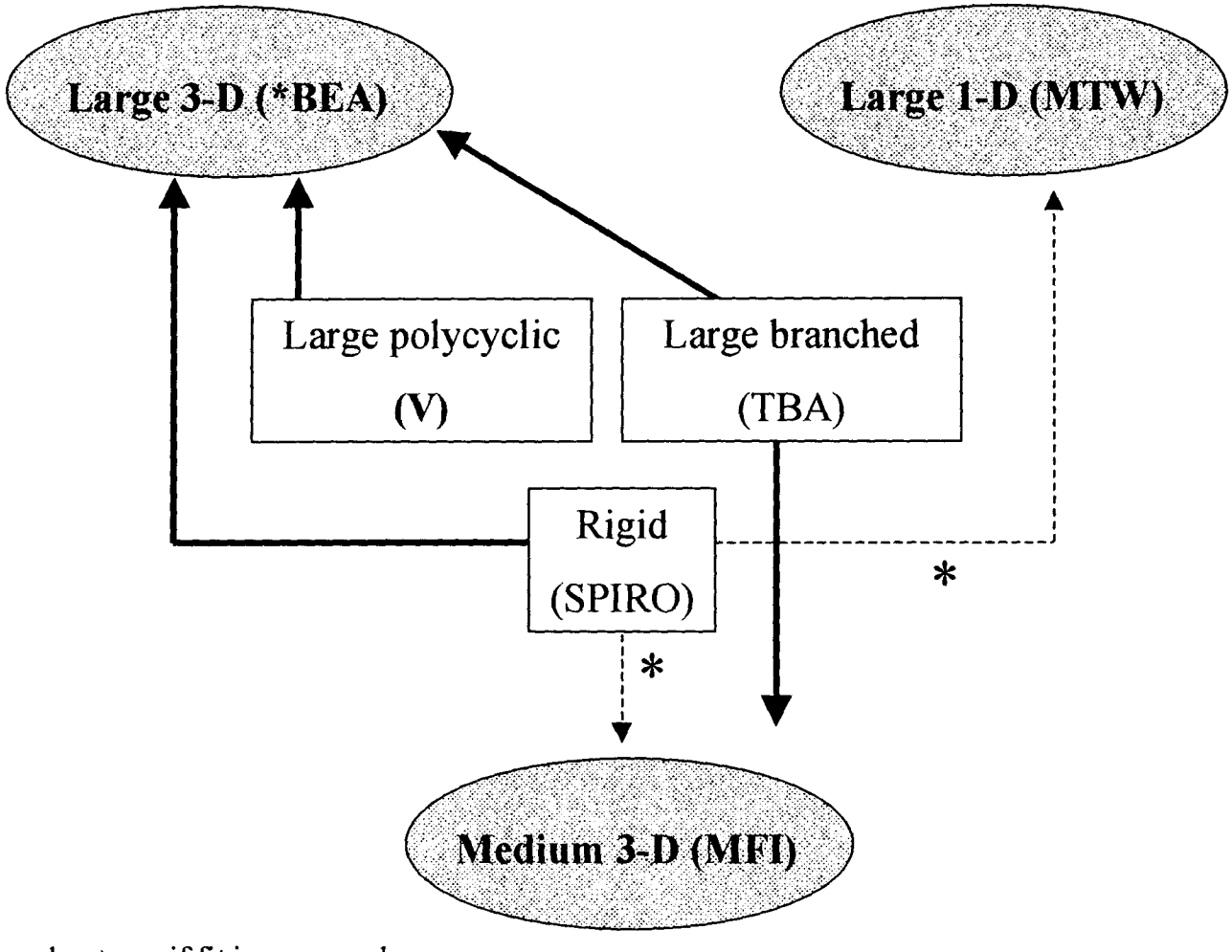

* can be strong if fit is very good

Figure 7.10. (Continued)

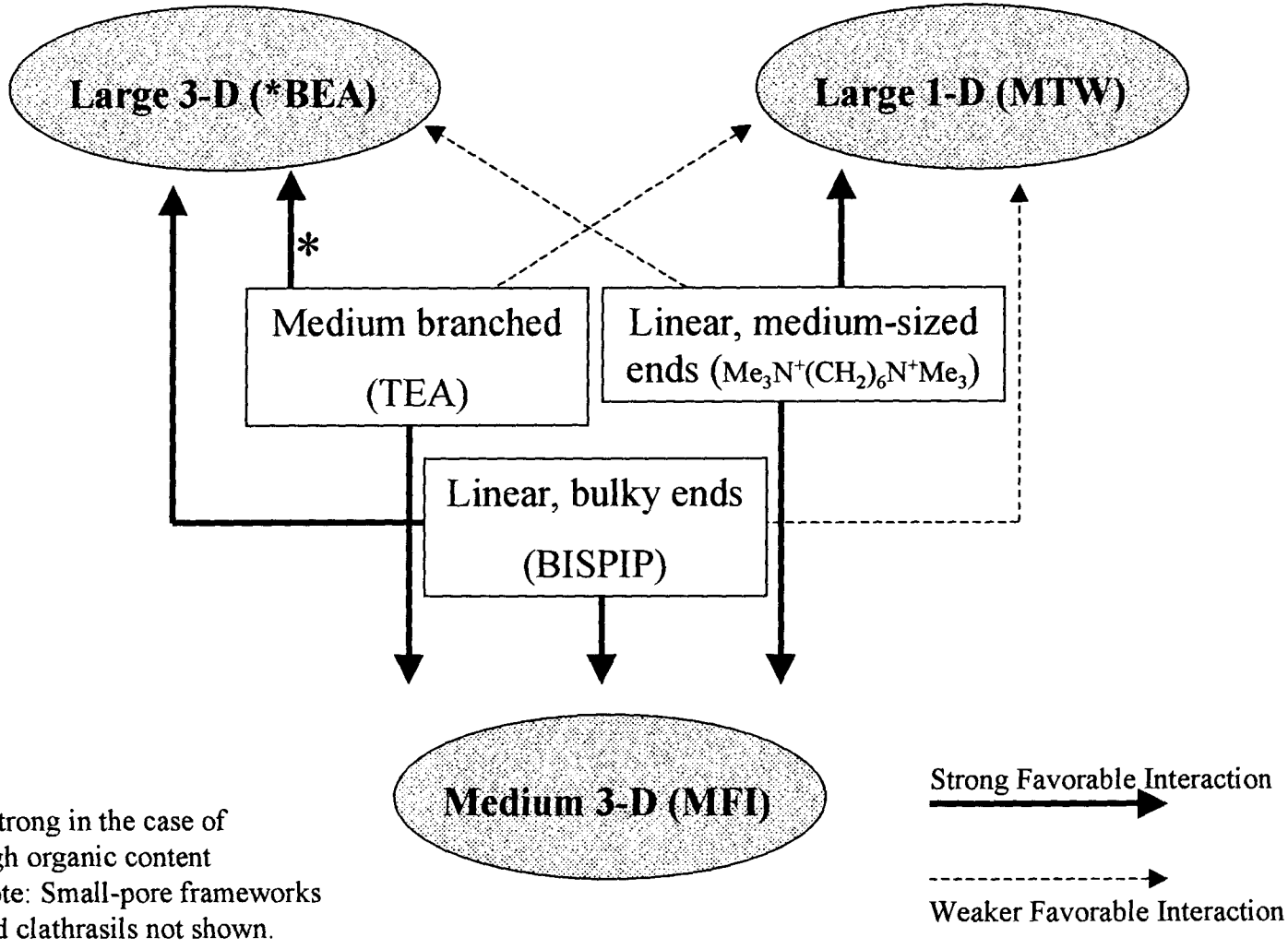

*Strong in the case of high organic content
Note: Small-pore frameworks and clathrasils not shown.

References

[1] Szostak, R. *Molecular Sieves*, **1989**, Van Nostrand Reinhold: NY.

[2] Davis, M. E. *Micro. Meso. Mater.* **1998**, *21*, 173.

[3] Breck, D. W. *Zeolite Molecular Sieves,* **1974**, Wiley: NY.

[4] Gies, H.; Marler, B. *Zeolites*, **1992**, *12*, 42.

[5] Lobo, R. F.; Zones, S. I.; Davis, M. E. *J. Incl. Phen. Mol. Recogn. Chem.* **1995**, *21*, 47.

[6] Davis, M. E.; Zones, S. I. in Occelli, M. L.; Kessler, H. *Synthesis of Porous Materials*, **1997**, Marcel Dekker: NY.

[7] Piccione, P. M.; Laberty, C. M.; Yang, S.; Camblor, M. A.; Navrotsky, A.; Davis, M. E. *J. Phys. Chem. B* **2000**, *101*, 10001.

[8] Petrovic, I.; Navrotsky, A.; Davis, M. E.; Zones, S. I. *Chem. Mater.* **1993**, *5*, 1805.

[9] http://www.iza-sc.ethz.ch/IZA-SC/Atlas/AtlasHome.html.

[10] Boerio-Goates, J.; Stevens, R.; Hom, B.; Woodfield, B. F.; Piccione, P. M.; Davis, M. E.; Navrotsky, A. *J. Chem. Thermodyn.* **2001** *submitted.*

[11] Piccione, P. M.; Woodfield, B. F.; Boerio-Goates, J.; Navrotsky, A.; Davis, M. E. *J. Phys. Chem. B* **2001**, 105, 6025.

[12] Robie, R. A.; Hemingway, B. S. *USGS Bulletin 2131,* **1995**.

[13] Patarin, J.; Soulard, M.; Kessler, H.; Guth, J.L.; Diot, M. *Thermochim. Acta* **1989**, *146*, 21.

[14] Patarin, J.; Kessler, H.; Soulard, M.; Guth, J. L. in *Zeolite Synthesis*; Occelli, M. L.; Robson, H. E., Eds.; *ACS Symposium Series 298*, **1989**, Ch. 16.

[15] Helmkamp, M. M.; Davis, M. E. *Annu. Rev. Mater. Sci.*, **1995**, *25*, 161.

[16] Flanigen, E. M.; Patton, R. L. *US Patent 4073865*, **1978**.

[17] Camblor, M. A.; Villaescusa, L. A.; Díaz-Cabañas, M.-J. *Top. Catal.* **1999**, *9*, 59.

[18] Barrett, P. A.; Camblor, M. A.; Corma, A.; Jones, R. H.; Villaescusa, L. A. *J. Phys. Chem. B* **1998**, *102*, 4147.

[19] Camblor, M. A.; Corma, A.; Valencia, S. *J. Mater. Chem.* **1998**, *8*, 2137.

[20] Tsuji, K.; Beck, L. W.; Davis, M. E. *Micro. Meso. Mater.* **1999**, *28*, 519.

[21] Koller, H.; Lobo, R. F.; Burkett, S. L.; Davis, M. E. *J. Phys. Chem.* **1995**, *99*, 12588.

[22] Nakagawa, Y.; Lee, G. S.; Harris, T. V.; Yuen, L. T.; Zones, S. I. *Micro Meso. Mater.* **1998**, *22*, 69.

[23] http://srmcatalog.nist.gov/srmcatalog/certificates/srm-1655.html.

[24] Derweik, S.; Sasson, Y. *J. Org. Chem.* **1989**, *54*, 4827.

[25] Christe, K. O.; Wilson, W. W.; Wilson, R. D.; Bau, R.; Feng, J. *J. Am. Chem. Soc.* **1990**, *112*, 7619.

[26] Lindenbaum, S. *J. Phys. Chem.* **1966**, *70*, 814.

[27] Parker, V. B. *Thermal Properties of Aqueous Uni-univalent Electrolytes*, **1965**, Nat. Stand. Ref. Data Ser., Nat. Bur. Stand. (U.S.).

[28] Bilger, S.; Soulard, M.; Kessler, H.; Guth, J. L. *Zeolites* **1991**, *11*, 784.

[29] Camblor, M. A.; Corma, A.; Valencia, S. *Chem. Comm.* **1996**, 2365.

[30] Hemingway, B. S.; Robie, R. A. *Jour. Research U.S. Geol. Survey.* **1977**, *5*, 413.

[31] Marthada, V. K.; Prosen, E. J. *Jour. Research N.B.S.* **1973**, *77A*, 205.

[32] Liou, J. G.; Donahoe, R. J. *U.S. DOE Report No. DOE/ER/12051-TI*, **1984**.

[33] Hummel, C.; Schwiete, H. E. *Glastech. Ber.* **1959**, *32*, 327.

[34] Johnson, G.K.; Tasker, I. R.; Howell, D. A.; Smith, J. V. *J. Chem. Thermodynamics* **1987**, *19*, 617.

[35] Wagner, P.; Zones, S. I.; Davis, M. E.; Medrud, R. C. *Angew. Chem. Int. Ed.* **1999**, *38*, 1269.

[36] Burkett, S. L.; Davis, M. E. *J. Phys. Chem.* **1994**, *98*, 4647.

[37] Burkett, S. L.; Davis, M. E. *Chem. Mater.* **1995**, *7*, 920, 1440.

[38] Koller, H.; Wölker, A.; Villaescusa, L. A.; Díaz-Cabañas, M. J.; Valencia, S.; Camblor, M. A. *J. Am. Chem. Soc.* **1999**, *121*, 3368.

[39] Tsuji, K.; Davis, M. E. *Microporous Materials* **1997**, *11*, 53.

[40] Harris, T. V.; Zones, S. I. *Stud. Surf. Sci. Catal.* **1994**, *84*, 29.

[41] Zones, S. I.; Olmstead, M. M.; Santilli, D. S. *J. Am. Chem. Soc.* **1992**, 114, 4195.

[42] Lewis, D. W.; Freeman, C. M.; Catlow, C. R. A. *J. Phys. Chem.* **1995**, *99*, 11194.

[43] Krishnan, C. V.; Friedman, H. L. *J. Phys. Chem.* **1969**, *73*, 3934.

[44] Frank, H. S.; Wen, W. Y. *Disc. Faraday Soc.* **1957**, *24*, 133.

[45] Johnson, D. A.; Martin, J. F. *J. Chem. Soc. Dalton Trans.* **1973**, 1585.

[46] Wagman, D.D.; Evans, W. H.; Parker, V. B.; Schumm, R. H.; Halow, I.; Bailey, S. M.; Churney, K. L.; Nuttall, R. L. *J. Phys. Chem. Ref. Data* **1982**, *11 suppl. 2*.

[47] Zones, S. I.; Hwang, S.-J.; Davis, M. E. *Chem. Eur. J.* **2001**, *7*, 1990.

[48] Zones, S. I. *Personal Communication* **2001**.

[49] Cox, B. G.; Hedwig, G. R.; Parker, A. J.; Watts, D. W. *Aust. J. Chem.* **1974**, *27*, 477.

[50] Pitzer, K. S. *Activity Coefficients in Electrolyte Solutions*, 2nd Edition, **1991**, CRC Press: Boca Raton.

[51] Wen, W. Y.; Saito, S.; Lee, C. *J. Phys. Chem.* **1966**, *70*, 1244.

[52] de Moor, P.-P. E. A.; Beelen, T. P. M.; Komanschek, B. U.; Beck, L. W.; Wagner, P.; Davis, M. E.; van Santen, R. A. *Chem. Eur. J.* **1999**, *5*, 7.

Chapter Eight

Conclusions

True catalyst design still hinges on a complete understanding of the molecular interactions resulting in the self-assembly of a given framework. As a first step towards this goal, systematic thermodynamic data pertinent to molecular sieve synthesis were determined in this investigation.

The enthalpies of a diverse set of pure-silica molecular sieves were determined by drop solution calorimetry in lead borate at 974 K. Despite the variety of their structural features, the molecular sieves span a narrow enthalpy range 6.8-14.4 kJ/mol above quartz. At typical pure-SiO_2 molecular sieve synthesis temperatures, the available thermal energy is RT = 3.5 kJ/mol. The enthalpies of pure-silica molecular sieves are therefore quite close to each other and also to quartz. The enthalpy variations were correlated with several structural parameters. A strong linear correlation between enthalpy and molar volume was observed, implying that it is the overall packing quality that determines the relative enthalpies of molecular sieve frameworks. Furthermore, the presence of internal silanol (Si-O-H) groups in calcined silica molecular sieves is only weakly ($\leq$2.4 kJ/mol) destabilizing. By extension, the enthalpies for all SiO_2 molecular sieves presently known are expected to lie within a narrow region approximately 6.8-14.4 kJ/mol above quartz.

In order to conclusively assess the relative stabilities of the various SiO_2 polymorphs, it was necessary to complement the enthalpy data with entropy measurements. Third-law entropies were determined for four silica molecular sieves by low-temperature heat capacity measurements. These frameworks were

chosen to span almost the entire range of molar volumes available to pure-silica molecular sieves. Their entropies lie in a very narrow range at 3.2-4.2 $J \cdot K^{-1} \cdot mol^{-1}$ above quartz, despite a 50% increase in molar volume between the least and most porous phases. At 1.4-1.8 kJ/mol, the resulting range of $T\Delta S$ is smaller than the available thermal energy at typical synthesis conditions, hence there are no significant entropy barriers to transformations between SiO_2 polymorphs.

The combination of the enthalpy and entropy data above enabled the calculation of the Gibbs free energy of transformation with respect to quartz for eight SiO_2 phases. All molecular sieve Gibbs free energies lie within twice the available thermal energy of each other at 423.15 K, a typical synthesis temperature. There are no large thermodynamic barriers to the interconversions among the many polymorphs of SiO_2. Rather, the narrowness of the energy range covered by different frameworks explains the multiplicity (around 30) of known SiO_2 polymorphs. The role of the structure-directing agent in molecular sieve synthesis cannot then be to help stabilize *otherwise* very unstable structures. Instead, it was concluded that the relatively frequent occurrence of all-SiO_2 molecular sieves as pure-phase materials must be due either to very slow transformation kinetics, or to significant interactions between the organic guest and inorganic host. To examine these possibilities in more detail, studies were undertaken to measure the energetics of the molecular sieve-SDA interaction.

The enthalpy of interaction between six pure-SiO_2 molecular sieve/SDA pairs were determined by HF solution calorimetry at 323.15 K. These values range

from -1.1 to -5.9 kJ/mol SiO_2. All enthalpies of interaction are negative, implying that the MS/SDA interaction is exothermic for all inorganic/organic pairs studied here. The interaction enthalpies are in no case more exothermic than twice the thermal energy at synthesis conditions. The relatively small magnitude of the interaction enthalpies is consistent with the interpretation of the MS/SDA interaction as consisting predominantly of weak, van der Waals forces between the hydrophobic silica species and hydrocarbon moieties of the SDA. The interaction enthalpies were shown to depend to some extent on the quality of the fit between inorganic host and organic guest, especially for more rigid and/or bulkier SDAs.

The entropy of interaction between molecular sieve and SDA fluoride was estimated by the negative of the entropy of hydration of the fluoride salt for *BEA/TEA, MFI/TEA, and MFI/TPA. The entropy for the MS/SDA interaction is positive in all cases, due to the release of ordered water upon SDA occlusion. The inorganic/organic interaction is thus simultaneously favored by its enthalpy (exothermic van der Waals contacts between hydrophobic silica species and hydrocarbon chains) and entropy (disordering of water around the SDA). Entropy contributions to the interaction energetics are comparable to the enthalpy contributions and must therefore be included in the thermodynamic description of molecular sieve formation. Within the approximations of this work, the entropy contribution was shown to preferentially stabilize higher organic contents, i.e., more porous frameworks.

Together with the experimentally determined enthalpies of interaction, the entropies of interaction enable the calculation of the Gibbs free energy of interaction for *BEA/TEA, MFI/TEA, and MFI/TPA. The magnitudes of the Gibbs free energies of interaction (-2.0 to -5.4 kJ/mol SiO_2) are comparable to differences between silica polymorphs. The MS/SDA interaction appreciably alters the energetics of molecular sieve self-assembly. The self-assembly of silica frameworks less stable than silica glass (e.g., *BEA) can become thermodynamically favorable when taking place simultaneously with the interaction between assembling inorganic framework and SDA species. Although favorable, the MS/SDA interaction is not sufficiently exergonic to explain the strong selectivity many organic cations exhibit towards a relatively small subset of porous silica frameworks. Rather, the modest energetics explain the ability of most organocations to direct syntheses towards more than one molecular sieve framework. These conclusions are not changed by considering all species present in the synthesis mixture, although the effective dilution of SDAF species upon enclathration is exergonic by an additional 1.6-4.4 kJ/mol SiO_2.

In conclusion, the results presented in this thesis conclusively show that no strong thermodynamic factors are at play in pure-silica molecular science synthesis. All silica polymorphs are similar in energy to each other. The role of the organic SDA is neither the stabilization of otherwise very unstable phases nor the preferential stabilization of one framework structure over others. The self-assembly thermodynamics depend on the delicate interplay between enthalpy

and entropy contributions to the energetics of the empty molecular sieves, to the energetics of the organic/inorganic interaction, and to the energetics of unreacting components of the synthesis mixture. Since thermodynamic differences are relatively modest, the crucial role of organic SDAs in molecular sieve synthesis must be related to kinetic effects, and synthetic data suggest that molecular sieve nucleation is most likely to be the rate-determining step. It is speculated that such activation energies may be related to the interaction energetics since several techniques have documented the existence of intimately bound inorganic/organic composites in early stages of molecular sieve syntheses.

Several directions for further work are suggested. Traditionally, attempts to model the interaction between molecular sieves and their organic SDAs have suffered from the lack of experimental data to which the calculations could be compared. The interaction enthalpies determined experimentally in Chapter Seven make up the first collection of interaction energy data for a molecular sieve framework other than MFI. It is recommended that the Chapter Seven interaction enthalpies be used to improve existing theoretical models for molecular sieve/SDA interactions.

The discrepancy in the enthalpies of transition from quartz to MTW determined by high-temperature lead borate calorimetry and by HF calorimetry should be resolved. The simplest approach is to measure the enthalpy of drop solution in lead borate for MTW free of silanol defects, prepared as described in Chapter Seven.

The calculations of Gibbs free energies of interaction in Chapter Seven relied on several assumptions in the estimations of the entropies of interaction. It is recommended that the entropies of interaction be determined experimentally for specimens representing the various possible combinations of molecular sieve and SDA. Since the shape of the third-law entropy (relative to quartz) versus temperature curve of pure-silica *BEA is different from those of the other three samples studied here, it may be instructive to perform heat capacity measurements on pure-silica *BEA prepared in hydroxide media to determine whether the difference in curve shapes is a property of the *BEA framework or of the particular sample studied in Chapter Four.

The relationship between interaction energetics and activation energies also needs to be investigated. Synthetic experiments to determine kinetic parameters for the nucleation and growth of the six materials studied in Chapter Seven are expected to be most informative in this regard.

The solution calorimetry experiments of Chapter Seven were performed at 323.15 K, approximately 100 K below typical synthesis conditions for pure-SiO_2 molecular sieves. While the interaction enthalpies are not expected to vary strongly with temperature, this assumption can be tested by collecting data closer to synthesis temperatures. No attempts were made in this thesis to determine the highest operating temperature of the calorimetry equipment (in particular, the highest temperature before significant leaks develop from the HF-containing cells), but this temperature is expected to lie in the 323-373 K range. It is therefore

recommended that solution calorimetry experiments be carried out at higher temperatures. Data for only a subset of the systems studied in Chapter Seven (e.g., *BEA/TEA and MFI/TPA) would be sufficient to evaluate the importance of temperature variations.